



## NEW DIRECTIONS IN AMINOCATALYSIS: VINYLOGY AND PHOTOCHEMISTRY

Mattia Silvi

**ADVERTIMENT.** L'accés als continguts d'aquesta tesi doctoral i la seva utilització ha de respectar els drets de la persona autora. Pot ser utilitzada per a consulta o estudi personal, així com en activitats o materials d'investigació i docència en els termes establerts a l'art. 32 del Text Refós de la Llei de Propietat Intel·lectual (RDL 1/1996). Per altres utilitzacions es requereix l'autorització prèvia i expressa de la persona autora. En qualsevol cas, en la utilització dels seus continguts caldrà indicar de forma clara el nom i cognoms de la persona autora i el títol de la tesi doctoral. No s'autoritza la seva reproducció o altres formes d'explotació efectuades amb finalitats de lucre ni la seva comunicació pública des d'un lloc aliè al servei TDX. Tampoc s'autoritza la presentació del seu contingut en una finestra o marc aliè a TDX (framing). Aquesta reserva de drets afecta tant als continguts de la tesi com als seus resums i índexs.

**ADVERTENCIA.** El acceso a los contenidos de esta tesis doctoral y su utilización debe respetar los derechos de la persona autora. Puede ser utilizada para consulta o estudio personal, así como en actividades o materiales de investigación y docencia en los términos establecidos en el art. 32 del Texto Refundido de la Ley de Propiedad Intelectual (RDL 1/1996). Para otros usos se requiere la autorización previa y expresa de la persona autora. En cualquier caso, en la utilización de sus contenidos se deberá indicar de forma clara el nombre y apellidos de la persona autora y el título de la tesis doctoral. No se autoriza su reproducción u otras formas de explotación efectuadas con fines lucrativos ni su comunicación pública desde un sitio ajeno al servicio TDR. Tampoco se autoriza la presentación de su contenido en una ventana o marco ajeno a TDR (framing). Esta reserva de derechos afecta tanto al contenido de la tesis como a sus resúmenes e índices.

**WARNING.** Access to the contents of this doctoral thesis and its use must respect the rights of the author. It can be used for reference or private study, as well as research and learning activities or materials in the terms established by the 32nd article of the Spanish Consolidated Copyright Act (RDL 1/1996). Express and previous authorization of the author is required for any other uses. In any case, when using its content, full name of the author and title of the thesis must be clearly indicated. Reproduction or other forms of for profit use or public communication from outside TDX service is not allowed. Presentation of its content in a window or frame external to TDX (framing) is not authorized either. These rights affect both the content of the thesis and its abstracts and indexes.

UNIVERSITAT ROVIRA I VIRGILI

NEW DIRECTIONS IN AMINOCATALYSIS: VINYLOGY AND PHOTOCHEMISTRY

Mattia Silvi

UNIVERSITAT ROVIRA I VIRGILI

NEW DIRECTIONS IN AMINOCATALYSIS: VINYLOGY AND PHOTOCHEMISTRY

Mattia Silvi

Mattia Silvi

# **New Directions in Aminocatalysis: Vinylogy and Photochemistry**

Doctoral Thesis

Supervised by Prof. Paolo Melchiorre

ICIQ – Institut Català d'Investigació Química



UNIVERSITAT ROVIRA I VIRGILI

Tarragona

2015

UNIVERSITAT ROVIRA I VIRGILI

NEW DIRECTIONS IN AMINOCATALYSIS: VINYLOGY AND PHOTOCHEMISTRY

Mattia Silvi



UNIVERSITAT ROVIRA I VIRGILI

Prof. Paolo Melchiorre, ICREA Research Professor & ICIQ Group Leader

I STATE that the present study, entitled "New Directions in Aminocatalysis: Vinylgy and Photochemistry", presented by MATTIA SILVI to receive the degree of Doctor, has been carried out under my supervision at the Institut Català d'Investigació Química (ICIQ).

Tarragona, September the 1st 2015

Doctoral Thesis Supervisor

A handwritten signature in blue ink, appearing to read 'P. Melchiorre', with a long horizontal stroke extending to the right.

Prof. Paolo Melchiorre

UNIVERSITAT ROVIRA I VIRGILI

NEW DIRECTIONS IN AMINOCATALYSIS: VINYLOGY AND PHOTOCHEMISTRY

Mattia Silvi

## Acknowledgements

Every single page of this manuscript has represented a personal challenge that I have approached with passion and dedication.

In this endeavor, of course, I have not been alone! The help of many people has been crucial to make this possible. First of all, thanks to my supervisor for giving me the possibility to carry out this research in a wonderful research institute such as ICIQ. It would be hard to make a list in a single page of everything he has taught me. I would like to thank him for motivating me and helping me to understand that carrying out successful research means: optimizing time WITHOUT forget the importance of high-quality research and the importance of details.

My thanks to John P. Wolfe and all my colleagues from the University of Michigan who gave me the possibility to spend 10 unforgettable weeks in USA teaching me interesting aspects of organometallic chemistry. Thanks for giving me your trust and allowing me to explore this field of chemistry with such a degree of freedom.

A challenge, such as carrying out a PhD in a foreign country, far from home and friends, would not have been achievable without the help of several people that made me feel at home, even if very far from Italy.

Thanks to my family, who have always supported me. From the day when I told them that I would be leaving Italy until the last day of this experience they have been close to me, making me feel like I never left home. Thanks to Martina, who always helped me in the difficult moments and always encouraged me to follow my dreams.

Grazie alla mia famiglia, che non ha mai cessato di mandarmi messaggi positivi e mi ha sempre incoraggiato a correre verso un sogno. Grazie di cuore davvero per non aver mai smesso di mandarmi tutto il vostro calore che, credetemi, è arrivato lontano migliaia di chilometri.

Grazie Martina, per avermi incoraggiato a seguire la mia vocazione verso la scienza, anche se questo ci ha portato distanti per qualche tempo. Grazie per esserci sempre stata, nei momenti bui per avermi supportato e al tempo stesso scosso e nei momenti di gioia per averli resi ancora più indimenticabili con la tua presenza.

Thanks to all my colleagues that helped me and taught me both practical and theoretical aspects of chemistry.

Thanks to Manuel, an unforgettable friend who shared with me most of this experience. From the first day we met, we supported each other and shared both the good and the bad times. I firmly believe that we will always keep in contact in the future. Grazie caro ragazzo!

Thanks to Igor and John, two outstanding post-docs that taught me many aspects of chemistry helping me to grow in a scientific point of view, but also have been close friends sharing with me many nice Friday nights.



Thanks to David, for being a good friend during this four years.

Thanks to Hamish for proofreading this manuscript and giving me his suggestions.

Thanks to Charlie, Luca and Mauro for continuing the iminium ion photochemistry projects and Giacomo for continuing the photochemical enamine-mediated alkylation project while I was writing this manuscript.

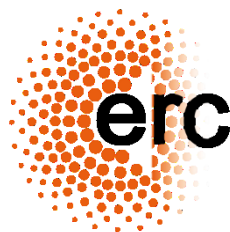
Thanks to all the colleagues from the Melchiorre group, for sharing with me this 4 years.

Thanks to Marco Bella from the University "Sapienza" of Rome, for all he taught me and for his suggestions and support when I made the decision to leave Italy.

Thanks to all ICIQ staff and technicians for their valuable work and their help.

Support from the Institute of Chemical Research of Catalonia (ICIQ) Foundation, from MICINN (grant CTQ2010-15513) and from the European Research Council (ERC Starting grant agreement no. 278541—ORGA-NAUT) are gratefully acknowledged.

I am personally grateful to ICIQ Foundation for a doctoral fellowship (ref. 06/211-2).



## List of Publications

Some of the results presented in this thesis have been published:

- “Enantioselective Organocatalytic Alkylation of Aldehydes and Enals Driven by the Direct Photoexcitation of Enamines”

Mattia Silvi, Elena Arceo, Igor D. Jurberg, Carlo Cassani and Paolo Melchiorre

*Journal of the American Chemical Society*, **2015**, *137*, 6120. Highlighted in Synfact 2015, 765.

- “Controlling the Molecular Topology of Vinylogous Iminium Ions by Logical Substrate Design: Highly Regio- and Stereoselective Aminocatalytic 1,6-Addition to Linear 2,4-Dienals”

Mattia Silvi, Indranil Chatterjee, Yiankai Liu and Paolo Melchiorre

*Angewandte Chemie International Edition*, **2013**, *52*, 10780.

- “Secondary Amine-Catalyzed Asymmetric  $\gamma$ -Alkylation of  $\alpha$ -Branched Enals via Dienamine Activation”

Mattia Silvi, Carlo Cassani, Antonio Moran and Paolo Melchiorre

*Helvetica Chimica Acta*, **2012**, *95*, 1985.

UNIVERSITAT ROVIRA I VIRGILI

NEW DIRECTIONS IN AMINOCATALYSIS: VINYLOGY AND PHOTOCHEMISTRY

Mattia Silvi

*Imagination, tenacity and doubt.*

*“I am enough of an artist to draw freely upon my imagination. Imagination is more important than knowledge. Knowledge is limited. Imagination encircles the world.”*

*Albert Einstein*

*“Let me tell you the secret that has led me to my goal. My strength lies solely in my tenacity.”*

*Louis Pasteur*

*“The intellect does not deserve this name, until the day when it starts to doubt itself.”*

*Arturo Graf*

UNIVERSITAT ROVIRA I VIRGILI

NEW DIRECTIONS IN AMINOCATALYSIS: VINYLGY AND PHOTOCHEMISTRY

Mattia Silvi

UNIVERSITAT ROVIRA I VIRGILI  
NEW DIRECTIONS IN AMINOCATALYSIS: VINYLOGY AND PHOTOCHEMISTRY  
Mattia Silvi

*To my family and Martina*

UNIVERSITAT ROVIRA I VIRGILI

NEW DIRECTIONS IN AMINOCATALYSIS: VINYLGY AND PHOTOCHEMISTRY

Mattia Silvi

## Table of Contents

<b>1. Introduction .....</b>	<b>1</b>
1.1. Asymmetric catalysis and organocatalysis.....	1
1.2. Aminocatalysis .....	2
1.3. The tools of aminocatalysis .....	5
1.4. Towards new frontiers in aminocatalysis .....	7
1.5. The principle of vinylogy .....	8
1.6. Photochemistry and organocatalysis.....	9
1.7. Objectives and summary of the present doctoral thesis .....	10
1.7.1. Vinylogous reactivity in aminocatalysis .....	10
1.7.2. The photochemistry of the covalent intermediates of aminocatalysis .....	11
<b>2. Secondary Amine-Catalyzed Asymmetric <math>\gamma</math>-Alkylation of <math>\alpha</math>-Branched Enals via Dienamine Activation .....</b>	<b>13</b>
2.1. Introduction .....	13
2.1.1. Dienamine activation in organocatalysis .....	14
2.1.2. $S_N1$ -type alkylation of aldehydes .....	20
2.2. Target of the project .....	22
2.3. Results and discussion .....	23
2.3.1. Optimization studies .....	23
2.3.2. Reaction scope.....	28
2.3.3. Mechanistic insights – Stereochemical model .....	30
2.4. Conclusions and remarks .....	36
2.5. Experimental section .....	36
<b>3. Controlling the Molecular Topology of Vinylogous Iminium Ions: Asymmetric 1,6-Addition to Linear 2,4-Dienals .....</b>	<b>47</b>
3.1. Introduction .....	47
3.2. Target of the project .....	52
3.3. Results and discussion .....	54
3.3.1. Starting material design .....	54
3.3.2. Optimization studies .....	62
3.3.3. The reaction scope .....	70
3.4. Conclusions and remarks .....	72
3.5. Experimental Section .....	72
Annex I – Iminium ion species <b>39d</b> analysis .....	92
<b>4. Enantioselective Organocatalytic <math>\alpha</math>-Alkylation of Aldehydes and Enals Driven by the Direct Photoexcitation of Enamines .....</b>	<b>95</b>
4.1. Introduction .....	95



4.1.1. Photocatalysis: the MacMillan approach .....	96
4.1.2. Photochemistry of EDA complex: our group approach .....	97
4.2. Target of the project .....	100
4.3. Results and discussion .....	100
4.3.1. Enamine synthesis and characterization .....	104
4.3.2. Photophysical studies of the Enamine .....	108
4.3.3. Enamine redox properties .....	112
4.3.4. Proposed mechanism .....	115
4.3.5. Scope of the reaction .....	118
4.4. Towards novel applications: formal asymmetric methylation of aldehydes .....	119
4.4.1. Preliminary optimization studies .....	122
4.5. Conceptual implications and conclusions .....	124
4.6. Experimental section.....	125
<b>5. Iminium ion photochemistry: a novel route for the unconventional asymmetric <math>\beta</math>-functionalization of enals .....</b>	<b>141</b>
5.1. Introduction .....	141
5.1.1. From enamine excitation to iminium ion excitation: the idea of exploiting the redox proprieties of the excited iminium ion ....	143
5.1.2. A brief overview of photophysical and electrochemical properties of iminium ions.....	144
5.1.3. The identification of the donor partner .....	145
5.2. Target of the project .....	147
5.3. Catalytic asymmetric conjugate allylation and benzylation of electron-poor olefins: challenging reactions .....	148
5.4. Results and discussion.....	150
5.4.1. Spectroscopic investigations and mechanistic considerations ..	155
5.5. Future directions .....	158
5.5.1. Introduction of $-\text{CH}_2\text{X}$ fragments in $\beta$ position of enals .....	158
5.5.2. The employment of trifluoroborate salts: forging quaternary stereocenters .....	159
5.5.3. Iminium photochemistry and trifluoroborate salts, a general alkylation strategy? .....	161
5.6. Conclusions .....	162
5.7. Experimental section.....	162

# Chapter I

## Introduction

---

### 1.1 Asymmetric catalysis and organocatalysis

As the main aim of this research thesis is the development of new enantioselective catalytic reactions, the definition of *catalysis* is reminded. A catalyst is a compound that takes part in a reaction increasing the rate of the process without modifying the overall standard Gibbs energy change. Since the catalyst is not consumed during a given reaction, it can be employed in sub-stoichiometric amounts. The employment of efficient catalysts in organic synthesis gives the possibility to overcome prohibitive energy activation barriers often faced in common organic transformations.<sup>1</sup>

The growing request for enantiopure chiral compounds by the pharmaceutical, fragrances and material industries have led to the development of asymmetric catalysis, where the concept of catalysis is exploited for synthesizing chiral compounds such that formation of one particular stereoisomer is favored. The fact that the valuable and often expensive chiral catalysts could be used in a sub-stoichiometric amount can help keeping a process cost-effective while enhancing the atom economy of the reaction.<sup>2</sup>

The employment of small chiral organic molecules as catalysts (later defined as *asymmetric organocatalysis*) has been known for more than a century. The earliest example was the hydrocyanation of benzaldehyde promoted by quinine (Scheme 1.1, a) while another remarkable early example, published in the 1970's, was the L-proline-catalyzed Hajos-Parrish reaction (Scheme 1.1, b).<sup>3,4,5</sup> However, the synthetic potential of organocatalysis was not recognized by the chemistry community until the year 2000, when two seminal publications, published by MacMillan and List, Lerner, and Barbas III,<sup>6,7</sup> conceptualized the field of asymmetric aminocatalysis.

---

<sup>1</sup> a) Anslyn, E. V.; Dougherty, D. A. "Catalysis" Chapter 9, p. 489 in *Modern Physical Organic Chemistry*, 2006, University Science Books. b) Laider, K. J. "A Glossary of Terms Used in Chemical Kinetics, Including Reaction Dynamics (IUPAC Recommendations 1996)" *Pure and App. Chem.* **1996**, 68, 149.

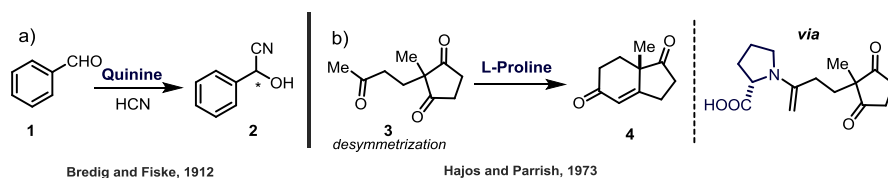
<sup>2</sup> a) [http://www.nobelprize.org/nobel\\_prizes/chemistry/laureates/2001/advanced-chemistryprize2001.pdf](http://www.nobelprize.org/nobel_prizes/chemistry/laureates/2001/advanced-chemistryprize2001.pdf)  
b) Noyori, R. "Introduction" Chapter 1, p. 1 in *Asymmetric Catalysis in Organic Synthesis*, 1994, Wiley.

<sup>3</sup> Hajos, Z. G; Parrish, D. R. "Asymmetric Synthesis of Bicyclic Intermediates of Natural Product Chemistry" *J. Org. Chem.* **1974**, 39, 1615.

<sup>4</sup> List, B. "Emil Knoevenagel and the Roots of Aminocatalysis" *Angew. Chem. Int. Ed.* **2010**, 49, 1730.

<sup>5</sup> Berkessel, A.; Gröger, H. "Introduction: Organocatalysis - From Biomimetic Concepts to Powerful Methods for Asymmetric Synthesis" Chapter 1, p. 1 in *Asymmetric Organocatalysis*, 2005, Wiley-VCH.

<sup>6</sup> Ahrendt, K. A.; Borths, C. J.; MacMillan, D. W. C. "New Strategies for Organic Catalysis: The First Highly Enantioselective Organocatalytic Diels-Alder Reaction" *J. Am. Chem. Soc.* **2000**, 122, 4243.



Bredig and Fiske, 1912

Hajos and Parrish, 1973

Scheme 1.1 – Early examples of asymmetric organic catalysis.

While the turnover numbers of organocatalytic processes are typically lower than those observed using metal-based catalysts and high catalyst loadings are often required, the benefit of using inexpensive organic catalysts and the ability to run the reaction in open air with wet solvents often more than compensate the drawbacks, justifying the popularity of the field in current organic chemistry.<sup>8</sup>

## 1.2 Aminocatalysis

One of the most exploited and efficient strategies in asymmetric organocatalysis is the generation of active covalent intermediates (enamine and iminium ions) through the condensation of chiral amines with carbonyl compounds, a concept commonly known as *aminocatalysis*.<sup>9</sup> Such a catalytic strategy could be considered biologically inspired, since it is employed by some enzymes to overcome the high activation energy barriers encountered in chemical transformations. Class I aldolase can be considered as a representative example of the occurrence of aminocatalytic activation in enzymatic catalysis (Scheme 1.2).<sup>10</sup> In the active site of this enzyme, the formation of the highly reactive iminium ion **6** mediates the carbon-carbon bond scission (retro-aldol reaction) to form the two fragments **7** and **8**. This chemical reaction is pivotal for one of the primary biochemical processes: glycolysis.

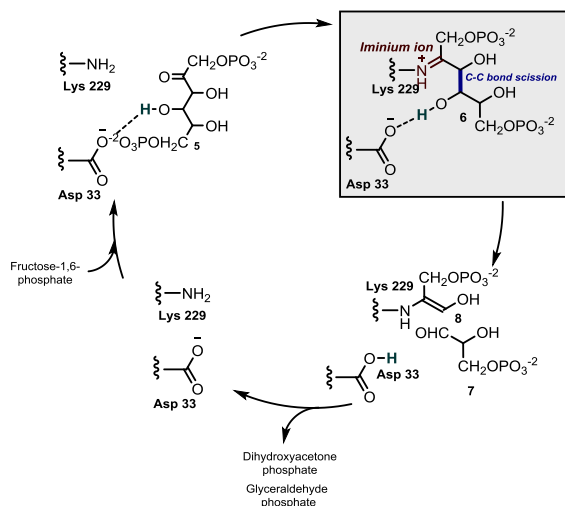
The analogies in the mechanism of catalysis between enamine activation and Class I aldolase prompted Hajos and Parrish to consider their catalytic system, in which condensation of an amine-derived catalyst with a carbonyl compound plays a key role, as *a simplified model of a biological system in which (S)-proline plays the role of an enzyme* (Figure 1.1, b).<sup>3</sup>

<sup>7</sup> List, B.; Lerner, R. A.; Barbas III, C. F. "Proline-Catalyzed Direct Asymmetric Aldol Reactions" *J. Am. Chem. Soc.* **2000**, *122*, 2395.

<sup>8</sup> MacMillan, D. W. C. "The Advent and Development of Organocatalysis" *Nature* **2008**, *455*, 304.

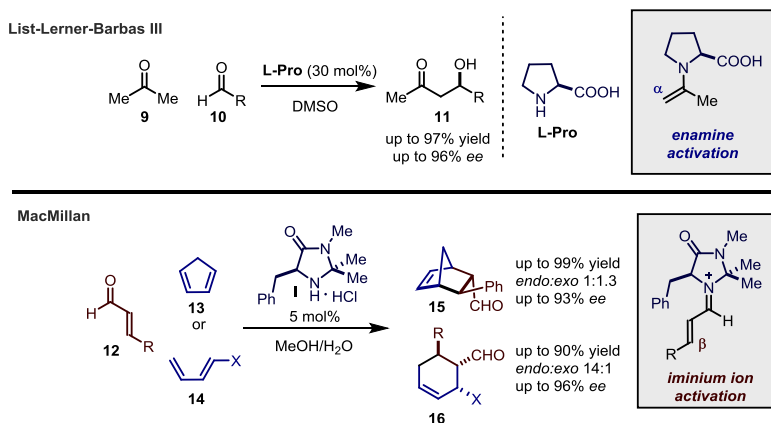
<sup>9</sup> Melchiorre, P.; Marigo, M.; Carlone, A.; Bartoli, G. "Asymmetric Aminocatalysis – Gold Rush in Organic Chemistry" *Angew. Chem. Int. Ed.* **2008**, *47*, 6138.

<sup>10</sup> Voet, D.; Voet, J. G. "Glycolysis" Chapter 17, p. 602 in *Biochemistry*, 4<sup>th</sup> Edition, **2011**, Wiley.



Scheme 1.2 – Class I aldolase: iminium ion mediated C-C scission.

Despite the synthetic potential of both enamines and iminium ions were well-known, thanks to the pioneering work by Stork *et al.* in the early sixties<sup>11</sup> and Baum *et al.* in the middle seventies of the last century,<sup>12</sup> their employment as active intermediates in catalytic reactions remained relatively unexplored for years. In 2000, Barbas III, Lerner, and List and MacMillan reported two remarkable examples of asymmetric functionalization of carbonyl compounds exploiting the concept of aminocatalysis: the enamine-mediated aldol reaction and the iminium-ion mediated Diels-Alder reaction (Scheme 1.3).<sup>6,7</sup>



Scheme 1.3 – Early examples of modern aminocatalysis.

<sup>11</sup> Stork, G.; Brizzolara, A.; Landesman, H.; Szmuszkovicz, J.; Terrell, R. "The Enamine Alkylation and Acylation of Carbonyl Compounds" *J. Am. Chem. Soc.* **1963**, *85*, 207.

<sup>12</sup> Baum, J. S.; Viehe, H. G. "Synthesis and Cycloaddition Reactions of Acetylenic Iminium Compounds" *J. Org. Chem.* **1976**, *41*, 183.

For those transformations, two cheap and readily available catalysts were employed: L-proline (**L-Pro**) and L-phenylglycine-derived imidazolidinone **I**.

These two seminal works were fundamental for the conceptualization of the field of organocatalysis and the scientific community quickly realized the potential of the aminocatalytic activation of carbonyl compounds. MacMillan himself highlighted the importance of defining the field as *organocatalysis*,<sup>8,13</sup> which provided a strong identity to the field and attracted the attention of the broad synthetic community.<sup>8</sup> A great number of transformations were developed since then, and the research groups involved in asymmetric catalysis effectively considered organocatalysis as a new fundamental tool in their catalysis toolbox. The *aminocatalytic gold rush*<sup>9</sup> began and the covalent activation of carbonyl compounds provided a novel and reliable synthetic platform for generating stereogenic centers at the  $\alpha$ - and  $\beta$ -position of unmodified carbonyl compounds.<sup>9,14,15</sup>

In enamine-mediated reactions, an aminocatalyst quickly condenses with carbonyl compounds, generating iminium ions carrying highly acidic  $\alpha$ -protons (**18**). The deprotonation of such species generate enamines (**19**), enol synthetic equivalents with increased HOMO energies and high nucleophilicities (Scheme 1.4). These chiral enamines can stereoselectively trap a variety of electrophiles providing, after release of the catalyst,  $\alpha$ -functionalized carbonyl compounds **20**.

In iminium ion-mediated reactions, the condensation of secondary amines with unsaturated carbonyl compounds generates cationic iminium ions (**22**), compounds with reduced LUMO orbital energy and increased electrophilicity compared to the starting enone. For conjugated  $\pi$ -systems, the electronic redistribution induced by iminium ion intermediates facilitates nucleophilic additions and pericyclic reactions. As a result, this activation mode, termed iminium ion activation, allows the asymmetric  $\beta$ -functionalization of carbonyl compounds. This kind of catalysis displays analogies with some examples of organometallic activation, where coordination by Lewis acids decreases the LUMO energy of carbonyl compounds (LUMO lowering effect).<sup>16</sup>

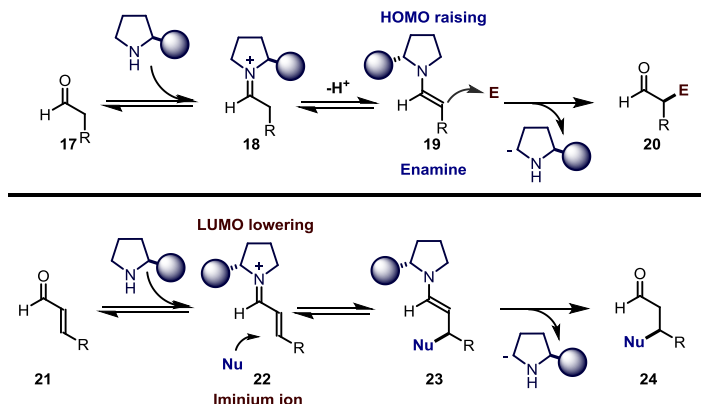
---

<sup>13</sup> In reality the name “organocatalysis” is much older than one could expect. In fact Langenbeck, in 1937, had an entire research program devoted to studying organic catalysts (“die Organischen Katalysatoren”). See ref. 4 for further details.

<sup>14</sup> Mukherjee, S.; Yang, J. W.; Hoffmann, S.; List, B. “Asymmetric Enamine Catalysis” *Chem. Rev.* **2007**, *107*, 5471.

<sup>15</sup> Erkkilä, A.; Majander, I.; Pihko, P. M. “Iminium Catalysis” *Chem. Rev.* **2007**, *107*, 5416.

<sup>16</sup> Fleming, I. “The Effect of Lewis Acids on Diels-Alder Reactions” Chapter 6, p. 318 in *Molecular Orbitals and Organic Chemical Reactions, Reference Edition*, **2010**, Wiley.

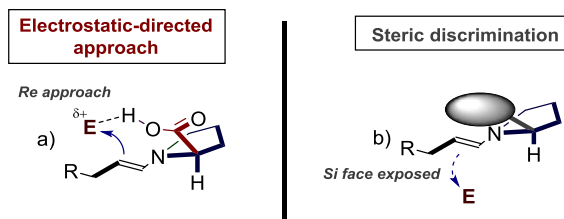


**Scheme 1.4** – General activation in organocatalytic transformations, water additions/eliminations and protonation/deprotonation steps (a part the one between **18** and **19**) are not reported for brevity.

### 1.3 The tools of aminocatalysis

The well-defined geometry of the covalently bound catalyst-substrate adducts is considered one of the reasons for the high stereoselectivity observed in asymmetric aminocatalytic reactions. Thus, it is no surprise that extensive efforts have been devoted to the optimization of the chiral aminocatalyst structure, in order to identify more efficient and general scaffolds. Both chiral secondary or primary amines could be successfully employed as catalysts. In this section, a brief description of common chiral secondary amine catalysts is reported, since it will be functional for the discussion carried out in the entire manuscript.

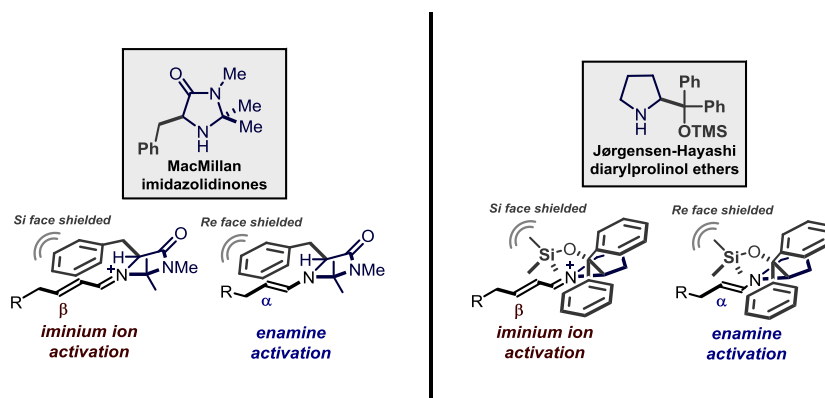
In enamine-mediated reactions, a chiral aminocatalyst condenses with a carbonyl compound (*i.e.* an aldehyde) to form a reactive enamine intermediate. The chiral catalyst scaffold creates a stereo-electronic bias directing the electrophile approach preferentially towards one of the two prochiral faces of the  $sp^2$ -hybridized enamine intermediate (Scheme 1.5). Usually, hydrogen bonding or steric interactions are exploited to induce  $\pi$ -facial discrimination.



**Scheme 1.5** – General facial discrimination operated by secondary amines in enamine-mediated organocatalysis.

Although cases of electrostatic guidance of the nucleophile are known in iminium ion activation as well,<sup>17</sup> steric preferences for the approach of the nucleophile are more common.

Since in the investigations discussed herein the steric discrimination approach (Scheme 1.5, b) has been extensively used for developing new asymmetric reactions, the most common catalysts used for the strategy are briefly discussed. Between the myriad of effective catalysts developed for efficient aminocatalytic reactions, the most prevalent and general are undoubtedly the MacMillan type imidazolidinones and the Jørgensen-Hayashi type diarylprolinol silylethers (Scheme 1.6).<sup>18</sup> The reactive intermediates, generated upon condensation of these chiral secondary amines with carbonyl substrates, have been widely studied and their geometry has been determined in the solid state (through single crystal X-ray diffraction) and in solution (through NMR spectroscopic analysis).<sup>19</sup> It is important to remark that these chiral scaffolds are able to catalyze a wide variety of aminocatalytic processes with exceptional reliability and constantly high stereoselectivity. The observed enantioselectivities are barely dependent on the nature of the reaction partner but more on the intrinsic geometric features of the reactive covalent intermediates.



Scheme 1.6 – Steric shielding discrimination operated by the most popular secondary amine organocatalysts.

<sup>17</sup> a) Kawara, A.; Taguchi, T. “An Enantioselective Michael Addition of Soft Nucleophiles to Prochiral Enone Catalyzed by (2-Pyrrolidyl)Alkyl Ammonium Hydroxide” *Tetrahedron Lett.* **1994**, *35*, 8805. b) Kunz, R. K.; MacMillan, D. W. C. “Enantioselective Organocatalytic Cyclopropanations. The Identification of a New Class of Iminium Catalyst Based upon Directed Electrostatic Activation” *J. Am. Chem. Soc.* **2005**, *127*, 3240.

<sup>18</sup> a) Lelais, G.; MacMillan, D. W. “Modern Strategies in Organic Catalysis: The Advent and Development of Iminium Activation” *Aldrichim. Acta* **2006**, *39*, 79. b) Jensen, K.; Dickmeiss, G.; Jiang, H.; Albrecht, Ł.; Jørgensen, K. A. “The Diarylprolinol Silyl Ether System: A General Organocatalyst” *Acc. Chem. Res.* **2012**, *45*, 248.

<sup>19</sup> a) Seebach, D.; Grošelj, U.; Badine, M.; Schweizer, W. B.; Beck, A. K. “Isolation and X-Ray Structure of Reactive Intermediates of Organocatalysis with Diphenylprolinol Ethers and with Imidazolidinones” *Helv. Chim. Acta* **2008**, *91*, 1999. b) Schmid, M. B.; Zeitler, K.; Gschwind, R. M. “Distinct Conformational Preferences of Prolinol and Prolinol Ether Enamines in Solution Revealed by NMR” *Chem. Sci.* **2011**, *2*, 1793. c) Peelen, T. J.; Chi, Y.; Gellman, S. H. “Enantioselective Organocatalytic Michael Additions of Aldehydes to Enones with Imidazolidinones: Cocatalyst Effects and Evidence for an Enamine Intermediate” *J. Am. Chem. Soc.* **2005**, *127*, 11598.

As schematically reported in Scheme 1.6, the chiral amine  $\alpha$ -substituent induces specific geometrical features in the reactive intermediate. Furthermore, it induces  $\pi$ -facial discrimination of the covalent reactive intermediate, providing the steric bias responsible for the highly reliable and predictable enantioselectivity observed in aminocatalytic reactions.<sup>9,14,15</sup>

## 1.4 Towards new frontiers in aminocatalysis

During the last 15 years, the field of organocatalysis has been growing at an impressive pace. The cheap and relatively easy-to-perform experimental procedures, together with the high reliability of the modern organocatalytic tools to ensure high reaction efficiency, attracted a great number of research groups. In 2008, Melchiorre described the highly competitive field with the image reported in Figure 1.1, drawing an analogy to the Californian Gold Rush of 1848-1855.<sup>9</sup>

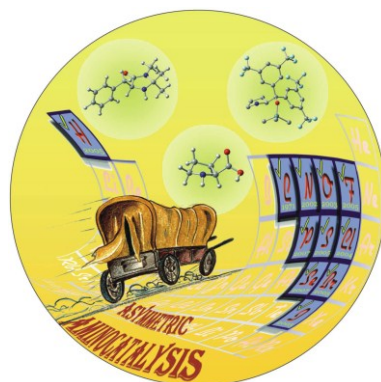


**Figure 1.1** – Aminocatalysis in 2008, the high competition of the field was compared to the one of the “California Gold Rush”.<sup>9</sup> Figure reproduced under the permission of John Wiley and Sons, licence number 3686971199013.

The improved knowledge and the continued optimization of the tools of organocatalysis (*i.e.* optimization of catalyst scaffold, better knowledge of reaction mechanisms) resulted in the field being even more crowded than it was 7 years ago. After the “gold rush”, chemists focused their attention on the development of new concepts, such as cascade procedures, or on the application of organocatalytic strategies in total synthesis.<sup>20</sup> The competition and the level of sophistication reached such high levels that finding novel organocatalytic transformations became constantly harder.

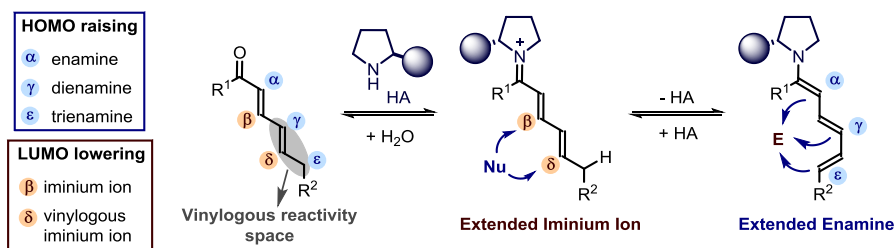
<sup>20</sup> Bertelsen, S.; Jørgensen, K. A. “Organocatalysis – After the Gold Rush” *Chem. Soc. Rev.* **2009**, *38*, 2178.



In order to further expand the synthetic potential of aminocatalysis, we sought to develop novel synthetic strategies that could allow new directions to be explored. We investigated the possibility of merging aminocatalytic reactivities with the concept of vinylogy to develop new strategies for the remote functionalization of unmodified carbonyl compounds. At the same time, our recent interest in the field of photochemistry led us to consider the intrinsic photoactivity of the reactive intermediates of organocatalysis for developing new light-driven asymmetric reactions. Indeed, the chemical reactivity of electronically excited molecules differs fundamentally from that in the ground state and could provide unexplored opportunities for developing processes which cannot be realized using thermal activation. These reactivity concepts will pervade the whole dissertation and they will be briefly introduced in the following paragraphs.

## 1.5 The principle of vinylogy

In 1934, Reynold Fuson stated: "When, in a compound of the type  $A-E_1=E_2$ , a structural unit of the type  $-(C=C)_n-$  is interposed between  $A$  and  $E_1$  the function of  $E_2$  remains qualitatively unchanged but that of  $E_1$  may be usurped by the carbon atom attached to  $A$ ".<sup>21</sup> As a consequence of this general principle (*the vinylogy principle*), the general activation modes of aminocatalysis, enamine and iminium ion, can be transmitted through the  $\pi$ -system of polyunsaturated carbonyl compounds allowing for the stereoselective functionalization at distal positions, such as the  $\gamma$ -,  $\delta$ - and  $\epsilon$ -carbon atoms.



Scheme 1.7 – Types of vinylogous aminocatalytic activation of unsaturated carbonyl compounds.

The combination of aminocatalysis and vinylogous reactivity was exploited for developing enantioselective Diels-Alder reactions and remote functionalizations of carbonyls with simple electrophiles or nucleophiles.<sup>22</sup> Achieving high levels of site- and stereo-selectivity represent the main challenges, since it requires the ability of the chiral aminocatalyst to control the stereochemical outcome and the selectivity at remote positions, many atoms apart from the

<sup>21</sup> Fuson, R. C. "The Principle of Vinylogy" *Chem. Rev.* **1934**, *16*, 1.

<sup>22</sup> a) Jurberg, I. D.; Chatterjee, I.; Tannert, R.; Melchiorre P. "When Asymmetric Aminocatalysis Meets the Vinylogy Principle" *Chem. Commun.* **2013**, *49*, 4869. b) Jiang, H.; Albrecht, Ł.; Jørgensen, K. A. "Aminocatalytic Remote Functionalization Strategies" *Chem. Sci.* **2013**, *4*, 2287.

anchoring point. This was mainly achieved linking an appropriate hydrogen-bonding directing group to the catalyst, or designing a conformationally rigid starting material.

The combination of the vinylogy principle with aminocatalysis, and the exploitation of its potential, will be widely discussed and analyzed in Chapters 2 and 3 of the present dissertation.

## 1.6 Photochemistry and organocatalysis

In 1912, Giacomo Ciamician remarked how the modern civilization should greatly focus on exploiting an inexhaustible energy source: sunlight. It is remarkable how apt his analysis was, even after more than a century from its expression.<sup>23</sup> Nowadays, the main sources of energy exploited by the modern society are the fossil fuels like petroleum and coal.<sup>24</sup> The growing attention of current environmental issues has led the scientific community to focus on renewable energy sources and in particular light. The energy of light is exploited by nature for a great number of biochemical processes, the most important being photosynthesis, responsible for the synthesis of carbohydrates from the endergonic reduction of CO<sub>2</sub> and oxidation of H<sub>2</sub>O.<sup>25</sup> In the past decade, the potential of photochemistry has been re-discovered and the branch of organic photochemistry, in particular photocatalysis, is currently of high interest with the development of new powerful methodologies and concepts covering all aspects of organic chemistry, including asymmetric catalysis.<sup>26</sup>

Upon light absorption, a chemical species undergoes an electronic transition and an excited state of the molecule is obtained. The excited-state molecule differs from the corresponding ground state not only in terms of energy content, but also in terms of electronic distribution. For this reason, the excited molecule should not be considered as a “hot” ground state molecule, but as a new chemical species, with an inherently different chemical and physical behavior.<sup>27</sup>

Excited molecules can undergo a number of peculiar physical and chemical processes, for instance electron transfer reactions, energy transfer to other molecules, isomerization, pericyclic reactions and rearrangements, processes that are inaccessible with traditional ground state chemistry.<sup>28</sup> As already explored by a number of research groups,<sup>29</sup> photochemistry could be successfully coupled to asymmetric aminocatalysis in order to achieve chemical transformations that the simple ground state of reactive intermediates of organocatalysis does not allow. The

---

<sup>23</sup> Ciamician, G. “The Photochemistry of the Future” *Science* **1912**, *36*, 385.

<sup>24</sup> [https://ec.europa.eu/energy/sites/ener/files/documents/2014\\_pocketbook.pdf](https://ec.europa.eu/energy/sites/ener/files/documents/2014_pocketbook.pdf)

<sup>25</sup> Voet, D.; Voet, J. G. “Photosynthesis” Chapter 24, p. 901 in *Biochemistry*, 4<sup>th</sup> edition **2011**, Wiley.

<sup>26</sup> Prier, C. K.; Rankic, D. A.; MacMillan, D. W. C. “Visible Light Photoredox Catalysis with Transition Metal Complexes: Applications in Organic Synthesis” *Chem. Rev.* **2013**, *113*, 5322.

<sup>27</sup> Balzani, V.; Ceroni, P.; Juris, A. “Excited states: Physical and Chemical Properties” Chapter 4, p. 103 in *Photochemistry and photophysics*, **2014**, Wiley-VCH.

<sup>28</sup> Coyle, J. D. *Introduction to Organic Photochemistry*, **1986**, Wiley.

<sup>29</sup> For a seminal example: Nicewicz, D. A.; MacMillan, D. W. C. “Merging Photoredox Catalysis with Organocatalysis: The Direct Asymmetric Alkylation of Aldehydes” *Science* **2008**, *322*, 77.

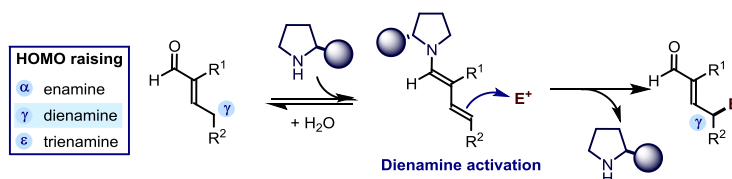
combination of two powerful methods of molecule activation, photochemistry and organocatalysis, has been extensively investigated within the course of the present research.

## 1.7 Objectives and summary of the present doctoral thesis

The main objective of the present doctoral thesis is the development of new catalytic methodologies in the field of aminocatalysis. The research studies have been divided in two main parts. First, enamine and iminium ion activation were successfully combined with the principle of vinylogy to develop new stereoselective remote functionalizations of carbonyl substrates. In the second part, the unexplored photochemical behavior of the active covalent intermediates of aminocatalysis has been explored upon direct light excitation of enamines and iminium ions. The resulting reactivity served to develop novel photochemical asymmetric organocatalytic reactions.

### 1.7.1 Vinylogous reactivity in aminocatalysis

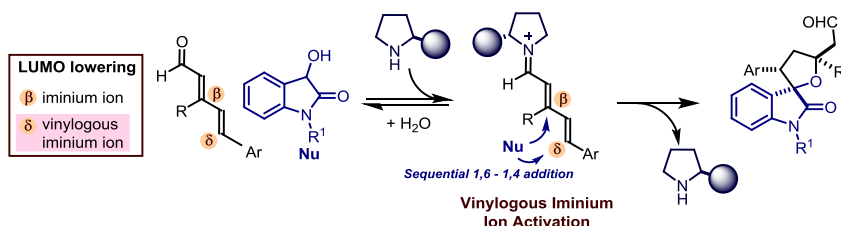
In Chapter II, a benchmark reaction in enamine mediated reactions, the  $S_N1$ -type alkylation of aldehydes with highly stabilized carbocations, has been used as a model reaction to demonstrate the feasibility of vinylogous reactivity in the context of a highly regio- and stereoselective  $\gamma$ -alkylation of  $\alpha,\beta$ -unsaturated aldehydes (Scheme 1.8).



**Scheme 1.8** – Asymmetric  $S_N1$ -type  $\gamma$ -alkylation of  $\alpha$ -branched dienals through dienamine activation. The Blue circle represents a bulky  $\alpha$ -substituent in the chiral aminocatalyst scaffold.

The reactive dienamine intermediate was successfully synthesized and a conformational analysis was carried out through NMR spectroscopic techniques in order to glean insights into the mechanism of stereinduction operated by the chiral aminocatalyst. The work was undertaken in collaboration with Carlo Cassani, who set up the first catalytic reaction, and Dr. Antonio Moran, who carried out computational studies on the reactive intermediate.

In Chapter III, the concept of vinylogy is further explored in the realm of iminium ion activation in order to regio- and stereo-selectively functionalize  $\alpha,\beta,\gamma,\delta$ -conjugated dienals. The stereoselective synthesis of highly valuable spirooxindoles were achieved through a sequence of 1,6-/1,4-conjugate additions (Scheme 1.9).



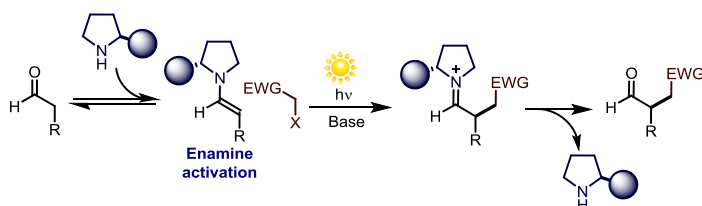
**Scheme 1.9** – Synthesis of spirooxindoles through vinyllogous iminium ion mediated cascade reaction.

The introduction of an opportune  $\beta$ -substituent on the dienal scaffold was crucial for obtaining both high regio- and stereo-selectivity. The vinyllogous iminium ion intermediate was successfully synthesized upon catalyst condensation with the dienal. A careful conformational analysis, carried out by NMR analysis, highlighted the importance of the peculiar conformation adopted by the chiral iminium ion for the stereochemical outcome of the reaction.

The work was undertaken in collaboration with Dr. Indranil Chatterjee, who set up the first catalytic reaction and carried out a part of the scope of the transformation, and with Yankai Liu, who helped with stimulating discussions.

### 1.7.2 The photochemistry of the covalent intermediates of aminocatalysis

In Chapter IV, the asymmetric aminocatalytic photochemical reaction of aldehydes with electron-poor alkyl halides is reported. The process proceeds through an open-shell mechanistic pathway. Interestingly, the reaction is fast and high yielding and occurs in the absence of external sensitizers, which are commonly needed to generate the radical intermediates.

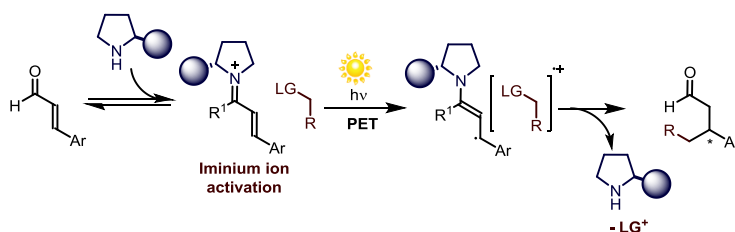


**Scheme 1.10** – Photochemical enamine mediated  $\alpha$ -alkylation of aldehydes with electron-poor alkyl halides. X = Br, I; EWG = Electron-withdrawing group.

Photophysical investigations revealed the direct involvement of the transiently formed chiral enamine in the photochemical activation event, highlighting the ability of this species to trigger the formation of the radical species. The work was undertaken in collaboration with Dr. Elena Arceo, who set up the first catalytic reaction, Dr. Igor Dias Jurberg, who evaluated most of the substrate scope, and Carlo Cassani, whose role was to investigate the vinyllogous reactivity of

dienals in this photochemical reaction. My role mainly focused on the elucidation of the mechanism of photoactivation and in expanding the activation mode with sulfone-derived alkyl halides.

In Chapter V, unprecedented photochemical stereoselective aminocatalytic  $\beta$ -alkylations of unsaturated carbonyl compounds are discussed. The chemistry exploits the transient generation of radical intermediates. Again the reaction does not rely upon the use of external photosensitizer, but it does employ the intrinsic photochemical tendency of iminium ions to participate in photoinduced electron transfer processes upon light excitation.



**Scheme 1.11** – Photochemical iminium ion  $\beta$ -alkylation of aldehydes. LG = leaving group

The choice of a readily fragmenting group (LG) within the reaction partner was crucial to modulate the redox potential of the donor and to reduce the competing (and synthetically unproductive) back electron transfer, a common drawback in photoinduced electron-transfer reactions. Notably, this strategy led to the development of an unprecedented  $\beta$ -alkylation of cinnamaldehyde.

## Chapter II

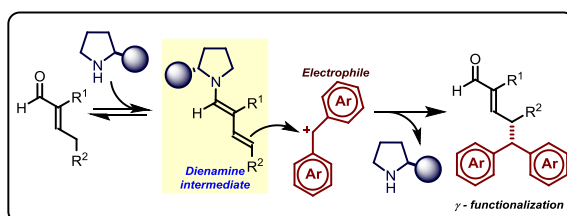
# Secondary Amine-Catalyzed Asymmetric $\gamma$ -Alkylation of $\alpha$ -Branched Enals via Dienamine Activation

### Target

The direct and enantioselective  $\gamma$ -alkylation of  $\alpha$ -substituted  $\alpha,\beta$ -unsaturated aldehydes proceeding under dienamine catalysis.

### Tool

Ability of diphenylprolinol silyl ether aminocatalysts to promote high yielding  $S_N1$ -type alkylation of  $\alpha$ -branched enals, while ensuring complete  $\gamma$ -site selectivity and high stereocontrol.<sup>1</sup>

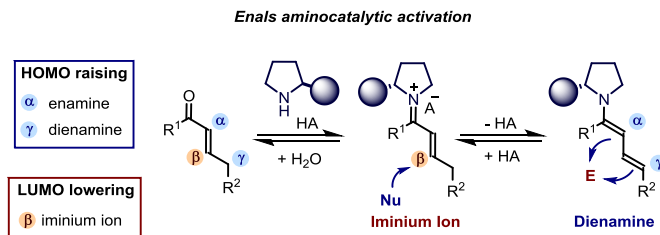


## 2.1 Introduction

Over the past decade, enamine and iminium-ion activations have become reliable synthetic platforms for generating stereogenic centers at the  $\alpha$ - and  $\beta$ -positions of carbonyl compounds with very high fidelity. These activation strategies have been extensively used for developing a wide variety of enantioselective catalytic methodologies, bringing the field of aminocatalysis to reach high levels of sophistication. At a certain time, because of the difficulties in finding new reactivities in an intensively explored field, the research community became interested in using aminocatalysis for targeting stereocenters remote from the catalyst's point of action. This was achieved by combining asymmetric aminocatalysis with the principle of vinylogy, which allowed to functionalize a carbonyl compound at distant positions. Key to success was the ability of the amine catalyst to propagate the electronic effects inherent to aminocatalytic reactivity modes (*i.e.* the HOMO-raising and the LUMO-lowering activating effects) through the conjugated  $\pi$ -system of poly-unsaturated carbonyls while transmitting the stereochemical information at distant positions.

<sup>1</sup> The work discussed in this chapter has been published in a special issue celebrating the 75<sup>th</sup> birthday of Prof. Dr. Dieter Seebach, see: Silvi, M.; Cassani, C.; Moran, A.; Melchiorre, P. "Secondary Amine-Catalyzed Asymmetric  $\gamma$ -Alkylation of  $\alpha$ -Branched Enals via Dienamine Activation" *Helv. Chim. Acta* **2012**, *95*, 1985.

In particular, the condensation of a secondary amine with an enal compound induces vinylogous nucleophilicity resulting in extended enamines, activating the remote  $\gamma$ -carbon position towards electrophiles (Scheme 2.1).



Such activation, known as dienamine activation, is expected to be rather intricate considering the established ability of the aminocatalyst to activate the  $\beta$ -position of the enal towards the addition of nucleophiles through iminium ion activation and the bidentate nucleophilic nature of the dienamine intermediate, which could lead to regioselectivity issues.

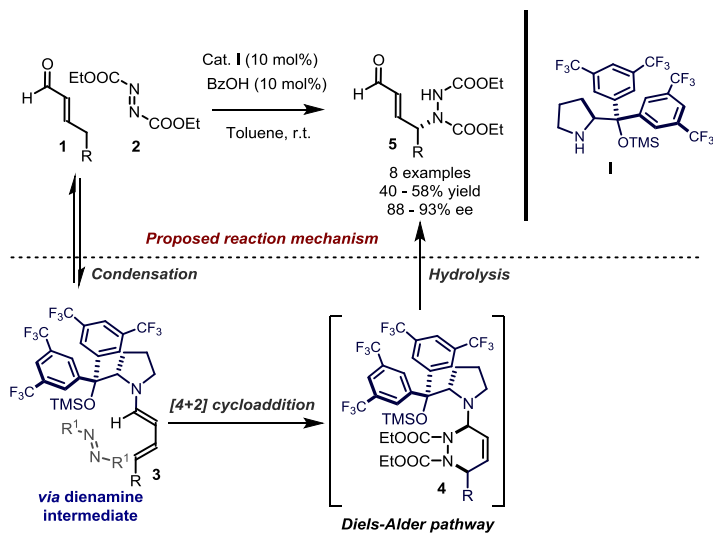
### 2.1.1 Dienamine activation in organocatalysis

Organocatalytic dienamine activation was firstly introduced by Jørgensen *et al.* who successfully developed a secondary amine catalyzed  $\gamma$ -regioselective asymmetric amination of enals (Scheme 2.2).<sup>2</sup> Mixing the diaryl-prolinol silyl ether aminocatalyst **I**, pentenal (**1**), and benzoic acid, the authors observed the formation of a dienamine intermediate through <sup>1</sup>H NMR spectroscopy. This observation led to the idea of exploiting the intrinsic nucleophilicity of this species for achieving remote functionalizations.

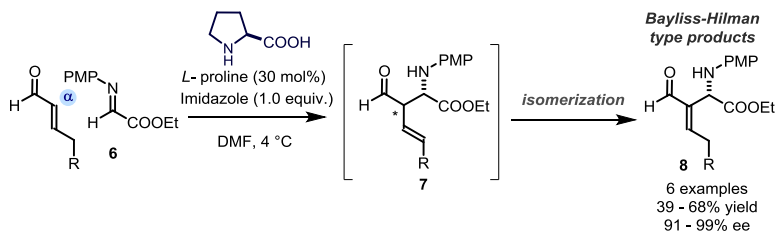
On the basis of the absolute configuration of the final product **5** and theoretical calculations, the reaction was proposed to proceed *via* a [4+2] cycloaddition pathway and subsequent hydrolysis of the cyclic emiaminal **4** (Scheme 2.2). The proposed mechanism is consonant with the well-known high reactivity of dienamine species towards Diels-Alder pathways.<sup>3</sup>

<sup>2</sup> Bertelsen, S.; Marigo, M.; Brandes, S.; Dinér, P.; Jørgensen, K. A. "Dienamine Catalysis: Organocatalytic Asymmetric  $\gamma$ -Amination of  $\alpha,\beta$ -Unsaturated Aldehydes" *J. Am. Chem. Soc.* **2006**, *128*, 12973.

<sup>3</sup> For examples of Diels-Alder reactions on stoichiometric dienamines: a) Wu, T.; Houk, T. N. "Intramolecular Diels-Alder Reactions of Dienamines with Acrylates: Trends in Stereoselectivity Upon Substitution" *Tetrahedron Lett.* **1985**, *26*, 2293. b) Snowden, R. L.; Wüst, M. "Dienamines as Diels-Alder Dienes. An Efficient Cyclohexannulation Sequence" *Tetrahedron Lett.* **1986**, *27*, 699.



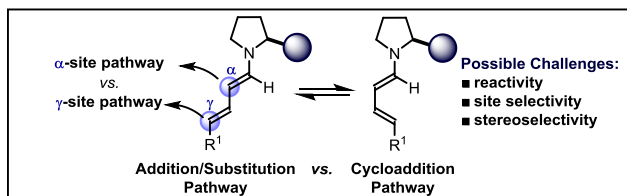
In spite of its potential, dienamine catalysis initially found limited application. This was probably because the  $\gamma$ -amination of unsaturated aldehydes **1** followed a [4+2] cycloaddition path, instead of a more general nucleophilic addition pathway. Moreover, initial studies suggested that chiral secondary amines, such as proline and its derivatives, activated  $\gamma$ -enolizable unsaturated aldehydes toward the formation of the dienamine intermediate, but generally promoted  $\alpha$ -site selective alkylation *via* an enamine pathway in the presence of suitable electrophiles (Scheme 2.3).<sup>4</sup>



$\gamma$ -Site selective transformation based on dienamine activation remained limited to few examples due to the many challenges offered by this activation mode (Scheme 2.4).

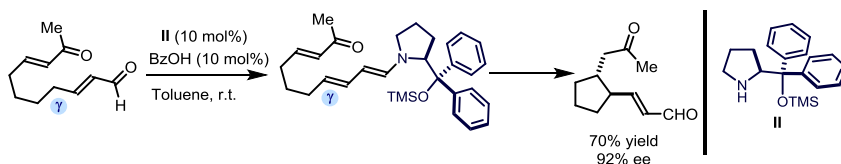
<sup>4</sup> Utsumi, N.; Zhang, H.; Tanaka, F.; Barbas III, C. F. "A Way to Highly Enantiomerically Enriched aza-Morita-Baylis-Hillman-Type Products" *Angew. Chem. Int. Ed.* **2007**, *46*, 1878.





Scheme 2.4 Designing vinylogous processes by means of dienamine activation: challenges.

The first use of dienamine activation in a direct nucleophilic  $\gamma$ -addition was successfully reported by Christmann in 2008, as a single isolated example within the framework of a [4+2] type reaction of  $\alpha,\beta$ -unsaturated aldehydes (Scheme 2.5). In this case, the tendency to form a thermodynamically favored five membered ring over higher energy structures completely directed the regioselectivity of the reaction, which proceeded with high efficiency.<sup>5</sup>

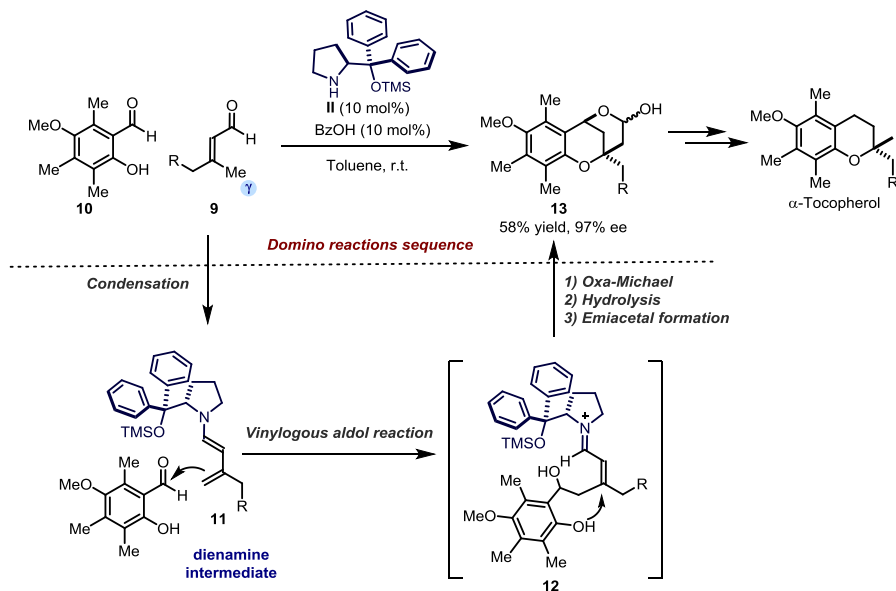


Scheme 2.5 – Dienamine-mediated intramolecular asymmetric  $\gamma$ -regioselective conjugate addition.

$\gamma$ -Regioselectivity could be achieved in specific cascade processes. In 2008, the group of Woggon developed a short and efficient synthetic route to  $\alpha$ -tocopherol based on a  $\gamma$ -regioselective aldol reaction through a dienamine intermediate (Scheme 2.6).<sup>6</sup> The highly reactive terminal dienamine **11**, formed upon condensation of catalyst **II** with the  $\beta$ -methyl substituted enal **9**, was responsible for the initial step in a domino sequence. This report provided a powerful annulation strategy while also demonstrating the potential of dienamine activation to streamline the total synthesis of natural compounds.

<sup>5</sup> De Figueiredo, R. M.; Fröhlich, R.; Christmann, M. "Amine-Catalyzed Cyclizations of Tethered  $\alpha,\beta$ -Unsaturated Carbonyl Compounds" *Angew. Chem. Int. Ed.* **2008**, *47*, 1450.

<sup>6</sup> Liu, K.; Chougnat, A.; Woggon, W.-D. "A Short Route to  $\alpha$ -Tocopherol" *Angew. Chem. Int. Ed.* **2008**, *47*, 582.



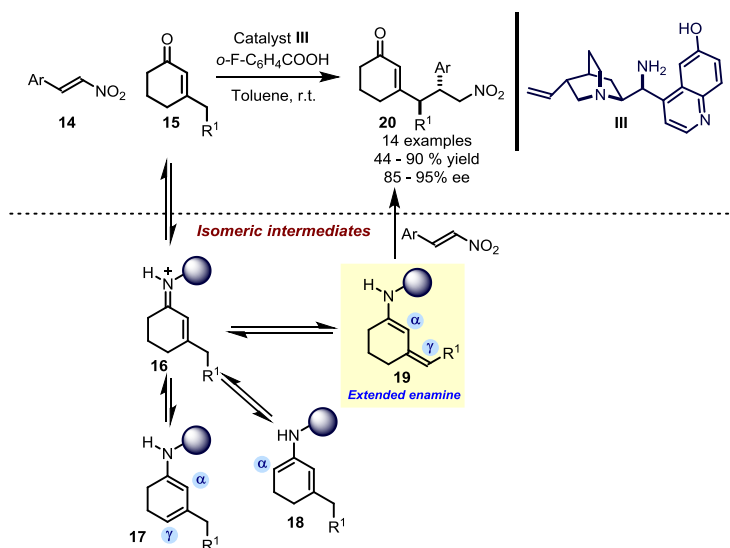
Scheme 2.6 – Organocatalytic short route to  $\alpha$ -Tocopherol.

In 2010, our research group reported an intermolecular example of dienamine-mediated reaction of various Michael acceptors with cyclohexenones. The reaction was catalyzed by the *Cinchona* alkaloid derivative III (Scheme 2.7).<sup>7</sup> Key to reaction development was the unique ability of the cinchona-derived amine catalyst III, in combination with an acidic cocatalyst, to perturb the iminium-enamine equilibrium leading to the selective formation of the extended dienamine 19 (responsible for the formation of products 20) over the *endo*-isomer 17 or the cross-conjugated dienamine 18.

Interestingly, in sharp contrast, the employment of a chiral secondary amine, in the presence of the same reagent combination, induced the formation of the crossed-conjugated dienamine 18, catalyzing a Diels-Alder-type reaction pathway.<sup>8</sup>

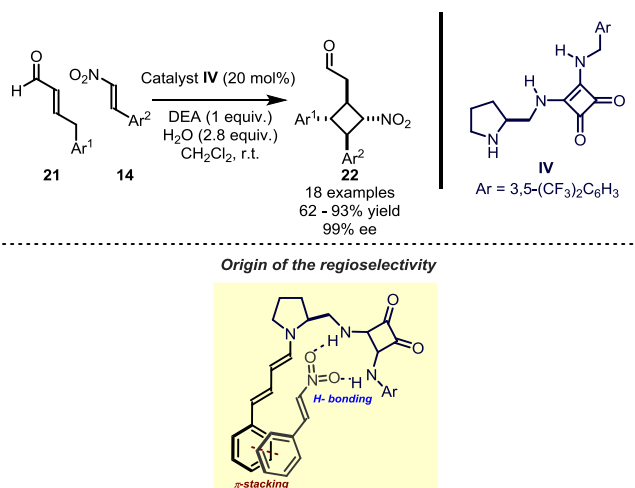
<sup>7</sup> Bencivenni, G.; Galzerano, P.; Mazzanti, A.; Bartoli, G.; Melchiorre, P. "Direct Asymmetric Vinylogous Michael Addition of Cyclic Enones to Nitroalkenes via Dienamine Catalysis" *Proc. Natl. Acad. Sci. U. S. A.* **2010**, *107*, 20642.

<sup>8</sup> Xu, D.-Q. Xia, A.-B.; Luo, S.-P.; Tang, J.; Zhang, S.; Jiang, J.-R.; Xu, Z.-Y "In Situ Enamine Activation in Aqueous Salt Solutions: Highly Efficient Asymmetric Organocatalytic Diels-Alder Reaction of Cyclohexenones with Nitroolefins" *Angew. Chem. Int. Ed.* **2009**, *48*, 3821.



Scheme 2.7 – Dienamine-promoted vinylogous Michael addition reaction.

An elegant example of how the catalyst scaffold can direct the approach of an electrophile towards the  $\gamma$ -position of a dienamine intermediate was reported by Jørgensen *et al.* in 2012. When mixing dienals and  $\beta$ -nitrostyrene **14** in the presence of catalyst **IV**, cyclobutanes **22** were formed in high yield and complete stereoselectivity (Scheme 2.8).<sup>9</sup>

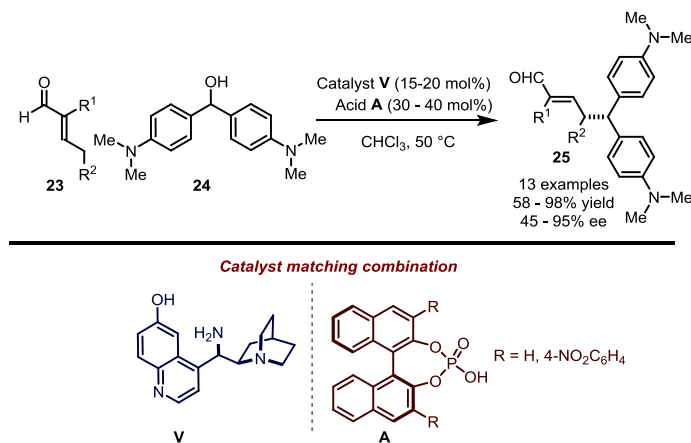


Scheme 2.8 – Dienamine-mediated formal [2+2] cycloaddition. DEA: diethyl acetamide.

<sup>9</sup> Albrecht, Ł.; Dickmeiss, G.; Acosta, F. C.; Rodríguez-Esrich, C.; Davis, R. L.; Jørgensen, K. A. "Asymmetric Organocatalytic Formal [2 + 2]-Cycloadditions via Bifunctional H-Bond Directing Dienamine Catalysis" *J. Am. Chem. Soc.* **2012**, *134*, 2543.

On the basis of computational studies, the authors proposed the involvement of a complex net of interactions between the dienamine intermediate and  $\beta$ -nitrostyrene **14** to rationalize the observed reactivity, regioselectivity and stereoselectivity.

In 2011, our research group envisioned to control the regioselectivity of dienamine-mediated reactions by opportunely introducing substituents in the  $\alpha$ -position of the enal scaffold. The aim was to induce a steric bias and direct the electrophile attack towards the  $\gamma$ -position (Scheme 2.9).<sup>10</sup> This strategy was successfully employed for the development of a  $\gamma$ -selective version of  $S_N1$ -type alkylation of aldehydes, a reaction discussed in details in paragraph 2.1.2.



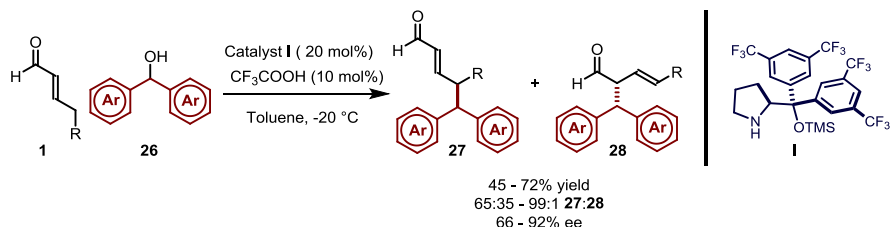
**Scheme 2.9** – Primary amine catalyzed asymmetric  $\gamma$ -alkylation of  $\alpha$ -branched dienal.

The introduction of an alkyl substituent in  $\alpha$ -position to an enal (**23**) was crucial to obtain complete regioselectivity, leading to corresponding  $\gamma$ -functionalized compounds **25**. Finding the opportune combination of chiral amine **V** and phosphoric acid **A** was pivotal for obtaining the desired products in high yield and stereoselectivity.

The importance of enal  $\alpha$ -substitution for achieving high regioselectivity was further evidenced by a work published by Christmann *et al.* in 2012. The group reported that linear enals **1** are reactive towards an analogous transformation as in Scheme 2.9 under secondary amine catalysis (Scheme 2.10).<sup>11</sup> Despite a high stereoselectivity was generally obtained in this transformation, a poor regioselectivity was usually observed and the corresponding  $\gamma$ -adducts **27** were usually isolated in low yields.

<sup>10</sup> Bergonzini, G.; Vera, S.; Melchiorre, P. "Cooperative Organocatalysis for the Asymmetric  $\gamma$  Alkylation of  $\alpha$ -Branched Enals" *Angew. Chem. Int. Ed.* **2010**, *49*, 9685.

<sup>11</sup> Stiller, J.; Marque, E.; Marqués-Lopez, E.; Herrera, R. P.;Fröhlich, R.; Strohmman, C.; Christmann, M. "Enantioselective  $\alpha$ - and  $\gamma$ -Alkylation of  $\alpha,\beta$ -Unsaturated Aldehydes Using Dienamine Activation" *Org. Lett.* **2011**, *13*, 70.



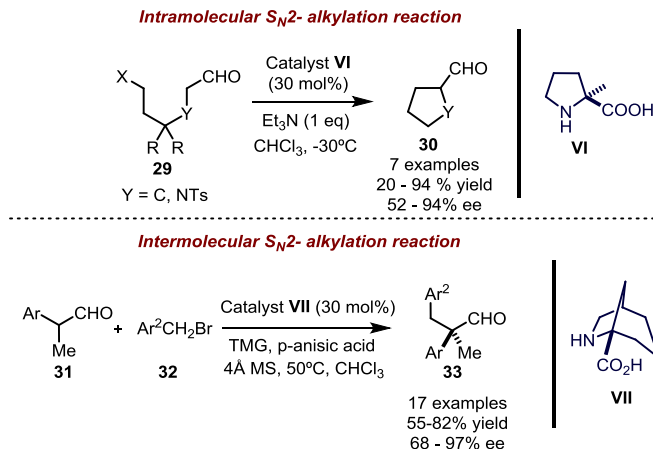
**Scheme 2.10** –  $S_N1$ -type  $\alpha$ -alkylation of aldehydes. Highly stabilized carbocations are generated *in situ* from acid-catalyzed dehydration of benzhydrols.

The transformations depicted in Scheme 2.9 and 2.10 are examples of  $S_N1$ -type alkylation of dienamines with stabilized carbocations, a benchmark reaction developed for enamine mediated  $\alpha$ -functionalization of aldehydes.

### 2.1.2 $S_N1$ -type alkylation of aldehydes

Despite the alkylation of stoichiometric enamines could be considered a milestone in organic chemistry and is well-known for more than 50 years,<sup>12</sup> a general catalytic, enamine-mediated stereoselective  $\alpha$ -alkylation of aldehydes remains a difficult target to achieve.

Only a couple of examples of  $S_N2$ -type reactions have been published by the group of List, albeit with rather limited scope (Scheme 2.11).<sup>13,14</sup>



**Scheme 2.11** – Examples of  $S_N2$ -type asymmetric catalytic  $\alpha$ -alkylation of aldehydes, a challenging reaction. TMG = tetramethyl guanidine, Ts = -tosyl, MS = molecular sieves.

<sup>12</sup> Stork, G.; Brizzolara, A.; Landesman, H.; Szmuszko, J.; Terrell, R. J. "The Enamine Alkylation and Acylation of Carbonyl Compounds" *J. Am. Chem. Soc.* **1963**, *85*, 207.

<sup>13</sup> Vignola, N.; List, B. "Catalytic Asymmetric Intramolecular  $\alpha$ -Alkylation of Aldehydes" *J. Am. Chem. Soc.* **2004**, *126*, 450.

<sup>14</sup> List, B.; Coric, I.; Grygorenko, O. O.; Kaib, P. S. J.; Komarov, I.; Lee, A.; Leutsch, M.; Chandra Pan, S.; Tyntsunikm, A. V.; Van Gemmeren, M. "The Catalytic Asymmetric  $\alpha$ -Benzoylation of Aldehydes" *Angew. Chem. Int. Ed.* **2014**, *53*, 282.

The lack of general procedures based on  $S_N2$ -type alkylation strategy is thought to be connected to the occurrence of side reactions, *e.g.* deactivation of aminocatalyst due to *N*-alkylation.

The difficulties in developing effective methods for  $S_N2$ -type alkylation chemistry prompted the aminocatalysis community to evaluate alternative strategies to develop the enantioselective  $\alpha$ -alkylation of aldehydes, including the combination of enamine activation with radical or cationic  $S_N1$ -type reaction pathways.<sup>15</sup> The extensive studies by Herbert Mayr on the reactivity of  $\pi$ -nucleophiles indicate that enamines are highly nucleophilic compounds, strong enough to engage in productive reaction pathways with highly stabilized carbocations.<sup>16,17</sup>

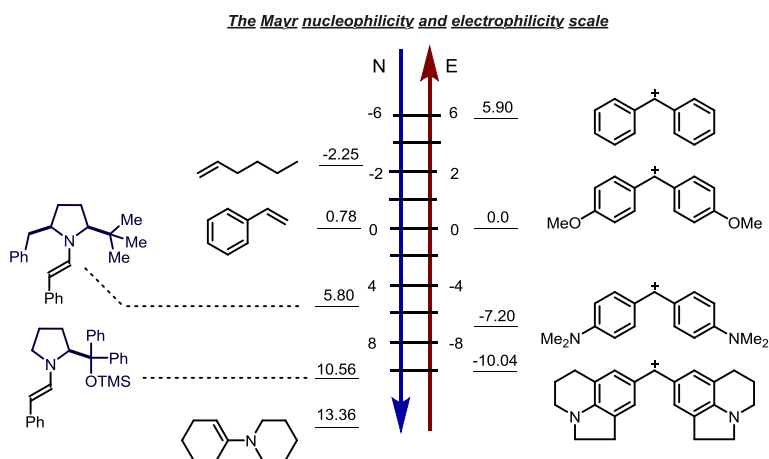


Figure 2.1 – The Mayr nucleophilicity and electrophilicity scale.

The Mayr scale quantitatively defines nucleophilicity and electrophilicity of organic compounds. In the representation in Figure 2.1, nucleophiles at the top do not react with the electrophiles at the bottom, while nucleophiles at the bottom react with the electrophiles at the top with diffusion control.

In particular, the relationship reported in eq. (1) quantitatively defines the kinetic constant for the bimolecular reaction between the two partners.

$$(1) \quad \log k = s (N + E)$$

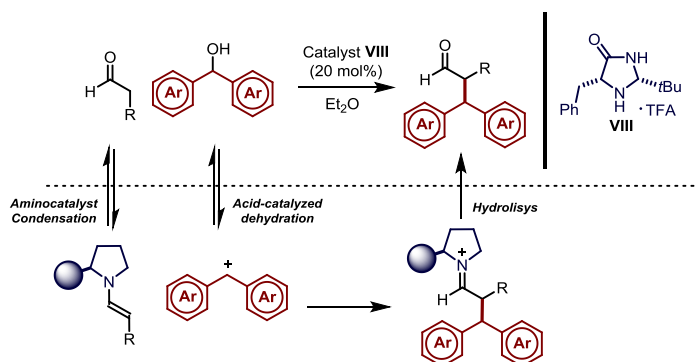
<sup>15</sup> For a review: Vesely, J.; Rios, R. "Organocatalytic Enantioselective  $\alpha$ -Alkylation of Aldehydes" *ChemCatChem* **2012**, *4*, 942.

<sup>16</sup> For a review: Mayr, H.; Kempf, B.; Ofial, A. R. " $\pi$ -Nucleophilicity in Carbon–Carbon Bond-Forming Reactions" *Acc. Chem. Res.* **2003**, *36*, 66.

<sup>17</sup> For a quantitative study of the nucleophilicity of transient enamines formed in organocatalysis: Lakhdar, S.; Maji, B.; Mayr, H. "Imidazolidinone-Derived Enamines: Nucleophiles with Low Reactivity" *Angew. Chem. Int. Ed.* **2012**, *51*, 5739.

The parameters  $N$  and  $s$  are correlated to the nature of the nucleophile employed, whereas the parameter  $E$  quantitatively describes the reactivity of the electrophile considered. Equation (1) is not only useful because it defines a quantitative scale of reactivity for organic compounds, but also because it can predict whether a reaction will occur or not. The “rule of thumb” of Mayr defines that electrophiles are expected to react with nucleophiles at room temperature when  $E + N > -5$ . Considering the high  $N$  value of enamines, the rule of thumb of Mayr will be favorable to most of the reactions between these species and carbocationic species.

In 2009, the group of Cozzi reported a remarkable enamine mediated  $S_N1$ -type asymmetric  $\alpha$ -alkylation of aldehydes with stabilized carbocations (Scheme 2.12).<sup>18</sup>



**Scheme 2.12** –  $S_N1$ -type  $\alpha$ -alkylation of aldehydes. Highly stabilized carbocations are generated *in situ* from acid-catalyzed dehydration of benzhydrols.

Inspired by this pioneering work, many examples of enamine-mediated enantioselective  $S_N1$ -type alkylations of aldehydes were reported.<sup>19</sup>

## 2.2 Target of the project

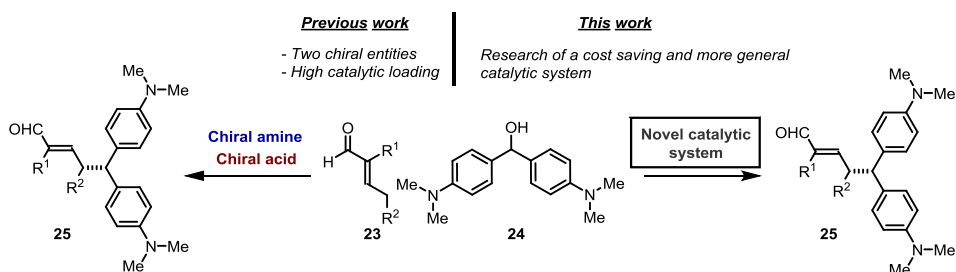
Although the catalytic system in Scheme 2.9 leads to high efficient and stereoselective  $\gamma$ -alkylation of enals, it involves the employment of two chiral entities in rather high catalytic loading.<sup>10</sup> In this dual-catalyst system, the enantioselectivity was found to be significantly higher when a chiral phosphoric acid was used in place of an achiral cocatalyst such as trifluoroacetic

<sup>18</sup> Cozzi, P. G.; Benfatti, F.; Zoli, L. “Organocatalytic Asymmetric Alkylation of Aldehydes by  $S_N1$ -Type Reaction of Alcohols” *Angew. Chem. Int. Ed.* **2009**, *48*, 1313.

<sup>19</sup> a) Capdevila, M. G.; Benfatti, F.; Zoli, L.; Stenta, M.; Cozzi, P. G. “Merging Organocatalysis with an Indium(III)-Mediated Process: A Stereoselective  $\alpha$ -Alkylation of Aldehydes with Allylic Alcohols” *Chem. Eur. J.* **2010**, *16*, 11237. b) Benfatti, F.; Capdevila, M. G.; Zoli, L.; Benedetto, E.; Cozzi, P. G. “Catalytic Stereoselective Benzylic C–H Functionalizations by Oxidative C–H Activation and Organocatalysis” *Chem. Commun.* **2009**, 5919. c) Brown, A. R.; Kuo, W.-H.; Jacobsen, E. N. “Enantioselective Catalytic  $\alpha$ -Alkylation of Aldehydes via an  $S_N1$  Pathway” *J. Am. Chem. Soc.* **2010**, *132*, 9286. d) Gualandi, A.; Emer, E.; Capdevila, M. G.; Cozzi, P. G. “Highly Enantioselective  $\alpha$  Alkylation of Aldehydes with 1,3-Benzodithiolium Tetrafluoroborate: A Formal Organocatalytic  $\alpha$  Alkylation of Aldehydes by the Carbenium Ion” *Angew. Chem. Int. Ed.* **2011**, *50*, 7842.

acid, thus indicating that the intrinsic potential of the chiral primary amine to forge the  $\gamma$  stereogenic center, by means of dienamine activation, was moderate.

In order to develop a more efficient synthetic platform for dienamine mediated reactions, we envisioned the design of a new catalytic system in which only one chiral entity was required: the aminocatalyst. As a model reaction, again, we chose the  $S_N1$ -type alkylation of enals **23** with activated benzhydrols **24** (Scheme 2.13).



**Scheme 2.13** – Target of the project: development of a general, cost-saving and efficient synthetic platform for  $\gamma$ -alkylation of aldehydes.

## 2.3 Results and discussion

### 2.3.1 Optimization studies

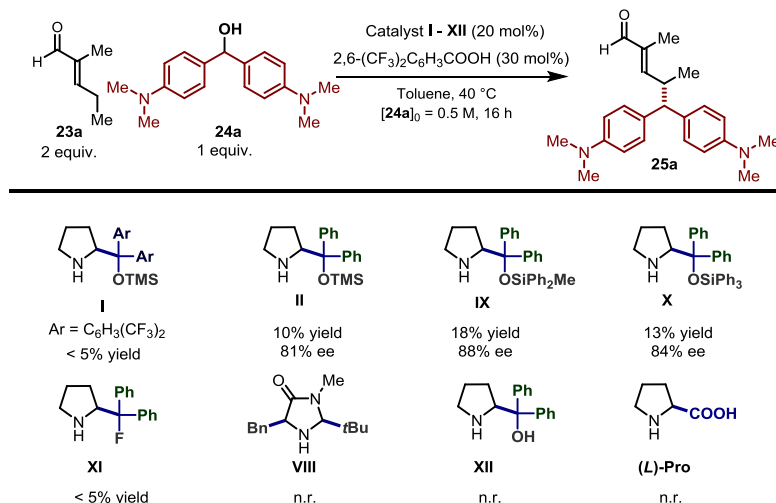
We started out our optimization studies seeking an efficient aminocatalyst for the desired transformation.  $\alpha$ -Branched enals **23** have been used in asymmetric organocatalysis prevalently under iminium ion activation.<sup>20</sup> Chiral primary amines were usually employed as catalysts, likely due to the difficult condensation of secondary amines with these rather bulky substrates. Nevertheless, our preliminary experiments led us to an unexpected observation: the commercially available secondary amine diphenylprolinol silyl ether **II** (the so-called Jørgensen-Hayashi catalyst) could indeed catalyze the process with full regioselectivity.<sup>21</sup> Several chiral secondary amines were tested in the reaction; selected results are reported in Scheme 2.14.

<sup>20</sup> For selected examples: a) Ishihara, K.; Nakano, K. "Design of an Organocatalyst for the Enantioselective Diels-Alder Reaction with  $\alpha$ -Acyloxyacroleins" *J. Am. Chem. Soc.* **2005**, *127*, 10504. b) Ishihara, K.; Nakano, K. "Enantioselective [2 + 2] Cycloaddition of Unactivated Alkenes with  $\alpha$ -Acyloxyacroleins Catalyzed by Chiral Organoammonium Salts" *J. Am. Chem. Soc.* **2007**, *129*, 8930. c) Galzerano, P.; Pescioli, F.; Mazzanti, F.; Bartoli, G.; Melchiorre, P. "Asymmetric Organocatalytic Cascade Reactions with  $\alpha$ -Substituted  $\alpha,\beta$ -Unsaturated Aldehydes" *Angew. Chem. Int. Ed.* **2009**, *48*, 7892. d) Erkkilä, A.; Pihko, P. M.; Clarke, M.-R. "Simple Primary Anilines as Iminium Catalysts for the Epoxidation of  $\alpha$ -Substituted Acroleins" *Adv. Synth. Catal.* **2007**, *349*, 802. e) Lifchits, O.; Reisinger, C.; List, B. "Catalytic Asymmetric Epoxidation of  $\alpha$ -Branched Enals" *J. Am. Chem. Soc.* **2010**, *132*, 10227.

<sup>21</sup> Hayashi, Y.; Gotoh, H.; Hayashi, T.; Shoji, M. "Diphenylprolinol Silyl Ethers as Efficient Organocatalysts for the Asymmetric Michael Reaction of Aldehydes and Nitroalkenes" *Angew. Chem. Int. Ed.* **2005**, *44*, 4212.



The observed regioselectivity control is another evidence of the crucial importance of the  $\alpha$ -substitution on the enal scaffold, as the employment of linear unsaturated aldehydes and analogous secondary aminocatalysts in the same reaction led to mixture of both  $\alpha$ - and  $\gamma$ -functionalized products, as already detailed in Scheme 2.10.<sup>11</sup>



**Scheme 2.14** – Secondary amines tested in the model reaction. Reactions performed at 40 °C on a 0.1 mmol scale, without any precaution for excluding air. Yield determined by <sup>1</sup>H NMR analysis of the crude reaction mixture using 1,3,5-trimethoxybenzene as the internal standard. Enantiomeric excess determined by HPLC analysis on a chiral stationary phase. n.r. = no reaction.

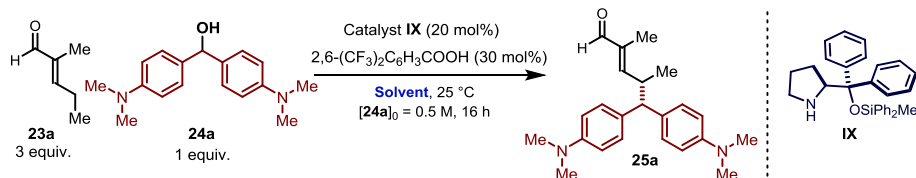
Gratifyingly, both reactivity and stereocontrol were sensitive to catalyst structural modifications, the bulkier silyl protective group of the catalyst leading to a significant improvement (compare the results obtained with catalyst IX and II). Catalyst IX was first reported by Seebach *et al.*, who predicted, based on X-ray crystallographic analysis, a more effective shielding of the chiral fragment over the pro-chiral face of the reactive intermediate, in comparison with the standard trimethylsilyl group within the catalyst II.<sup>22</sup> Further increasing the steric hindrance of the pendant silyl group did not provide higher stereoselectivity (catalyst X). Interestingly, other widely employed chiral secondary amines (proline or the second-generation MacMillan catalyst VIII) were not able to promote this transformation. Thus, the chiral amine IX was selected for further investigations.

Examination of the reaction media, detailed in Table 2.1 (reactions performed at 25 °C), revealed that solvents with a high polarity strongly increased the reactivity (a correlation between reaction yield and solvent dielectric constant was observed) but at the expense of the

<sup>22</sup> Although Seebach's study concerned iminium ion activation, we speculated that an analogous increased shielding effect on the prochiral face of enamine intermediates could be operative: Seebach, D.; Großelj, U.; Badine, D. M.; Schweizer, W. B.; Beck, A. K. "Isolation and X-Ray Structures of Reactive Intermediates of Organocatalysis with Diphenylprolinol Ethers and with Imidazolidinones" *Helv. Chim. Acta* **2008**, *91*, 1999.

enantioselectivity. The employment of strongly apolar solvents was found to be crucial in order to obtain high enantioselectivity (Table 2.1).

Table 2.1 – Reaction media screening.



entry	Solvent	Dielectric constant ( $\epsilon$ ) <sup>23</sup>	Yield (%)	ee (%)
1	Hexane	2.0	5	87
2	Toluene	2.4	5	94
3	Diethyl ether	4.0	11	77
4	Chloroform	5.0	10	81
5	Dichloromethane	9.1	18	81
6	Acetonitrile	36	46	78

Reactions carried out on a 0.1 mmol scale. Yield determined by <sup>1</sup>H NMR analysis of the crude reaction mixture using 1,3,5-trimethoxybenzene as the internal standard. Enantiomeric excess determined by HPLC analysis on a chiral stationary phase.

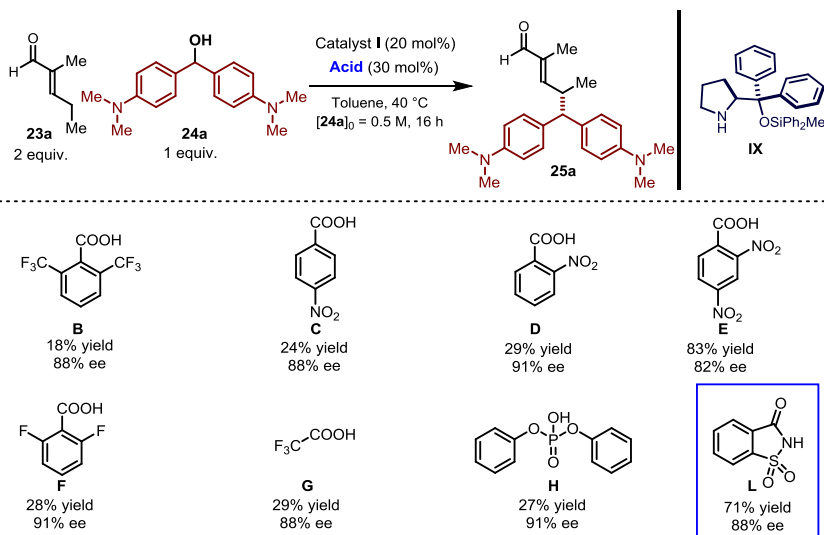
Encouraged by the high enantioselectivity obtained using toluene, we attempted improving the reaction efficiency slightly modifying the reaction parameters. Increasing the reaction temperature to 40 °C and modifying the nature of the acidic additive was found to be crucial for obtaining better chemical yields (Scheme 2.15).

The intrinsic acidity of the acidic additive was strictly correlated to the reaction efficiency. Comparing the results among the homologous acidic additives **C** - **E** ( $pK_a$  (DMSO) = 9.04; 8.18; 6.72, respectively),<sup>24</sup> it becomes apparent that moderately high acidity was required to obtain higher yields. Less acidic carboxylic acids (**F**,  $pK_a$  (DMSO) = 8.59) or highly acidic trifluoroacetic acid (**G**,  $pK_a$  (H<sub>2</sub>O) = 0.52)<sup>25</sup> led to worst results. The decrease of reactivity could also be due to the hydrolysis of the silyl ether moiety of catalyst **IX**, which could be hydrolyzed under highly acidic conditions or to full protonation of the aminocatalyst.

<sup>23</sup> Anslyn, E. V.; Dougherty, D. A. "Solutions and Non-Covalent Binding Forces" Chapter 3, p. 147 in *Modern Physical Organic Chemistry*, 2006, University Science Book.

<sup>24</sup> Jover, J.; Bosque, R.; Sales, J. "QSPR Prediction of  $pK_a$  for Benzoic Acids in Different Solvents" *QSAR Comb. Sci.* 2008, 27, 563.

<sup>25</sup> Anslyn, E. V.; Dougherty, D. A. "Acid-Base Chemistry" Chapter 5, p. 278 in *Modern Physical Organic Chemistry*, 2006, University Science Books.



**Scheme 2.15** – Acidic additives tested in the model reaction. Reactions carried out on a 0.1 mmol scale. Yield determined by <sup>1</sup>H NMR analysis of the crude reaction mixture using 1,3,5-trimethoxybenzene as the internal standard. Enantiomeric excess determined by HPLC analysis on a chiral stationary phase.

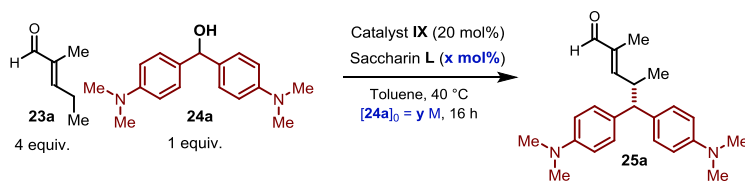
The rather acidic additive saccharin **L** ( $pK_a$  (DMSO) = 3.81)<sup>26</sup> was identified as the most promising additive towards the design of an effective amine **IX**-based catalytic system.

A final cycle of optimization with 20 mol% of the catalyst **IX** in toluene established a 2:1 saccharin/amine ratio as the most effective combination, while revealing that the reagent concentration was also crucial for modulating the efficiency (Table 2.2).

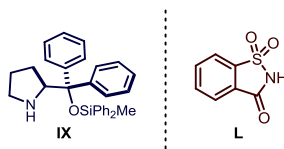
Carrying out the reaction at 40 °C with an excess of enal **23a** (4 equiv.) while diluting the mixture ([**24a**] = 0.25 M) provided the product **25a** with synthetically useful results over a 25-hour reaction time (entry 8: **25a** isolated in 88% yield and 93% ee).

<sup>26</sup> Christ, P.; Lindsay, A. G.; Vormittag, S. S.; Neudörfl, J.-M.; Berkessel, A.; Donoghue, A.-M. C. O. "pKa Values of Chiral Brønsted Acid Catalysts: Phosphoric Acids/Amides, Sulfonyl/Sulfuryl Imides, and Perfluorinated TADDOLs (TEFDDOLs)" *Chem. Eur. J.* **2011**, *17*, 8524.

**Table 2.2** – Final optimization cycle.



**Catalyst combination**



entry	Saccharin L (x mol%)	[24a] = y (M)	t (h)	Yield (%)	ee (%)
1 <sup>a</sup>	30	0.5	16	71	88
2	30	0.5	16	83	92
3	20	0.5	16	45	95
4	40	0.5	16	93	91
5	40	0.15	16	44	96
6	75	0.15	16	54	95
7	40	0.25	16	81	94
8	<b>40</b>	<b>0.25</b>	<b>25</b>	<b>88<sup>b</sup></b>	<b>93</b>

Reactions carried out on a 0.1 mmol scale. Yield determined by <sup>1</sup>H NMR analysis of the crude reaction mixture using 1,3,5-trimethoxybenzene as the internal standard. Enantiomeric excess determined by HPLC analysis on a chiral stationary phase. <sup>a</sup>Reaction carried out with 2 equiv. of **23a**. <sup>b</sup>Yield of the isolated product after flash column chromatography on silica gel.

With the optimized conditions in hand, we evaluated the scope of the secondary amine catalyzed  $\gamma$ -alkylation of  $\alpha$ -branched enals.

## 2.3.2 Reaction scope

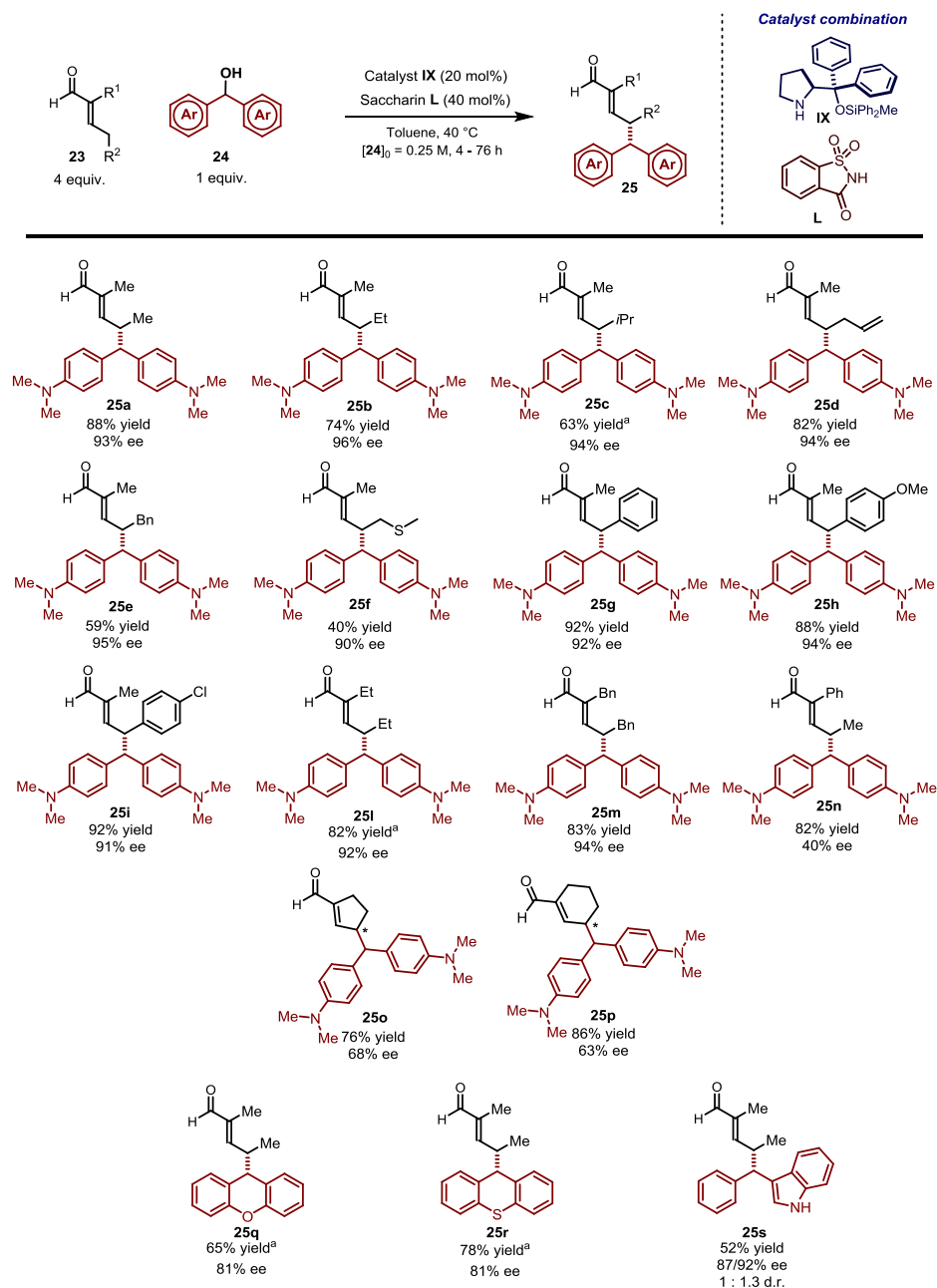


**Figure 2.2** – Reaction scope. Reactions carried out on a 0.1 mmol scale. <sup>a</sup>The standard procedure was slightly modified, see experimental section for further details.

As shown in Figure 2.2, different alkyl substituents, including a heteroatom-containing moiety, could be accommodated at the enal  $\gamma$ -position without affecting either the site-selectivity or the enantioselectivity of the process (compounds **25a-25m**). Furthermore,  $\gamma$ -aryl substituted enals were competent substrates for this catalytic system, showing an increased reactivity (compounds **25g-25i**). For these substrates, the  $\gamma$ -alkylation protocol opened a direct access to enantiomerically enriched benzylic stereogenic centers. Different aliphatic substituents at the  $\alpha$ -position of the enals were well-tolerated, enabling access to a broad variety of multifunctional molecules with complete  $\gamma$ -site selectivity and high levels of enantioselectivity (compounds **25l** and **25m**). As a limitation of the system, 2-phenylpent-2-enal, bearing a phenyl group at the  $\alpha$ -position, reacted smoothly providing the corresponding product with a modest level of stereocontrol (40% ee; compound **25n**).

We also explored the possibility of extending chiral secondary-amine-induced vinylogous nucleophilicity to cyclic  $\alpha$ -branched enals. The protocol developed for the linear substrates can be translated to cyclopent-1-ene-1-carboxaldehyde and cyclohex-1-ene-1-carboxaldehyde, maintaining a good level of reactivity but with moderate stereoselectivity (compounds **25o**, **25p**). Notably, the five-membered substrate proved very reactive, the reaction reaching completion over 4 h (**25o**).

To further delineate the reaction scope, we tested other benzylic alcohol able to generate stable carbocations through acid-catalyzed ionization. The  $\gamma$ -alkylated products **25q**, **25r**, and **25s** were obtained with synthetically meaningful results. Remarkably, an indole-containing compound **25s** could be synthesized, albeit it was obtained with low diastereoselectivity.

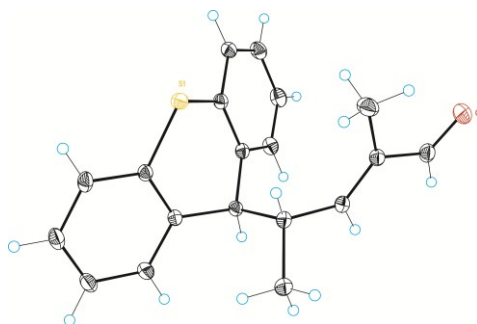


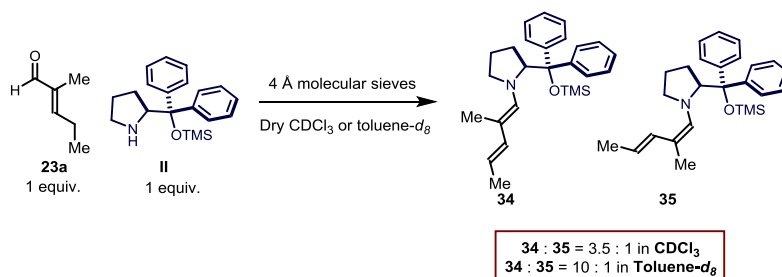
Figure 2.3 – X-ray diffraction analysis of compound **25r**.

The absolute configuration of compound **25r** was unambiguously determined by anomalous-dispersion X-ray crystallographic analysis: an (*S*) absolute configuration at the newly formed  $\gamma$ -stereogenic center was inferred (Figure 2.3).

### 2.3.3 Mechanistic insights – Stereochemical model

We carried out preliminary mechanistic investigations in order to elucidate the origin of the stereoselectivity. NMR spectroscopic analyses were used to gain information on the conformational behavior of the covalent dienamine intermediate, which is actively involved in the stereoselectivity determining step.<sup>27</sup>

Dienamines **34** - **35** could be synthesized by simply stirring aldehyde **23a** and catalyst **II** in dry deuterated solvent in the presence of 4 Å molecular sieves under a dry argon atmosphere.<sup>28</sup>



Scheme 2.16 – Synthesis of the dienamine intermediates.

Compounds **34** and **35** were stable enough to investigate their conformational behavior by means of conventional NMR techniques, particularly vicinal coupling constant analysis and nuclear Overhauser enhancement (nOe) spectroscopy.

<sup>27</sup> For conformational studies on classical enamine intermediates derived from the condensation of the Jørgensen-Hayashi catalyst with saturated aldehydes, see: X-ray techniques: a) Seebach, D.; Grošelj, U.; Badine, D. M.; Schweizer, W. B.; Beck, A. K. "Isolation and X-Ray Structures of Reactive Intermediates of Organocatalysis with Diphenylprolinol Ethers and with Imidazolidinones" *Helv. Chim. Acta* **2008**, *91*, 1999. b) Grošelj, U.; Seebach, D.; Badine, M.; Schweizer, W. B.; Beck, A. K. "Structures of the Reactive Intermediates in Organocatalysis with Diarylprolinol Ethers" *Helv. Chim. Acta* **2009**, *92*, 1225. Computational studies: c) Dinér, P.; Kjærsgaard, A.; Lie M. A.; Jørgensen K. A. "On the Origin of the Stereoselectivity in Organocatalysed Reactions with Trimethylsilyl-Protected Diarylprolinol" *Chem. Eur. J.* **2008**, *14*, 122. NMR studies: d) Schmid, M. B.; Zeitler, K.; Gschwind, R. M. "Distinct conformational preferences of prolinol and prolinol ether enamines in solution revealed by NMR" *Chem. Sci.* **2011**, *2*, 1793. e) Schmid, M. B.; Zeitler, K., Gschwind, R. M. *J. Am. Chem. Soc.*, **2011**, *133*, 7065.

<sup>28</sup> The dienamine intermediates derived from the catalyst **IX** were too unstable for allowing an exhaustive NMR analysis. We assumed the dienamines derived from the parent amine **II** to be structurally similar to the one obtained from the bulkier catalyst **IX**.

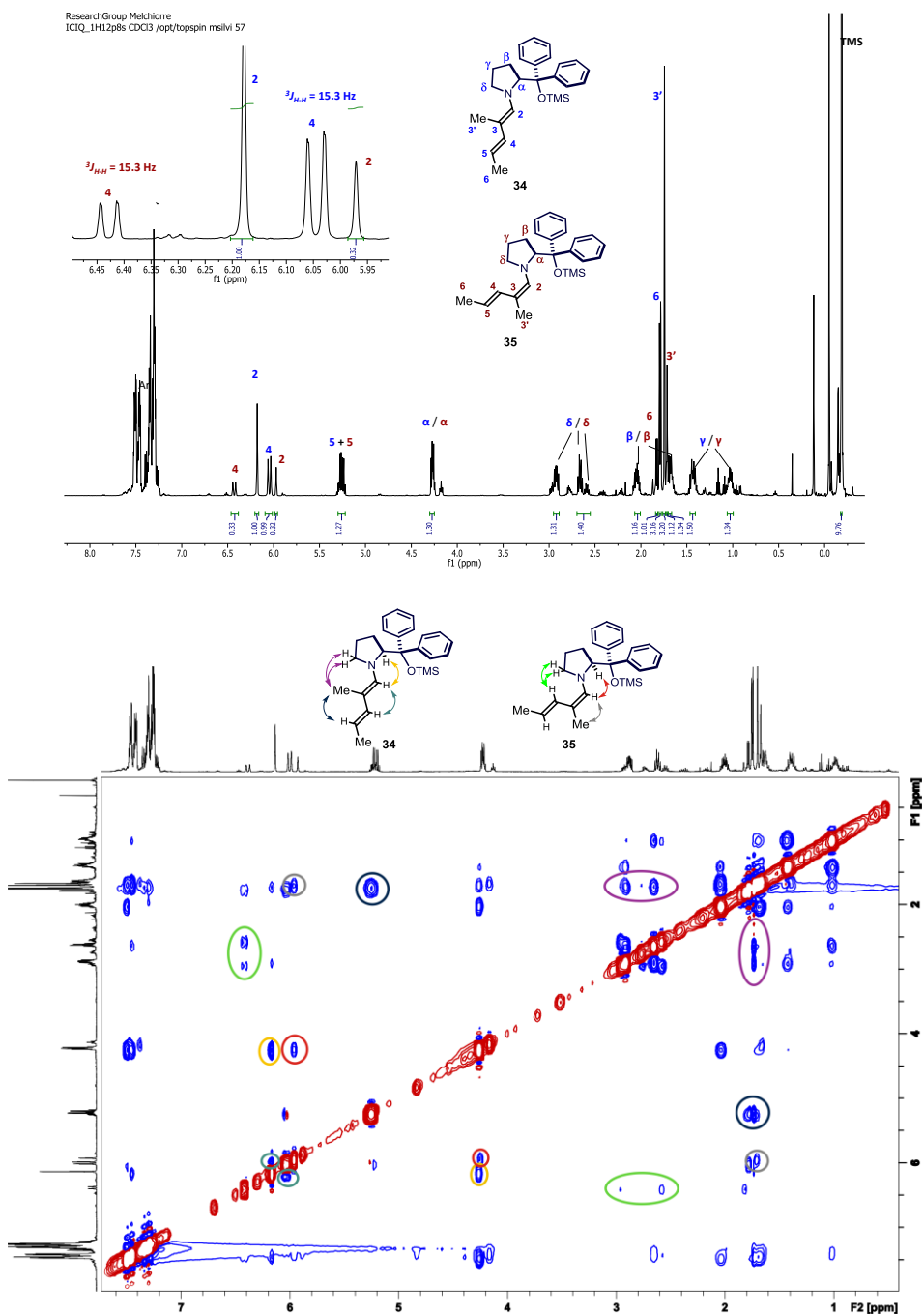


Figure 2.4 – Selected NMR spectra ( $^1\text{H}$  and NOESY) for compounds **34** and **35**. Conformational study carried out in  $\text{CDCl}_3$ .



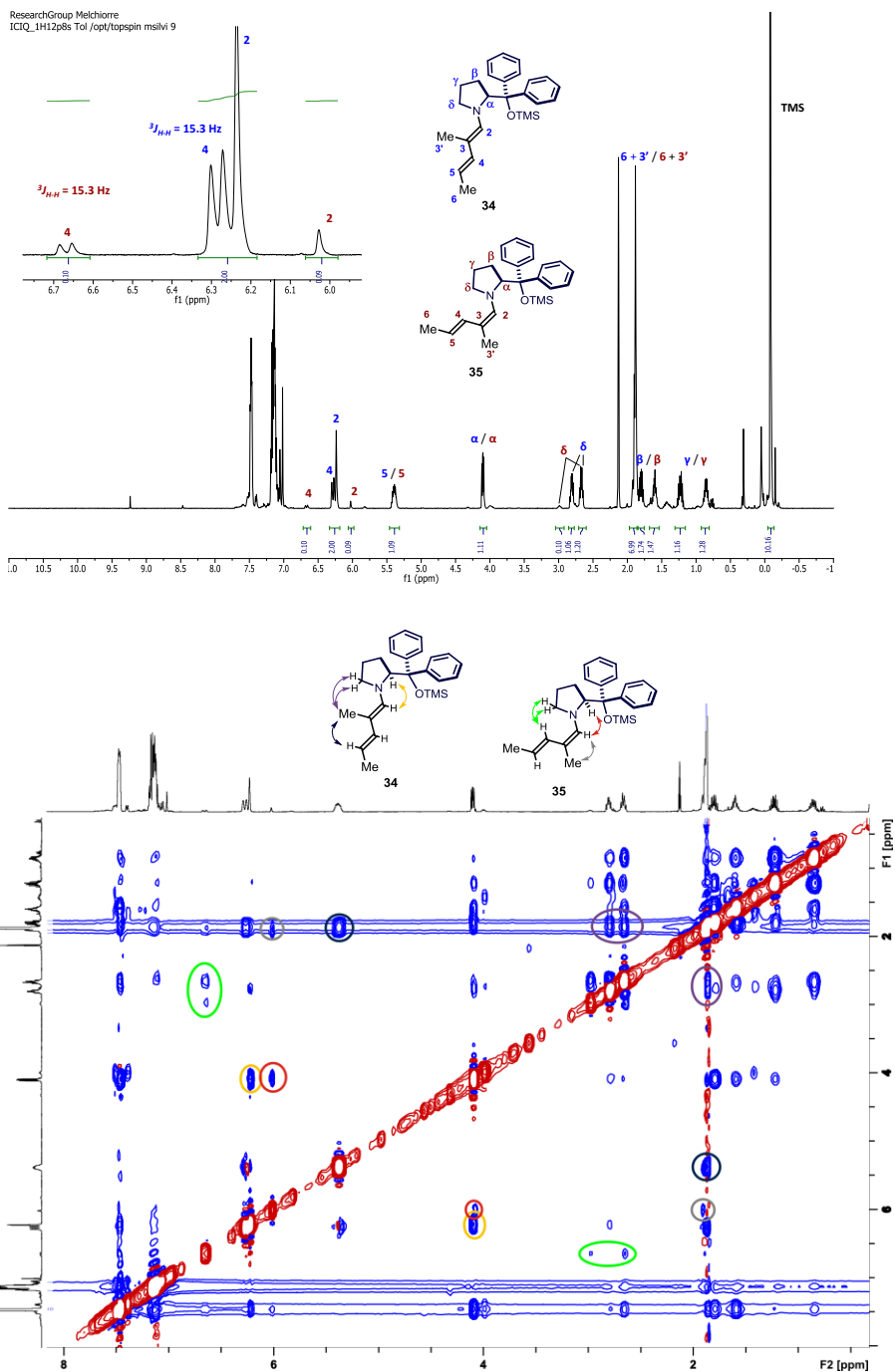
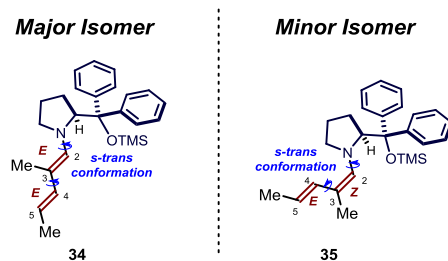


Figure 2.5 – Selected NMR spectra (<sup>1</sup>H and NOESY) for compounds **34** and **35**. Conformational study carried out in toluene-*d*<sub>6</sub>.

In  $\text{CDCl}_3$ , two different isomers **34** and **35** (shown in Scheme 2.16) were found in 3.5 : 1 abundance ratio (conformational analysis in Figure 2.4).

Several topological elements have the same geometry in the major and the minor isomers **34** and **35**, respectively. The presence of strong NOESY cross-peak between the H-C(2) and H-C( $\alpha$ ) (yellow arrow for major and red arrow for minor species) indicates a *s-trans* conformation of the single bond connecting N-C(2) (Figure 2.4). Additionally, the value of 15.3 Hz for the two  $^3J_{H-H}$  coupling constants between H-C(4) and H-C(5) for the intermediates **34** and **35**, respectively, are proof of an *E*-configured C(4)-C(5) double bond. Finally, the NOESY cross-peak between H-C(3') and H-C(5) (dark blue arrow, H-atom signal overlap for the major and the minor species) suggests an *s-trans* conformation of the C(3)-C(4) bond. The two dienamine species differ in the configuration of the C(2)-C(3) bond. The major isomer **34** has an *E*-configured C-C bond, assigned on the basis of the two NOESY cross-peaks between H-C(3') and H-C( $\delta$ ) (violet arrow), and H-C(4) and H-C(2) (dark green arrow). In contrast, the minor isomer **35** has a *Z*-configured C-C bond, as assigned on the basis of the two diagnostic NOESY signals H-C(3')/H-C(2) (grey arrow) and H-C(4)/H-C( $\delta$ ) (light green arrow). Overall, these studies establish an *E-E* configuration for the major dienamine isomer, having preferential *s-trans* conformation of the C(3)-C(4) and N-C(2) single bonds, while the minor isomer has a *Z-E* configuration of the two double bonds, with analogous *s-trans* preferential conformation of the C(2)-N bond and the C(3)-C(4) bond. The two isomers found in solution are depicted in Figure 2.6, with their respective conformational preferences.



**Figure 2.6** – The two dienamine isomers detected in solution. The major isomer has *E,E* configuration of the double bonds, whereas the minor differs for the configuration of the double bond closer to the nitrogen atom. In both of the cases the conformation of the N-C(2) and C(3)-C(4) is preferentially *s-trans*.

We then carried out conformational studies in toluene- $d_8$ , the deuterated analog of the reaction medium. As reported in the conformational analysis in Figure 2.5, two isomers, having the same topological arrangement as in  $\text{CDCl}_3$ , were detected. However, the major dienamine isomer **34** was formed in a much higher relative abundance (**34/35** = 10 : 1; Figure 2.5).

Computational analysis, carried out by Dr. Antonio Moran, a postdoctoral fellow at the Melchiorre group, showed good agreement with the results of our NMR conformational analysis. The hybrid functional B3LYP with the 6-31G(d) basis was used for this calculation.

Single-point energy calculations were performed with M06-2X/6-311++G(d,p) on B3LYP/6-31G(d) geometries to reproduce the dispersion effect, indicating that the two geometries found in solution are remarkably more stable than the other possible ones (Figure 2.7).

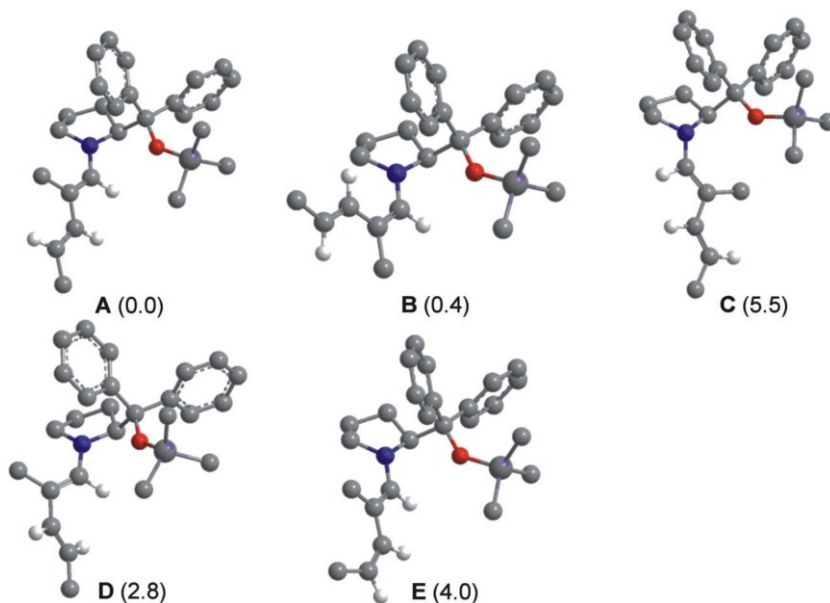
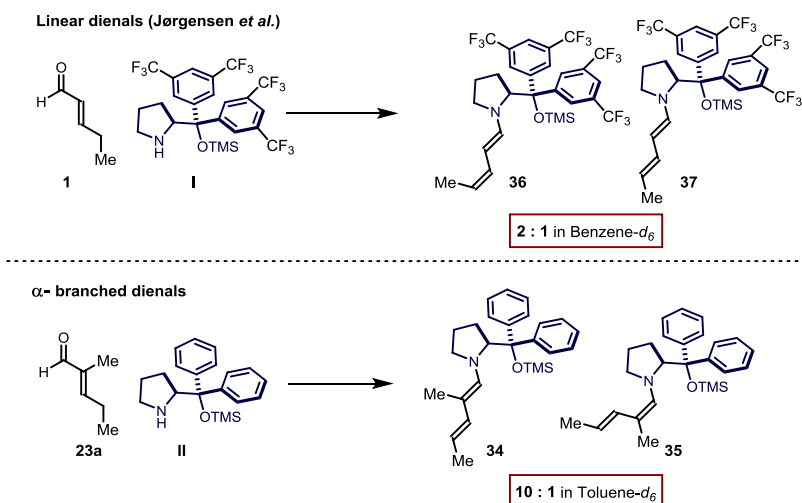


**Figure 2.7** – Optimized geometries and relative energies (in kcal/mol in parenthesis) at M06-2X/6-311++G(d,p)//B3LYP/6-31G(d) level of the more stable dienamine geometries.

These findings provoke interesting mechanistic considerations when compared with the spectroscopic studies carried out by Jørgensen and co-workers, who observed *in situ* the dienamine adduct derived by condensation of a similar catalyst (amine **1**) with a linear unsubstituted  $\alpha,\beta$ -unsaturated aldehyde **1** (Scheme 2.17).<sup>2</sup> For this system, two possible geometrical isomers were detected in C<sub>6</sub>D<sub>6</sub> solution, differing in the configuration of the second C-C double bond, more distant from the N-atom. In their case, the major isomer showed a Z-configuration of the second double bond. Remarkably, both detected dienamines derived from the  $\alpha$ -branched enal **23a** show an exclusive *E*-configuration of the remote C-C double bond. There thus arises the interesting prospect that the  $\alpha$ -branched enals, which are generally difficult substrates for enamine and iminium ion catalysis, have the structural properties (namely A<sup>1,3</sup> strain interactions generated by the  $\alpha$ -substituent)<sup>29</sup> to bias the dienamine geometry, a necessary requirement for forging a stereogenic center at the  $\gamma$ -position with high fidelity.

<sup>29</sup> Anslyn, E. V.; Dougherty, D. A. "Strain and Stability" Chapter 2, p. 100 in *Modern Physical Organic Chemistry*, 2006, University Science Book.



**Scheme 2.17** – Geometry difference between analogous linear dienamines and  $\alpha$ -branched dienamines.

Our conformational study has identified the *E-E* isomer having *s-trans* conformation of both the C(2)-N and the C(3)-C(4) single bonds as the thermodynamically more stable geometry in solution (Figure 2.6). The dominance of the major isomer upon the minor is higher in toluene solution than in chloroform solution, and this could be connected to the better enantioselectivity obtained in the aromatic solvent.

Based on these findings, a model for rationalizing the stereoselectivity of the  $\gamma$ -alkylation of  $\alpha$ -branched enals can be proposed (Figure 2.8). The classical steric control approach generally invoked to rationalize the stereochemical outcome of a process catalyzed by the Jørgensen-Hayashi type catalyst is consistent with the sense of asymmetric induction observed.<sup>30,31</sup>

### Stereochemical model

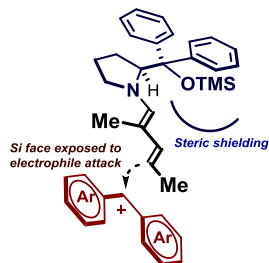


**Figure 2.8** – Proposed stereochemical model.

<sup>30</sup> Jensen, K.; Dickmeiss, G.; Jiang, H.; Albrecht, Ł.; Jørgensen, K. A. "The Diarylprolinol Silyl Ether System: A General Organocatalyst" *Acc. Chem. Res.* **2012**, *45*, 248.

<sup>31</sup> In our model, we assume that the minor isomer **35** is not significantly more reactive than the major **34** observed in solution. In fact, it is reasonable to consider that isomers **34** and **35** can convert each other in the reaction conditions and a much higher reactivity of **35** would lead to a Curtin-Hammett scenario in which the minor isomer is in reality the reactive one.

Indeed, the efficient shielding by the bulky substituent determines the selective engagement of the *in situ* generated carbocation with the *Si*-face of the most stable dienamine intermediate (Figure 2.8).

## 2.4 Conclusions and remarks

We have reported an effective catalytic system for the direct  $\gamma$ -site selective alkylation of  $\alpha$ -branched enals. Key to the development of the chemistry was the unexpected ability of chiral secondary-amine catalysis to activate  $\alpha$ -substituted  $\alpha,\beta$ -unsaturated aldehydes towards vinylogous nucleophilicity. NMR-based conformational analysis of the transient extended enamine intermediate allowed us to propose a stereochemical model and to rationalize the role of the  $\alpha$ -substituent in biasing the geometry of the reactive intermediate.

## 2.5 Experimental section

**General information:** The NMR spectra were recorded at 400 MHz and 500 MHz for  $^1\text{H}$  NMR or at 100 MHz and 125 MHz for  $^{13}\text{C}$ , respectively. The chemical shifts ( $\delta$ ) for  $^1\text{H}$  and  $^{13}\text{C}$  are given in ppm relative to residual signals of the solvents ( $\text{CHCl}_3$  @ 7.26 ppm  $^1\text{H}$  NMR, 77.16 ppm  $^{13}\text{C}$  NMR). Coupling constants are given in Hz. The following abbreviations are used to indicate the multiplicity: s, singlet; t, triplet; q, quartet; p, pentuplet; hept, heptuplet; m, multiplet.

High-resolution mass spectra (HRMS) were obtained from the ICIQ High Resolution Mass Spectrometry Unit on Waters GCT gas chromatograph coupled time-of-flight mass spectrometer (GC/MS-TOF) with electron ionization (EI) or MicroTOF II (Bruker Daltonics): HPLC-MS-TOF (ESI). X-Ray data were obtained from the ICIQ X-Ray unit using a Bruker-Nonius diffractometer equipped with an APPEX 2 4K CCD area detector.

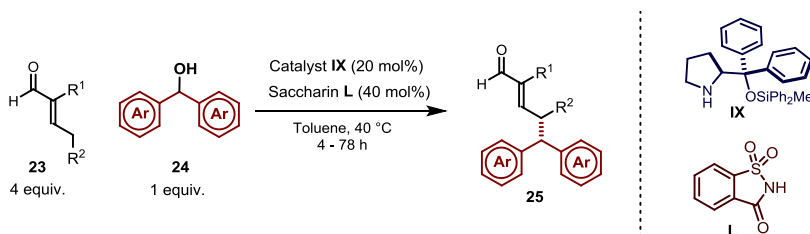
**General procedures:** All the reactions were set up under air and using synthesis grade solvents, without any precautions to exclude moisture, unless otherwise noted. Chromatographic purification of products was accomplished using force-flow chromatography on silica gel (35-70 mesh). For thin layer chromatography (TLC) analysis throughout this work, Merck precoated TLC plates (silica gel 60 GF254, 0.25 mm) were employed, using UV light as the visualizing agent and potassium permanganate stain solution and heat as developing agents. Organic solutions were concentrated under reduced pressure on a Büchi rotatory evaporator.

**Determination of Yields in the Optimization Studies:** All the yields reported in the optimization studies were obtained through  $^1\text{H}$  NMR analysis using 1,3,5-trimethoxybenzene as the internal standard (3.75 (s, 3 MeO); 6.08 (s, 3 arom. H)) and comparing these signals with those of the aldehyde H-atom of the product (s, 9.24 ppm). Analogous results were always obtained integrating other protons of the product.

**Determination of Enantiomeric Purity:** Enantiomeric excesses were determined by HPLC Analysis on chiral stationary phase, performed on an Agilent 1200 series instrumentation. Daicel

Chiralpak IA and IC columns with *i*PrOH/hexane as the eluent were used. HPLC traces were compared to racemic samples prepared by performing the reactions in the presence of a catalytic amount of an equimolar mixture of (*R*)- and (*S*)-diphenylprolinol trimethylsilyl ether catalyst II.

**Materials:** Reagents were purchased at the highest commercial quality from Sigma Aldrich, Fluka, and Alfa Aesar and used as received, without further purification, unless otherwise stated. Catalyst **IX** and **X** were prepared starting from commercially available (*S*)-diphenylprolinol according to the procedure described in literature.<sup>27a</sup> Aldehydes **23** were purchased from commercial suppliers and used without further purification; otherwise, they were synthesized according to the procedure described in literature.<sup>10</sup> Aldehyde **23m** has been obtained from autocondensation of hydrocinnamaldehyde following the procedure reported by Pihko *et al.*<sup>32</sup> Bis[4-(dimethylamino)phenyl]methanol (**24a**) and xanthidrol (**24q**) are commercially available. (1*H*-Indol-2-yl)(phenyl)methanol (**24s**) and thioxanthidrol (**24r**) were synthesized according to procedures reported in the literature.<sup>33,34</sup>



**General Procedure for the  $\gamma$ -Alkylation of  $\alpha$ -Branched Enals.** All the reactions were carried out in toluene (synthesis grade, >99%) without any precaution for excluding air and moisture. An ordinary 1-ml vial equipped with a Teflon-coated stir bar and a plastic screw cap was charged with 0.1 mmol of the alcohol **24**, 0.02 mmol of (*S*)-diphenylpyrrolidine-2-methanol methyl(diphenyl)silyl ether **IX** and 0.4 mmol of the enal **23** in 400  $\mu$ L of toluene (0.25 M). Then, 0.04 mmol of saccharin **L** was added. The vial was sealed and immersed in a 40 °C thermostatically controlled oil bath, and stirring was continued for the stated time. The mixture assumed a green color that disappeared upon complete consumption of the starting material (generally 24 – 36 h). The mixture was then directly charged on SiO<sub>2</sub> and subjected to chromatographic purification with hexane/Et<sub>2</sub>O or toluene/Et<sub>2</sub>O. All the products were stable if conserved in sealed vials flushed with Ar and stored at -20 °C in the absence of traces of acid (for spectroscopic analysis, chloroform was previously passed through basic aluminium oxide).

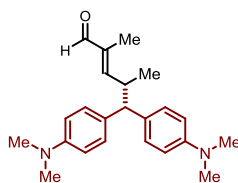
<sup>32</sup> Erkkilä, A.; Pihko, P. M. "Rapid Organocatalytic Aldehyde-Aldehyde Condensation Reactions" *Eur. J. Org. Chem.* **2007**, 4205.

<sup>33</sup> Guo, Q.-X.; Peng, Y.-G.; Zhang, J.-W.; Song, L.; Feng, Z.; Gong, L.-Z "Highly Enantioselective Alkylation Reaction of Enamides by Brønsted-Acid Catalysis" *Org. Lett.* **2009**, *11*, 4620.

<sup>34</sup> Fujii, T.; Hao, W.; Yoshimura, T. "New method for the preparation of dibenzo[*b,f*][1,4]thiazepines" *Heteroat. Chem.* **2004**, *15*, 246.

Products were fully characterized, all the spectra for previously reported compounds match with literature.<sup>10</sup> The absolute configuration of the  $\gamma$ -alkylated products **25** was assigned by comparison of the optical rotation to those of known compounds,<sup>10</sup> while the absolute configuration for compound **25r** was unambiguously determined by anomalous-dispersion X-ray crystallographic analysis.<sup>35</sup>

#### 5,5-Bis[4-(dimethylamino)phenyl]-2,4-dimethylpent-2-enal (**25a**).

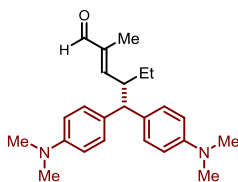


The reaction was carried out following the general procedure. After 27 hours of reaction the title compound **25a** was isolated by flash column chromatography (eluent hexane:diethyl ether 4:1) as a colorless oil (31 mg, 0.088 mmol, 88% yield). The enantiomeric excess was determined to be 93% by HPLC analysis on a Daicel Chiralpak IA column: 95/5 hexane/*i*-PrOH, flow rate 1.00 mL/min,  $\lambda$  =

254 nm:  $\tau_{\text{major}} = 8.4$  min,  $\tau_{\text{minor}} = 9.6$  min.  $[\alpha]_{\text{D}}^{26} = +30.41$  ( $c = 0.73$ ,  $\text{CHCl}_3$ , 93% ee).

<sup>1</sup>H-NMR (500 MHz,  $\text{CDCl}_3$ ): 9.24 (s, 1 H); 7.17 – 7.10 (m, 2 H); 7.07 – 7.00 (m, 2 H); 6.72 – 6.63 (m, 2 H); 6.61 – 6.54 (m, 2 H); 6.32 (dq,  $J = 9.9, 1.4$  Hz, 1 H); 3.62 (d,  $J = 10.5$  Hz, 1 H); 3.50 – 3.40 (m, 1 H); 2.86 (s, 6H); 2.90 (s, 6H); 1.74 (d,  $J = 1.4$  Hz, 3 H); 1.01 (d,  $J = 6.6$  Hz, 3 H). <sup>13</sup>C-NMR (125 MHz,  $\text{CDCl}_3$ ): 195.6, 160.1, 149.1, 149.0, 137.6, 132.1, 132.0, 128.6, 128.3, 112.8, 112.6, 56.2, 40.7, 40.6, 38.2, 19.0, 9.3.

#### 4-[Bis[4-(dimethylamino)phenyl]methyl]-2-methylhex-2-enal (**25b**).



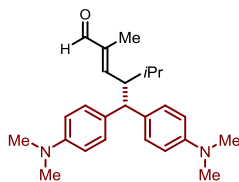
The reaction was carried out following the general procedure. After 32 hours of reaction the title compound **25b** was isolated by flash column chromatography (eluent hexane:diethyl ether 5:1) as a white solid (27 mg, 0.074 mmol, 74% yield). The enantiomeric excess was determined to be 96% by HPLC analysis on a Daicel Chiralpak IA column: 95/5 hexane/*i*-PrOH, flow rate 1.00 mL/min,  $\lambda = 254$  nm:

$\tau_{\text{major}} = 8.4$  min,  $\tau_{\text{minor}} = 9.5$  min.  $[\alpha]_{\text{D}}^{25} = +7.11$  ( $c = 1.24$ ,  $\text{CHCl}_3$ , 96% ee). HRMS calcd for ( $\text{C}_{24}\text{H}_{32}\text{ON}_2\text{H}^+$ ): 365.2593, found 365.2596.

<sup>1</sup>H-NMR (500 MHz,  $\text{CDCl}_3$ ): 9.27 (s, 1 H), 7.20 – 7.11 (m, 2 H), 7.09 – 6.92 (m, 2 H), 6.76 – 6.63 (m, 2 H), 6.63 – 6.52 (m, 2 H), 6.23 (dq,  $J = 10.3, 1.3$  Hz, 1 H), 3.69 (d,  $J = 10.3$  Hz, 1 H), 3.30 (qd,  $J = 10.3, 3.2$  Hz, 1 H), 2.90 (s, 6H), 2.85 (s, 6H), 1.74 (d,  $J = 1.3$  Hz, 3 H), 1.71 – 1.65 (m, 1 H), 1.26 – 1.20 (m, 1 H); 0.80 (t,  $J = 7.4$  Hz, 3 H). <sup>13</sup>C-NMR (125 MHz,  $\text{CDCl}_3$ ): 195.5, 158.9, 149.1, 148.9, 139.4, 132.1, 132.1, 128.5, 128.3, 112.8, 112.6, 54.8, 45.3, 40.7, 40.6, 26.5, 11.5, 9.9. HRMS: 365.2596 [ $\text{M}+\text{H}^+$ ], calc. for  $\text{C}_{24}\text{H}_{33}\text{ON}_2^+$  365.2593.

<sup>35</sup> CCDC-894226 contains the supplementary crystallographic data for compound **25r**. These data can be obtained free of charge via [http://www.ccdc.cam.ac.uk/data\\_request/cif](http://www.ccdc.cam.ac.uk/data_request/cif).

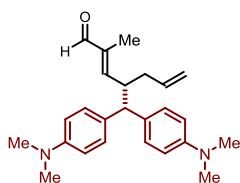
#### 4-{Bis[4-(dimethylamino)phenyl]methyl}-2,5-dimethylhex-2-enal (**25c**).



The reaction was carried out following the general procedure using 200  $\mu$ l of toluene). After 48 hours of reaction the title compound **25c** was isolated by flash column chromatography (eluent hexane:diethyl ether 4:1) as a white solid (24 mg, 0.063 mmol, 63% yield). The enantiomeric excess was determined to be 94% by HPLC analysis on a Daicel Chiralpak IA column: 80/20 hexane/*i*-PrOH, flow rate 1.00 mL/min,  $\lambda = 254$  nm:  $\tau_{\text{major}} = 4.7$  min,  $\tau_{\text{minor}} = 5.8$  min.  $[\alpha]_{\text{D}}^{26} = -12.50$  ( $c = 0.7$ ,  $\text{CHCl}_3$ , 94% ee).

$^1\text{H-NMR}$  (500 MHz,  $\text{CDCl}_3$ ): 9.25 (s, 1 H), 7.22 – 7.15 (m, 2 H), 7.06 – 7.00 (m, 2 H), 6.70 – 6.66 (m, 2 H), 6.55 – 6.51 (m, 2 H), 6.30 (dq,  $J = 11.1$ , 1.3 Hz, 1 H), 3.85 (d,  $J = 11.1$  Hz, 1 H), 3.38 (td,  $J = 11.1$ , 3.1 Hz, 1 H); 2.90 (s, 6 H); 2.84 (s, 6H); 1.92 (heptd,  $J = 7.0$ , 3.1 Hz, 1 H); 1.71 (d,  $J = 1.3$  Hz, 3 H); 0.89 (d,  $J = 7.0$  Hz, 3 H); 0.83 (d,  $J = 7.0$  Hz, 3 H).  $^{13}\text{C-NMR}$  (125 MHz,  $\text{CDCl}_3$ ): 195.5, 156.2, 149.1, 148.9, 140.5, 132.3, 132.0, 128.3, 128.1, 112.9, 112.6, 52.7, 48.6, 40.7, 40.6, 29.8, 22.1, 15.7, 10.1.

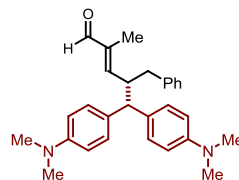
#### 4-{Bis[4-(dimethylamino)phenyl]methyl}-2-methylhepta-2,6-dienal (**25d**).



The reaction was carried out following the general procedure. After 50 hours of reaction the title compound **25d** was isolated by flash column chromatography (eluent in gradient hexane:diethyl ether 4:1 – 3:1) as a white solid (31 mg, 0.082 mmol, 82% yield). The enantiomeric excess was determined to be 94% by HPLC analysis on a Daicel Chiralpak IA column: 94/6 hexane/*i*-PrOH, flow rate 1.00 mL/min,  $\lambda = 254$  nm:  $\tau_{\text{major}} = 8.2$  min,  $\tau_{\text{minor}} = 8.9$  min.  $[\alpha]_{\text{D}}^{27} = -12.92$  ( $c = 1.00$ ,  $\text{CHCl}_3$ , 94% ee).

$^1\text{H NMR}$  (500 MHz,  $\text{CDCl}_3$ )  $\delta$  9.26 (s, 1H), 7.21 – 7.13 (m, 2H), 7.08 – 6.99 (m, 2H), 6.73 – 6.66 (m, 2H), 6.61 – 6.53 (m, 2H), 6.25 (dq,  $J = 10.4$ , 1.3 Hz, 1H), 5.66 (ddt,  $J = 17.3$ , 10.2, 7.2 Hz, 1H), 5.00 – 4.89 (m, 2H), 3.74 (d,  $J = 10.4$  Hz, 1H), 3.55 – 3.41 (m, 1H), 2.91 (s, 6H), 2.85 (s, 6H), 2.42 – 2.32 (m, 1H), 2.10 – 1.98 (m, 1H), 1.70 (d,  $J = 1.3$  Hz, 3H).  $^{13}\text{C NMR}$  (125 MHz,  $\text{CDCl}_3$ )  $\delta$  195.4, 158.0, 149.2, 149.0, 139.2, 135.4, 131.7(x2), 128.6, 128.3, 116.8, 112.9, 112.6, 54.4, 43.6, 40.7, 40.6, 37.8, 9.9.

#### 4-Benzyl-5,5-bis[4-(dimethylamino)phenyl]-2-methylpent-2-enal (**25e**).



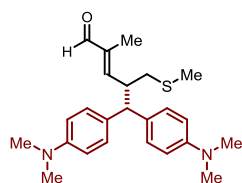
The reaction was carried out following the general procedure. After 43 hours of reaction the title compound **25e** was isolated by flash column chromatography (eluent hexane:diethyl ether 4:1) as a white solid (25 mg, 0.059 mmol, 59% yield). The enantiomeric excess was determined to be 95% by HPLC analysis on a Daicel Chiralpak IC column: 85/15 hexane/*i*-PrOH, flow rate 1.00 mL/min,  $\lambda = 254$  nm:

$\tau_{\text{major}} = 19.4$  min,  $\tau_{\text{minor}} = 21.0$  min.  $[\alpha]_{\text{D}}^{26} = +5.16$  ( $c = 0.94$ ,  $\text{CHCl}_3$ , 95% ee).



$^1\text{H}$  NMR (500 MHz,  $\text{CDCl}_3$ )  $\delta$  9.20 (s, 1H), 7.29 – 7.21 (m, 2H), 7.21 – 7.09 (m, 3H), 7.07 – 6.96 (m, 4H), 6.77 – 6.71 (m, 2H), 6.61 – 6.52 (m, 2H), 6.22 (dq,  $J = 10.3, 1.3$  Hz, 1H), 3.79 (d,  $J = 10.3$  Hz, 1H), 3.63 (qd,  $J = 10.3, 3.2$  Hz, 1H), 3.02 (dd,  $J = 13.4, 3.2$  Hz, 1H), 2.93 (s, 6H), 2.85 (s, 6H), 2.42 (dd,  $J = 13.4, 10.3$  Hz, 1H), 1.19 (d,  $J = 1.3$  Hz, 3H).  $^{13}\text{C}$  NMR (125 MHz,  $\text{CDCl}_3$ )  $\delta$  195.3, 157.3, 149.2, 149.0, 139.8, 139.6, 131.8, 131.7, 129.1, 128.6, 128.2, 128.1, 126.0, 113.1, 112.6, 54.9, 46.4, 40.7, 40.6, 39.8, 9.1.

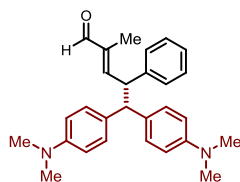
#### 5,5-Bis[4-(dimethylamino)phenyl]-2-methyl-4-[(methylsulfanyl)methyl]pent-2-enal (25f).



The reaction was carried out following the general procedure. After 48 hours of reaction the title compound **25f** was isolated by flash column chromatography (eluent in gradient hexane:diethyl ether 5:1 – 4:1) as a yellowish solid (16 mg, 0.040 mmol, 40% yield). The enantiomeric excess was determined to be 90% by HPLC analysis on a Daicel Chiralpak IA-3 column: 97/3 hexane/*i*-PrOH, flow rate 0.80 mL/min,  $\lambda = 254$  nm:  $\tau_{\text{major}} = 14.0$  min,  $\tau_{\text{minor}} = 15.0$  min.  $[\alpha]_{\text{D}}^{25} = +19.71$  ( $c = 1.07$ ,  $\text{CHCl}_3$ , 90% ee). HRMS calcd for  $(\text{C}_{24}\text{H}_{32}\text{N}_2\text{OS}^+)$ : 397.2314, found 397.2333.

$^1\text{H}$  NMR (500 MHz,  $\text{CDCl}_3$ )  $\delta$  9.29 (s, 1H), 7.20 – 7.14 (m, 2H), 7.06 – 7.01 (m, 2H), 6.72 – 6.66 (m, 2H), 6.61 – 6.54 (m, 2H), 6.31 (dq,  $J = 10.3, 1.4$  Hz, 1H), 3.89 (d,  $J = 10.3$  Hz, 1H), 3.64 (tdd,  $J = 10.3, 8.7, 3.6$  Hz, 1H), 2.91 (s, 6H), 2.86 (s, 6H), 2.73 (dd,  $J = 12.8, 3.6$  Hz, 1H), 2.48 (dd,  $J = 12.8, 8.7$  Hz, 1H), 2.02 (s, 3H), 1.74 (d,  $J = 1.4$  Hz, 3H).  $^{13}\text{C}$  NMR (125 MHz,  $\text{CDCl}_3$ )  $\delta$  195.3, 156.6, 149.2, 149.0, 140.1, 131.1(x2), 128.5, 128.4, 113.0, 112.6, 53.9, 43.6, 40.7, 40.6, 38.6, 16.7, 10.0.

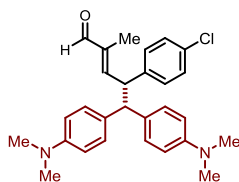
#### 5,5-Bis[4-(dimethylamino)phenyl]-2-methyl-4-phenylpent-2-enal (25g).



The reaction was carried out following the general procedure. After 6 hours of reaction the title compound **25g** was isolated by flash column chromatography (eluent hexane:diethyl ether 4:1) as a white solid (38 mg, 0.092 mmol, 92% yield). The enantiomeric excess was determined to be 92% by HPLC analysis on a Daicel Chiralpak IA column: 93/7 hexane/*i*-PrOH, flow rate 1.00 mL/min,  $\lambda = 254$  nm:  $\tau_{\text{major}} = 8.3$  min,  $\tau_{\text{minor}} = 9.2$  min.  $[\alpha]_{\text{D}}^{26} = +6.98$  ( $c = 1.05$ ,  $\text{CHCl}_3$ , 92% ee).

$^1\text{H}$  NMR (400 MHz  $\text{CDCl}_3$ )  $\delta$  9.25 (s, 1H), 7.23 – 7.17 (m, 2H), 7.17 – 7.09 (m, 5H), 6.96 – 6.91 (m, 2H), 6.65 – 6.59 (m, 3H), 6.54 – 6.45 (m, 2H), 4.50 (t,  $J = 10.9$  Hz, 1H), 4.26 (d,  $J = 10.9$  Hz, 1H), 2.89 (s, 6H), 2.83 (s, 6H), 1.70 (s, 3H).  $^{13}\text{C}$  NMR (100 MHz,  $\text{CDCl}_3$ )  $\delta$  195.3, 157.0, 149.1, 148.7, 141.7, 137.9, 131.2, 131.1, 128.7(x2), 128.5, 128.3, 126.5, 112.6, 112.5, 55.4, 50.3, 40.6(x2), 9.5.

### 5,5-Bis[4-(dimethylamino)phenyl]-4-(4-chlorophenyl)-2-methylpent-2-enal (**25h**).

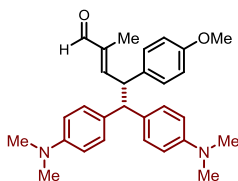


The reaction was carried out following the general procedure. After 5.5 hours of reaction the title compound **25h** was isolated by flash column chromatography (eluent hexane:diethyl ether 2:1) as a white solid (39 mg, 0.088 mmol, 88% yield). The enantiomeric excess was determined to be 94% by HPLC analysis on a Daicel Chiralpak IC-3 column: 80/20 hexane/*i*-PrOH, flow rate 0.80 mL/min,

$\lambda = 254$  nm:  $\tau_{\text{major}} = 25.9$  min,  $\tau_{\text{minor}} = 30.8$  min.  $[\alpha]_{\text{D}}^{26} = -2.08$  ( $c = 1.00$ ,  $\text{CHCl}_3$ , 94% ee).

$^1\text{H NMR}$  (500 MHz,  $\text{CDCl}_3$ )  $\delta$  9.25 (s, 1H), 7.14 – 7.03 (m, 4H), 6.99 – 6.92 (m, 2H), 6.79 – 6.72 (m, 2H), 6.66 – 6.57 (m, 3H), 6.55 – 6.47 (m, 2H), 4.47 (dd,  $J = 11.1, 9.9$  Hz, 1H), 4.21 (d,  $J = 11.1$  Hz, 1H), 3.74 (s, 3H), 2.89 (s, 6H), 2.83 (s, 6H), 1.70 (d,  $J = 1.3$  Hz, 3H).  $^{13}\text{C NMR}$  (125 MHz,  $\text{CDCl}_3$ )  $\delta$  195.4, 158.0, 157.4, 149.1, 148.7, 137.6, 133.8, 131.4, 131.2, 129.2, 128.7(x2), 113.9, 112.6, 112.5, 55.5, 55.1, 49.4, 40.6(x2), 9.4..

### 4-(4-Chlorophenyl)-5,5-bis[4-(dimethylamino)phenyl]-2-methylpent-2-enal (**25i**).

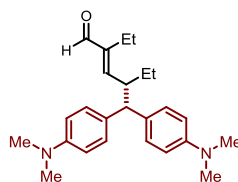


The reaction was carried out following the general procedure. After 6 hours of reaction the title compound **25i** was isolated by flash column chromatography (eluent hexane:diethyl ether 3:1) as a white solid (41 mg, 0.092 mmol, 92% yield). The enantiomeric excess was determined to be 91% by HPLC analysis on a Daicel Chiralpak IA-3 column: 90/10 hexane/*i*-PrOH, flow rate 0.80 mL/min,  $\lambda = 254$  nm:

$\tau_{\text{minor}} = 10.1$  min,  $\tau_{\text{major}} = 10.9$  min.  $[\alpha]_{\text{D}}^{26} = +12.45$  ( $c = 1.00$ ,  $\text{CHCl}_3$ , 91% ee).

$^1\text{H NMR}$  (400 MHz,  $\text{CDCl}_3$ )  $\delta$  9.25 (s, 1H), 7.20 – 7.14 (m, 2H), 7.12 – 7.03 (m, 4H), 6.95 – 6.89 (m, 2H), 6.64 – 6.55 (m, 3H), 6.53 – 6.48 (m, 2H), 4.47 (dd,  $J = 11.1, 9.7$  Hz, 1H), 4.18 (d,  $J = 11.1$  Hz, 1H), 2.89 (s, 6H), 2.83 (s, 6H), 1.67 (d,  $J = 1.3$  Hz, 3H).  $^{13}\text{C NMR}$  (100, MHz,  $\text{CDCl}_3$ )  $\delta$  195.1, 156.1, 149.2, 148.8, 140.4, 138.4, 132.1, 130.8, 130.7, 129.6, 128.7, 128.6, 128.6, 112.6, 112.5, 55.5, 49.7, 40.6(x2), 9.5.

### 4-[Bis[4-(dimethylamino)phenyl]methyl]-2-ethylhex-2-enal (**25l**).



The reaction was carried out following the general procedure using 200  $\mu\text{L}$  of solvent. After 78 hours of reaction, the title compound **25l** was isolated by flash column chromatography (eluent hexane:diethyl ether 4:1) as a white solid (31 mg, 0.082 mmol, 82% yield). The enantiomeric excess was determined to be 92% by HPLC analysis on a Daicel Chiralpak IC column: 90/10 hexane/*i*-PrOH, flow rate 1.00

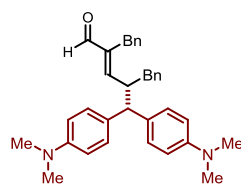
mL/min,  $\lambda = 254$  nm:  $\tau_{\text{major}} = 15.7$  min,  $\tau_{\text{minor}} = 18.4$  min.  $[\alpha]_{\text{D}}^{27} = -16.73$  ( $c = 0.85$ ,  $\text{CHCl}_3$ , 92% ee).

$^1\text{H NMR}$  (400 MHz,  $\text{CDCl}_3$ )  $\delta$  9.23 (s, 1H), 7.19 – 7.13 (m, 2H), 7.06 – 7.00 (m, 2H), 6.71 – 6.65 (m, 2H), 6.59 – 6.53 (m, 2H), 6.16 (d,  $J = 10.6$  Hz, 1H), 3.70 (d,  $J = 10.2$  Hz, 1H), 3.35 – 3.23 (m, 1H),

2.90 (s, 6H), 2.84 (s, 6H), 2.22 (q,  $J = 7.5$  Hz, 2H), 1.73 – 1.62 (m, 1H), 1.26 – 1.20 (m, 1H), 0.91 (t,  $J = 7.5$  Hz, 3H), 0.80 (t,  $J = 7.5$  Hz, 3H).  $^{13}\text{C}$  NMR (100 MHz,  $\text{CDCl}_3$ )  $\delta$  195.6, 158.5, 149.1, 149.0, 144.9, 132.1, 131.8, 128.6, 128.4, 112.8, 112.6, 54.8, 45.0, 40.7, 40.7, 26.5, 18.2, 12.8, 11.6.

### 2,4-Dibenzyl-5,5-bis[4-(dimethylamino)phenyl]pent-2-enal (25m).

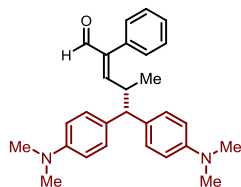
The reaction was carried out following the general procedure. After 48 hours of reaction the title compound **25m** was isolated by flash column chromatography (eluent in gradient toluene:diethyl ether 97:3 – 95:5) as a white solid (42 mg, 0.083 mmol, 83% yield). The



enantiomeric excess was determined to be 94% by HPLC analysis on a Daicel Chiralpak IA column: 96/4 hexane/*i*-PrOH, flow rate 1.00 mL/min,  $\lambda = 254$  nm:  $\tau_{\text{minor}} = 11.8$  min,  $\tau_{\text{major}} = 12.5$  min.  $[\alpha]_{\text{D}}^{26} = -33.60$  ( $c = 1.00$ ,  $\text{CHCl}_3$ , 94% ee).

$^1\text{H}$  NMR (500 MHz,  $\text{CDCl}_3$ )  $\delta$  9.29 (s, 1H), 7.24 – 7.19 (m, 5H), 7.15 – 7.12 (m, 3H), 7.03 – 7.00 (m, 2H), 6.88 – 6.82 (m, 2H), 6.76 – 6.72 (m, 4H), 6.49 – 6.44 (m, 2H), 6.38 (d,  $J = 10.2$  Hz, 1H), 3.77 (d,  $J = 10.3$  Hz, 1H), 3.70 – 3.63 (m, 1H), 3.12 (d,  $J = 15.1$  Hz, 1H), 3.01 (dd,  $J = 13.4$ , 3.2 Hz, 1H), 2.93 (s, 6H), 2.85 (s, 6H), 2.69 (d,  $J = 15.1$  Hz, 1H), 2.46 (dd,  $J = 13.4$ , 9.4 Hz, 1H).  $^{13}\text{C}$  NMR (125 MHz,  $\text{CDCl}_3$ )  $\delta$  194.8, 158.8, 149.2, 148.9, 142.3, 139.3, 138.8, 131.4, 131.4, 129.4, 128.7, 128.5, 128.5, 128.3, 128.1, 126.2, 125.7, 113.0, 112.6, 54.9, 46.4, 40.7, 40.6, 39.8, 29.3.

### 5,5-Bis[4-(dimethylamino)phenyl]-4-methyl-2-phenylpent-2-enal (25n).

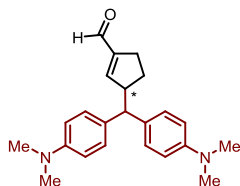


The reaction was carried out following the general procedure. After 26 hours of reaction the title compound **25n** was isolated by flash column chromatography (eluent hexane:diethyl ether 4:1) as a yellowish oil (34 mg, 0.082 mmol, 82% yield). The enantiomeric excess was determined to be 40% by HPLC analysis on a Daicel Chiralpak IA column: 95/5 hexane/*i*-PrOH, flow rate 1.00 mL/min,  $\lambda =$

254 nm:  $\tau_{\text{major}} = 9.9$  min,  $\tau_{\text{minor}} = 12.8$  min.  $[\alpha]_{\text{D}}^{25} = +38.98$  ( $c = 1.3$ ,  $\text{CHCl}_3$ , 40% ee).

$^1\text{H}$  NMR (400 MHz,  $\text{CDCl}_3$ )  $\delta$  9.44 (s, 1H), 7.48 – 7.39 (m, 3H), 7.08 – 6.98 (m, 4H), 6.92 – 6.87 (m, 2H), 6.65 – 6.60 (m, 2H), 6.59 – 6.51 (m, 3H), 3.63 (d,  $J = 10.5$  Hz, 1H), 3.41 – 3.28 (m, 1H), 2.88 (s, 6H), 2.87 (s, 6H), 1.07 (d,  $J = 6.5$  Hz, 3H).  $^{13}\text{C}$  NMR (100 MHz,  $\text{CDCl}_3$ )  $\delta$  193.9, 161.4, 149.1(x2), 142.8, 133.1, 132.0, 131.6, 129.3, 128.5(x2), 128.2, 127.8, 112.8, 112.6, 56.5, 40.7(x2), 38.5, 19.7.

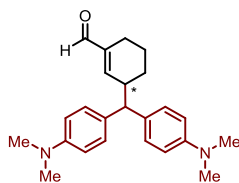
### 3-{Bis[4-(dimethylamino)phenyl]methyl}cyclopent-1-ene-1-carbaldehyde (**25o**).



The reaction was carried out following the general procedure. After 4 hours of reaction the title compound **25o** was isolated by flash column chromatography (eluent toluene:diethyl ether 96:4 – 95:5) as a yellowish oil (26 mg, 0.076 mmol, 76% yield). The enantiomeric excess was determined to be 68% by HPLC analysis on a Daicel Chiralpak IA column: 90/10 hexane/*i*-PrOH, flow rate 1.00 mL/min,  $\lambda$  = 254 nm:  $\tau_{\text{major}}$  = 11.2 min,  $\tau_{\text{minor}}$  = 12.2 min.  $[\alpha]_{\text{D}}^{27}$  = + 76.23 (*c* = 1.0, CHCl<sub>3</sub>, 68% ee). HRMS calcd for (C<sub>23</sub>H<sub>27</sub>N<sub>2</sub>OH<sup>+</sup>): 349.2280, found 349.2263.

<sup>1</sup>H NMR (500 MHz, CDCl<sub>3</sub>)  $\delta$  9.69 (s, 1H), 7.18 – 7.10 (m, 4H), 6.72 – 6.64 (m, 5H), 3.77 – 3.68 (m, 1H), 3.60 (d, *J* = 11.2 Hz, 1H), 2.91 (s, 6H), 2.90 (s, 6H), 2.62 – 2.51 (m, 1H), 2.50 – 2.40 (m, 1H), 2.17 – 2.06 (m, 1H), 1.71 – 1.60 (m, 1H). <sup>13</sup>C NMR (125 MHz, CDCl<sub>3</sub>)  $\delta$  190.4, 156.3, 149.1, 149.1, 147.0, 132.6, 132.1, 128.4, 128.3, 112.9, 112.8, 55.0, 51.8, 40.7, 29.3, 27.8.

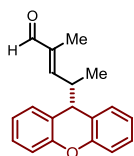
### 3-[Bis[4-(dimethylamino)phenyl]methyl]cyclohex-1-ene-1-carbaldehyde (**25p**).



The reaction was carried out following the general procedure. After 32 hours of reaction the title compound **25p** was isolated by flash column chromatography (eluent toluene:diethyl ether 5:1) as a yellowish solid (31 mg, 0.086 mmol, 86% yield). The enantiomeric excess was determined to be 63% by HPLC analysis on a Daicel Chiralpak IA column: 90/10 hexane/*i*-PrOH, flow rate 1.00 mL/min,  $\lambda$  = 254 nm:  $\tau_{\text{major}}$  = 8.5 min,  $\tau_{\text{minor}}$  = 9.9 min.  $[\alpha]_{\text{D}}^{26}$  = + 8.72 (*c* = 1.0, CHCl<sub>3</sub>, 63% ee).

<sup>1</sup>H NMR (500 MHz, CDCl<sub>3</sub>)  $\delta$  9.28 (s, 1H), 7.20 – 7.11 (m, 4H), 6.73 – 6.65 (m, 4H), 6.66 – 6.61 (m, 1H), 3.56 (d, *J* = 11.2 Hz, 1H), 3.20 – 3.09 (m, 1H), 2.92 (s, 6H), 2.90 (s, 6H), 2.33 – 2.25 (m, 1H), 2.11 – 2.03 (m, 1H), 1.87 – 1.76 (m, 1H), 1.77 – 1.70 (m, 1H), 1.56 – 1.47 (m, 1H), 1.27 – 1.19 (m, 1H). <sup>13</sup>C NMR (125 MHz, CDCl<sub>3</sub>)  $\delta$  194.9, 154.6, 149.1, 149.1, 141.5, 132.0, 131.4, 128.6, 128.3, 113.0, 112.9, 54.9, 41.0, 40.7, 28.0, 21.7, 20.6.

### 2-Methyl-4-(9H-xanthen-9-yl)pent-2-enal (**25q**).



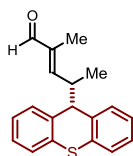
The reaction was carried out following the general procedure, but using 200  $\mu$ L of acetonitrile as solvent and 2,4-dinitrobenzoic acid as acidic additive. After 30 hours of reaction the reaction mixture was subjected to flash column chromatography purification (eluent hexane:diethyl ether 95:5) obtaining a mixture of the product **25q** and xanthone (this compound shows fluorescence at 354 nm). This mixture was finally purified on preparative TLC using methylene chloride as eluent (product *RF* = 0.6) affording the product as a white solid (18 mg - 0.065 mmol – 65% yield). The enantiomeric excess was determined to be 81% by HPLC analysis on a Daicel Chiralpak IA column: 95/5 hexane/*i*-PrOH, flow rate 1.00 mL/min,  $\lambda$  = 254 nm:  $\tau_{\text{minor}}$  = 5.6 min,

$\tau_{\text{major}} = 5.8$  min.  $[\alpha]_{\text{D}}^{26} = + 13.87$  ( $c = 1.00$ ,  $\text{CHCl}_3$ , 81% ee). HRMS calcd for  $(\text{C}_{19}\text{H}_{18}\text{O}_2\text{Na}^+)$ : 301.1204, found 301.1210.

$^1\text{H}$  NMR (500 MHz,  $\text{CDCl}_3$ )  $\delta$  9.30 (s, 1H), 7.29 – 7.22 (m, 2H), 7.22 – 7.14 (m, 2H), 7.13 – 7.04 (m, 4H), 6.11 (dq,  $J = 10.3, 1.4$  Hz, 1H), 3.98 (d,  $J = 5.0$  Hz, 1H), 3.00 (dq,  $J = 10.3, 6.8, 5.0$  Hz, 1H), 1.36 (d,  $J = 1.4$  Hz, 3H), 1.03 (d,  $J = 6.8$  Hz, 3H).  $^{13}\text{C}$  NMR (125 MHz,  $\text{CDCl}_3$ )  $\delta$  195.2, 155.8, 153.0, 152.9, 139.4, 129.2, 129.0, 128.1, 123.3, 123.2, 123.0, 122.7, 116.5, 116.4, 45.0, 42.4, 16.7, 8.8.

### 2-Methyl-4-(9H-thioxanthen-9-yl)pent-2-enal (25r)

The reaction was carried out following the general procedure but two times more concentrated, using 200  $\mu\text{L}$  of acetonitrile as solvent. After 30 hours of reaction the title compound **25r** was



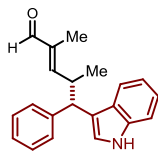
isolated by flash column chromatography (eluent hexane:diethyl ether 10:1) as a white solid (23 mg - 0.078 mmol – 78% yield).

The enantiomeric excess was determined to be 81% by HPLC analysis on a Daicel Chiralpak IA column: 90/10 hexane/*i*-PrOH, flow rate 1.00 mL/min,  $\lambda = 254$  nm:  $\tau_{\text{minor}} = 6.2$  min,  $\tau_{\text{major}} = 8.4$  min.  $[\alpha]_{\text{D}}^{26} = - 106.69$  ( $c = 0.85$ ,  $\text{CHCl}_3$ , 81%

ee). HRMS calcd for  $(\text{C}_{19}\text{H}_{18}\text{OSNa}^+)$ : 317.0976, found 317.0961.

$^1\text{H}$  NMR (500 MHz,  $\text{CDCl}_3$ )  $\delta$  9.31 (s, 1H), 7.54 – 7.44 (m, 1H), 7.45 – 7.33 (m, 1H), 7.35 – 7.24 (m, 3H), 7.21 – 7.03 (m, 3H), 6.28 (dq,  $J = 10.5, 1.3$  Hz, 1H), 3.84 (d,  $J = 9.8$  Hz, 1H), 3.52 – 3.37 (m, 1H), 1.18 (d,  $J = 1.3$  Hz, 3H), 0.94 (d,  $J = 6.6$  Hz, 3H).  $^{13}\text{C}$  NMR (125 MHz,  $\text{CDCl}_3$ )  $\delta$  195.2, 157.1, 139.7, 136.2, 135.7, 132.7, 132.5, 130.3, 129.8, 127.2, 126.9, 126.8, 126.7, 126.2, 126.0, 55.0, 33.2, 18.6, 8.5.

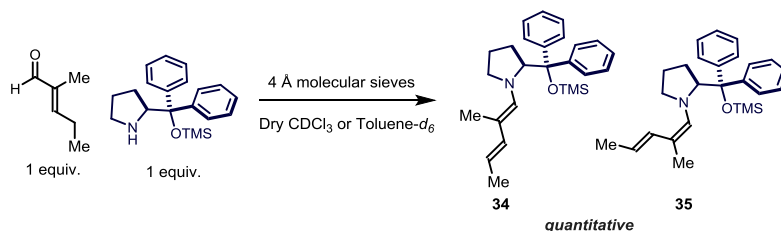
### 5-(1H-Indol-3-yl)-2,4-dimethyl-5-phenylpent-2-enal (25s).



The reaction was carried out following the general procedure. After 25 hours of reaction the title compound **25s** was isolated by flash column chromatography (eluent in gradient toluene:diethyl ether 98:2 – 95:5) as a white solid (16 mg, 0.052 mmol, 52% yield) as a mixture of diastereoisomers in a ratio of 1.3:1 with an enantiomeric excess respectively of 87% and 92%.

The enantiomeric excess was determined by HPLC analysis on a Daicel Chiralpak IA column: 80/20 hexane/*i*-PrOH, flow rate 1.00 mL/min,  $\lambda = 254$  nm:  $T_{\text{minor}} = 6.5$  min,  $T_{\text{major}} = 14.5$  min and  $\tau_{\text{minor}} = 6.5$  min,  $\tau_{\text{major}} = 14.5$  min. HRMS calcd for  $(\text{C}_{21}\text{H}_{21}\text{NONa}^+)$ : 326.1521, found 326.1522.

$^1\text{H}$  NMR (400 MHz, Benzene- $d_6$ )  $\delta$  9.17 (s, 1H), 7.63 (d,  $J = 7.6$  Hz, 1H), 7.23 – 6.89 (m, 10H), 6.59 – 6.50 (m, 1H), 6.01 (d,  $J = 9.9$  Hz, 1H), 3.98 (d,  $J = 9.0$  Hz, 1H), 3.41 – 3.31 (m, 1H), 1.62 (d,  $J = 1.4$  Hz, 3H), 0.92 (d,  $J = 6.7$  Hz, 3H).  $^{13}\text{C}$  NMR (100 MHz,  $\text{C}_6\text{D}_6$ )  $\delta$  195.1, 158.5, 144.4, 139.2, 138.7, 137.4, 129.4, 129.2, 127.4, 123.2, 122.2, 120.6, 120.4, 118.9, 112.3, 49.8, 39.5, 19.9, 10.2.



#### Procedure for Preparing the Dienamine Intermediate.

An anhydrous Schlenk tube under argon atmosphere was charged with freshly activated 4 Å molecular sieves, 2-methyl-2-pentenal (19.6 mg, 0.2 mmol) and (*S*)-diphenylprolinol trimethylsilylether (65 mg, 0.2 mmol) in dry deuterated solvent (200  $\mu$ L – 1M). The reaction was stirred overnight (16 h) at r.t. and then an aliquote of 50  $\mu$ L of the reaction crude, diluted with 500  $\mu$ L of dry deuterated solvent, was poured in a dry Young NMR tube under argon atmosphere and directly analyzed through NMR.

**Theoretical Calculations of Structures.** The different structures of the dienamine intermediate were fully optimized at the B3LYP/6-31G(d) level.<sup>36</sup> For each structure, a frequency calculation has been performed to verify that it is an energy minimum, i.e., having no imaginary frequency. Energy evaluations of the B3LYP/6-31G(d)-optimized structures were carried out at the M06-2X levels using a larger basis set, 6-311++G(d,p). The B3LYP calculations do not reproduce dispersion effects, but the M06-2X calculations do consider them, at least in part. The Gaussian 09 program was used for all theoretical calculations.

<sup>36</sup> a) Becke, A.D. "Density-functional thermochemistry. III. The role of exact exchange" *J. Chem. Phys.* **1993**, *98*, 5648 b) Lee, C.; Yang, W.; Parr, R. G. "Development of the Colle-Salvetti correlation-energy formula into a functional of the electron density" *Phys. Rev. B: Condens. Matter* **1988**, *37*, 785. c) Miehlich, B.; Savin, A.; Stoll, H.; Preuss, H. "Results obtained with the correlation energy density functionals of becke and Lee, Yang and Parr" *Chem. Phys. Lett.* **1989**, *157*, 200. c) Hariharan, P. C.; Pople, J. A. "The influence of polarization functions on molecular orbital hydrogenation energies" *Theor. Chim. Acta* **1973**, *28*, 213.

UNIVERSITAT ROVIRA I VIRGILI

NEW DIRECTIONS IN AMINOCATALYSIS: VINYLOGY AND PHOTOCHEMISTRY

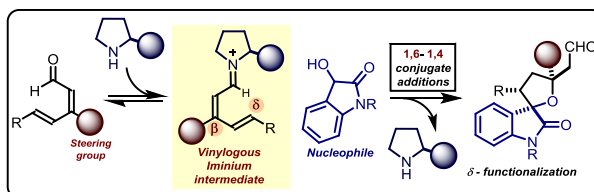
Mattia Silvi

## Chapter III

# Controlling the Molecular Topology of Vinylogous Iminium Ions: Asymmetric 1,6-Addition to Linear 2,4-Dienals

### Target

Synthesis of valuable tetrahydrofuran spirooxindoles through a regio- and stereo-selective sequential 1,6/1,4-conjugate addition to acyclic 2,4-dienals proceeding under iminium ion activation.



### Tool

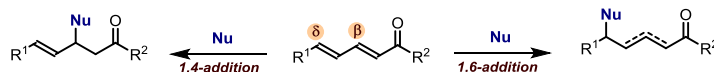
Use of a steering group at the  $\beta$ -dienal position to control the molecular topology of the catalytically active vinylogous iminium ion intermediate in order to secure high stereo- and regio-selectivity.<sup>1</sup>

## 3.1 Introduction

In spite of the large body of literature dealing with asymmetric 1,4-conjugate additions, the analogous 1,6-additions have remained largely underdeveloped. Such reactions are undoubtedly difficult since nucleophilic conjugate additions to  $\alpha,\beta,\gamma,\delta$ -diunsaturated carbonyl compounds are complicated by the presence of three possible competing pathways: 1,2-, 1,4-, and 1,6-addition manifolds are all feasible (Scheme 3.1).

### Competing conjugate addition pathways

$\alpha,\beta,\gamma,\delta$ -unsaturated carbonyl compounds



Scheme 3.1 – Conjugate addition on unsaturated and bis-unsaturated carbonyl compounds (1,2-addition not shown).

Although the possibility of exploiting the principle of vinylogy (see Chapter I and II) for developing 1,6-conjugate additions has been known for several decades,<sup>2</sup> channeling the

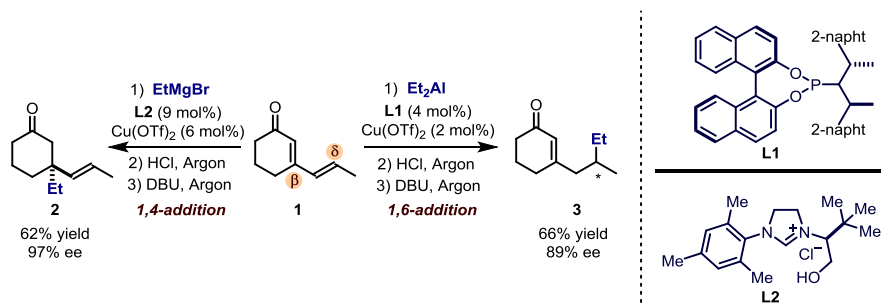
<sup>1</sup> The work discussed in this chapter has been published, see: Silvi, M; Chatterjee, I.; Liu, Y.; Melchiorre, P. "Controlling the Molecular Topology of Vinylogous Iminium Ions by Logical Substrate Design: Highly Regio- and Stereoselective Aminocatalytic 1,6-Addition to Linear 2,4-Dienals" *Angew. Chem. Int. Ed.* **2013**, *52*, 10780.



reaction with high regioselectivity toward 1,6-addition manifold is far from easy. The site-selectivity depends on both steric and electronic effects within the starting unsaturated systems, along with the nature of the nucleophile used. The development of an enantioselective catalytic strategy for such reactions is even more challenging, since it requires the formation of stereogenic centers remote from the catalyst's point of action.

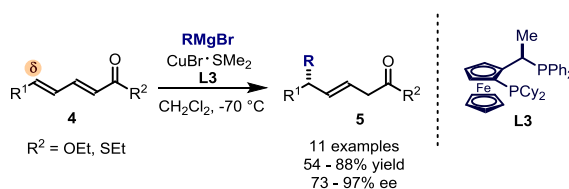
Recently, organometallic chemistry successfully achieved this target, mainly using copper or rhodium-based catalytic systems.<sup>3</sup> In 2008, Alexakis *et al.* reported a remarkable regiodivergent approach for the asymmetric  $\delta$ -site functionalization of cyclic  $\alpha,\beta,\gamma,\delta$ -unsaturated dienones (Scheme 3.2).<sup>4</sup> By simply modulating the reaction conditions, either the 1,6-addition product (**3**) or the 1,4- functionalized adduct **2** could be selectively accessed "at will" with good yield and high enantioselectivity.

**Regiodivergent approach**



**Scheme 3.2** – A regiodivergent approach for the asymmetric functionalization of cyclic dienones.

The same year, Feringa *et al.* reported a highly efficient methodology for the enantioselective  $\delta$ -site selective addition of Grignard reagents to linear esters (Scheme 3.3).<sup>5</sup>



**Scheme 3.3** – Asymmetric alkylation of linear dienones at the  $\delta$  position.

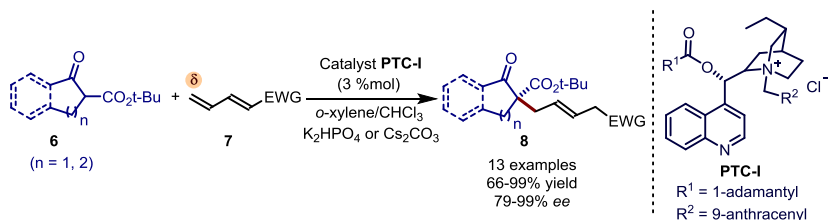
<sup>2</sup> J. W. Ralls. "Unsymmetrical 1,6-Additions to Conjugated Systems" *Chem. Rev.* **1959**, 59, 329.

<sup>3</sup> For reviews see: a) Csáký, A. C.; de la Herrán, G.; Murcia, M. C. "Conjugate Addition Reactions of Carbon Nucleophiles to Electron-Deficient Dienes" *Chem. Soc. Rev.* **2010**, 39, 4080. b) Silva, E. M. P.; Silva, A. M. S. "1,6-Conjugate Addition of Nucleophiles to  $\alpha,\beta,\gamma,\delta$ -Diunsaturated Systems" *Synthesis* **2012**, 44, 3109.

<sup>4</sup> Hénon, H.; Mauduit, M.; Alexakis, A. "Regiodivergent 1,4 versus 1,6 Asymmetric Copper-Catalyzed Conjugate Addition" *Angew. Chem. Int. Ed.* **2008**, 47, 9122.

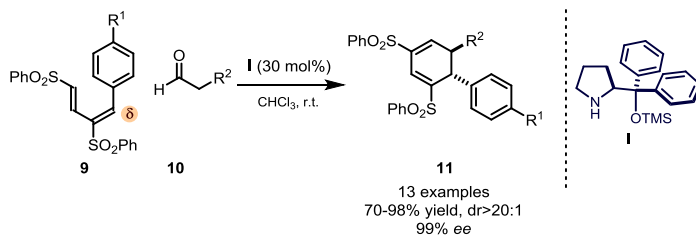
<sup>5</sup> Den Hartog, T.; Harutyunyan, S. R.; Font, D.; Minnaard, A. J.; Feringa, B. L. "Catalytic Enantioselective 1,6-Conjugate Addition of Grignard Reagents to Linear Dienoates" *Angew. Chem. Int. Ed.* **2008**, 47, 398.

Recent studies have demonstrated that organocatalysis can provide useful alternatives for the design of enantio- and regio-selective 1,6-addition reactions. In 2007, Jørgensen and coworkers reported the  $\delta$ -site selective, asymmetric addition of  $\beta$ -ketoesters **6** to terminal  $\alpha,\beta,\gamma,\delta$ -diunsaturated ketones and nitrocompounds **7** using *Cinchona* alkaloid-based phase transfer catalysts (Scheme 3.4).<sup>6</sup>



**Scheme 3.4** – Organocatalytic asymmetric 1,6-addition to terminal electron-poor dienes under phase transfer catalysis.  
EWG = Electron-withdrawing group.

Organocatalytic 1,6-additions could also be achieved employing transiently formed chiral enamines as nucleophiles. The group of Alexakis and Stephens recently reported a regio- and stereo-selective conjugate addition of catalytically generated enamines to the *ad hoc* designed butadiene **9**.<sup>7</sup> Key to reaction development was the inability of a single sulfonyl group to induce 1,4-enamine addition to vinyl derivatives. This lack of reactivity toward the  $\beta$ -carbon has set the stage for designing a 1,6-conjugate addition, by exploiting the delocalizing ability of a second sulfonyl group placed in  $\gamma$  position. Spontaneous cyclization of the 1,6-conjugate addition product led to the formation of products **11** in high yield and stereoselectivity.



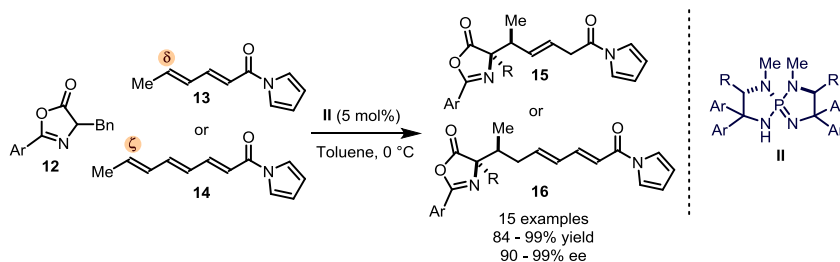
**Scheme 3.5** – Asymmetric 1,6-addition of aldehydes to 1,3-dienic sulfones.

A remarkable example of asymmetric remote conjugate addition to polyenals was reported by Ooi *et al.* Chiral phosphazene base **II** was used as the catalyst in order to ionize azlactones **12**,

<sup>6</sup> Bernardi, L.; López-Cantarero, J.; Niess, B.; Jørgensen, K. A. "Organocatalytic Asymmetric 1,6-Additions of  $\alpha$ -Ketoesters and Glycine Imine" *J. Am. Chem. Soc.* **2007**, *129*, 5772.

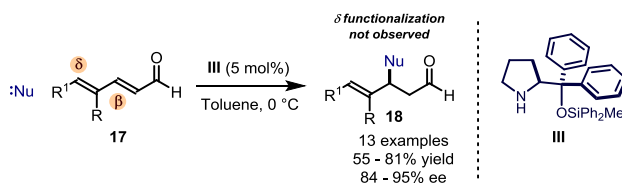
<sup>7</sup> Murphy, J. J.; Quintard, A.; McArdle, P.; Alexakis, A.; Stephens, J. C. "Asymmetric Organocatalytic 1,6-Conjugate Addition of Aldehydes to Dienic Sulfones" *Angew. Chem. Int. Ed.* **2011**, *50*, 5095.

which added stereoselectively to the remote  $\delta$  or  $\zeta$  position of a linear polyunsaturated amide with high efficiency.<sup>8</sup> The product of kinetic protonation was eventually isolated.



**Scheme 3.6** – Asymmetric remote addition of azlactones to unsaturated *N*-acylpyrroles.

As discussed in Chapter II of this dissertation, the propagation of the HOMO-raising electronic effect through the conjugated  $\pi$ -system of poly-unsaturated carbonyl compounds (dienamine and trienamine activations) has become an established aminocatalytic strategy for the direct, regio-, and stereo-selective remote functionalization of carbonyl compounds. In contrast, the possibility of productively merging the iminium ion strategy with the concept of vinylogy has only recently been explored.<sup>9</sup> The successful transmission of the LUMO-lowering effect within the extended  $\pi$ -system of  $\alpha,\beta,\gamma,\delta$ -diunsaturated carbonyl compounds could serve for the stereoselective functionalization of unmodified carbonyl compounds at the remote  $\delta$ -position. The simultaneous control of the regio- and stereo-selectivity in such processes is however difficult, thus justifying the underdevelopment of the field. The difficulties in controlling the stereoselectivity of remote nucleophile addition to vinylogous iminium ion intermediates could be easily figured out considering the large distance between the chiral catalyst and the reactive  $\delta$  carbon. Furthermore, the regioselectivity of the addition of simple nucleophiles to linear conjugated diene in iminium ion-mediated reactions has been recently studied in detail by Hayashi *et al.*,<sup>10</sup> who demonstrated that nitromethane and other simple nucleophiles exclusively added to the  $\beta$  position (Scheme 3.7).



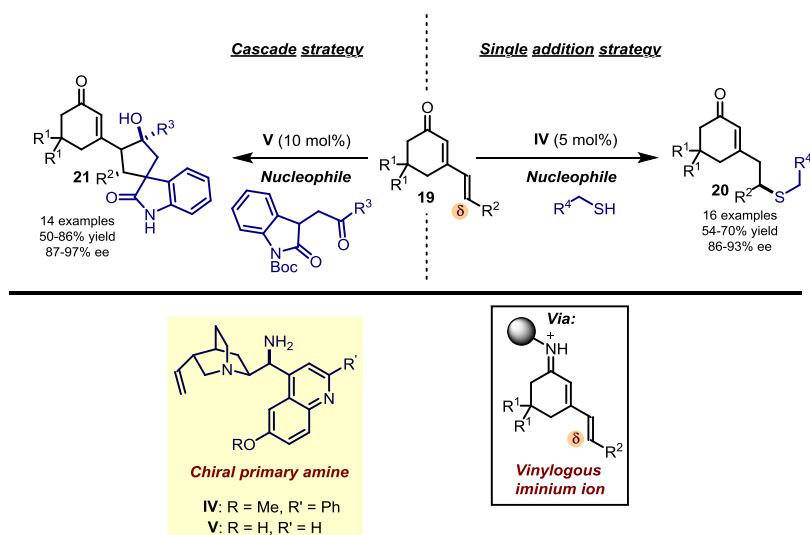
**Scheme 3.7** – Asymmetric addition of various nucleophiles to dienals. The 1,4-addition manifold is preferred.

<sup>8</sup> Uraguchi, D.; Yoshioka, K.; Ueki, Y.; Ooi, T. "Highly Regio-, Diastereo- and Enantioselective 1,6- and 1,8- Additions of Azlactones to Di- and Trienyl *N*-Acylpyrroles" *J. Am. Chem. Soc.* **2012**, *134*, 19370.

<sup>9</sup> Jurberg, I. D.; Chatterjee, I.; Tannert, R.; Melchiorre, P. "When Asymmetric Aminocatalysis Meets the Vinylogy Principle" *Chem. Commun.* **2013**, *49*, 4869.

<sup>10</sup> Hayashi, Y.; Okamura, D.; Umeyama, S.; Uchimarui, T. "Organocatalytic 1,4- Addition Reaction of  $\alpha,\beta,\gamma,\delta$  Diunsaturated Aldehydes versus 1,6-Addition Reaction" *ChemCatChem* **2012**, *4*, 959.

Our research group extensively studied the possibility of directing the regio- and stereo-selectivity of vinylogous iminium ion-mediated reactions by rationally designing structurally defined substrates. Based on our experience on the employment of *Cinchona* alkaloids derivatives as efficient catalysts for the dienamine activation of cyclic enones (Chapter II, Scheme 2.7), we envisioned the possibility to employ an analogous strategy for the vinylogous iminium ion activation of structurally related polyunsaturated carbonyl compounds. This strategy was successfully exploited for the direct 1,6-addition of thiols to unsaturated ketones **19** and for the design of a vinylogous iminium ion-dienamine cascade reactions for the synthesis of complex cyclic compounds **21** (Scheme 3.8).<sup>11</sup>

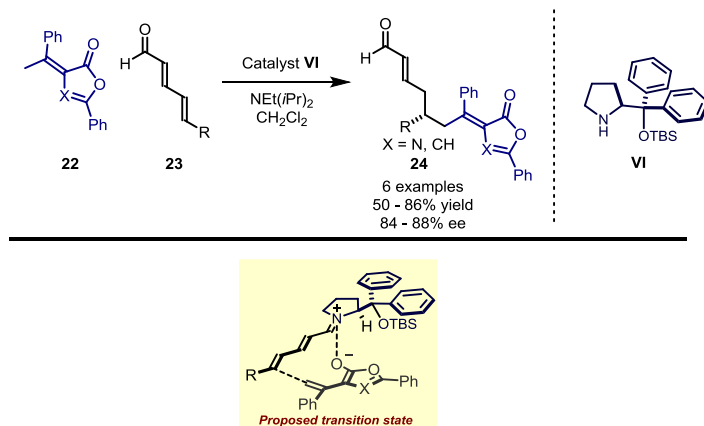


**Scheme 3.8** – Organocatalytic 1,6-addition under vinylogous iminium ion activation. The peculiar cyclic scaffold of **19** leads to complete  $\delta$ -site selectivity.

During the work carried out in this chapter, the group of Jørgensen reported a remarkable conjugate 1,6-addition on linear dienals. They discovered that a particular class of nucleophiles (cyclic azlactones or olefinic butyrolactones) added regioselectively to the  $\delta$  position of aliphatic, completely unbiased, linear dienals under iminium ion activation. The desired products were obtained with high stereoselectivity (Scheme 3.9).<sup>12</sup>

<sup>11</sup> a) Tian, X.; Liu, Y.; Melchiorre, P. "Aminocatalytic Enantioselective 1,6-Additions of Alkyl Thiols to Cyclic Dienones: Vinylogous Iminium Ion Activation" *Angew. Chem. Int. Ed.* **2012**, *51*, 6439. b) Tian, X.; Melchiorre, P. "Control of Remote Stereochemistry in the Synthesis of Spirocyclic Oxindoles by Means of Vinylogous Organocascade Catalysis" *Angew. Chem. Int. Ed.* **2013**, *52*, 5360.

<sup>12</sup> Dell'Amico, L.; Albrecht, Ł.; Naicker, T.; Poulsen, P. H.; Jørgensen, K. A. "Beyond Classical Reactivity Patterns: Shifting from 1,4- to 1,6- Additions in Regio- and Enantioselective Organocatalyzed Vinylogous Reactions of Olefinic Lactones with Enals and 2,4-Dienals" *J. Am. Chem. Soc.* **2013**, *135*, 8063.



Scheme 3.9 – Organocatalytic 1,6- addition of azlactones to linear dienals under vinylogous iminium ion activation.

Although an explanation for the remarkable regioselectivity is not trivial, the authors speculated the existence of a complex net of interactions responsible for directing the conjugate addition towards the remote  $\delta$  position mainly for geometric reasons. Further studies are in need to better elucidate the unexpected reactivity.

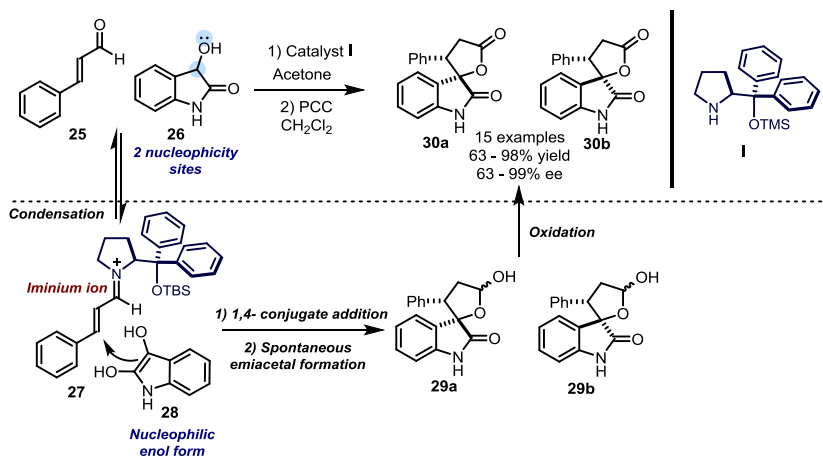
### 3.2 Target of the project

After the success in developing asymmetric 1,6-additions to cyclic dienones (Scheme 3.8), we wondered if the synthetic potential of the vinylogous iminium ion activation could be further harnessed to develop a remote functionalizations of linear dienals. While in the precedent approach we capitalized upon the ability of a chiral amine to stereochemically bias intermediary cyclic vinylogous iminium ion intermediates (as depicted in Scheme 3.8), controlling the molecular topology of an acyclic intermediate, so to ensure highly predictable reaction outcomes, poses a more difficult problem. In particular, we decided to exploit the vinylogous iminium ion reactivity to promote the regio- and stereo-selective 1,6-additions of nucleophiles to linear dienals.

We recently discovered that dioxindole **26** is characterized by a bidentate nucleophilic behavior, which we exploited in iminium ion-mediated reactions to access interesting chiral spirocompounds with high stereocontrol (Scheme 3.10).<sup>13</sup>

<sup>13</sup> a) Bergonzini, G.; Melchiorre, P. "Dioxindole in Asymmetric Catalytic Synthesis: Routes to Enantioenriched 3-Substituted 3-Hydroxyoxindoles and the Preparation of Maremycin A" *Angew. Chem. Int. Ed.* **2012**, *51*, 971. b) Retini, M.; Bergonzini, G.; Melchiorre, P. "Dioxindole in Asymmetric Catalytic synthesis: Direct Access to 3-Substituted 3-Hydroxy-2-oxindoles via 1,4-Additions to Nitroalkenes" *Chem. Commun.* **2012**, *48*, 3336.

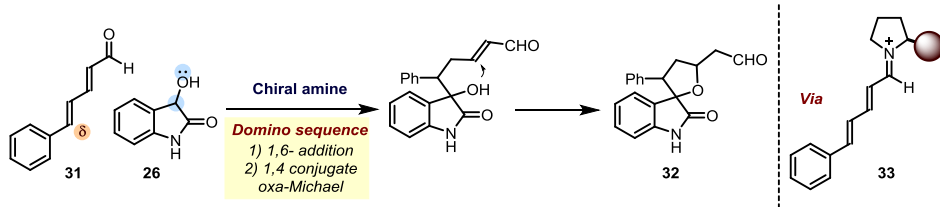
**Dioxindole as bidentate nucleophile**



**Scheme 3.10** – Dioxindole as a bidentate nucleophile for the synthesis of spirooxindoles. PCC = pyridinium chlorochromate

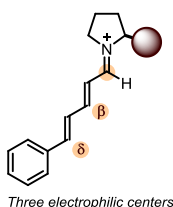
We envisioned to exploit the bidentate nucleophilicity of dioxindole **26** to realize a 1,6- conjugate addition on acyclic dienals while synthesizing biologically interesting, complex chiral molecules. Our design plan, based on the domino reactions sequence detailed in Scheme 3.11, would conclude with an intramolecular *oxa*-Michael cyclization event to forge the spiro-stereocenter within the tetrahydrofuran spirooxindole products **32**.

**The strategy**

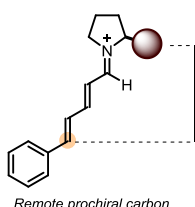


**Challenges**

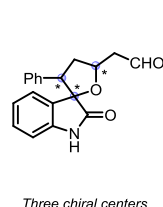
1. Site-selectivity



2. Enantioselectivity

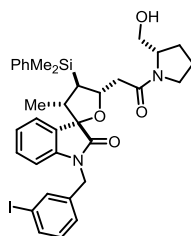


3. Diastereoselectivity



**Scheme 3.11** – The design plan to realize vinylogous organocascade catalysis: 1,6-addition/*oxa*-Michael sequence driven by vinylogous iminium ion/iminium ion activation leading to tetrahydrofuran spirooxindoles **32**.

Spirooxindoles are privileged structures since they carry an appealing spiro architecture often associated with significant biological activity.<sup>14</sup> For this reason, they have been interesting synthetic targets for organic chemists. Schreiber *et al.* studied the bio-activity of tetrahydrofuran spirooxindoles (Figure 3.1).<sup>15</sup> These compounds are powerful antitumor agents and their preparation usually requires a multi-step synthesis and a racemate resolution.



Potent antitumor agent

Figure 3.1 – A tetrahydrofuran spirooxindole with potent cytotoxicity.

As highlighted in Scheme 3.11, several challenges should be addressed in order to successfully develop the strategy. Firstly, the first Michael addition should regioselectively occur at the remote  $\delta$  position over the possible three electrophilic sites. An undesired  $\beta$  addition would result in the formation of products of type **30**, as in Scheme 3.10. Second, the chiral amine catalyst should forge a stereogenic center with high fidelity at the remote  $\delta$  position, six atoms away from the chiral center within the catalyst scaffold. Third, in order to develop a synthetically useful strategy, the product should be formed with high diastereoselectivity. This is not trivial considering that the product structure is adorned with three stereogenic centers.

## 3.3 Results and discussion

### 3.3.1 Starting material design

In our initial experiments, we examined the reactivity of *N*-methyl dioxindole **35** towards the proposed vinylogous cascade reaction with the linear (*E,E*)-hexa-2,4-dienal **34** (Table 3.1). The commercially available diphenylprolinol silyl ether **I** was selected because of its established ability to activate  $\alpha,\beta$ -unsaturated aldehydes toward asymmetric transformations.<sup>16</sup> As

<sup>14</sup> a) Marti, C.; Carreira, E. M. "Construction of Spiro[pyrrolidine-3,3-oxindoles]: Recent Applications to the Synthesis of Oxindole Alkaloids" *Eur. J. Org. Chem.* **2003**, 2209. b) Chowdhury, S.; Chafeev, M.; Liu, S.; Sun, J.; Raina, J.; Chui, R.; Young, W.; Kwan, R.; Fu, J.; Cadieux, J. A. "Discovery of XEN907, a Spirooxindole Blocker of NaV1.7 for the Treatment of Pain" *Bioorg. Med. Chem. Lett.* **2011**, *21*, 3676. c) Eastwood, P.; Gonzalez, J.; Gomez, E.; Caturla, F.; Aguilar, N.; Mir, M.; Aiguade, J.; Matassa, V.; Balague, C.; Orellana, A.; Dominguez, M. "Indolin-2-one p38a Inhibitors III: Bioisosteric Amide Replacement" *Bioorg. Med. Chem. Lett.* **2011**, *21*, 6253.

<sup>15</sup> Franz, A. K.; Dreyfuss, P. D.; Schreiber, S. L. "Synthesis and Cellular Profiling of Diverse Organosilicon Small Molecules" *J. Am. Chem. Soc.* **2007**, *129*, 1021.

<sup>16</sup> Jensen, K. L.; Dickmeiss, G.; Jiang, H.; Albrecht, Ł.; Jørgensen, K. A. "The Diarylprolinol Silyl Ether System: A General Organocatalyst" *Acc. Chem. Res.* **2012**, *45*, 248.

expected, in consonance with the traditional reactivity of vinylogous iminium ion intermediates depicted in Scheme 3.7, the reaction followed an exclusive  $\beta$ -site selective pathway.

As discussed in Chapter 2 of this dissertation, the inherent steric bias created by the introduction of an opportune alkyl substituent within the starting material structure can modulate the regioselectivity in reactions involving vinylogous organocatalytic intermediates. Aware of this lesson, we envisioned to place a suitable alkyl substituent at the  $\beta$  position of the starting dienal in order to suppress the competing 1,4-addition pathway.

Table 3.1 – Influence of the  $\beta$  substituent on the reaction outcome.

entry	34	R	R <sup>1</sup>	Yield of 37 (%)	Yield of 36 (%)	ee of 37 (%)	dr of 37
1	a	H	Me	0	69	-	-
2	b	Me	<i>n</i> -Bu	0	70	-	-
3	c	Me	Ph	35	35	n.d.	3:1
4	d	Ph	Ph	72 <sup>a</sup>	0	46	8:1

Reactions carried out on a 0.1 mmol scale. Yield determined by <sup>1</sup>H NMR analysis of the crude reaction mixture using 2,6-dimethylfuran as the internal standard. Enantiomeric excess determined by HPLC analysis on a chiral stationary phase. In every occasion, products **36** were obtained as an equimolar mixture of diastereoisomers. <sup>a</sup>Yield of the isolated single major diastereoisomer after purification through silica gel flash column chromatography.

As presented in Table 3.1, the introduction of a methyl substituent in  $\beta$  position did not provide enough steric bias to ensure a good level of regioselectivity in the desired reaction, although 35% yield of the desired remote  $\delta$ -functionalization product was observed in the reaction crude in entry 3. Introducing a phenyl moiety at the  $\beta$ -position of **34** completely switched the site selectivity toward the desired 1,6-addition driven by vinylogous iminium ion activation (entry 4). The tetrahydrofuran spirooxindole **37** was formed in good yield with a good control over the relative stereochemistry of the three stereogenic centers (8:1 d.r.). However, the enantioselectivity of the process was far below a synthetically useful level (46% ee), and no improvement were observed modifying the reaction parameters (solvent, acid, temperature). Notably, during our investigations, we noticed that the dienal **34d** was not configurationally stable, since a scrambling of the  $\alpha,\beta$ -carbon double bond configuration was observed in the presence of the catalyst **I** (from *E* to *Z*), see Figures 3.2 and 3.3.



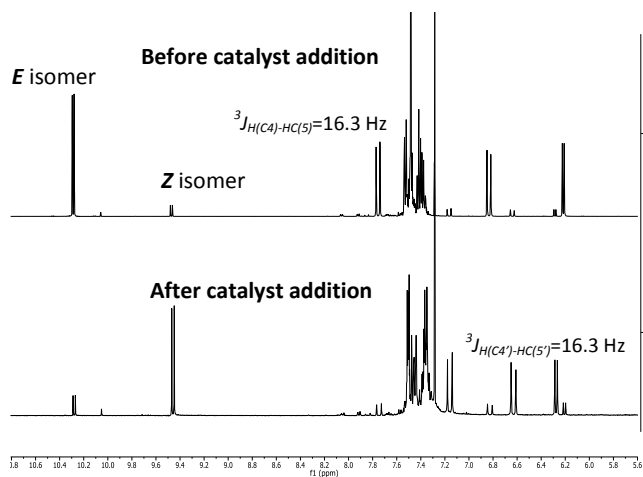


Figure 3.2 – Isomerization of the aldehyde **34d** upon exposure to amine **I** in  $\text{CDCl}_3$ .

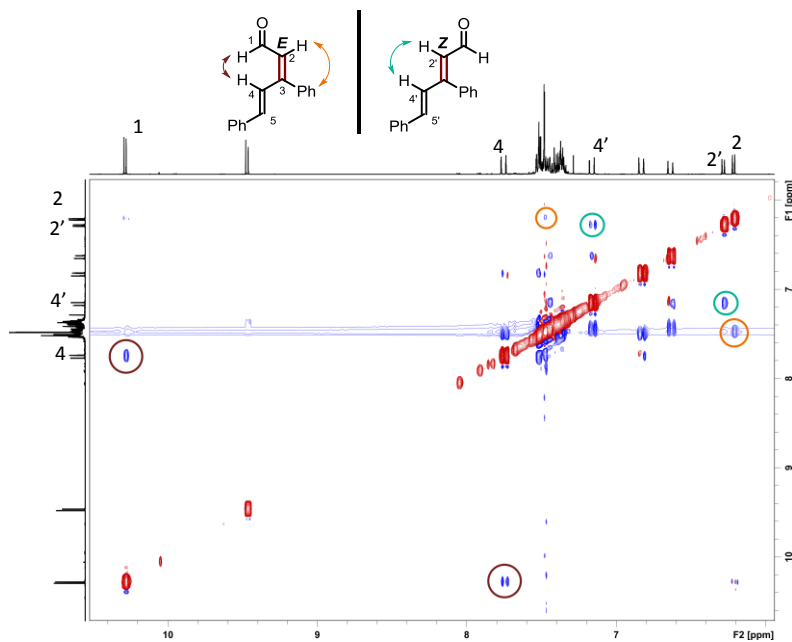
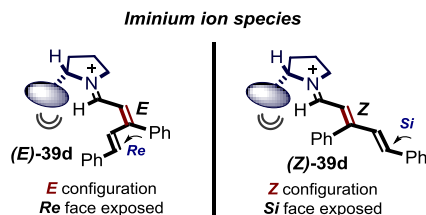


Figure 3.3 – NOESY spectrum of a mixture ~ 1:1 of the two isomers of **34d** observed in solution.

We ascribed the low enantioselectivity observed in the cascade reaction to the configurational lability of the substrate, which is translated directly to the iminium ion intermediate. NMR spectroscopic studies of the covalent vinylogous iminium ion intermediate, formed in  $\text{CDCl}_3$  by condensation of **I** and **34d** in the presence of molecular sieves, confirmed that the geometrical promiscuity of the dienal **34d** is translated into the catalytically active species: two geometries

for the iminium ion **39d** were detected.<sup>17</sup> The lack of structural preorganization makes it difficult for the chiral catalyst **I** to ensure configurational control and  $\pi$ -facial discrimination of the covalent intermediate, factors which are essential in enforcing high levels of enantioselectivity in iminium ion based chemistry (Figure 3.4).<sup>18</sup>



**Figure 3.4** – Rationalization for the poor enantioselectivity observed using aldehyde **34d** as starting material.

We hypothesized that the presence of a bulky substituent at the  $\beta$ -position of the starting dienal could serve for freezing out a specific geometry of the molecular iminium ion assembly by enhancing repulsive steric interactions. The dienal **38**, bearing a *tert*-butyl moiety, was purposely synthesized (Figure 3.5). We were pleased to confirm that the defined *E,E* double bond geometry was stable under the reaction conditions, since no isomerization was observed in the presence of catalyst **I**.

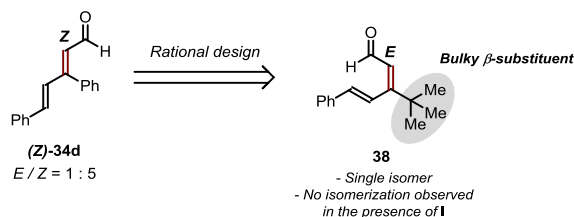


**Figure 3.5** – Rational starting material design.

NOESY spectra of the starting material revealed that the role of the *tert*-butyl group is not limited to fixing the geometry of the  $C(\alpha)$ - $C(\beta)$  double bond. Indeed, the steric prominence of the  $\beta$ -substituent makes it a topologically dominant element, since it is able to enforce an uncommon *s-cis* conformation around the single  $C(\beta)$ - $C(\gamma)$  bond, as inferred on the basis of NOESY investigation (Figure 3.7).<sup>19</sup> In order to correctly assign the identity of the two protons in

<sup>17</sup> See annex I for details.

<sup>18</sup> Grošelj, U.; Seebach, D.; Badine, M.; Schweizer, W. B.; Beck, A. K. "Structures of the Reactive Intermediates in Organocatalysis with Diarylprolinol Ethers" *Helv. Chim. Acta* **2009**, *92*, 1225.

<sup>19</sup> The tendency of *tert*-butyl substituted olefins to enforce a *s-cis* conformational preference in vicinal single bonds has been already observed and reported in literature: a) Ernst, L.; Hopf, H.; Krause, N. "Retinoids. 6. Preparation of Alkyl and Trimethylsilyl-Substituted Retinoids via Conjugate Addition of Cuprates to Acetylenic Esters" *J. Org. Chem.* **1987**, *52*, 398. b) De Lera, A. R.; Okamura, W. H. "19,19- and 20,20,20-Trimethylretinal: Side Chain *tert*-Butyl Substituted Retinals" *Tetrahedron Lett.* **1987**, *28*, 2921. c) De Lera, A. R.; Reischl, W.; Okamura, W. H. "On the Thermal Behavior of Schiff Bases of Retinal and its Analogues: 1,2-

C( $\gamma$ )-C( $\delta$ ), crucial for the correct interpretation of the NOESY signals, a deuterium labelling experiment was performed (Figure 3.6),<sup>20</sup> since traditional bidimensional analysis (HSQC, HMBC) were not sufficient for an unambiguous assignment.

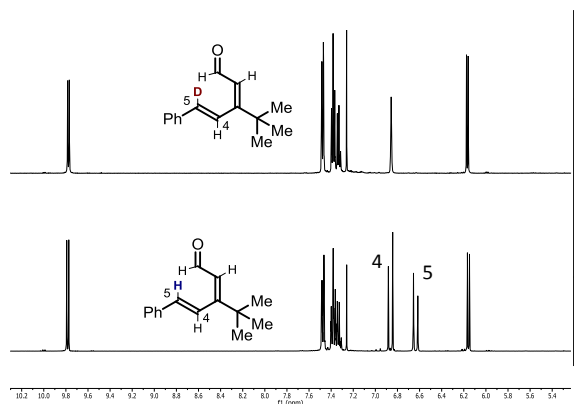


Figure 3.6 – Deuterium labelling experiment for unambiguous assignment of protons 4 and 5 in compound **38**.

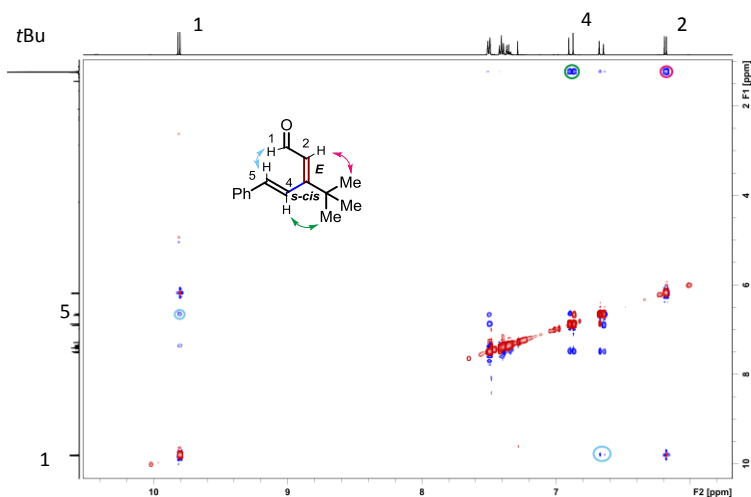


Figure 3.7 – NOESY spectrum of compound **38**.

The peculiar geometry of compound **38** prompted us to further investigate the system in order to study whether the conformational rigidity observed in the starting material was maintained in the transient vinylogous iminium ion **39**, the reactive intermediate of the studied reaction.

Dihydropyridine Formation *via* Six- $\pi$ -Electron Electrocyclization of 13-Cis Isomers" *J. Am. Chem. Soc.* **1989**, *111*, 4051. The conformational preference could be observed also in an increased reactivity towards particular reactions *i.e.* Diels-Alder reactions: d) Craig, D.; Shipman, J. J.; Fowler, R. B. "The Rate of Reaction of Maleic Anhydride with 1,3-Dienes as Related to Diene Conformation" *J. Am. Chem. Soc.* **1961**, *83*, 2885.

<sup>20</sup> The deuterium labelled compound was synthesized starting from benzaldehyde- $\alpha$ - $d_1$  according to Scheme 3.17 (see the Experimental Section).

Compound **39** was synthesized by simply stirring an equimolar amount of starting aldehyde **38**, catalyst **I** and benzoic acid in dry  $\text{CDCl}_3$  under an argon atmosphere. The crude reaction mixture was then placed in a dry Young NMR tube under an argon atmosphere and analyzed through NMR spectroscopy (Figure 3.8). A single isomer was detected, and the conformational behavior was investigated by conventional NMR techniques, particularly vicinal coupling constant analysis and monodimensional nOe experiments. The results of the investigation are highlighted in Figures 3.8 - 3.11.

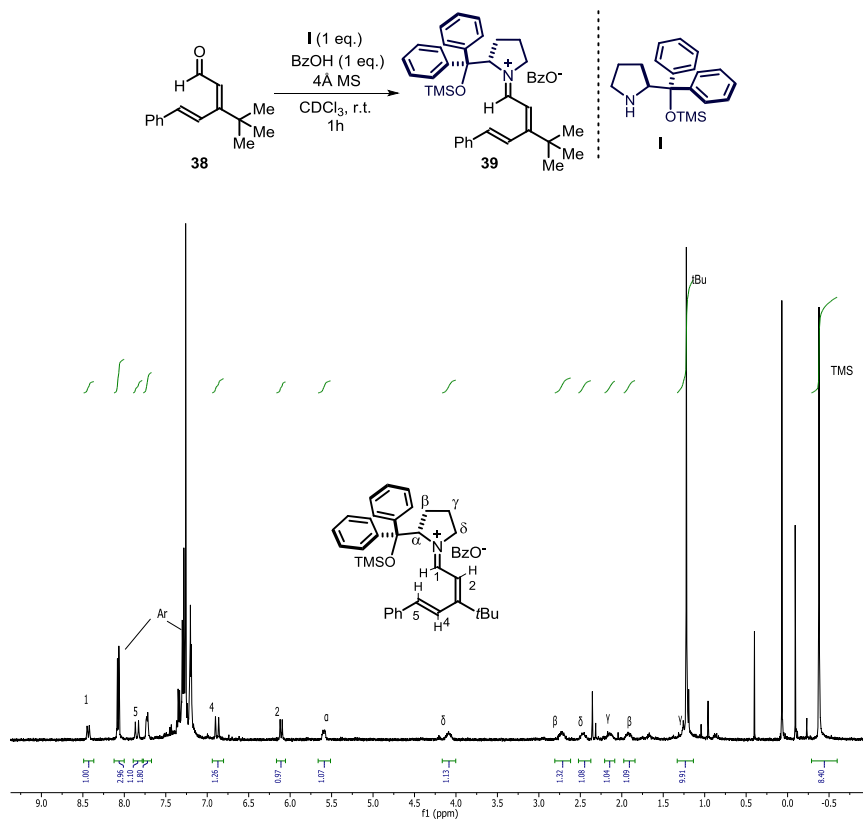


Figure 3.8 –  $^1\text{H}$  NMR spectrum of iminium ion **39**.

Again, deuterium labelling of the substrate **38** helped us to unambiguously assign protons 4 and 5 of compound **39**.

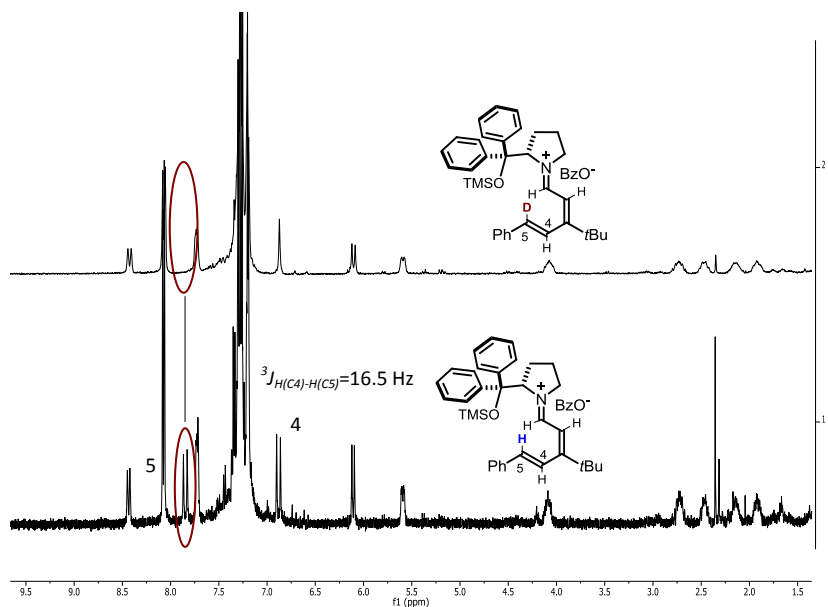


Figure 3.9 – Deuterium labelling experiment for the unambiguous assignment of protons 4 and 5 in compound 39.

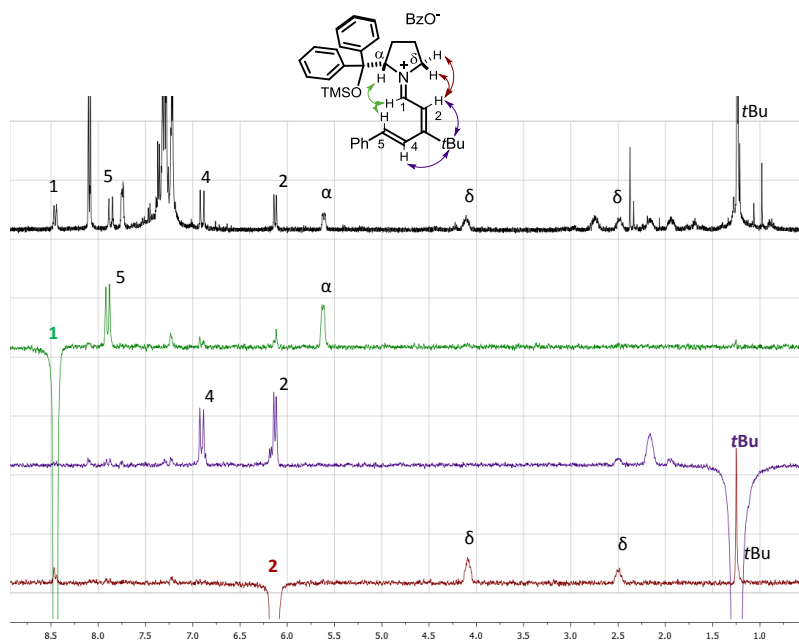
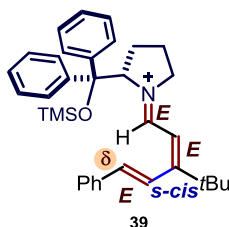
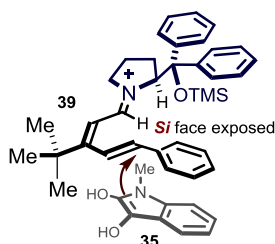


Figure 3.10 – Conformational analysis carried out on compound 39. Selected monodimensional NOE experiments are shown.



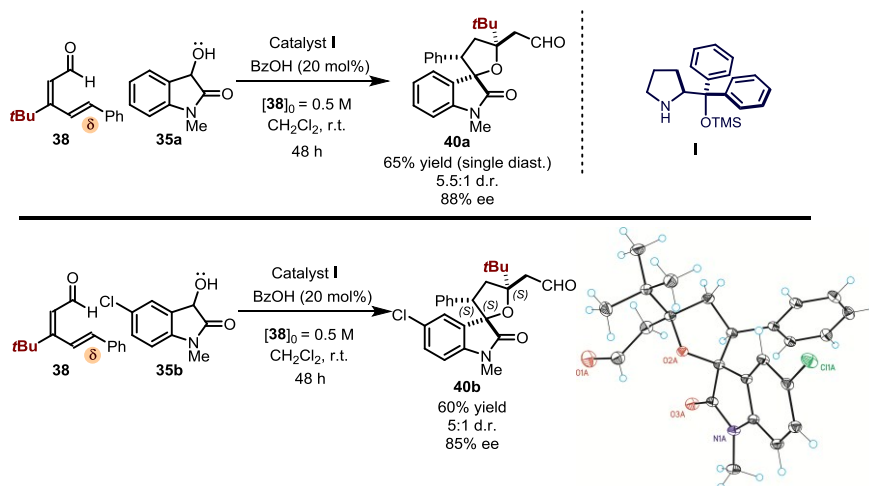
**Figure 3.11** - The conformational preference of compound **39**: the chiral fragment of catalyst **I** lays surprisingly close to the reactive  $\delta$  carbon.

Overall, the NMR studies indicated that the transient vinylogous iminium ion **39** in solution has an (*E,E,E*) configuration of the three double bonds. Interestingly, the peculiar *s-cis* conformation of the single C( $\beta$ )-C( $\gamma$ ) bond observed in the starting aldehyde is conserved within the vinylogous iminium ion reactive intermediate. Collectively, these features contribute to a highly preorganized, configurationally stable, transient intermediate (Figure 3.11). Indeed, the chiral fragment in **39** seems positioned close enough to the reactive  $\delta$ -carbon atom to determine an effective shielding of the *Re* face of the extended iminium ion, thus leaving the opposite *Si* face available for the approach of the dioxindole **35** (Figure 3.12).



**Figure 3.12** – Possible stereochemical outcome of the nucleophile addition to vinylogous iminium ion **39**.

To verify our predictions, we evaluated the impact of the *tert*-butyl group of **38** on the stereochemical outcome of the vinylogous cascade reaction. We were delighted to observe that the spirocompound **40a** was obtained with perfect  $\delta$ -site selectivity and an enantioselectivity as high as 88%. The use of the chloro-containing dioxindole **35b** resulted in similar reaction efficiency. The corresponding tetrahydrofuran spirooxindole **40b** was obtained with synthetically useful results (Scheme 3.12).



**Scheme 3.12** – Results obtained using dienal **38** as the starting aldehyde and the absolute configuration of the product **40b**, as unambiguously inferred through x-ray diffraction analysis.

The absolute and relative configuration for the major diastereomer of compound **40b** was unambiguously determined by anomalous dispersion X-ray crystallographic analysis: an (*S*)-absolute configuration at the newly formed  $\delta$ -stereocenter was inferred. The sense of asymmetric induction is in perfect agreement with the stereochemical model extrapolated from the conformational analysis discussed above.<sup>21</sup>

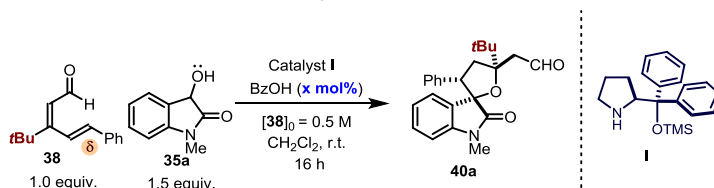
Having identified a viable strategy to control the regio- and stereo-selectivity of the vinylogous cascade, we sought to increase the efficiency of the catalytic system.

### 3.3.2 Optimization studies

Starting from the conditions detailed in Scheme 3.12, we evaluated variations of the standard reaction parameters. Interestingly, reducing the reaction time to 16 hours, a third diastereoisomer was detected in the crude reaction mixture (the product was isolated and characterized). The amount of this diastereoisomer was strictly correlated to the acidic additive loading (Table 3.2).

<sup>21</sup> In this model we assume that minor conformers do not show much higher reactivity than the major one observed in solution. In fact this eventuality would lead to a Curtin-Hammett scenario in which minor conformers, although not clearly observable through NMR techniques, would be the real reactive species in the chemistry.

**Table 3.2** – Influence of the  $\beta$  substituent on the reaction outcome.



entry <sup>a</sup>	Acid ( <b>x mol%</b> )	Conv. (%)	ee (%)	d.r. <b>40a</b>
1	0	n.r.	-	-
2	20	>99	87	54:15:31
3	50	>99	89	70:13:14
4	75	>99	90	78:13:9
5	100	>99	90	79:12:9

The reactions were carried out in capped vials in freshly distilled  $\text{CH}_2\text{Cl}_2$  (SPS system) on a 0.05 mmol scale and analyzed after 16 hours. Conversion measured by  $^1\text{H}$  NMR as reported in the experimental part.

In order to explain the phenomenon, we carefully studied the crude reaction mixture composition over the time. Interestingly, we observed that one of the diastereoisomer was interconverting into the other during the course of the reaction (**40a-3**  $\rightarrow$  **40a-1**, Figure 3.13). The study was carried out by means of NMR analysis, using 1 equivalent of 2,5-dimethylfuran as the internal standard. The use of an internal standard in this study is pivotal in order to rule out the possibility of product degradation, which could vary the relative amount of diastereoisomers also in absence of any interconversion.



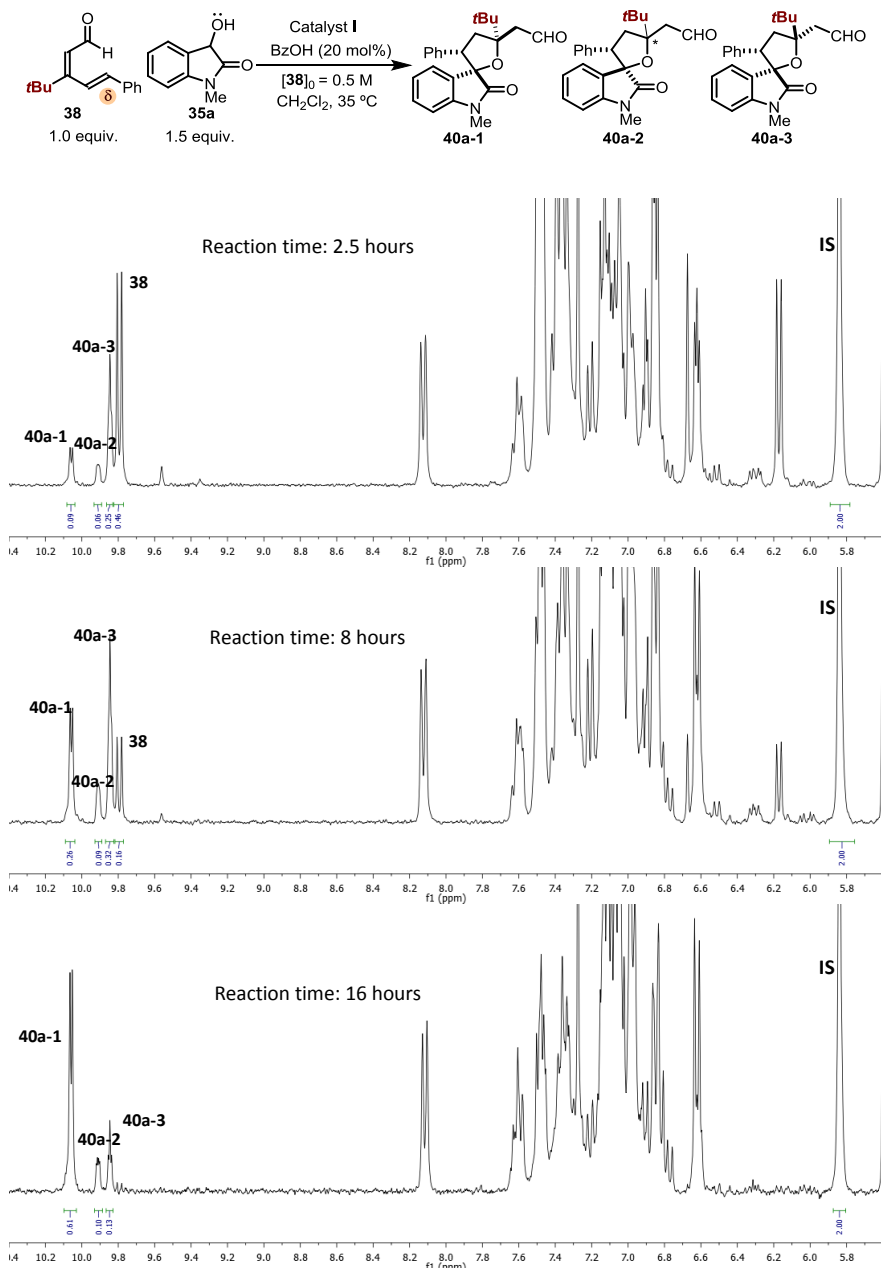
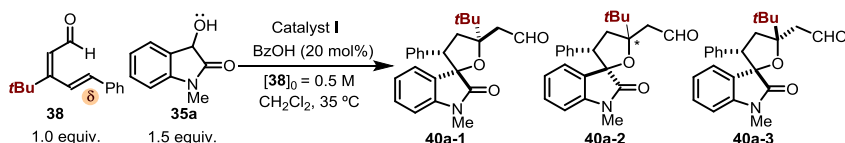


Figure 3.13 – Evolution of the product distribution over the time. Conversion of diastereoisomer 40a-3 into 40a-1 was observed during the time.

As presented in Figure 3.13, a first kinetic diastereoisomer (**40a-3**) was firstly generated in the reaction mixture. The compound is slowly converted into the final compound **40a-1**, the thermodynamically favored diastereoisomer. More interesting was the analysis of the enantiomeric excess of the final reaction product **40a-1**, which increased during the time (Table 3.3).

**Table 3.3** – Monitoring the reaction over the time. An unexpected increase of the compound **40a-1**'s enantiomeric excess was observed over the time.



entry	Time (h)	Conv. (%)	ee of <b>40a-1</b> (%)	ee of <b>40a-3</b> (%)	yield <b>40a(1-2-3)</b>
1	2.5	64	60	97	9:6:25
2	8	81	81	95	26:9:32
3	16	>99	89	n.d.	61:10:13

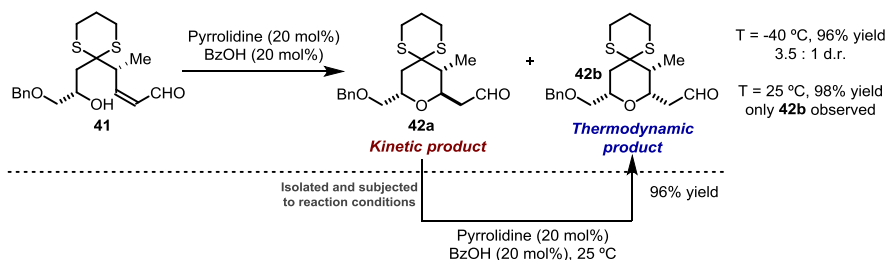
The reactions were carried out in capped vials in freshly distilled  $\text{CH}_2\text{Cl}_2$  (SPS system) on a 0.1 mmol scale. NMR yields obtained using 2,6-dimethyl furan as internal standard (see Figure 3.13 for details). Conversion measured by  $^1\text{H}$  NMR analysis, as detailed in the experimental part.

In a separate test experiment, we observed that the isolated kinetic diastereoisomer **40a-3** could be quantitatively converted into the thermodynamic **40a-1** by simply mixing it with benzoic acid in  $\text{CH}_2\text{Cl}_2$  solution. This phenomenon explains the strict correlation between the diastereomeric ratio and the acidic additive loading.

It is known that *oxa*-Michael additions are usually reversible processes, a fact which renders the development of asymmetric versions extremely difficult, due to the occurrence of product racemization.<sup>22</sup> It has been already reported that intramolecular iminium ion-mediated *oxa*-Michael reactions can be reversible while showing phenomena of diastereoisomer interconversions (Scheme 3.13).<sup>23</sup> The authors reported that the intramolecular *oxa*-Michael cyclization reaction of compound **41** led to the two diastereoisomers **42a** and **42b**. At low temperature ( $-40 \text{ }^\circ\text{C}$ ), the compound **42a** was the major product, whereas conducting the reaction at room temperature compound **42b** was the only one detected in the reaction mixture. Purification of compound **42a** and subjection to the reaction conditions led to compound **42b** as the only product in high yield.

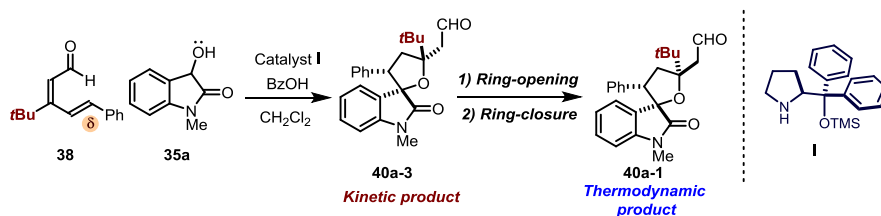
<sup>22</sup> Bertelsen, S.; Dinér, P.; Johansen, R. L.; Jørgensen, K. A. "Asymmetric Organocatalytic  $\beta$ -Hydroxylation of  $\alpha,\beta$ -Unsaturated Aldehydes" *J. Am. Chem. Soc.* **2007**, *129*, 1536.

<sup>23</sup> Lee, K.; Kim, H.; Hong, J. "Stereoselective Synthesis of Tetrahydropyrans through Tandem and Organocatalytic *oxa*-Michael Reactions: Synthesis of the Tetrahydropyran Cores of *ent*-(+)-Sorangicin A" *Eur. J. Org. Chem.* **2012**, 1025.



**Scheme 3.13** – Iminium ion mediated intramolecular oxa-Michael cyclization. Diastereoisomer interconversion was observed under the reaction conditions.

We believe that the inherent reversibility of the oxa-Michael reaction serves as the vehicle of diastereoisomer interconversion also in our system. The first stereogenic center is forged in an irreversible carbon-carbon bond forming process (1,6-addition), so the reversibility of the oxa-Michael reaction simply leads to an epimerization process and, consequently, to the thermodynamically favored diastereoisomer.

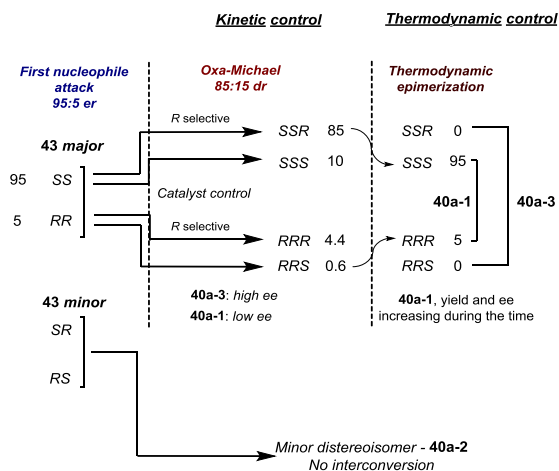
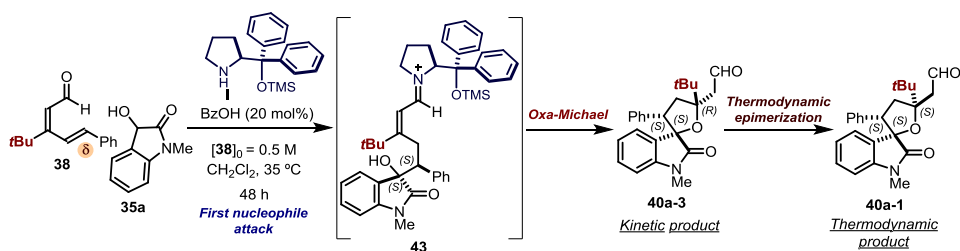


**Scheme 3.14** – Rationale for the observed isomerization.

To rationalize the peculiar increase of enantiomeric excess during the time, we recall the concept of statistical asymmetric amplification during multiple asymmetric processes, a concept whose chemists sometimes refer to as the “Horeau principle”.<sup>25,26</sup>

<sup>25</sup> The first statistical asymmetric amplifications were observed and quantified in dimerization reactions, and were used in order to increase the optical purity of chiral compounds: a) Vigneron, J. P.; Dhaenens, M.; Horeau, A. “Nouvelle Methode pour Porter au Maximum la Pureté Optique d’un Produit Partiellement Dedouble Sans l’Aide d’Acune Substance Chirale” *Tetrahedron* **1973**, *29*, 1055. From there, several examples have been reported, some examples: b) Fleming, I.; Ghosh, S. K. “A Simple Method for Enriching the Enantiomeric Purity of a Functional Molecule Already Rich in One Enantiomer.” *J. Chem. Soc., Chem. Commun.* **1994**, 99. c) Han, X.; Corey, E. J. “A Catalytic Enantioselective Total Synthesis of (-)-Wodeshiol” *Org. Lett.* **1999**, *1*, 1871.

<sup>26</sup> For an elegant example of asymmetric amplification in a catalytic multiple enantioselective transformation, see: Huo, S.; Negishi, E.-I. “A Convenient and Asymmetric Protocol for the Synthesis of Natural Products Containing Chiral Alkyl Chains via Zr-Catalyzed Asymmetric Carboalumination of Alkenes. Synthesis of Phytol and Vitamins E and K” *Org. Lett.* **2001**, *3*, 3253.



**Scheme 3.15** – A rational model to explain the increase of enantiomeric excess of the final product **40a-1** observed under the reaction conditions.

In the model reported in Scheme 3.15, we propose a possible explanation for the stereochemical outcome. In the first 1,6 nucleophilic addition, expected to be irreversible, two stereogenic centers are simultaneously generated and the intermediate **43** is formed as a couple of diastereoisomers (indicated in Scheme 3.15 as **43 major** and **43 minor**). The minor diastereoisomer **43 minor** (which is present as the couple of enantiomers *SR* and *RS*) will follow an *oxa*-Michael reaction leading to the final minor diastereoisomer **40a-2** observed at the end of the process. This compound does not have possibility of interconversion in the final product **40a-1** (opposite absolute configuration of the stable spiro-stereocenter), and cannot interfere with the enantiomeric excess of the final products **40a-1** – **40a-3**. Instead, the fate of the diastereoisomer **43 major** (present as the couple of enantiomers *SS* and *RR*) is more interesting since it is directly involved in the stereoselectivity of the final products **40a-1** – **40a-3**. The first 1,6-addition forges **43 major** with a certain enantiomeric ratio, which we assume to be 95:5 (Scheme 3.15). We consider that the following *oxa*-Michael cyclization is completely under catalyst control (absence of matched/mismatched effects when forging the third stereocenter in **40a-3**). This condition is often indicated as *absence of internal chiral recognition* in similar

processes.<sup>27</sup> The chiral catalyst would induce a specific stereoselectivity in the *oxa*-Michael step (we assume in the model a dr of 85:15 favoring the R stereocenter), which would build upon the original enantiomeric distribution established after the 1,6-addition event. This model would be a classical example of statistical asymmetric amplification, leading the formation of **40a-3** in extremely high enantiomeric excess (see Scheme 3.15, compound **40a-3**, *kinetic control*). Under kinetic control, the stereoisomer **40a-1** (which is the thermodynamically favored) would have a low enantiomeric excess (Scheme 3.15, compound **40a-1**). This peculiar distribution of enantiomeric excess values is consonant with our observations (see Table 3.3).<sup>28</sup>

In case of reversibility of the second step (*oxa*-Michael, a process well-known to be reversible), the kinetic diastereoisomer **40a-3** would be progressively converted into the thermodynamic diastereoisomer **40a-1**, constantly increasing its enantiomeric excess (see scheme 3.15, conversion from *kinetic control* to *thermodynamic control*). The final d.r. between the two diastereoisomers **40a-1** and **40a-3** will reach the thermodynamic ratio at the end of the process. In the limit case presented in Scheme 3.15, the kinetic diastereoisomer **40a-3** will be completely converted into the thermodynamic **40a-1**. An important observation of this model is that *in the case of a complete conversion of the kinetic diastereoisomer 40a-3 into the thermodynamic 40a-1, the enantiomeric excess observed in the final product 40a-1 would be identical to the enantiomeric excess of the 1,6-addition of the dioxindole to the transient iminium ion species (compound 43 major)*, and this can give information about the entity of asymmetric induction operated by catalyst I in the first nucleophile attack of the process.

Carrying out the reaction for longer reaction time (*i.e.* 48 h) the amount of kinetic diastereoisomer **40a-3** is below 5% yield (see Figure 3.14). For this reason we believe that the model presented in Scheme 3.15 describes with good fidelity our reaction.

---

<sup>27</sup> We considered a simplified model in which no internal chiral recognition is present in order to build a clear and comprehensible model. In the presence of partial internal chiral recognition (partial substrate control), the value of enantiomeric excess of the kinetic isomer would not be possible to calculate with a simple mathematical model. Anyway, the final result of thermodynamic equilibration reported in Scheme 3.15 would be the same as in our simplified model.

<sup>28</sup> In our model, we considered the hypothetical values of 19:1 er (90% ee) for the first attack and 8.5:1 dr for the second process, these values are reported just as exemplificative numbers for explaining our model.

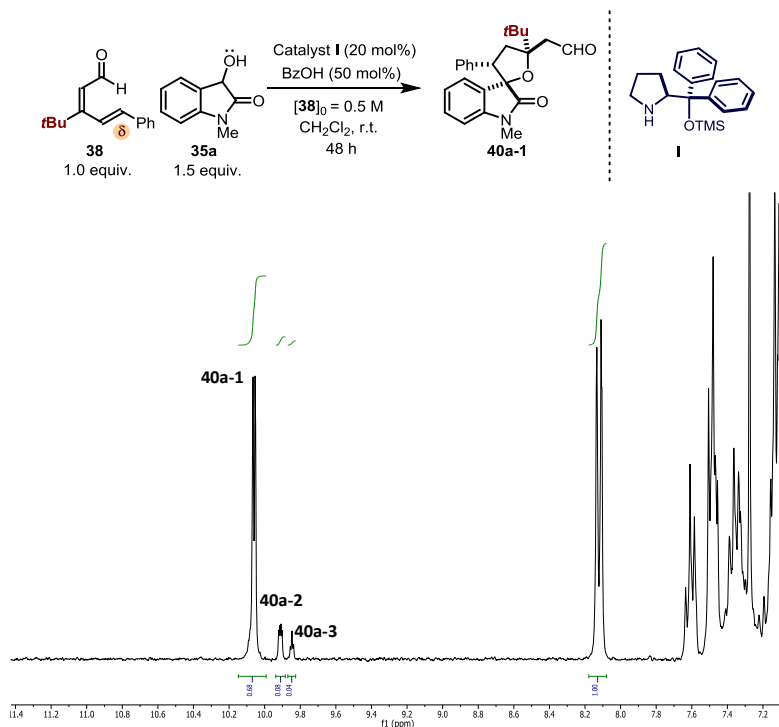


**Figure 3.14** – Reaction carried out for 48 h. The amount of kinetic diastereoisomer is below 5% yield. NMR yield calculated using benzoic acid as internal standard.

On the basis of the observation reported above, we focused our optimization studies in speeding up the conversion of the kinetic product **40a-3** into the final compound **40a-1**.

**Table 3.4** – Final optimization cycle.

entry <sup>a</sup>	T (°C)	Acid (x % mol)	Conv. (%)	ee (%)	d.r. <b>40a(1-2-3)</b>
1	r.t.	37.5	81	84	46:15:40
2	r.t.	50	86	86	55:13:31
3	35	10	81	82	38:16:47
4	35	20	>99	89	67:14:19
5	35	50	>99	90	81:12:7

The reactions were carried out in capped vials in freshly distilled CH<sub>2</sub>Cl<sub>2</sub> (SPS system) on a 0.05 mmol scale. The reactions were analyzed after 16 hours. Conversion measured by <sup>1</sup>H NMR as reported in the experimental part.

Slightly modifying the reaction parameters (temperature and acid loading) we could obtain the desired product **40a-1** with high stereoselectivity using half catalyst loading (10 mol%).

### 3.3.3 The reaction scope

With the optimized conditions in hand, we sought to evaluate the scope of the transformation. In order to make sure to reach full equilibration of the diastereoisomers in all the cases, we increased the reaction time from 16 hours to 24 hours.

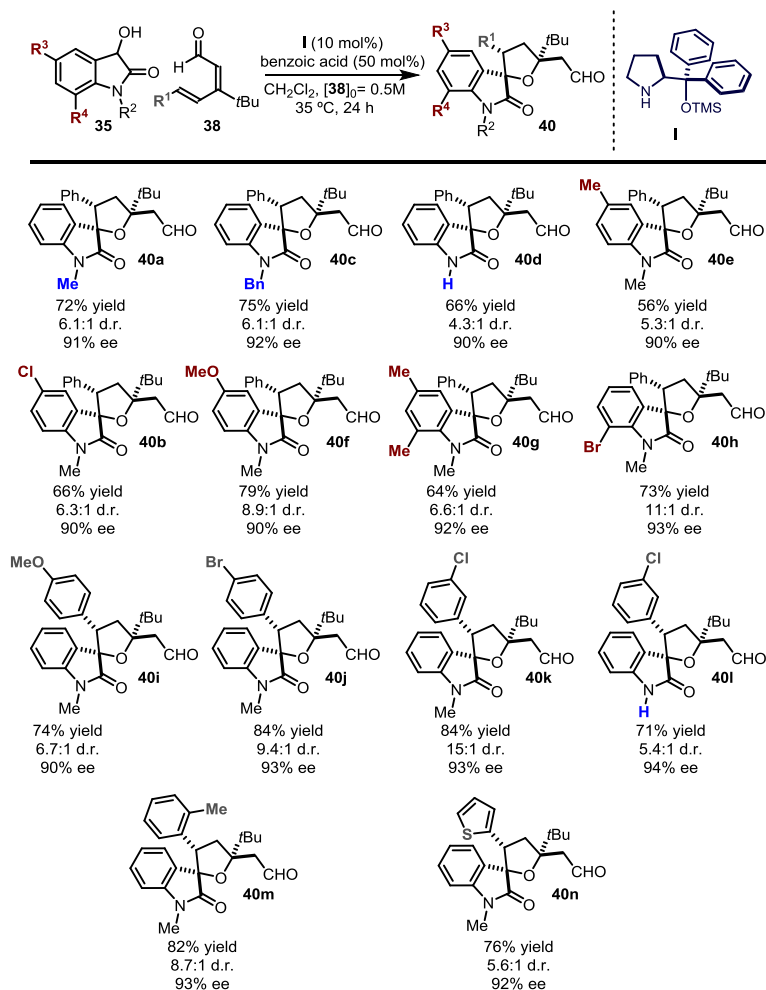


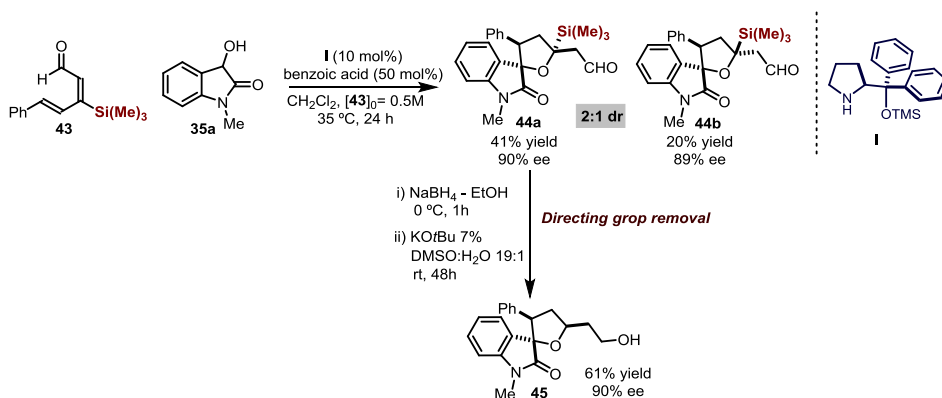
Figure 3.15 – Reaction scope.

As highlighted in Figure 3.15, there appears to be significant tolerance for structural and electronic variations of both substrates to access a variety of complex spiro-tetrahydrofurans **35** with good diastereomeric ratio, a high optical purity, and exquisite site-selectivity. It is of

synthetic relevance that a simple chromatographic purification on silica gel afforded the isolation of the pure major diastereoisomer of **40**. A wide range of dioxindole derivatives are compatible with the catalytic system. The presence of a different substituent at the nitrogen atom or the use of unprotected dioxindole preserved the stereoselectivity of the process (compounds **40a-c**), while substrates with different substituents at the C5 and C7 positions (compounds **40e-h**) performed well under the reaction conditions. As for the  $\delta$ -position of the dienal substrate **38**, different substitution patterns at the aromatic moiety were well-tolerated, regardless of their electronic properties and position on the phenyl ring (products **40i-m**). A heteroaryl framework could be included in the final product, as shown for the thiophenyl-substituted adduct **40n**. As a limitation of the system, an aliphatic R<sup>1</sup> substituent in **38** resulted in a complete loss of reactivity.

The main limitation of the present methodology is the need of a sterically demanding *tert*-butyl group in the scaffold of **38** in order to control the geometry of the transient intermediate **39**. Although the study of such a pivotal effect in the geometry control of the vinylogous iminium ion was key for reaction development, the need of a  $\beta$ -*tert*-butyl group drastically reduced the synthetic interest of the transformation.

We wondered whether we could employ a traceless directing group which could emulate the role of the bulky *tert*-butyl substituent. The trimethylsilyl moiety has very similar chemical features compared to the *tert*-butyl group, and it is characterized by a very similar steric profile.<sup>29</sup>



Scheme 3-16 – Employment of a traceless directing group.

<sup>29</sup> The trimethylsilyl moiety has a similar Charton parameter compared to the *tert*-butyl group: *t*Bu  $\sigma = 1.24$ ; (Me)<sub>3</sub>Si,  $\sigma = 1.40$ . Charton, M. "Steric Effects. I. Esterification and Acid-Catalyzed Hydrolysis of Esters" *J. Am. Chem. Soc.* **1975**, *97*, 1552.



Subjecting dienal **43** under the reaction conditions, compound **44** was obtained in high enantiomeric excess, albeit with lower diastereomeric ratio. The two diastereoisomers **44a-b** could be easily separated through silica gel chromatography. This approach can be useful for directly accessing biologically relevant silicon-containing spiro-compounds (see structure in Figure 3.1). Remarkably, we could easily access the enantio-enriched compound **45** upon protodesilylation of the isolated major diastereoisomer **44a** under basic conditions.<sup>30</sup> This highlights that the trimethylsilyl moiety can be used as a traceless directing group to achieve  $\delta$ -site selectivity, providing a formal 1,6-addition of geometrically unbiased, linear dienals.

### 3.4 Conclusions and remarks

In conclusion, we have developed a novel aminocatalytic vinylogous cascade reaction, yielding valuable tetrahydrofuran spirooxindole derivatives. The chemistry is based on a rare example of asymmetric 1,6-addition to linear 2,4-dienals proceeding with high  $\delta$ -site and stereo-selectivity. Central to this study was the rational design of the substrate, as inspired by conformational studies. A steering group at the  $\beta$ -dienal position ensured molecular preorganization of the catalytically active vinylogous iminium ion intermediate, which was essential to achieve highly predictable reaction outcomes. This design blueprint could be useful for the development of other asymmetric aminocatalytic remote functionalization strategies. The crucial steps for developing the present methodology were motivated by rational considerations, from the design of the starting material, to the optimization studies and including the design of a traceless directing group for iminium ion mediated  $\delta$ -functionalizations of dienals.

### 3.5 Experimental section

**General information:** The NMR spectra were recorded at 400 MHz and 500 MHz for  $^1\text{H}$  NMR or at 100 MHz and 125 MHz for  $^{13}\text{C}$ . The chemical shifts ( $\delta$ ) for  $^1\text{H}$  and  $^{13}\text{C}$  are given in ppm relative to residual signals of the solvents ( $\text{CHCl}_3$  @ 7.26 ppm  $^1\text{H}$  NMR, 77.16 ppm  $^{13}\text{C}$  NMR). Coupling constants are given in Hz. The following abbreviations are used to indicate the multiplicity: s, singlet; t, triplet; q, quartet; p, quintuplet; hept, septuplet; m, multiplet.

High-resolution mass spectra (HRMS) were obtained from the ICIQ High Resolution Mass Spectrometry Unit on Waters GCT gas chromatograph coupled time-of-flight mass spectrometer (GC/MS-TOF) with electron ionization (EI) or MicroTOF II (Bruker Daltonics): HPLC-MS-TOF (ESI). X-Ray data were obtained from the ICIQ X-Ray unit using a Bruker-Nonius diffractometer equipped with an APPEX 2 4K CCD area detector.

**General procedures:** All the reactions were set up under air and using synthesis grade solvents, without any precautions to exclude moisture, unless otherwise noted. Chromatographic

<sup>30</sup> Hudrlik, P. F.; Hudrlik, A. M.; Kulkarni, A. K. "Protodesilylation Reactions of Simple  $\beta$ -Hydroxysilanes (and  $\alpha$ -Hydroxysilanes). Homo-Brook Rearrangements" *J. Am. Chem. Soc.* **1982**, *104*, 6809.

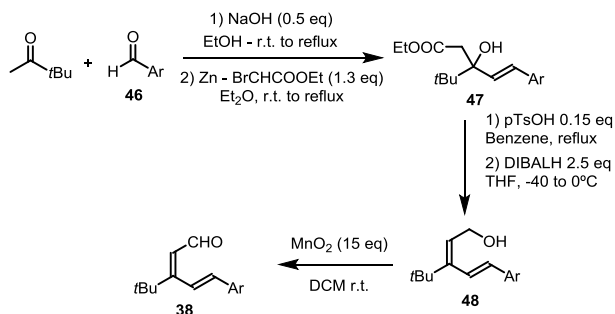
purification of products was accomplished using force-flow chromatography on silica gel (35-70 mesh). For thin layer chromatography (TLC) analysis throughout this work, Merck precoated TLC plates (silica gel 60 GF254, 0.25 mm) were employed, using UV light as the visualizing agent and potassium permanganate stain solution and heat as developing agents. Organic solutions were concentrated under reduced pressure on a Büchi rotatory evaporator.

**Determination of yields and conversions in the optimization studies:** All the yields reported in the optimization studies are obtained through  $^1\text{H}$  NMR analysis using 2,5-dimethylfuran as the internal standard ( $\delta$  5.82 ppm, 2H) and comparing these signals with those of the aldehyde H-atom of the product. Analogous results were always obtained integrating other protons of the product. Conversions value were obtained comparing the aldehydic peak of product **40a** ( $\delta$  10.05 ppm) to the one of aldehyde **38** ( $\delta$  = 9.78 ppm).

**Determination of Enantiomeric Purity:** Enantiomeric excesses were determined upon HPLC Analysis on chiral stationary phase on an Agilent 1200 series instrumentation. Daicel Chiralpak IA, IC, columns with *i*PrOH/hexane as the eluent were used. HPLC Traces were compared to racemic samples prepared by performing the reactions in the presence of a catalytic amount of an equimolar mixture of (*R*)- and (*S*)-diphenylprolinol trimethylsilyl ether I.

**Materials:** Reagents were purchased at the highest commercial quality from Sigma Aldrich, Fluka, and Alfa Aesar and used as received, without further purification, unless otherwise stated. Carrying out the reactions with distilled SPS solvent (without the need of strictly anhydrous conditions) is generally beneficial for this transformation, for this reason we used SPS solvent for the reaction scope. The  $^1\text{H}$  NMR and  $^{13}\text{C}$  NMR spectra traces are available in literature and are not reported in the present dissertation.<sup>1</sup>

### Synthesis of aldehydes **38**



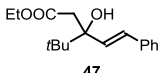
Scheme 3.17 – Synthetic pathway for synthesizing aldehydes **38**.

**General procedure for preparing compounds **47**:** The aromatic aldehyde **46** (1.1 equiv) was slowly added to a solution of pinacolone (1M in EtOH). Then a 10% aqueous solution of NaOH

(0.5 equiv) was added dropwise over a period of 5 minutes. The reaction was stirred overnight until full conversion of the ketone was achieved, as determined by  $^1\text{H}$  NMR analysis of the crude mixture. When needed, warming up the reaction to reflux (1-2 h) allowed to reach full conversion. The pH of the aqueous solution was then adjusted to  $\approx 4$  by slowly adding a 1M HCl solution. The mixture was diluted with water (30 mL for each mmol of starting ketone) and extracted 3 times with diethyl ether (20 mL for each mmol of starting ketone). The organic layers were combined and washed with a saturated solution of sodium bicarbonate and brine. After drying over sodium sulphate, solvents were removed under vacuum affording the crude condensation products.

Freshly activated zinc in pellets was kept in a dry flask under argon atmosphere. For complete activation of the zinc, traces of iodine and 4 mL of dry diethyl ether were added and the solution stirred until decolouration occurred. Then, ethyl bromoacetate (1.1 eq) and a solution of crude condensation product (1.5 M in dry diethyl ether) were added under vigorous stirring. The reaction was refluxed until complete consumption of the starting material was achieved, as judged by TLC analysis (30 min approximately). The reaction mixture was then filtered and diluted with diethyl ether (10 mL for each mmol of III), washed with 1 M aqueous solution of HCl, saturated with a solution of sodium bicarbonate and finally with brine. After drying over sodium sulphate, the organic layers were removed under vacuum affording the crude compounds IV, which were purified through flash chromatography on silica gel (Hexane/EtOAc 99:1 – 95:5 as the eluent). All the products **47** were obtained with an overall yield over two steps of 60 – 80%.

**Characterization of the model substrate (47a):** The title compound was obtained following the general procedure as a colourless oil (24 g – 87 mmol) starting from pinacolone (11.6 g - 116 mmol) 75% yield for two steps. HRMS calcd for ( $\text{C}_{17}\text{H}_{24}\text{O}_3\text{Na}^+$ ): 299.1618, found 299.1631

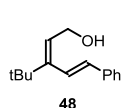
  
 $^1\text{H}$  NMR (500 MHz,  $\text{CDCl}_3$ )  $\delta$  7.37 – 7.29 (m, 4H), 7.24 – 7.20 (m, 1H), 6.64 (d,  $J$  = 16.0 Hz, 1H), 6.31 (d,  $J$  = 16.0 Hz, 1H), 4.15 (s, 1H), 4.12-4.04 (m, 2H), 2.74 (d,  $J$  = 14.6 Hz, 1H), 2.66 (d,  $J$  = 14.6 Hz, 1H), 1.16 (t,  $J$  = 7.1 Hz, 3H), 1.00 (s, 9H).

$^{13}\text{C}$  NMR (125 MHz,  $\text{CDCl}_3$ )  $\delta$  174.0, 137.4, 132.2, 130.4, 128.9, 127.7, 126.8, 78.0, 61.2, 40.0, 38.5, 25.6, 14.5.

**General procedure for preparing compounds 48:** The alcohol **47** was dissolved in benzene (0.2 M solution) and heated to reflux. *p*-Toluensulfonic acid (0.15 eq) was added all at once to the boiling mixture. The reaction was stirred until complete consumption of the starting material, as judged by TLC analysis (approximately 30 minutes). A saturated solution of sodium bicarbonate served to quench the reaction (20 mL for each mmol of **47**) and the mixture was extracted three times with diethyl ether (10 mL). The organic layers were collected, washed with brine (10 mL) and dried over sodium sulphate. Quick chromatographic purification (hexane:EtOAc 99:1- 97:3)

afforded the crude elimination product as an oil, which was employed in the next step without further purification. The crude elimination product was placed in a dry flask and dissolved in dry THF (0.2 M solution). The solution was then cold to  $-40\text{ }^{\circ}\text{C}$  and 2.5 equiv of DIBAL-H (1M solution in hexanes) was added dropwise over a period of 20 minutes. The reaction was then stirred for further 30 minutes at  $0\text{ }^{\circ}\text{C}$ . A saturated solution of Rochelle salt in water (10 mL for each mmol of the starting material) was then carefully added dropwise at  $0\text{ }^{\circ}\text{C}$  in order to quench the reaction. The mixture was stirred overnight at room temperature and then extracted 3 times with diethyl ether. The combined organic layers were washed with brine and dried over sodium sulphate. Removal of the solvent under vacuum and purification through flash chromatography on silica gel (hexanes/EtOAc 95:5-80:20 as the eluent) afforded the compound **48** as a colourless oil. All the products **48** were obtained with an overall yield over two steps of 40 – 60%. When the Ar substituent in **48** was a 4-OMe-Ph moiety, the elimination protocol was modified to follow a procedure reported in the literature.<sup>31</sup>

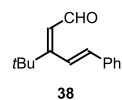
**Characterization of the model substrate (48):** The title compound was obtained as a colourless oil (2.2 g, 10 mmol) from its precursor **47** (6.1 g - 22mmol) in 45% overall yield over two steps. HRMS calcd for ( $\text{C}_{15}\text{H}_{19}^+$ ): 199.1481, found 199.1479



$^1\text{H}$  NMR (500 MHz,  $\text{CDCl}_3$ )  $\delta$  7.46 – 7.39 (m, 2H), 7.37 – 7.31 (m, 2H), 7.29 – 7.23 (m, 1H), 6.68 (d,  $J = 16.1$ , 1H), 6.32 (d,  $J = 16.1$  Hz, 1H), 5.65 (t,  $J = 6.5$  Hz, 1H), 4.34 (d,  $J = 6.5$  Hz, 2H), 1.14 (s, 9H).  $^{13}\text{C}$  NMR (125 MHz,  $\text{CDCl}_3$ )  $\delta$  150.6, 137.5, 134.2, 129.0, 127.9, 126.7, 125.9, 123.2, 61.3, 36.3, 30.0.

**Preparation of enals 38:** Compound **48** was dissolved in dry  $\text{CH}_2\text{Cl}_2$  (0.1 M solution) under an argon atmosphere. Then, activated  $\text{MnO}_2$  (15 equiv) was added to the solution and the reaction stirred until complete consumption of the starting material, as determined by TLC analysis (generally 16 hours). The reaction mixture was then filtered through a pad of Celite and solvents were removed under vacuo to afford the crude product. Purification by flash chromatography on silica gel (Hexanes/EtOAc 90:10) afforded the enals **38**. The yield of the oxidation was ranging from 90 to 99%.

**Characterization of the model substrate (38):** The title compound was obtained following the general procedure as a yellowish oil (2.0 g – 9.3 mmol) starting from compound **48** (2.1 g – 9.7 mmol) 96% yield. HRMS calcd for ( $\text{C}_{15}\text{H}_{19}\text{O}^+$ ): 215.1430, found 215.1433

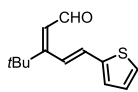


<sup>31</sup> Frija, L. M. T.; Afonso C. A. M. "Amberlyst (R)-15: a Reusable Heterogeneous Catalyst for the Dehydration of Tertiary Alcohols" *Tetrahedron* **2012**, *68*, 7414.

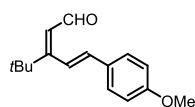
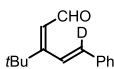
$^1\text{H}$  NMR (500 MHz,  $\text{CDCl}_3$ )  $\delta$  9.78 (d,  $J = 7.4$  Hz, 1H), 7.52 – 7.42 (m, 2H), 7.42 – 7.30 (m, 3H), 6.86 (d,  $J = 15.6$  Hz, 1H), 6.64 (d,  $J = 15.6$  Hz, 1H), 6.16 (d,  $J = 7.4$  Hz, 1H), 1.21 (s, 9H).  $^{13}\text{C}$  NMR (125 MHz,  $\text{CDCl}_3$ )  $\delta$  194.2, 172.4, 139.9, 136.1, 129.2, 129.2, 127.4, 127.0, 123.7, 37.5, 29.6.

### Characterization of the other starting enals 38:

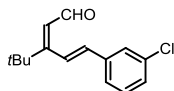
$^1\text{H}$  NMR (400 MHz,  $\text{CDCl}_3$ )  $\delta$  9.77 (d,  $J = 7.4$  Hz, 1H), -7.32-7.27 (m, 1H), 7.15 – 6.97 (m, 2H), 6.77 (d,  $J = 15.4$  Hz, 1H), 6.66 (d,  $J = 15.4$  Hz, 1H), 6.13 (d,  $J = 7.4$  Hz, 1H), 1.20 (s, 9H).  $^{13}\text{C}$  NMR (100 MHz,  $\text{CDCl}_3$ )  $\delta$  193.9, 171.7, 141.3, 132.8, 128.5, 128.2, 126.9, 126.4, 123.0, 37.5, 29.6. HRMS calcd for  $(\text{C}_{13}\text{H}_{17}\text{OS}^+)$ : 221.0995, found 221.1000



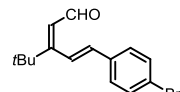
$^1\text{H}$  NMR (500 MHz,  $\text{CDCl}_3$ )  $\delta$  9.78 (d,  $J = 7.4$  Hz, 1H), 7.53 – 7.44 (m, 2H), 7.42 – 7.29 (m, 3H), 6.86 (t,  $J = 2.0$  Hz, 1H), 6.17 (d,  $J = 7.4$  Hz, 1H), 1.21 (s, 9H).  $^{13}\text{C}$  NMR (125 MHz,  $\text{CDCl}_3$ )  $\delta$  194.3, 172.6, 136.0, 129.2, 129.2, 127.4, 127.0, 123.5, 37.5, 29.6. The carbon linked to the deuterium atom is missing due to the longer relaxation time. HRMS calcd for  $(\text{C}_{15}\text{H}_{18}\text{DO}^+)$ : 216.1493, found 216.1487.



$^1\text{H}$  NMR (300 MHz,  $\text{CDCl}_3$ )  $\delta$  9.74 (d,  $J = 7.4$  Hz, 1H), 7.47 – 7.35 (m, 2H), 6.97 – 6.83 (m, 2H), 6.72 (d,  $J = 15.5$  Hz, 1H), 6.57 (d,  $J = 15.5$  Hz, 1H), 6.12 (d,  $J = 7.4$  Hz, 1H), 3.81 (s, 3H), 1.19 (s, 9H).  $^{13}\text{C}$  NMR (75 MHz,  $\text{CDCl}_3$ )  $\delta$  194.0, 172.5, 160.4, 139.5, 128.7, 128.7, 126.4, 121.2, 114.4, 55.5, 37.2, 29.4. HRMS calcd for  $(\text{C}_{16}\text{H}_{20}\text{O}_2\text{Na}^+)$ : 267.1356, found 267.1356.

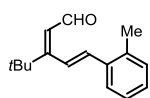


$^1\text{H}$  NMR (400 MHz,  $\text{CDCl}_3$ ):  $\delta$  9.76 (d,  $J = 7.5$  Hz, 1H), 7.47-7.46 (m, 1H), 7.33-7.29 (m, 3H), 6.86 (d,  $J = 15.7$  Hz, 1H), 6.56 (d,  $J = 15.7$  Hz, 1H), 6.16 (d,  $J = 7.5$  Hz, 1H), 1.21 (s, 9H) ppm.  $^{13}\text{C}$  NMR (100 MHz,  $\text{CDCl}_3$ ):  $\delta$  193.6, 171.4, 137.8, 137.6, 134.9, 130.1, 128.8, 127.0, 126.7, 125.4, 124.8, 37.2, 29.2 ppm. HRMS calcd for  $(\text{C}_{15}\text{H}_{17}\text{ClNaO}^+)$ : 271.0860, found 271.0862.



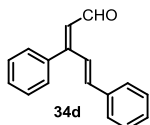
$^1\text{H}$  NMR (500 MHz,  $\text{CDCl}_3$ ):  $\delta$  9.75 (d,  $J = 7.4$  Hz, 1H), 7.52-7.49 (m, 2H), 7.34-7.32 (m, 2H), 6.84 (d,  $J = 15.7$  Hz, 1H), 6.56 (d,  $J = 15.7$  Hz, 1H), 6.16 (d,  $J = 7.4$  Hz, 1H), 1.20 (s, 9H) ppm.  $^{13}\text{C}$  NMR (100 MHz,  $\text{CDCl}_3$ ):  $\delta$  193.6, 171.6, 138.2, 134.6, 132.0, 128.5, 126.8, 124.1, 122.9, 37.2, 29.2 ppm. HRMS calcd for  $(\text{C}_{15}\text{H}_{17}\text{BrNaO}^+)$ : 315.0355, found 315.0351.

$^1\text{H}$  NMR (400 MHz,  $\text{CDCl}_3$ ):  $\delta$  9.82 (d,  $J = 7.4$  Hz, 1H), 7.55-7.52 (m, 1H), 7.25-7.19 (m, 3H), 6.86 (d,  $J = 15.5$  Hz, 1H), 6.73 (d,  $J = 15.5$  Hz, 1H), 6.17 (d,  $J = 7.4$  Hz, 1H), 2.36 (s, 3H), 1.22 (s, 9H)



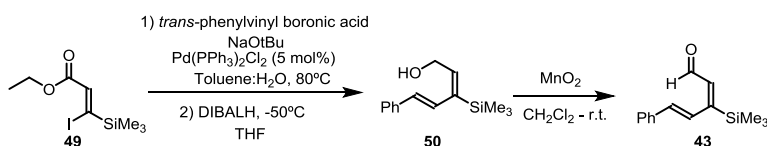
ppm. <sup>13</sup>C NMR (100 MHz, CDCl<sub>3</sub>): δ 193.8, 172.4, 137.6, 136.4, 135.1, 130.7, 128.7, 126.6, 126.3, 125.9, 124.8, 37.1, 29.2, 19.9 ppm. HRMS calcd for (C<sub>16</sub>H<sub>20</sub>NaO<sup>+</sup>): 251.1406, found 251.1406.

Enal **34d** was prepared according to scheme S1 starting from commercially available III chalcone and obtained as a mixture 11:1 of E/Z isomers.



<sup>1</sup>H NMR (500 MHz, CDCl<sub>3</sub>) δ 10.26 (d, *J* = 7.6 Hz, 1H), 7.73 (d, *J* = 15.8, Hz, 1H), 7.58 – 7.28 (m, 12H), 6.81 (d, *J* = 15.9 Hz, 1H), 6.19 (d, *J* = 7.5 Hz, 1H). The spectra matches to the one reported in literature.<sup>32</sup>

### Synthesis of the β-branched dienal **43**.



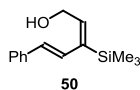
Scheme 3.18 – Synthetic pathway for the synthesis of aldehyde **43**

**Procedure for preparing compound 50.** 35 mg of Pd(PPh<sub>3</sub>)<sub>2</sub>Cl<sub>2</sub> (0.05 mmol – 0.05 equiv), 185 mg of trans-phenylvinyl boronic acid (1.25 mmol – 1.25 equiv) and 192 mg of NaOtBu (2 mmol – 2 equiv) were weighted in a flask. Then, 298 mg of the alkenyl iodide<sup>33</sup> (1 mmol – 1 equiv) and a 5:1 water/toluene mixture (2 mL) was added. The reaction mixture was warmed to 80 °C for 3 hours under an argon atmosphere, after which it was diluted with EtOAc (20 ml) and plugged through celite and silica gel. Solvents were evaporated and the crude compound was roughly purified on silica gel (Hex:EtOAc 97:3) to afford a yellowish-brown oil.

The oil was dissolved in dry THF (5 mL) and the mixture cooled down to -50 °C. 2.5 mL of DIBAL-H solution (1 M in hexanes, 2.5 mmol – 2.5 equiv) was then slowly added over a period of 20 minutes. The solution was stirred for additional 30 minutes at the same temperature, after which it was carefully quenched with 10 mL of saturated Rochelle salts solution in an ice bath. The mixture was stirred for 1 hour at room temperature and then extracted 3 times with diethyl ether (10 mL). The combined organic layers were washed with 10 mL of brine and dried over sodium sulphate. Removal of the solvent under vacuo and purification through flash chromatography (hexanes/EtOAc 95:5-80:20) afforded compound **50** as a colourless oil (129 mg – 0.56 mmol- 56% yield over two steps).

<sup>32</sup> Gravel, D.; Leboeuf, C. "On the origin of regioselectivity in the photorearrangement of 4,4-diphenyl-2,5-cyclohexadiene systems. Synthesis and photochemistry of 4,4-diphenyl-γ-thiopyran and -γ-thiopyran-1,1-dioxide" *Can. J. Chem.* **1982**, *60*, 574.

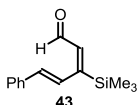
<sup>33</sup> The synthesis of the alkenyl iodide was reported in literature: Piers, E.; Wong, T.; Coish, P. D.; Rogers, C. "A Convenient Procedure for the Efficient Preparation of Alkyl (Z)-3-Iodo-2-Alkenoates" *Can. J. Chem.* **1994**, *72*, 1816.



<sup>1</sup>H NMR (400 MHz, CDCl<sub>3</sub>) δ 7.45 – 7.37 (m, 2H), 7.37 – 7.30 (m, 2H), 7.28 – 7.18 (m, 1H), 7.01 (d, J = 16.3, 1H), 6.52 (d, J = 16.3 Hz, 1H), 6.02 (t, J = 6.0 Hz, 1H), 4.47 (d, J = 6.0 Hz, 2H), 0.22 (s, 9H). <sup>13</sup>C NMR (100 MHz, CDCl<sub>3</sub>) δ 141.3, 140.7, 137.7, 132.3, 128.8, 127.7, 127.3, 126.4, 60.4, -0.6.

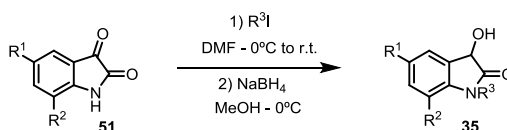
### Preparation of compound 43:

Compound **50** was oxidized following the general procedure used to prepare dienals **38** reported above to afford the enal **43** as a yellow oil (129 mg – 0.53 mmol – 95% yield).



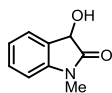
<sup>1</sup>H NMR (500 MHz, CDCl<sub>3</sub>) δ 10.13 (d, J = 8.0 Hz, 1H), 7.49 – 7.30 (m, 6H), 6.74 (d, J = 16.0 Hz, 1H), 6.27 (d, J = 8.0 Hz, 1H), 0.28 (s, 9H). <sup>13</sup>C NMR (125 MHz, CDCl<sub>3</sub>) δ 191.2, 163.7, 137.4, 136.8, 136.4, 129.0, 128.9, 127.1, 125.7, -1.1. HRMS calcd for (C<sub>14</sub>H<sub>18</sub>ONaSi<sup>+</sup>): 253.1019, found 253.1023.

### Synthesis of dioxindoles 35.



Scheme 3.19 – Synthetic pathway for the synthesis of dioxindoles **35**

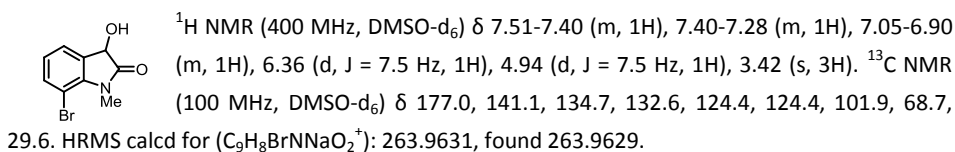
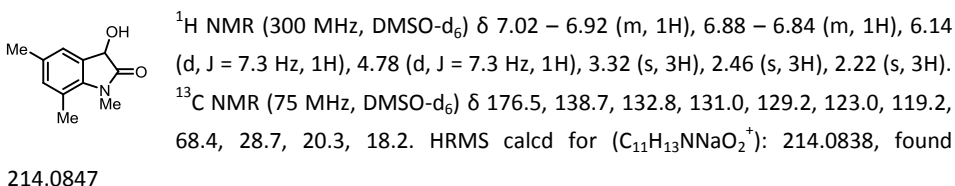
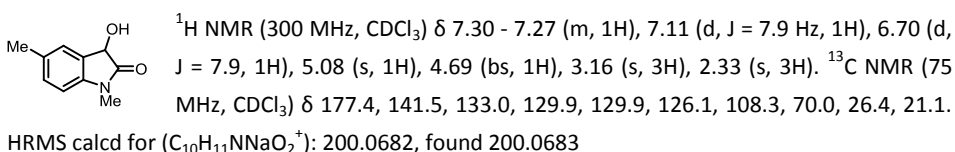
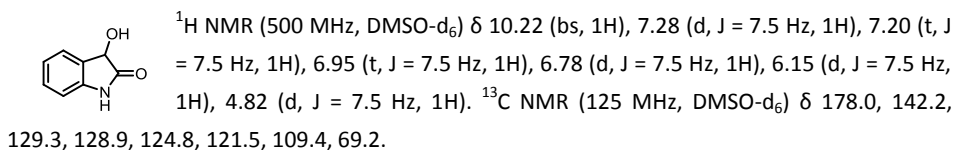
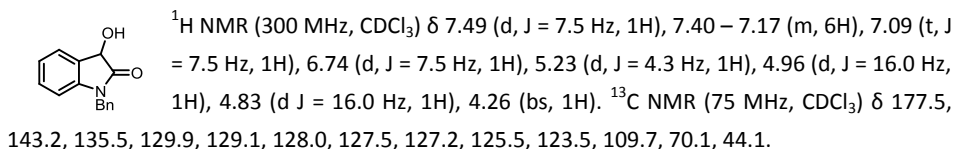
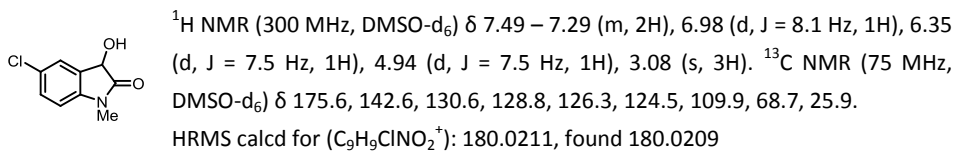
**General procedure for preparing compounds 35.** Isatin **51** was dissolved in dry DMF (1 M solution) under an argon atmosphere. The solution was then cooled down to 0 °C and NaH (60% in petroleum, 1.05 equiv) was added in portions. Iodomethane or benzyl iodide (1.05 equiv) was added dropwise to this mixture over a period of 5 minutes. The reaction was then allowed to stir for 30 minutes at 0 °C and 10 minutes at r.t., after which it was carefully quenched with water at 0 °C. The mixture was then poured into cold water. The solid that precipitated was filtered and recrystallized from boiling AcOEt. The obtained crystalline solid was suspended in EtOH at 0 °C (0.5 M solution). Sodium borohydride (1.3 equiv) was added in portions. The solution was stirred for 5 minutes. The reaction was quenched with the addition of water (2 mL for each mmol of isatin employed) and extracted three times with CH<sub>2</sub>Cl<sub>2</sub>. The organic layers were collected and dried over sodium sulphate. Solvent removal afforded the reaction crude as an amorphous solid that was recrystallized from boiling EtOAc to afford dioxindole **35** as crystalline white solids



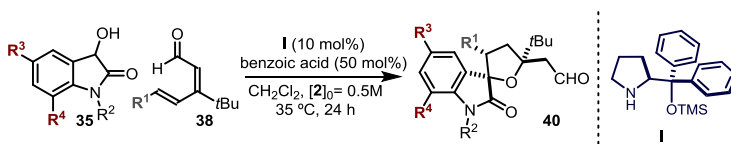
(overall yields of the reduction ranging from 40 to 80%).

Characterization of the dioxindoles **35**:

<sup>1</sup>H NMR (400 MHz, DMSO-d<sub>6</sub>) δ 7.38 – 7.26 (m, 2H), 7.07 – 7.01 (m, 1H), 6.98 – 6.93 (m, 1H), 6.25 (bs, 1H), 4.90 (bs, 1H), 3.08 (s, 3H). <sup>13</sup>C NMR (100 MHz, DMSO-d<sub>6</sub>) δ 176.1, 143.7, 129.1, 128.6, 124.4, 122.2, 108.4, 68.8, 25.8.



### Synthesis of spirooxindoles 40.



Scheme 3.20 – 1,6-1,4 cascade addition of dioxindoles 35 to dienals 38

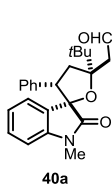


**General procedure for 1,6-1,4 cascade addition of dioxindoles to dienals**

The dienal **38** (0.1 mmol), benzoic acid (0.05 mmol – 0.5 equiv) and catalyst **I** (0.01 mmol – 0.1 equiv) were added to an oven dried hand-capped vial, avoiding direct contact between the catalyst and the aldehyde. The compounds were dissolved in 200  $\mu$ L of freshly distilled dichloromethane (SPS system) and the dioxindole **35** (0.15 mmol – 1.5 equiv) was added. The vial was quickly flushed with argon, closed with a Teflon-coated cap and the reaction stirred at 35  $^{\circ}$ C for 24 hours, unless otherwise stated. The reaction was then directly subjected to chromatographic purification employing eluent in gradient (Hexane – Hexane:EtOAc 85:15) affording spiro-tetrahydrofuran-oxindoles **40**. When necessary the compounds were filtered through a thin layer of basic alumina to remove co-eluted benzoic acid.

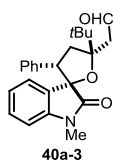
During the reaction, a third minor diastereoisomer was interconverting into the major product. This phenomenon can be explained on the basis of a retro-*oxa*-Michael reaction that converts the kinetic (minor) product into the thermodynamic final major **40** (see the main text for details). At the end of the reaction, a negligible amount (ranging from 0 to 5%) of such a minor diastereomer has been sporadically detected.

**Compound 40a** – The reaction was carried out following the general procedure to furnish the crude product as a 6.1:1 mixture of diastereoisomers; d.r. determined by integration of  $^1\text{H}$  NMR signal:  $\delta_{\text{major}}$  10.05 (dd),  $\delta_{\text{minor}}$  9.91 ppm (dd). After chromatographic purification the title compound **3a** was isolated as a single diastereoisomer (27 mg, 0.072 mmol, 72% yield). The enantiomeric excess was determined to be 91% by HPLC analysis on a Daicel Chiralpak IC column: 70:20:10 hexane/*i*-PrOH/DCM, flow rate 1.00 mL/min,  $\lambda = 254$  nm:  $\tau_{\text{minor}} = 9.6$  min,  $\tau_{\text{major}} = 28.1$  min.  $[\alpha]_{\text{D}}^{26} = -13.06$  ( $c = 1.00$ ,  $\text{CHCl}_3$ ). HRMS *calcd* for  $(\text{C}_{24}\text{H}_{27}\text{NNAO}_3)^+$ : 400.1883, found 400.1886.



$^1\text{H}$  NMR (500 MHz,  $\text{CDCl}_3$ )  $\delta$  10.05 (dd,  $J = 4.2, 1.0$  Hz, 1H), 7.12 – 6.95 (m, 7H), 6.82 (td,  $J = 7.6, 1.0$  Hz, 1H), 6.60 (d,  $J = 7.6$  Hz, 1H), 4.42 (dd,  $J = 13.0, 6.5$  Hz, 1H), 3.19 (s, 3H), 3.16 (d,  $J = 17.0$  Hz, 1H), 2.91 – 3.02 (m, 2H), 2.24 (dd,  $J = 13.0, 6.5$  Hz, 1H), 1.12 (s, 9H).  $^{13}\text{C}$  NMR (125 MHz,  $\text{CDCl}_3$ )  $\delta$  204.6, 177.8, 143.5, 136.5, 129.4, 128.2, 128.0, 127.4, 127.1, 126.1, 122.3, 108.3, 90.5, 88.0, 51.9, 49.0, 38.5, 37.3, 26.8, 26.6.

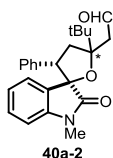
**Compound 40a-3:** The kinetic diastereoisomer **40a-3** was isolated after a first chromatographic purification as a strongly impure mixture. In order to remove impurities the compound was purified again with sequential preparative TLCs (respectively eluent hex:EOAc 70:30 and Toluene:EtO<sub>2</sub> 1:1). The amount of compound did not allow a  $^{13}\text{C}$  NMR analysis, but  $^1\text{H}$  NMR and bidimensional analysis (COSY, HSQC) are in perfect agreement with the proposed structure. The enantiomeric excess was determined over the time by HPLC analysis of the purified sample using



a Daicel Chiralpak IA column: 95:5 hexane/*i*-PrOH, flow rate 1.00 mL/min,  $\lambda = 254$  nm:  $\tau_{\text{major}} = 16.8$  min,  $\tau_{\text{minor}} = 18.2$  min.

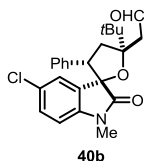
$^1\text{H}$  NMR (400 MHz, Chloroform-*d*)  $\delta$  9.86 (t,  $J = 2.8$  Hz, 1H), 7.25 - 6.85 (m, 8H), 6.63 (d,  $J = 7.8$ , 1H), 4.37 (t,  $J = 10.7$  Hz, 1H), 3.20 (s, 3H), 3.08 - 3.06 (m, 2H), 2.87 (d,  $J = 10.7$  Hz, 2H), 1.22 (s, 9H).

**Compound 40a-2:** The minor diastereoisomer **40a-2** was isolated after a first chromatographic purification as a strongly impure mixture. In order to remove impurities the compound was purified again with sequential preparative TLCs (respectively eluent hex:EOAc 80:20 and Toluene:EtO<sub>2</sub> 1:1). The amount of compound did not allow a  $^{13}\text{C}$  NMR analysis, but  $^1\text{H}$  NMR and bidimensional analysis (COSY, HSQC) are in perfect agreement with the proposed structure.



$^1\text{H}$  NMR (400 MHz, CDCl<sub>3</sub>)  $\delta$  9.91 (dd,  $J = 3.9, 1.9$  Hz, 1H), 7.63 - 7.52 (m, 1H), 7.36 - 7.29 (m, 1H), 7.21 - 7.07 (m, 4H), 6.98 - 6.90 (m, 2H), 6.64 - 6.51 (m, 1H), 3.88 (dd,  $J = 13.0, 8.1$  Hz, 1H), 3.63 (dd,  $J = 16.1, 1.9$  Hz, 1H), 3.34 (dd,  $J = 16.1, 3.9$  Hz, 1H), 3.07 (t,  $J = 13.0$  Hz, 1H), 2.79 - 2.66 (m, 4H), 1.14 (s, 9H).

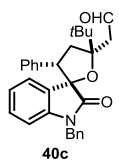
**Compound 40b** – The reaction was carried out following the general procedure to furnish the crude product as a 6.3:1 mixture of diastereoisomers; d.r. determined by integration of  $^1\text{H}$  NMR signal:  $\delta_{\text{major}}$  10.05 (dd),  $\delta_{\text{minor}}$  9.90 ppm (dd). After chromatographic purification the title compound **40b** was isolated as a single diastereoisomer (27 mg, 0.066 mmol, 66% yield). The enantiomeric excess was determined to be 90% by HPLC analysis on a Daicel Chiralpak IC column: 70:20:10 hexane/*i*-PrOH/DCM, flow rate 1.00 mL/min,  $\lambda = 254$  nm:  $\tau_{\text{minor}} = 8.6$  min,  $\tau_{\text{major}} = 18.3$ .  $[\alpha]_{\text{D}}^{26} = +44.2273$  ( $c = 1.1$ , CHCl<sub>3</sub>). HRMS *calcd* for (C<sub>24</sub>H<sub>26</sub>ClNNaO<sub>3</sub>)<sup>+</sup>: 434.1493, found 434.1504.



$^1\text{H}$  NMR (500 MHz, CDCl<sub>3</sub>)  $\delta$  10.05 (dd,  $J = 4.1, 1.0$  Hz, 1H), 7.17 - 7.04 (m, 5H), 7.04 - 6.93 (m, 2H), 6.54 (d,  $J = 8.2$  Hz, 1H), 4.43 (dd,  $J = 13.4, 6.5$  Hz, 1H), 3.20 (s, 3H), 3.16 (d,  $J = 16.9, 1H$ ), 3.01 (dd,  $J = 16.9, 4.1$  Hz, 1H), 2.95 (t,  $J = 13.4$  Hz, 1H), 2.27 (dd,  $J = 13.4, 6.5$  Hz, 1H), 1.15 (s, 9H).  $^{13}\text{C}$  NMR (126 MHz, CDCl<sub>3</sub>)  $\delta$  204.2, 177.4, 142.0, 135.9, 129.7, 129.2, 128.4, 127.7, 127.4, 127.3, 126.5, 109.2, 91.0, 87.9, 52.2, 48.9, 38.5, 37.1, 26.8, 26.7.

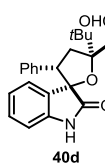
**Compound 40c** – The reaction was carried out following the general procedure to furnish the crude product as a 6.5:1 mixture of diastereoisomers; d.r. determined by integration of  $^1\text{H}$  NMR signal:  $\delta_{\text{major}}$  10.09 (dd),  $\delta_{\text{minor}}$  9.94 ppm (dd). After chromatographic purification the title compound **40c** was isolated as mixture of diastereoisomers 13.5:1 (34 mg, 0.075 mmol, 75% yield - 7% of the minor diastereoisomer as impurity). The enantiomeric excess was determined to be 92% by HPLC analysis on a Daicel Chiralpak IC column: 70:20:10 hexane/*i*-PrOH/DCM, flow

rate 1.00 mL/min,  $\lambda = 254$  nm:  $\tau_{\text{minor}} = 8.5$  min,  $\tau_{\text{major}} = 13.9$  min (other two peaks are detected due to the minor diastereoisomer).  $[\alpha]_{\text{D}}^{26} = -44.14$  ( $c = 1.00$ ,  $\text{CHCl}_3$ ). HRMS *calcd* for  $(\text{C}_{30}\text{H}_{31}\text{NNaO}_3)^+$ : 476.2196, found 476.2197.



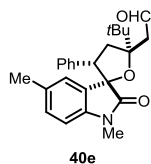
$^1\text{H}$  NMR (400 MHz,  $\text{CDCl}_3$ )  $\delta$  10.09 (dd,  $J = 4.1, 1.0$  Hz, 1H), 7.38 – 7.25 (m, 5H), 7.19 – 7.13 (m, 1H), 7.05 – 6.90 (m, 6H), 6.81 (td,  $J = 7.6, 1.0$  Hz, 1H), 6.61 – 6.50 (m, 1H), 5.08 (d,  $J = 15.4$  Hz, 1H), 4.68 (d,  $J = 15.4$  Hz, 1H), 4.46 (dd,  $J = 13.4, 6.6$  Hz, 1H), 3.19 (d,  $J = 16.7$ , 1H), 3.06 – 2.89 (m, 2H), 2.25 (dd,  $J = 12.4, 6.6$  Hz, 1H), 1.13 (s, 9H).  $^{13}\text{C}$  NMR (100 MHz,  $\text{CDCl}_3$ )  $\delta$  204.6, 178.0, 142.8, 136.2, 135.7, 129.3, 128.8, 128.1, 128.1, 127.8, 127.7, 127.7, 127.2, 126.3, 122.3, 109.2, 90.6, 87.9, 52.3, 49.0, 44.3, 38.5, 37.4, 26.9.

**Compound 40d** – The reaction was carried out following the general procedure to furnish the crude product as a 4.3:1 mixture of diastereoisomers; d.r. determined by integration of  $^1\text{H}$  NMR signal:  $\delta_{\text{major}} 10.05$  (dd),  $\delta_{\text{minor}} 9.92$  ppm (dd). After chromatographic purification the title compound **40d** was isolated as a single diastereoisomer (24 mg, 0.066 mmol, 66% yield). The enantiomeric excess was determined to be 90% by HPLC analysis on a Daicel Chiralpak IC column: 70:20:10 hexane/*i*-PrOH/DCM, flow rate 1.00 mL/min,  $\lambda = 254$  nm:  $\tau_{\text{minor}} = 11.0$  min,  $\tau_{\text{major}} = 11.8$ .  $[\alpha]_{\text{D}}^{26} = -13.99$  ( $c = 1.10$ ,  $\text{CHCl}_3$ ). HRMS *calcd* for  $(\text{C}_{23}\text{H}_{25}\text{NNaO}_3)^+$ : 386.1727, found 386.1730.



$^1\text{H}$  NMR (500 MHz,  $\text{CDCl}_3$ )  $\delta$  10.05 (d,  $J = 4.0$  Hz, 1H), 8.43 (bs, 1H), 7.18 – 6.96 (m, 7H), 6.79 (td,  $J = 7.6, 1.0$  Hz, 1H), 6.68 (d,  $J = 7.6$  Hz, 1H), 4.42 (dd,  $J = 13.3, 6.6$  Hz, 1H), 3.14 (d,  $J = 16.9$  Hz, 1H), 3.04 – 2.89 (m, 2H), 2.24 (dd,  $J = 12.4, 6.6$  Hz, 1H), 1.12 (s, 9H).  $^{13}\text{C}$  NMR (126 MHz,  $\text{CDCl}_3$ )  $\delta$  204.7, 180.3, 140.6, 136.4, 129.5, 128.4, 128.3, 127.4, 127.2, 126.5, 122.4, 110.3, 90.5, 88.3, 51.8, 48.8, 38.5, 37.4, 26.8.

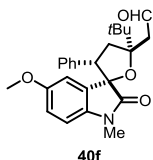
**Compound 40e** – The reaction was carried out following the general procedure (the reaction time is modified to 48 h) to furnish the crude product as a 5.3:1 mixture of diastereoisomers; d.r. determined by integration of  $^1\text{H}$  NMR signal:  $\delta_{\text{major}} 10.04$  (dd),  $\delta_{\text{minor}} 9.91$  ppm (dd). After chromatographic purification the title compound **40e** was isolated as a single diastereoisomer (22 mg, 0.056 mmol, 56% yield). The enantiomeric excess was determined to be 90% by HPLC analysis on a Daicel Chiralpak IC column: 70:20:10 hexane/*i*-PrOH/DCM, flow rate 1.00 mL/min,  $\lambda = 254$  nm:  $\tau_{\text{minor}} = 10.2$  min,  $\tau_{\text{major}} = 24.2$  min.  $[\alpha]_{\text{D}}^{26} = +26.3810$  ( $c = 1.05$ ,  $\text{CHCl}_3$ ). HRMS *calcd* for  $(\text{C}_{25}\text{H}_{29}\text{NNaO}_3)^+$ : 414.2040, found 414.2059.



$^1\text{H}$  NMR (500 MHz,  $\text{CDCl}_3$ )  $\delta$  10.04 (dd,  $J = 4.2, 1.0$  Hz, 1H), 7.09 – 6.98 (m, 3H), 6.98 – 6.93 (m, 2H), 6.91–6.88 (m, 1H), 6.88–6.83 (m, 1H), 6.48 (d,  $J = 7.9$  Hz, 1H), 4.40 (dd,  $J = 13.4, 6.6$  Hz, 1H), 3.17 (s, 4H), 3.01 – 2.90 (m, 2H), 2.23 (dd,  $J = 12.4, 6.6$  Hz, 1H), 2.16 (s, 3H),

1.12 (s, 9H).  $^{13}\text{C}$  NMR (125 MHz,  $\text{CDCl}_3$ )  $\delta$  204.7, 177.7, 141.2, 136.6, 131.7, 129.5, 128.1, 128.0, 127.4, 127.1, 127.0, 107.9, 90.4, 88.1, 51.8, 49.0, 38.5, 37.3, 26.8, 26.6, 21.2.

**Compound 40f** – The reaction was carried out following the general procedure to furnish the crude product as a 8.9:1 mixture of diastereoisomers; d.r. determined by integration of  $^1\text{H}$  NMR signal:  $\delta_{\text{major}}$  10.04 (dd),  $\delta_{\text{minor}}$  9.90 ppm (dd). After chromatographic purification the title compound **40f** was isolated as a single diastereoisomer (32 mg, 0.079 mmol, 79% yield). The enantiomeric excess was determined to be 90% by HPLC analysis on a Daicel Chiralpak IC3 column: 70:20:10 hexane/ $i$ -PrOH/ DCM, flow rate 0.8 mL/min,  $\lambda = 254$  nm:  $\tau_{\text{minor}} = 14.6$  min,  $\tau_{\text{major}} = 30.3$  min.  $[\alpha]_{\text{D}}^{26} = +26.51$  ( $c = 0.85$ ,  $\text{CHCl}_3$ ). HRMS *calcd* for  $(\text{C}_{25}\text{H}_{29}\text{NNaO}_4^+)$ : 430.1989, found 430.1983.

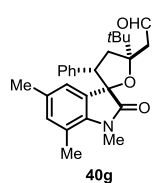


$^1\text{H}$  NMR (400 MHz,  $\text{CDCl}_3$ ):  $\delta$  10.04 (dd,  $J = 4.1, 0.9$  Hz, 1H), 7.09-7.0 (m, 3H), 6.98-6.96 (m, 2H), 6.73 (d,  $J = 2.5$  Hz, 1H), 6.59 (dd,  $J = 8.5, 2.5$  Hz, 1H), 6.50 (d,  $J = 8.5$  Hz, 1H), 4.42 (dd,  $J = 13.4, 6.6$  Hz, 1H), 3.65 (s, 3H), 3.18-3.13 (m, 1H), 3.17 (s, 3H), 3.0-2.89 (m, 2H), 2.23 (dd,  $J = 12.4, 6.6$  Hz, 1H), 1.12 (s, 9H) ppm.  $^{13}\text{C}$  NMR (100 MHz,  $\text{CDCl}_3$ ):  $\delta$  204.4, 177.3, 155.5, 137.0, 136.3, 129.1, 128.1, 127.2, 127.0, 113.9, 113.4, 108.3, 90.5, 88.1, 55.8, 51.7, 48.8, 38.4,

37.0, 26.7, 26.5 ppm.

**Compound 40g** – The reaction was carried out following the general procedure (reaction time 72 hours) to furnish the crude product as a 6.6:1 mixture of diastereoisomers; d.r. determined by integration of  $^1\text{H}$  NMR signal:  $\delta_{\text{major}}$  10.02 (dd),  $\delta_{\text{minor}}$  9.90 ppm (dd). After chromatographic purification the title compound **40g** was isolated as a single diastereoisomer (26 mg, 0.064 mmol, 64% yield).

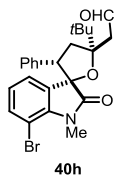
The enantiomeric excess was determined to be 92% by HPLC analysis on a Daicel Chiralpak IC column: 70:20:10 hexane/ $i$ -PrOH/DCM, flow rate 1.00 mL/min,  $\lambda = 254$  nm:  $\tau_{\text{minor}} = 11.7$  min,  $\tau_{\text{major}} = 24.8$  min.  $[\alpha]_{\text{D}}^{26} = +40.92$  ( $c = 0.8$ ,  $\text{CHCl}_3$ ). HRMS *calcd* for  $(\text{C}_{26}\text{H}_{31}\text{NNaO}_3^+)$ : 428.2196, found 428.2211.



$^1\text{H}$  NMR (400 MHz,  $\text{CDCl}_3$ )  $\delta$  10.02 (dd,  $J = 4.0, 1.0$  Hz, 1H), 7.15 – 6.91 (m, 5H), 6.79 – 6.68 (m, 1H), 6.62-6.55 (m, 1H), 4.39 (dd,  $J = 13.4, 6.6$  Hz, 1H), 3.45 (s, 3H), 3.18 (d,  $J = 16.8$  Hz, 1H), 3.05 – 2.82 (m, 2H), 2.35 (s, 3H), 2.21 (dd,  $J = 13.4, 6.6$  Hz, 1H), 2.10 (s, 3H), 1.11 (s, 9H).  $^{13}\text{C}$  NMR (100 MHz,  $\text{CDCl}_3$ )  $\delta$  204.8, 178.6, 138.8, 136.8, 133.6, 131.5, 128.7, 128.1, 127.5, 127.0, 125.0, 119.4, 90.3, 87.3, 51.9, 48.8, 38.5, 37.4, 30.1, 26.9, 20.9, 19.0.

**Compound 40h** - The reaction was carried out following the general procedure to furnish the crude product as a 11:1 mixture of diastereoisomers; d.r. determined by integration of  $^1\text{H}$  NMR signal:  $\delta_{\text{major}}$  10.00 (dd),  $\delta_{\text{minor}}$  9.87 ppm (dd). After chromatographic purification the title

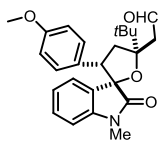
compound **40h** was isolated as a single diastereoisomer (33 mg, 0.073 mmol, 73% yield). The enantiomeric excess was determined to be 91% by HPLC analysis on a Daicel Chiralpak IC3 column: 70:20:10 hexane/*i*-PrOH/ DCM, flow rate 0.8 mL/min,  $\lambda = 254$  nm:  $\tau_{\text{minor}} = 10.7$  min,  $\tau_{\text{major}} = 21.6$  min.  $[\alpha]_{\text{D}}^{26} = -45.76$  ( $c = 0.4$ ,  $\text{CHCl}_3$ ). HRMS *calcd* for  $(\text{C}_{24}\text{H}_{26}\text{BrNNaO}_3)^+$ : 478.0988, found 478.0981.

**40h**

$^1\text{H}$  NMR (400 MHz,  $\text{CDCl}_3$ ):  $\delta$  10.00 (dd,  $J = 4.1, 1.0$  Hz, 1H), 7.15–7.20 (m, 1H), 7.12–7.01 (m, 4H), 6.95–6.93 (m, 2H), 6.60–6.70 (m, 1H), 4.42 (dd,  $J = 13.4, 6.6$  Hz, 1H), 3.60 (s, 3H), 3.16 (d,  $J = 16.6$  Hz, 1H), 2.98 (dd,  $J = 16.6, 4.1$  Hz, 1H), 2.91 (t,  $J = 13.4$  Hz, 1H), 2.25 (dd,  $J = 13.4, 6.6$  Hz, 1H), 1.10 (s, 9H) ppm.

$^{13}\text{C}$  NMR (125 MHz,  $\text{CDCl}_3$ ):  $\delta$  204.1, 178.4, 140.7, 136.0, 134.9, 131.1, 128.3, 127.2, 127.1, 125.0, 123.4, 102.5, 90.7, 87.0, 52.1, 48.6, 38.3, 37.0, 30.3, 26.7 ppm.

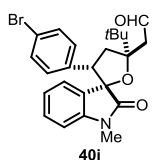
**Compound 40i** – The reaction was carried out following the general procedure to furnish the crude product as a 6.7:1 mixture of diastereoisomers; d.r. determined by integration of  $^1\text{H}$  NMR signal:  $\delta_{\text{major}} 10.04$  (dd),  $\delta_{\text{minor}} 9.90$  ppm (dd). After chromatographic purification the title compound **40i** was isolated as a single diastereoisomer (30 mg, 0.074 mmol, 74% yield). The enantiomeric excess was determined to be 90% by HPLC analysis on a Daicel Chiralpak IC column: 70:20:10 hexane/*i*-PrOH/DCM, flow rate 1.00 mL/min,  $\lambda = 254$  nm:  $\tau_{\text{minor}} = 12.0$  min,  $\tau_{\text{major}} = 38.9$  min.  $[\alpha]_{\text{D}}^{26} = -5.37$  ( $c = 1.5$ ,  $\text{CHCl}_3$ ). HRMS *calcd* for  $(\text{C}_{25}\text{H}_{29}\text{NNaO}_4)^+$ : 430.1989, found 430.2003.

**40i**

$^1\text{H}$  NMR (400 MHz,  $\text{CDCl}_3$ )  $\delta$  10.04 (dd,  $J = 4.3, 1.0$  Hz, 1H), 7.20 – 7.01 (m, 2H), 6.97 – 6.75 (m, 3H), 6.66 – 6.51 (m, 3H), 4.35 (dd,  $J = 13.0, 6.5$  Hz, 1H), 3.65 (s, 3H), 3.18 (s, 3H), 3.14 (d,  $J = 16.9$  Hz, 1H), 2.97 (dd,  $J = 16.9, 4.3$  Hz, 1H), 2.89 (t,  $J = 13.0$  Hz, 1H), 2.21 (dd,  $J = 13.0, 6.5$  Hz, 1H), 1.11 (s, 9H).  $^{13}\text{C}$  NMR (100 MHz,  $\text{CDCl}_3$ )  $\delta$  204.7, 177.9, 158.5, 143.5, 129.4, 128.5, 128.4, 128.1, 126.1,

122.4, 113.6, 108.3, 90.4, 88.0, 55.2, 51.4, 49.0, 38.5, 37.8, 26.8, 26.6.

**Compound 40j** – The reaction was carried out following the general procedure to furnish the crude product as a 9.4:1 mixture of diastereoisomers; d.r. determined by integration of  $^1\text{H}$  NMR signal:  $\delta_{\text{major}} 10.02$  (dd),  $\delta_{\text{minor}} 9.87$  ppm (dd).

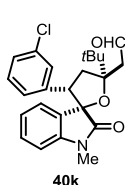
**40j**

compound **40j** was isolated as a single diastereoisomer (38 mg, 0.084 mmol, 84% yield). The enantiomeric excess was determined to be 93% by HPLC analysis on a Daicel Chiralpak IC column: 70:20:10 hexane/*i*-PrOH/ DCM, flow rate 0.8 mL/min,  $\lambda = 254$  nm:  $\tau_{\text{minor}} = 12.7$  min,  $\tau_{\text{major}} = 31.4$  min.  $[\alpha]_{\text{D}}^{26} = -29.96$  ( $c = 1.6$ ,  $\text{CHCl}_3$ ). HRMS *calcd* for  $(\text{C}_{26}\text{H}_{25}\text{BrNO}_3)^+$ : 478.1012, found 478.0989.

$^1\text{H}$  NMR (500 MHz,  $\text{CDCl}_3$ ):  $\delta$  10.02 (dd,  $J = 4.1, 1.0$  Hz, 1H), 7.19 – 7.17 (m, 2H), 7.13 – 7.09 (m, 2H), 6.87 – 6.82 (m, 3H), 6.64 (dt,  $J = 7.8, 0.7$  Hz, 1H), 4.34 (dd,  $J = 13.0, 6.5$  Hz, 1H), 3.19 (s, 3H), 3.13 (d,  $J = 16.6$  Hz, 1H), 2.98 (dd,  $J = 16.6, 4.1$  Hz, 1H), 2.88 (t,  $J = 13.0$  Hz, 1H), 2.24 (dd,  $J = 13.0,$

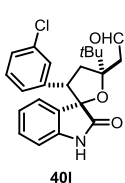
6.5 Hz, 1H), 1.10 (s, 9H).  $^{13}\text{C}$  NMR (125 MHz,  $\text{CDCl}_3$ ):  $\delta$  204.2, 177.4, 143.4, 135.4, 131.2, 129.6, 129.0, 127.5, 125.8, 122.4, 120.9, 108.4, 90.4, 87.5, 51.3, 48.8, 38.3, 37.3, 26.7, 26.5.

**Compound 40k** – The reaction was carried out following the general procedure to furnish the crude product as a 15:1 mixture of diastereoisomers; d.r. determined by integration of  $^1\text{H}$  NMR signal:  $\delta_{\text{major}}$  10.03 (dd),  $\delta_{\text{minor}}$  9.88 ppm (dd). After chromatographic purification the title compound **40k** was isolated as a single diastereoisomer (34.5 mg, 0.084 mmol, 84% yield). The enantiomeric excess was determined to be 93% by HPLC analysis on a Daicel Chiralpak IC3 column: 70:20:10 hexane/ $^i\text{PrOH}$ /DCM, flow rate 0.8 mL/min,  $\lambda = 254$  nm:  $\tau_{\text{minor}} = 10.9$  min,  $\tau_{\text{major}} = 24.3$  min.  $[\alpha]_{\text{D}}^{26} = -32.40$  ( $c = 0.55$ ,  $\text{CHCl}_3$ ). HRMS *calcd* for  $(\text{C}_{24}\text{H}_{26}\text{ClNNaO}_3)^+$ : 434.1493, found 434.1495.



$^1\text{H}$  NMR (400 MHz,  $\text{CDCl}_3$ ):  $\delta$  10.03 (dd,  $J = 4.0, 0.9$  Hz, 1H), 7.13-7.08 (m, 2H), 7.0-6.95 (m, 3H), 6.87-6.83 (m, 1H), 6.81-6.79 (m, 1H), 6.64 (d,  $J = 7.7$  Hz, 1H), 4.36 (dd,  $J = 13.4, 6.6$  Hz, 1H), 3.20 (s, 3H), 3.13 (d,  $J = 16.6$  Hz, 1H), 2.98 (dd,  $J = 16.6, 4.0$  Hz, 1H), 2.88 (t,  $J = 13.4$  Hz, 1H), 2.25 (dd,  $J = 13.4, 6.6$  Hz, 1H), 1.11 (s, 9H).  $^{13}\text{C}$  NMR (100 MHz,  $\text{CDCl}_3$ ):  $\delta$  204.1, 177.8, 143.4, 138.6, 134.0, 129.6, 129.3, 127.5, 127.3, 127.1, 125.8, 125.5, 122.4, 108.3, 90.5, 87.6, 51.5, 48.8, 38.3, 37.0, 26.7, 26.5.

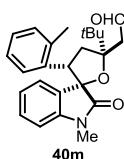
**Compound 40l** – The reaction was carried out following the general procedure to furnish the crude product as a 5.4:1 mixture of diastereoisomers; d.r. determined by integration of  $^1\text{H}$  NMR signal:  $\delta_{\text{major}}$  10.03 (dd),  $\delta_{\text{minor}}$  9.91 ppm (dd). After chromatographic purification the title compound **40l** was isolated as a single diastereoisomer (28 mg, 0.071 mmol, 71% yield). The enantiomeric excess was determined to be 94% by HPLC analysis on a Daicel Chiralpak IC column: 75:20:5 hexane/ $^i\text{PrOH}$ /DCM, flow rate 0.8 mL/min,  $\lambda = 254$  nm:  $\tau_{\text{major}} = 13.3$  min,  $\tau_{\text{minor}} = 14.5$  min.  $[\alpha]_{\text{D}}^{26} = -11.4$  ( $c = 0.7$ ,  $\text{CHCl}_3$ ). HRMS *calcd* for  $(\text{C}_{23}\text{H}_{24}\text{ClNNaO}_3)^+$ : 420.1337, found 420.1329.



$^1\text{H}$  NMR (400 MHz,  $\text{CDCl}_3$ ):  $\delta$  10.03 (dd,  $J = 4.0, 1.0$  Hz, 1H), 8.08 (bs, 1H), 7.08-7.03 (m, 3H), 7.02-6.98 (m, 2H), 6.92-6.89 (m, 1H), 6.85-6.81 (m, 1H), 6.70 (dd,  $J = 7.6, 1.1$  Hz, 1H), 4.37 (dd,  $J = 13.3, 6.6$  Hz, 1H), 3.11 (dd,  $J = 16.8, 1.0$  Hz, 1H), 2.96 (dd,  $J = 16.8, 4.0$  Hz, 1H), 2.89 (t,  $J = 13.3$  Hz, 1H), 2.25 (dd,  $J = 13.3, 6.6$  Hz, 1H), 1.12 (s, 9H).  $^{13}\text{C}$  NMR (126 MHz,  $\text{CDCl}_3$ ):  $\delta$  204.2, 179.5, 140.3, 138.5, 134.0, 129.6, 129.4, 127.9, 127.3, 127.3, 126.3, 125.7, 122.5, 110.2, 90.5, 87.9, 51.4, 48.6, 38.3, 37.2, 26.6.

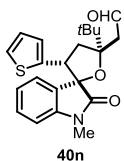
**Compound 40m** – The reaction was carried out following the general procedure to furnish the crude product as a 8.7:1 mixture of diastereoisomers; d.r. determined by integration of  $^1\text{H}$  NMR signal:  $\delta_{\text{major}}$  10.04 (dd),  $\delta_{\text{minor}}$  9.91 ppm (dd). After chromatographic purification the title

compound **40m** was isolated as a single diastereoisomer (32 mg, 0.082 mmol, 82% yield). The enantiomeric excess was determined to be 93% by HPLC analysis on a Daicel Chiralpak IC column: 70:20:10 hexane/*i*-PrOH/ DCM, flow rate 0.8 mL/min,  $\lambda = 254$  nm:  $\tau_{\text{minor}} = 10.0$  min,  $\tau_{\text{major}} = 16.1$  min.  $[\alpha]_{\text{D}}^{26} = -11.44$  ( $c = 1.55$ ,  $\text{CHCl}_3$ ). HRMS *calcd* for  $(\text{C}_{25}\text{H}_{29}\text{NNaO}_3^+)$ : 414.2040, found 414.2044.



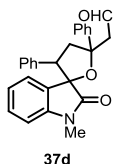
$^1\text{H}$  NMR (400 MHz,  $\text{CDCl}_3$ ):  $\delta$  10.04 (dd,  $J = 4.1$ , 0.9 Hz, 1H), 7.31-7.27 (m, 2H), 7.10-7.06 (m, 1H), 7.0-6.85 (m, 4H), 6.58 (d,  $J = 7.7$  Hz, 1H), 4.60 (dd,  $J = 13.1$ , 6.8 Hz, 1H), 3.26 (d,  $J = 16.7$  Hz, 1H), 3.10 (s, 3H), 3.07-2.97 (m, 2H), 2.18 (dd,  $J = 12.6$ , 6.8 Hz, 1H), 2.12 (s, 3H), 1.14 (s, 9H) ppm.  $^{13}\text{C}$  NMR (100 MHz,  $\text{CDCl}_3$ )  $\delta$  204.6, 178.2, 143.2, 136.9, 134.2, 130.5, 129.3, 128.0, 128.0, 126.8, 126.5, 125.3, 122.1, 108.1, 90.0, 87.4, 48.6, 48.4, 39.4, 38.5, 26.7, 26.3, 19.5 ppm.

**Compound 40n** – The reaction was carried out following the general procedure to furnish the crude product as a 5.6:1 mixture of diastereoisomers; d.r. determined by integration of  $^1\text{H}$  NMR signal:  $\delta_{\text{major}}$  10.03 (dd),  $\delta_{\text{minor}}$  9.88 ppm (dd). After chromatographic purification the title compound **40n** was isolated as a single diastereoisomer (29 mg, 0.076 mmol, 76% yield). The enantiomeric excess was determined to be 92% by HPLC analysis on a Daicel Chiralpak IC column: 70:20:10 hexane/*i*-PrOH/DCM, flow rate 1.00 mL/min,  $\lambda = 254$  nm:  $\tau_{\text{minor}} = 9.7$  min,  $\tau_{\text{major}} = 25.4$ .  $[\alpha]_{\text{D}}^{26} = -7.80$  ( $c = 1.1$ ,  $\text{CHCl}_3$ ). HRMS *calcd* for  $(\text{C}_{22}\text{H}_{25}\text{NNaO}_3\text{S}^+)$ : 406.1447, found 406.1455.



$^1\text{H}$  NMR (400 MHz,  $\text{CDCl}_3$ )  $\delta$  10.02 (dd,  $J = 4.1$ , 1.0 Hz, 1H), 7.24 – 7.08 (m, 2H), 7.01 – 6.83 (m, 2H), 6.75 – 6.58 (m, 3H), 4.59 (dd,  $J = 13.1$ , 6.7 Hz, 1H), 3.21 (s, 3H), 3.11 (d,  $J = 16.7$  Hz, 1H), 2.97 (dd,  $J = 16.7$ , 4.7 Hz, 1H), 2.85 (t,  $J = 13.1$  Hz, 1H), 2.40 (dd,  $J = 13.1$ , 6.7 Hz, 1H), 1.10 (s, 9H).  $^{13}\text{C}$  NMR (100 MHz,  $\text{CDCl}_3$ )  $\delta$  204.3, 177.4, 143.8, 139.9, 129.7, 127.6, 126.6, 126.3, 124.8, 124.2, 122.4, 108.3, 90.6, 87.7, 48.9, 48.0, 40.1, 38.4, 26.8, 26.6.

**Compound 37d** - The reaction was carried out following the general procedure, carrying out the reaction at r.t., with 20 mol% of catalyst and 20 mol% of acid for 3 hours to furnish the crude product as a 8:1 mixture of diastereoisomers  $\delta_{\text{major}}$  9.73 (dd),  $\delta_{\text{minor}}$  9.64 (dd). After chromatographic purification the title compound **37d** was isolated as a single diastereoisomer (28.5 mg – 0.072 mmol - 72% yield). The enantiomeric excess was determined to be 46% by HPLC analysis on a Daicel Chiralpak IC3 column: 70:20:10 hexane/*i*-PrOH/DCM, flow rate 0.8 mL/min,  $\lambda = 254$  nm:  $\tau_{\text{major}} = 15.8$  min,  $\tau_{\text{minor}} = 25.2$  min.  $[\alpha]_{\text{D}}^{26} = +4.5$  ( $c = 1.1$ ,  $\text{CHCl}_3$ ). HRMS *calcd* for  $(\text{C}_{26}\text{H}_{23}\text{NNaO}_3^+)$ : 420.1570, found 420.1570.

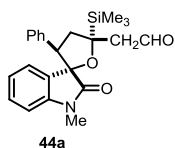


$^1\text{H}$  NMR (400 MHz,  $\text{CDCl}_3$ ):  $\delta$  9.73 (dd,  $J = 3.1$ , 2.3 Hz, 1H), 7.69-7.66 (m, 2H), 7.49-7.40 (m, 3H), 7.37-7.29 (m, 2H), 7.16-7.07 (m, 4H), 6.87-6.84 (m, 2H), 6.61 (d,  $J = 7.7$  Hz, 1H), 3.70-3.59 (m, 2H), 3.46 (dd,  $J = 15.7$ , 2.3 Hz, 1H), 3.17 (dd,  $J = 15.7$ , 3.1 Hz, 1H), 2.86 (dd,  $J =$

9.5, 3.4 Hz, 1H), 2.80 (s, 3H) ppm.  $^{13}\text{C}$  NMR (126 MHz,  $\text{CDCl}_3$ ):  $\delta$  201.8, 175.6, 145.3, 144.3, 133.7, 130.1, 128.7, 128.0, 128.0, 127.6, 127.6, 127.6, 125.5, 124.2, 123.0, 108.2, 88.9, 86.1, 56.7, 53.1, 41.6, 25.6 ppm.

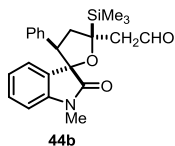
**Compound 44a-b** - The reaction was carried out following the general procedure to furnish the crude products as a 2:1 mixture of diastereoisomers; d.r. determined by integration of  $^1\text{H}$  NMR signal:  $\delta_{\text{major}}$  9.98 (dd),  $\delta_{\text{minor}}$  9.86 ppm (dd). After chromatographic purification the two compounds were isolated as single diastereoisomer (respectively 16 mg – 0.041 mmol - 41% yield; 8 mg – 0.02 mmol – 20% yield). The enantiomeric excess of both compounds were determined to be 90% and 89% by HPLC analysis.

**44a:** Daicel Chiralpak IA column: 95/5 hexane/ $^i$ PrOH flow rate 1 mL/min,  $\lambda$  = 290 nm.  $\tau_{\text{minor}}$  = 6.9 min,  $\tau_{\text{major}}$  = 7.9 min.  $[\alpha]_{\text{D}}^{26}$  = +53.1867 ( $c$  = 0.75,  $\text{CHCl}_3$ ). HRMS *calcd* for  $(\text{C}_{23}\text{H}_{27}\text{NNaO}_3\text{Si}^+)$ : 416.1652, found 416.1646.



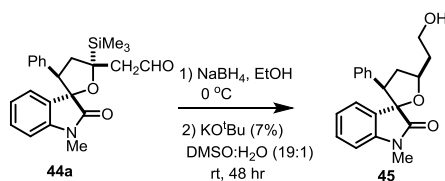
$^1\text{H}$  NMR (400 MHz,  $\text{CDCl}_3$ )  $\delta$  9.86 (dd,  $J$  = 3.8, 1.6 Hz, 1H), 7.47-7.43 (m, 1H), 7.32-7.26 (m, 1H), 7.20 – 7.06 (m, 4H), 6.98 – 6.88 (m, 2H), 6.57 (d,  $J$  = 7.8, Hz, 1H), 3.73 (dd,  $J$  = 13.1, 7.2 Hz, 1H), 3.59 (dd,  $J$  = 15.9, 1.6 Hz, 1H), 3.23 – 3.10 (m, 2H), 2.76 (s, 3H), 2.68 (dd,  $J$  = 13.1, 7.2 Hz, 1H), 0.22 (s, 9H).  $^{13}\text{C}$  NMR (100 MHz,  $\text{CDCl}_3$ )  $\delta$  203.5, 176.4, 144.3, 134.4, 130.1, 128.2, 128.2, 127.8, 127.6, 123.5, 123.1, 108.3, 88.7, 79.2, 55.9, 55.2, 39.1, 25.7, -2.5.

**44b:** Daicel Chiralpak IC column: 96/2/2 hexane/ $^i$ PrOH/DCM flow rate 1 mL/min,  $\lambda$  = 254 nm.  $\tau_{\text{minor}}$  = 9.0 min,  $\tau_{\text{major}}$  = 9.4 min.  $[\alpha]_{\text{D}}^{26}$  = + 16.9250 ( $c$  = 0.4,  $\text{CHCl}_3$ ).

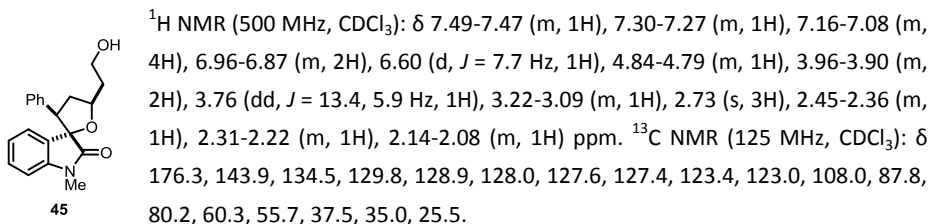


$^1\text{H}$  NMR (500 MHz,  $\text{CDCl}_3$ )  $\delta$  9.98 (t,  $J$  = 3.0 Hz, 1H), 7.40-7.45 (m, 1H), 7.35-7.29 (m, 1H), 7.22 – 7.07 (m, 4H), 6.99 – 6.85 (m, 2H), 6.62 (d,  $J$  = 7.8, 1H), 3.99 (dd,  $J$  = 13.2, 6.0 Hz, 1H), 3.38 (dd,  $J$  = 13.2, 12.1 Hz, 1H), 3.06 (dd,  $J$  = 15.7, 3.0 Hz, 1H), 2.89 (dd,  $J$  = 15.7, 3.0 Hz, 1H), 2.73 (s, 3H), 2.18 (dd,  $J$  = 12.1, 6.0 Hz 1H), 0.32 (s, 9H).  $^{13}\text{C}$  NMR (125 MHz,  $\text{CDCl}_3$ )  $\delta$  202.6, 174.6, 144.0, 134.4, 129.8, 129.2, 128.0, 127.7, 127.4, 123.6, 123.1, 107.9, 89.0, 78.2, 53.7, 53.0, 37.4, 25.4, -2.6.



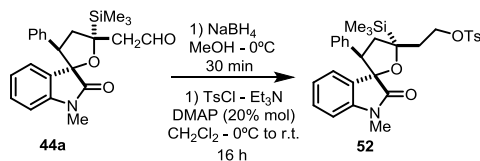
**Procedure for Protidesilylation of compound 44a:****Scheme 3.21** – Protidesilylation of compound **44a**.

The aldehyde **44a** (22 mg, 0.056 mmol) obtained by the general procedure described above was dissolved in 1.5 ml of EtOH and reduced by the slow addition of NaBH<sub>4</sub> (10 mg – 0.28 mmol – 5eq) at 0 °C. The reaction mixture was stirred for 1hr and then quenched by dropwise addition of saturated aqueous ammonium chloride solution (5 ml). The mixture was extracted 3 times with CH<sub>2</sub>Cl<sub>2</sub> (3 ml) and the organic phases were collected. The reaction crude was roughly purified through silica gel (hex-EtOAc 80/20) to remove impurities detectable on TLC. The resulting compound was then transferred to a round bottom flask and dissolved in 7% (w/v) KO<sup>t</sup>Bu in DMSO:H<sub>2</sub>O mixture (2.5 ml, 19:1). The reaction mixture was stirred for 48 hr at rt. The reddish-brown reaction mixture was diluted with 5 ml of ethyl acetate and washed 3 times with 2 ml of water and finally with 2 ml of brine. Solvents were removed under vacuum and the crude product was purified through flash column chromatography (Hexane:Ethyl acetate, 1:1) affording compound **45** as a single diastereoisomer (11 mg - 0.034 mmol – 61% yield for two steps). The enantiomeric excess was determined to be 90% by HPLC analysis on a Daicel Chiralpak IC3 column: 70/20/10 hexane/<sup>i</sup>PrOH/ DCM, flow rate 0.8 mL/min, λ = 254 nm: τ<sub>minor</sub> = 14.5 min, τ<sub>major</sub> = 24.7 min. [α]<sub>D</sub><sup>26</sup> = +39.42 (c = 0.45, CHCl<sub>3</sub>). HRMS *calcd* for (C<sub>20</sub>H<sub>21</sub>NNaO<sub>3</sub><sup>+</sup>): 346.1414, found 346.1421.

**Determination of the Product Configuration**

The absolute and relative configuration for the major diastereoisomer of compounds **40b**, **40k** and **44a** was unambiguously determined by anomalous dispersion X-ray crystallographic analysis.

In order to get a suitable single crystal for compound **44a**, the tosyl derivative has been synthesized according to Scheme S5.



Scheme 3.22 – Preparation of compound 52.

Crystallographic data for compound **40b**, **40k** and **52** are available free of charge from the Cambridge Crystallographic Data Centre, accession numbers CCDC 947750, CCDC 947751 and CCDC 953544 respectively.

For compounds **44b** and **45** (Scheme 3.16), the absolute configuration of the (C4) stereocenter has been established by analogy, considering the X-ray analysis carried out on compound **44a**. NMR study detailed below.

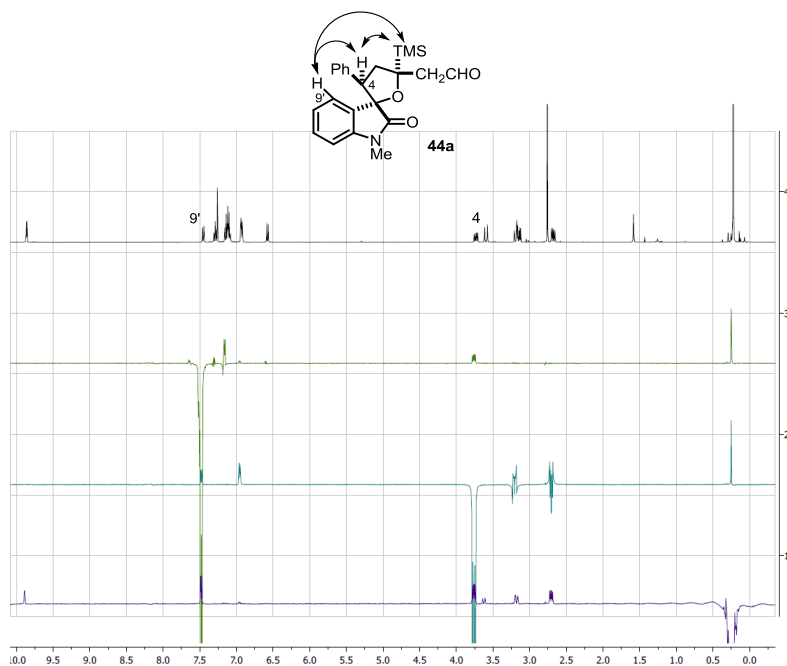


Figure 3.16 – nOe studies carried out on compound 44a.

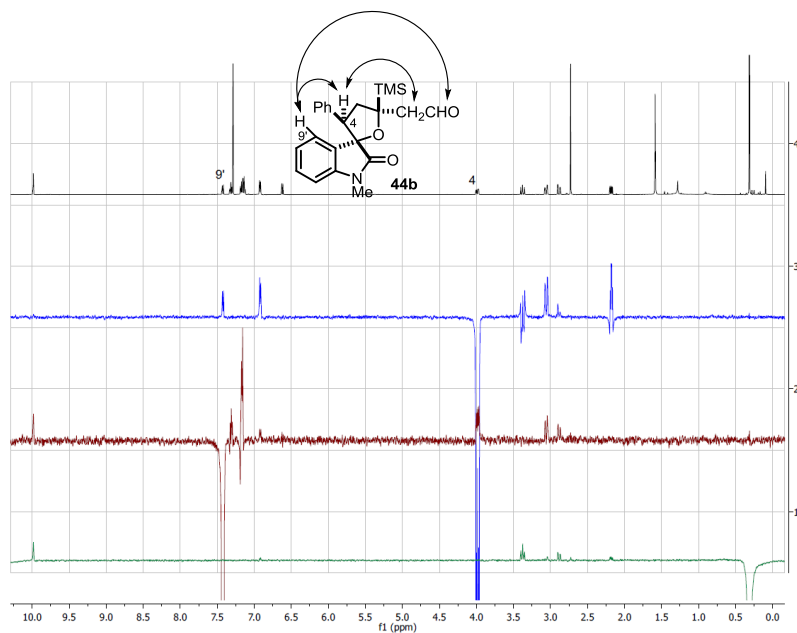


Figure 3.17 – nOe studies carried out on compound **44b**.

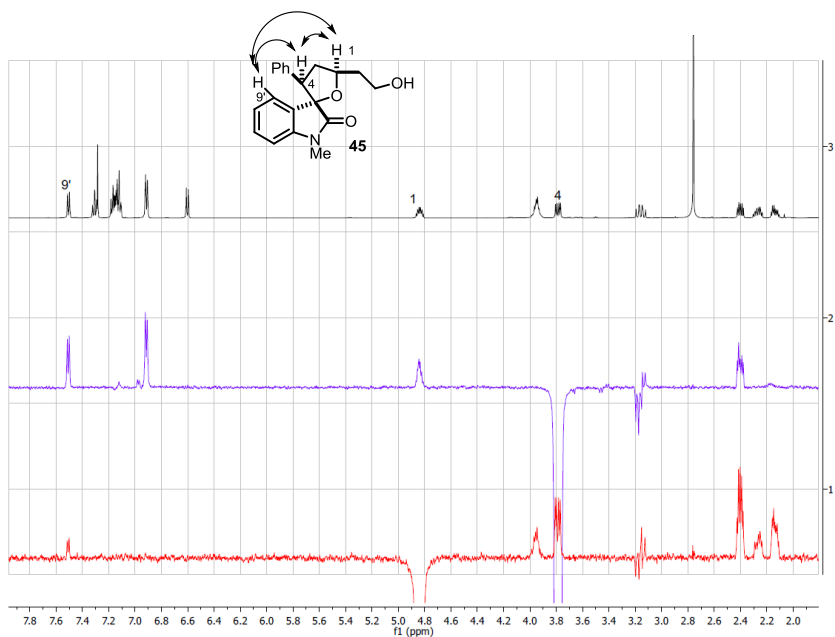
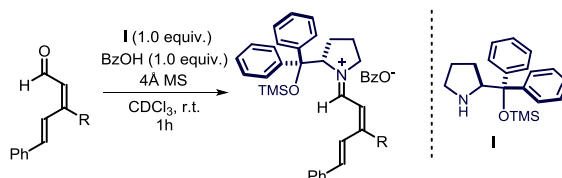


Figure 3.18 – nOe studies carried out on compound **45**.

**General procedure for preparing iminium ion species 39.**



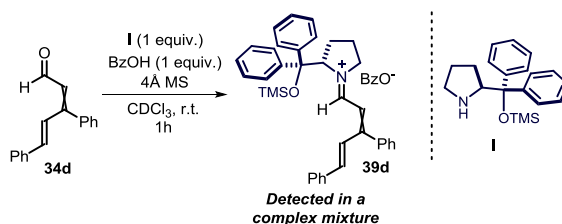
**Scheme 3.23** – Preparation of vinylogous iminium ion species.

19.5 mg (0.05 mmol – 1.0 equiv.) of catalyst **I**, 7.3 mg (0.05 mmol – 1.0 equiv.) of benzoic acid and 0.05 mmol (1.0 equiv.) of aldehydes **38** or **34d** were added in a dry schlenk tube charged with 80 mg of freshly activated 4 Å MS in powder under an argon atmosphere. 200 µL of freshly dried CDCl<sub>3</sub> were added and the mixture was stirred for 1 hour. 50 µL of this mixture were then added to a dry NMR tube under an argon atmosphere, followed by the addition of additional 500 µL of freshly dried CDCl<sub>3</sub>. The NMR tube was kept for 20 minutes under an argon atmosphere in order to let the molecular sieves to sediment on the bottom. The NMR analyses were then carried out on a Bruker 400 MHz machine.

## Annex I – Iminium ion species **39d** analysis

As presented in Figure 3.2 the starting material **34d** was present in solution as a pair of *E-Z* isomers. It is rational to assume that the presence of the two isomers of the starting material is directly translated in the formation of a pair of geometrical isomers in the reactive vinylogous iminium ions **39d**. This annex is devoted to the NMR studies carried out in order to detect the isomers of the vinylogous iminium ion **39d** in solution.

Attempts to synthesize pure vinylogous iminium ion derivatives **39d** derived from aldehyde **34d** have met with failure due to the high instability of these compounds. For this reason an exhaustive NMR conformational analysis of the species was not possible. Anyway, some amounts of the iminium species were detected in a complex mixture of byproducts.



Scheme 3.24 – Preparation of vinylogous iminium ion **39d**.

In order to verify the identity of compounds **39d** detected in the complex mixture we compared the chemical shifts of the species observed to the ones of compound **39** (see Figure 3.8), which was fully characterized by means of bidimensional and nOe NMR investigations.

After mixing aldehyde **34d** with catalyst **I** two broad doublets were detected respectively at 8.05 and 9.45 ppm (Figure 3.19, zoom in insert), chemical shifts feasible for iminium ion species (H1 of compounds **39d**, Figure 3.19). The signals are partially overlapped to other signals *e.g.* the starting aldehyde and other aromatic signals, but are sufficiently resolved to be detected. The two signals show clear COSY correlation with hydrogens at 6.0 – 7.0 ppm (Figure 3.20). The latter hydrogens show a doublet multiplicity and the lack of additional other COSY crosspeaks. The chemical shift of these two signals is comparable of the one of H2 in **39** (Figure 3.8). On the basis of the observed chemical shift, the signals multiplicity and the COSY profile, we consider feasible that the first signals could be assigned to H1 of compounds **39d** coupling with H2 (Figure 3.19). Compound **39d** is present as a mixture of two isomeric species.

In the region at 5.0 – 6.0 ppm, other two interesting signals were detected that we consider associated to the H $\alpha$  of the iminium species (the chemical shift is comparable of H $\alpha$  of compound **39**, Figure 3.8). Consonant with this hypothesis, these signals shown COSY crosspeaks with protons with chemical shift 2.5 – 3.0 ppm, comparable the H $\beta$  of compound **39**. In consonance with the proposed structure, irradiation of H $\alpha$  led to the detection of strong nOe on

H1 (Figure 3.21), indication of the presence of two iminium ion species having *E* configuration of the N-C bond.

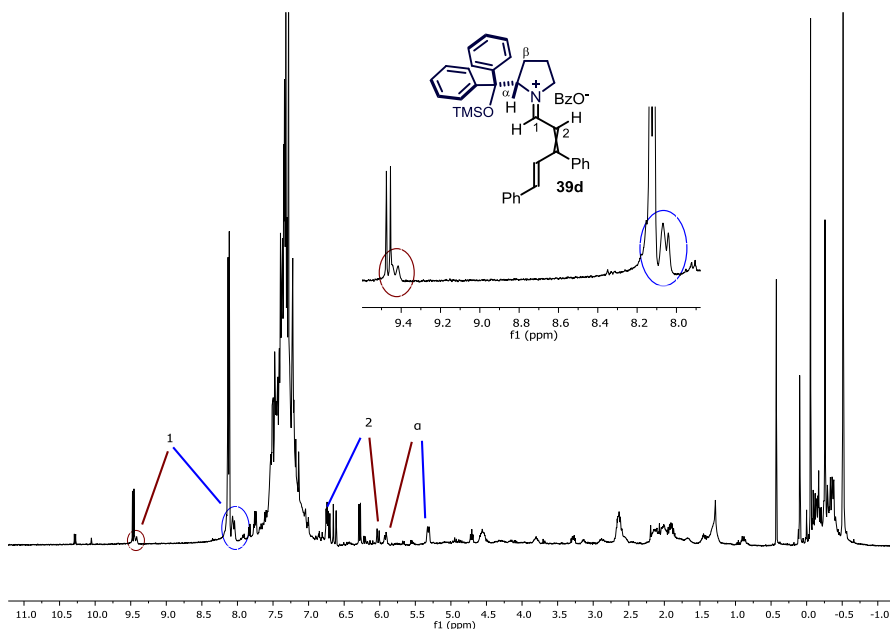


**Figure 3.19** – <sup>1</sup>H-NMR analysis of the reaction mixture for preparation of compounds 39d. A pair of isomers were detected in solution, in blue selected signals of the major and in red selected signals of the minor species.

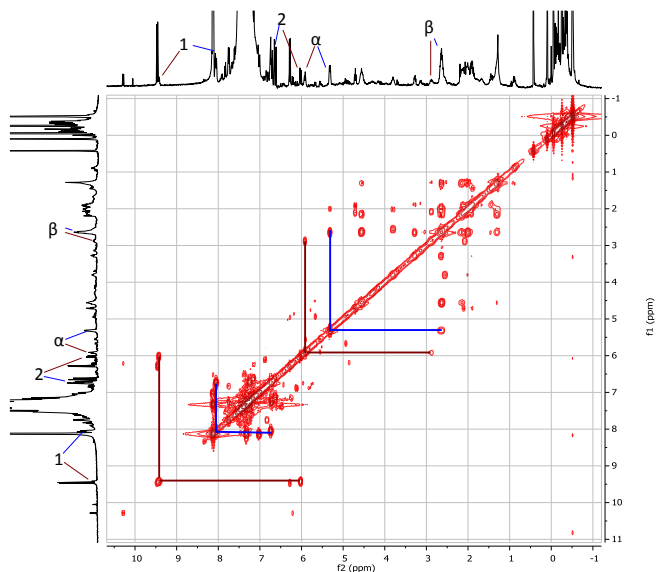


**Figure 3.20** – COSY-NMR analysis of reaction mixture for preparation of compounds 39d. Selected proton correlations of the major (blue) and the minor (red) iminium isomer are marked.

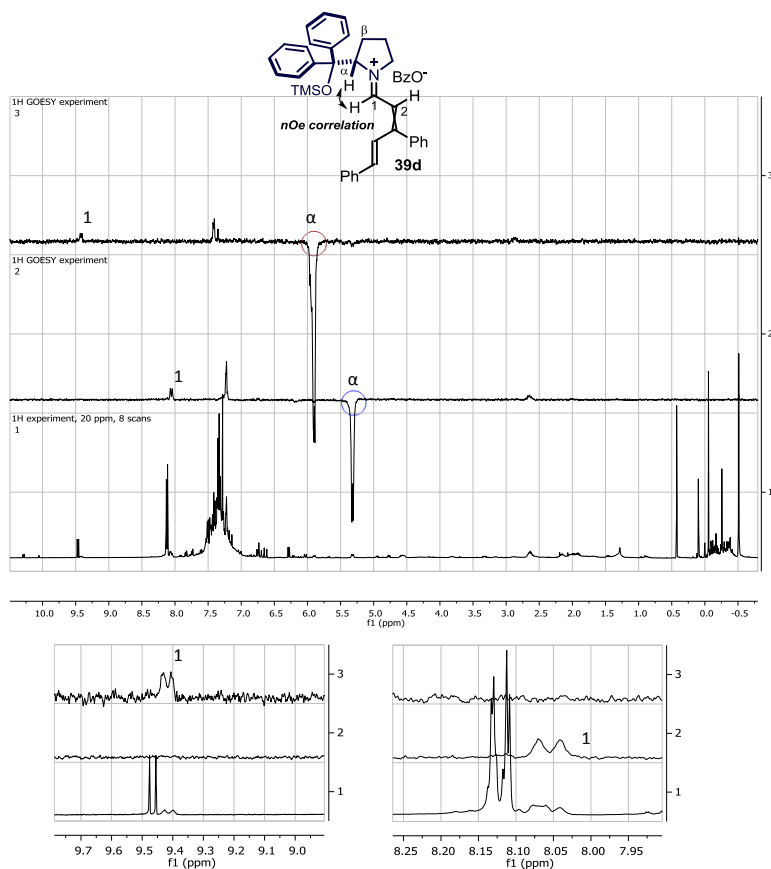


**Figure 3.21** – nOe investigation on compounds **39d**. Irradiation of  $\text{H}_\alpha$  lead to observation of nOe correlation with  $\text{H}_1$  in both the species detected in solution. This is a further evidence of the identity of the compounds and of the *E* configuration of the N-C bond in both the species. In the insert: zoom of the nOe correlation observed on the iminium hydrogen protons  $\text{H}_1$  in both the minor (left) and major (right) species.

It was impossible to perform additional conformational analysis of the iminium ion species detected in solution, as well as to provide a reliable quantification of the relative amount of the two isomers, due to the instability of the compounds and the complex mixture of byproducts detected in the mixture.

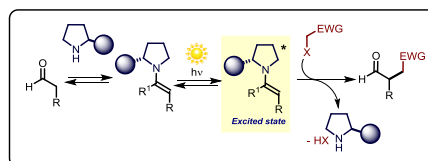
Anyway, on the basis of the above analysis we were able to confirm that the presence in solution of two isomers of starting aldehyde **34d** was directly translated in the formation of iminium ion **39d** as a couple of isomers. In contrast, as presented in Figure 3.8, iminium ion species **39** was synthesized as single isomer.

## Chapter IV

# Enantioselective Organocatalytic $\alpha$ -Alkylation of Aldehydes and Enals Driven by the Direct Photoexcitation of Enamines

### Target

Photochemical organocatalytic enantioselective synthesis of chiral  $\alpha$ -alkylated aldehydes proceeding through a radical pattern and in the absence of any external photoredox catalyst.



### Tool

Ability of photoexcited enamines to act as photoinitiators triggering the formation of reactive radical species from the organic halides.<sup>1</sup>

## 4.1 Introduction

Organocatalysis have been extensively explored over the last 15 years. The high level of competition within the field led to the development of a great number of novel concepts and chemical transformations at an impressive pace. Nowadays, it is remarkably hard to bring further innovation to the field.

In the first part of my PhD, we successfully merged the concept of vinylgy with organocatalysis in order to achieve asymmetric remote functionalizations of linear conjugated carbonyl compounds, a relatively unexplored topic in organocatalysis. In the second part of my PhD studies, I investigated the potential of key organocatalytic intermediates to directly reach an electronically excited state upon light absorption. Thus, I mainly focused on the development of novel reactivities triggered by the photoactivity of chiral organocatalytic intermediates in the excited state.

Using light excitation to bring a molecule from its ground state to an electronically excited state can open new dimensions for chemistry, since the chemical reactivity of electronically excited molecules differs fundamentally from that in the ground state. The excited state reactivity might provide unexplored possibilities for developing processes which cannot be realized using thermal activation. We believe that reconsidering photochemical reactivity using the knowledge,

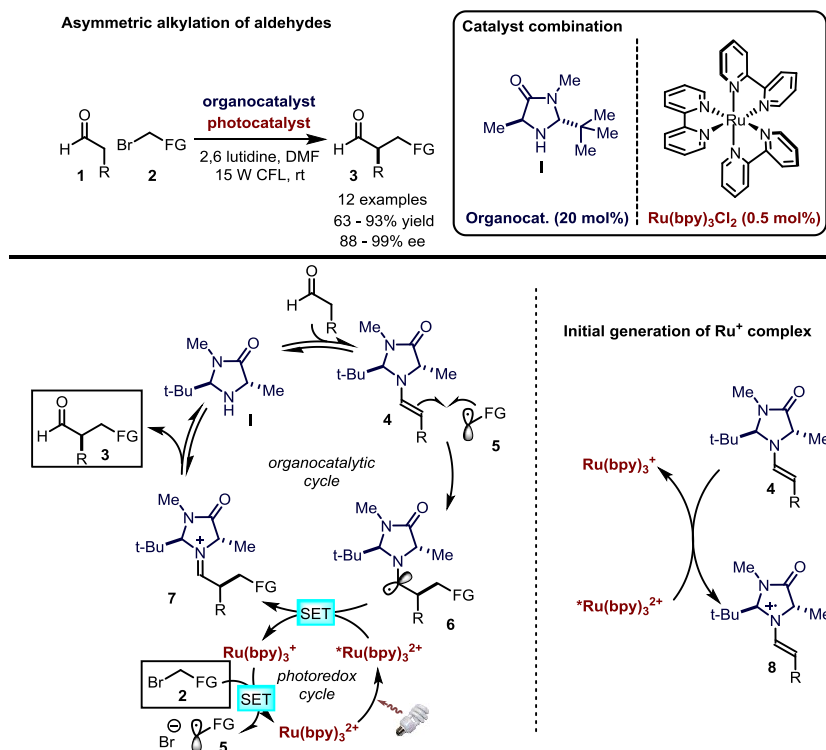
<sup>1</sup> The work discussed in this chapter has been published, see: Silvi, M.; Arceo E.; Jurberg, I. D.; Cassani, C.; Melchiorre, P. "Enantioselective Organocatalytic Alkylation of Aldehydes and Enals Driven by the Direct Photoexcitation of Enamines" *J. Am. Chem. Soc.* **2015**, *137*, 6120.



perspective, and tools of a modern organic chemist (*i.e.* aminocatalysis) can offer new opportunities for asymmetric catalytic synthesis, particularly when faced with the universal need for more environmentally responsible chemical processes.

#### 4.1.1 Photocatalysis: the MacMillan approach

The concept of merging photochemistry with organocatalysis was first explored by the group of MacMillan *et al.* (Scheme 4.1).<sup>2</sup> In this seminal work, the tendency of chiral enamines to react with electrophilic radicals was exploited for addressing the desired enantioselective  $\alpha$ -functionalization of aldehydes **1** with alkyl halides **2**, a sought-after transformation which could not be realized through classical polar pathways. A ruthenium-based catalyst was used as the photosensitizer to generate radicals under mild conditions.



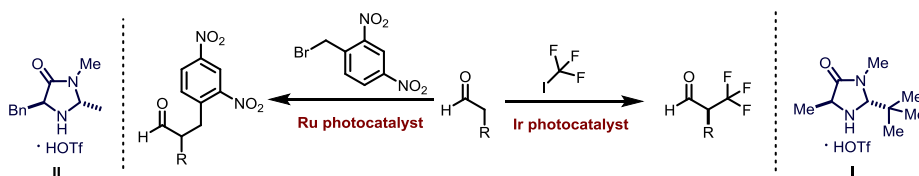
**Scheme 4.1** – MacMillan’s photochemical alkylation of enamines with alkyl halides. A photoredox catalytic cycle is merged with an organocatalytic one. CFL = compact fluorescent light; SET: single electron transfer.

<sup>2</sup> Nicewicz, D. A.; MacMillan, D. W. C. “Merging Photoredox Catalysis with Organocatalysis: The Direct Asymmetric Alkylation of Aldehydes” *Science* **2008**, *322*, 77.

In the proposed mechanism, the reductive cleavage of the electron-poor alkyl halide **2** induced by the strong reductant  $\text{Ru}^+(\text{bpy})_3$  ( $E_{1/2}^{\text{II/I}} = -1.33 \text{ V}$ ) affords electrophilic radicals **5**. Radical addition on the enamine double bond generates the  $\alpha$ -amino radical **6**, a strong electron-rich species.<sup>3</sup> Next, facile oxidation of **6** to the corresponding iminium ion **7** occurs to regenerate the reducing  $\text{Ru}^+$  species from the photoexcited  $^*\text{Ru}(\text{bpy})_3^{+2}$ . Luminescence quenching studies revealed that the reductant species  $\text{Ru}(\text{bpy})_3^+$  is initially generated by oxidation of a sacrificial amount of enamine **4** by photoexcited  $^*\text{Ru}(\text{bpy})_3^{+2}$  (Scheme 4.1).

At a later stage, the MacMillan group expanded the scope of the transformation to achieve the asymmetric  $\alpha$ -benzylation and  $\alpha$ -trifluoromethylation of aldehydes (Scheme 4.2).<sup>4,5</sup>

#### Asymmetric alkylation of aldehydes



Scheme 4.2 – Other enantioselective  $\alpha$ -alkylations of aldehydes accessible through MacMillan strategy.

It is important to remark that the idea developed by MacMillan *et al.* was to employ the ground state chemistry of chiral enamines in combination with the excited state reactivity of an external light-activated sensitizer.

### 4.1.2 Photochemistry of EDA complex: our group approach

In 2013, on the basis of a control experiment, colleagues within the Melchiorre group discovered that the enantioselective photochemical alkylation of aldehydes with electron-poor alkyl halides (benzyl and phenacyl bromides), could be successfully realized without the addition of external photosensitizers. Initial investigations revealed that light was required for the reaction to occur, and that radical intermediates were involved. Further studies established that crucial for the light-triggered generation of radicals was the photoactivity of ground state electron-donor

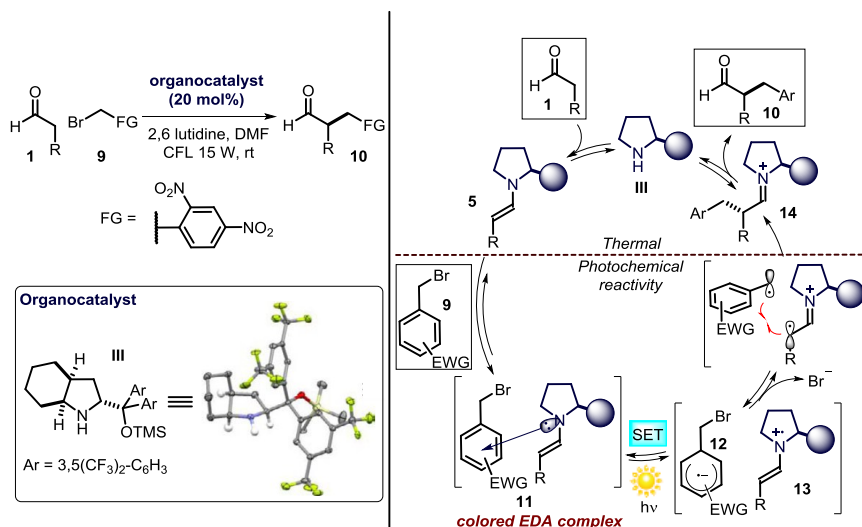
<sup>3</sup> Ismaili, H.; Pitre, S. P.; Scaiano, J. C. "Active Participation of Amine-Derived Radicals in Photoredox Catalysis as Exemplified by a Reductive Cyclization" *Catal. Sci. Technol.* **2013**, *3*, 935.

<sup>4</sup> Nagib, D. A.; Scott, M. E.; MacMillan D. W. C. "Enantioselective  $\alpha$ -Trifluoromethylation of Aldehydes via Photoredox Organocatalysis" *J. Am. Chem. Soc.* **2009**, *131*, 10875.

<sup>5</sup> Shih, H.-W.; Vander Wal, M. N.; Grange, R. L.; MacMillan, D. W. C. "Enantioselective  $\alpha$ -Benzylation of Aldehydes via Photoredox Organocatalysis" *J. Am. Chem. Soc.* **2010**, *132*, 13600.

acceptor complexes (EDA complexes, **11**), formed upon aggregation in the ground state of chiral enamines **5** and electron-poor alkyl halides **9** (Scheme 4.3).<sup>6</sup>

The instantaneous formation of the ground state EDA complex **11** could be detected just by visual observation, since a strong orange color developed immediately after mixing the achromatic reaction partners.



**Scheme 4.3** – Photoactivity of EDA complexes can drive  $\alpha$ -alkylation of aldehydes without the employment of external photosensitizers; CFL: compact fluorescence light; SET: single electron transfer.

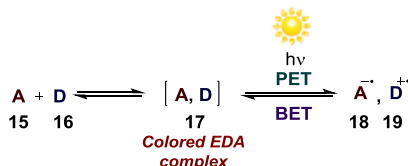
In the proposed mechanism, visible light irradiation of the colored EDA complex **11** leads to the occurrence of a single electron transfer between the enamine and the benzyl bromide, and the radical ion pair **12-13** is formed. The irreversible fragmentation of benzyl bromide radical anion **12** leads to the generation of benzylic radicals in solution, while avoiding an unproductive back electron transfer, which would return the ground state EDA complex. The generated open-shell species can initiate radical chain mechanisms or couple with the chiral enamine radical cation, as depicted in Scheme 4.3. The formation of the carbon-carbon bond leads to iminium ion **14**, whose hydrolysis furnishes the desired product **10** and regenerates the catalyst **III**.

The formation of EDA complexes between electron-rich and electron-poor partners (having a low ionization potential and a high electron affinity, respectively) has been widely studied and reported in the literature. The electronic spectra of EDA associations are characterized by a longer wavelength absorption band which is absent in the separate, individual components. This

<sup>6</sup> Arceo, E.; Jurberg, I. D.; Álvarez-Fernández, A.; Melchiorre, P. "Photochemical Activity of a Key Donor-Acceptor Complex can Drive Stereoselective Catalytic  $\alpha$ -Alkylation of Aldehydes" *Nat. Chem.* **2013**, *5*, 750.

absorption band is called “charge-transfer band” and it usually occurs in the visible region, justifying the intense color developed when mixing the partners.<sup>7</sup>

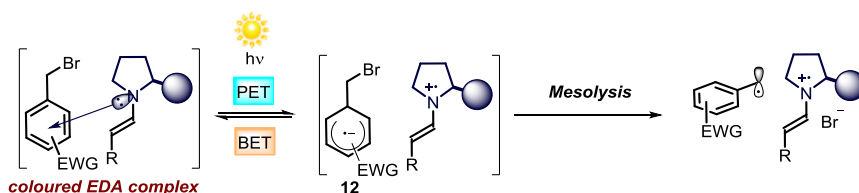
In Scheme 4.4, the photo-induced electron transfer event occurring between two generic partners (the acceptor **15** and the donor **16**) in an EDA complex **17** is depicted.



**Scheme 4.4** – Irradiation of EDA complex readily leads to electron-transfer between donor and acceptor partners to generate unstable radical ions. Back electron transfer is usually the only possible fate of the radical pair.

Irradiation of **17** leads to the formation of a radical ion pair **18-19**. This very high energy species has a great tendency to regenerate the starting materials **15** and **16** via a fast back electron transfer (BET). The tendency to undergo this process justifies the very limited employment of EDA complexes in synthetic photochemistry. In order to exploit the photoactivity of EDA complexes for synthetic purposes, the BET phenomenon has to be limited by a fast irreversible transformation involving the highly reactive open-shell species **18** or **19**.

Scheme 4.5 highlights the crucial step of the EDA complex-based enantioselective alkylation chemistry discussed in Scheme 4.3. The back electron transfer is limited by the irreversible fragmentation of the carbon-bromine bond within the alkyl halide radical anion **12**, which irreversibly generates highly reactive benzyl radicals.

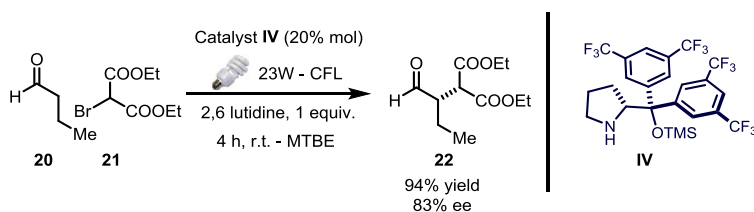


**Scheme 4.5** – Irreversible mesolysis of the carbon-bromine bond occurring within the radical anion **12** renders the electron-transfer synthetically useful, limiting the back electron transfer (BET) phenomenon.

<sup>7</sup> a) For an exhaustive review about EDA complexes in organic synthesis: Rathore, R.; Kochi, J. K. “Donor/Acceptor Organizations and the Electron-Transfer Paradigm for Organic Reactivity” Chapter 2, p. 193 in *Advances in Physical Organic Chemistry, Volume 35*, **2000**, Academic Press. b) For a representative example: Rathore, R.; Kochi, J. K. “ $\alpha$ -Nitration of Ketones via Enol Silyl Ethers. Radical Cations as Reactive Intermediates in Thermal and Photochemical Processes” *J. Org. Chem.* **1996**, *61*, 627.

## 4.2 Target of the project

During the investigation on the asymmetric  $\alpha$ -alkylation of aldehydes, it was discovered that diethyl bromomalonate **21** was a suitable candidate to react under photochemical conditions providing product **22** in high yield and stereoselectivity (Scheme 4.6). However, we did not observe any color formation during the entire reaction time.



**Scheme 4.6** – Photochemical  $\alpha$ -alkylation reaction of butyraldehyde with diethyl bromomalonate. The reaction smoothly affords the desired product using a commercially available compact fluorescent lamp (CFL) and does not require the use of any photocatalyst. The reaction mixture remained completely achromatic during the entire reaction time.

The lack of color development stands in sharp contrast with the mechanistic framework based on the formation of colored EDA complex, whose photoactivity was essential for driving the  $\alpha$ -alkylation of aldehydes with electron poor benzyl bromides. The target of my research endeavor within this project was to solve this mechanistic conundrum, providing a rationalization for the observed reactivity. The main question to address was: how could the radical be generated from bromomalonate **21** under light illumination if no EDA complex formation was detected? In other words, which is the photochemical mechanism of radical generation?

## 4.3 Results and discussion

The photochemical reaction depicted in Scheme 4.6 proceeds through visible light irradiation. In Figure 4.1, the vial containing the colorless reaction mixture is depicted.



**Figure 4.1** – Vial with the reaction components dissolved in MTBE at the same concentration employed for carrying out the reaction: aldehyde **20** (1.5 M), catalyst **IV** (0.1 M), 2,6-lutidine (0.5 M) and diethyl bromomalonate **21** (0.5 M) in MTBE.

The reaction does not show evident color.

As stated in the first law of photochemistry, also known as Grotthuss-Draper law, a photochemical process can occur if one (or more) of the species involved in the photochemical process can absorb the light employed for irradiation.<sup>8</sup> As a consequence, it is unexpected that a colorless reaction undergoes a photochemical process when irradiated by visible light. Spectroscopic studies carried out by means of a UV-vis spectrophotometer were carried out in order to give insights into the absorption proprieties of the reaction components (Figure 4.2).

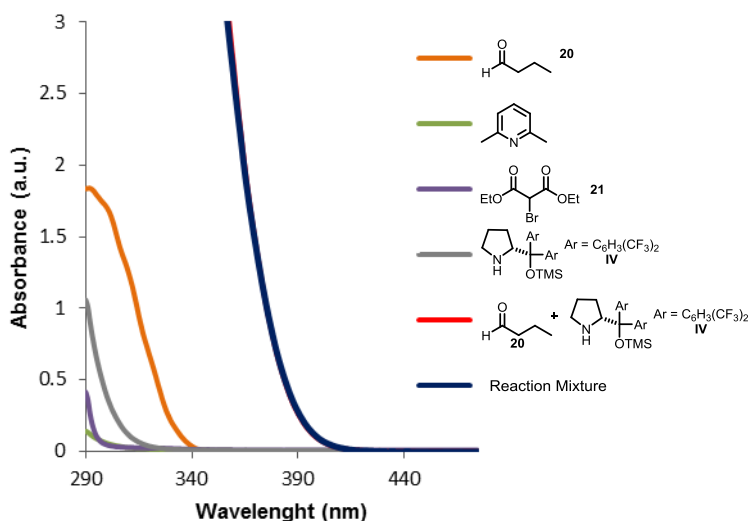


**Figure 4.2** – Spectroscopic study carried out on the reaction mixture at reaction conditions. Orange line: butyraldehyde **20** solution (1.5 M in MTBE). Green line: 2,6-lutidine (0.5 M in MTBE). Violet line: diethyl bromomalonate **21** (0.5 M in MTBE). Grey line: catalyst **IV** (0.1 M in MTBE). Red line (overlapped with blue line): aldehyde **20** (1.5 M in MTBE) + catalyst **IV** (0.1 M in MTBE). Blue line: reaction mixture: aldehyde **20** (1.5 M in MTBE), catalyst **IV** (0.1 M in MTBE), 2,6-lutidine (0.5 M in MTBE), diethyl bromomalonate **21** (0.5 M in MTBE).

Analysis of the reaction mixture revealed an absorption band in the near-visible UV light and a weak tail of light absorption until 420 nm (blue line). None of the separate reagents shown absorption in the near visible light, indicating that the profile observed in the reaction mixture was due to a transient species.

Registering the absorption of different mixtures of reagents, we realized that the mixture of aldehyde and catalyst (red line) perfectly overlaps the reaction mixture absorption (blue line) and is the only responsible for absorption at  $\lambda > 350$  nm. We ascribed the new band to the transient formation of an enamine intermediate **23**. This hypothesis was corroborated by an analogous absorption spectrum reported in literature for similar aliphatic aldehyde-derived

<sup>8</sup> Coyle, J. D. "Distinctive Features of Photochemical Reactions" Chapter 1, p. 3 in *Introduction to Organic Photochemistry*, 1986, Wiley.

enamines.<sup>9</sup> In consonance with our naked-eye observation, no EDA new absorption bands were detected during UV-vis spectroscopic studies.

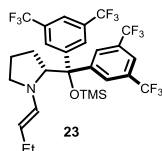


Figure 4.3 – Transient enamine formed after condensation of catalyst **IV** with aldehyde **20**.

The light absorption experiments suggested the possibility for enamines to be directly involved in the photochemical activation. We tried to get unambiguous evidence supporting the involvement of enamines in the photogeneration of radicals from the bromomalonate.

We recently demonstrated the ability of aromatic aldehydes, opportunely excited under compact fluoresce lamp illumination, to generate carbon-centered radicals from diethyl bromomalonate by a light-driven energy transfer mechanism.<sup>10</sup> In analogy, excitation of the  $n-\pi^*$  band of the aliphatic aldehyde **20** (orange line in Figure 4.2) due to weak UV emission spikes commonly present in commercially available fluorescent lamps may lead to sensitization of the alkyl halide **21**, followed by a homolytic cleavage of the excited alkyl halide **21** and development of free radicals which could initiate radical chain mechanisms.<sup>11</sup> Analogous considerations could be done in case of a direct photoexcitation of the alkyl halide **21**, so this possibility should be ruled out as well.<sup>12</sup> Additional experiments were carried out irradiating the reaction mixture with a 300 W xenon lamp equipped with high precision monochromatic or cut-off light filters (Figure 4.4).

Irradiating the mixture using a cut-off filter at 385 nm ( $\lambda > 385$  nm) and a band-pass filter at 400 nm (monochromatic irradiation at  $\lambda = 400$  nm) did not alter the reactivity of the model reaction, in spite of the inability of both the aldehyde **20** and the bromomalonate **21** to absorb light (orange and grey line in Figure 4.4). These results left the direct photoexcitation of the enamine as the most probable mechanism for triggering the radical generation from **21**. This mechanistic scenario was consonant with the experiment performed using a band-pass filter at 450 nm ( $\lambda > 450$  nm, a wavelength that could not be absorbed by the enamine), since a complete inhibition of the reaction was observed, leading to starting material recovery.

<sup>9</sup> González-Béjar, M.; Peters, K.; Hallett-Tapley, G. L.; Grenierb, M.; Scaiano, J. C. "Rapid One-pot propargylamine synthesis by plasmon mediated catalysis with gold nanoparticles on ZnO under ambient conditions" *Chem. Commun.* **2013**, 49, 1732.

<sup>10</sup> Arceo, E.; Montroni, E.; Melchiorre, P. "Photo-Organocatalysis of Atom-Transfer Radical Additions to Alkenes" *Angew. Chem. Int. Ed.* **2014**, 53, 12064.

<sup>11</sup> Aliphatic carbonyl compounds have been reported to act as photosensitizers in photochemical transformations, for an example: Borkman, R. F.; Kearns, D. R. "Triplet-State Energy Transfer in Liquid Solutions. Acetone-Photosensitized cis-trans Isomerization of Pentene-2" *J. Am. Chem. Soc.* **1962**, 88, 3467.

<sup>12</sup> "Photobehavior of Alkyl Halides" P. J. Kropp, Chapter 1, p. 1 in *Handbook of Organic Photochemistry and Photobiology*, 2<sup>nd</sup> edition CRC, **2004**, Boca Raton.

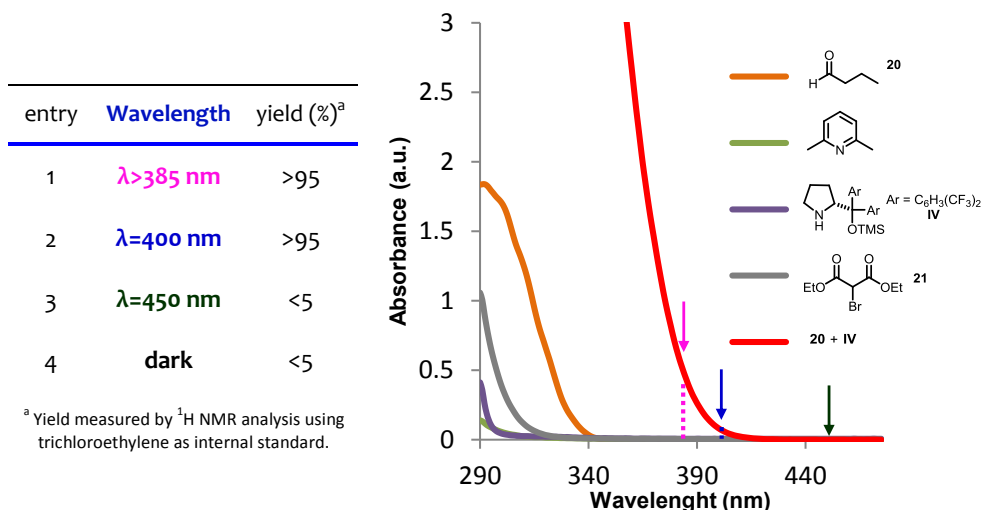


**Figure 4.4** – Results obtained carrying out the reaction with a 300 W – xenon lamp equipped with high-precision light filters.

Then, we registered the emission spectrum of the commercially available compact fluorescent light lamp used for the irradiation of the reaction mixture (Figure 4.5).

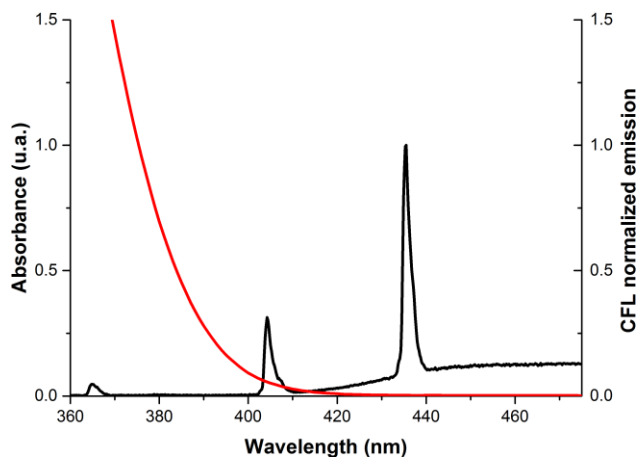


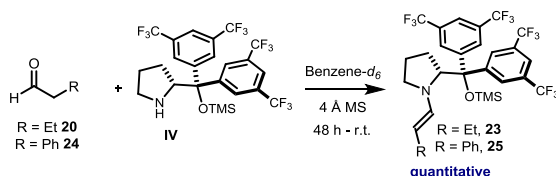
**Figure 4.5** – Overlay between emission spectrum of the compact fluorescent lamp employed for carrying out the reaction (black line) and absorption spectrum of the mixture aldehyde (1.5 M in MTBE) + catalyst (0.1 M in MTBE). Two emission peaks are involved in the photoexcitation (365 nm and 404 nm). In the region  $\lambda < 360 \text{ nm}$ , no emission was observed (the spectrum was registered until 190 nm).



Two light emission peaks (respectively a tiny one in the UV region and another one in the violet region) overlay the enamine **23** absorption. This explains why the commercially available compact fluorescent lamp can promote the photochemical reaction.

### 4.3.1 Enamine synthesis and characterization

To further examine the possible implication of the enamine within the photochemical regime, we decided to investigate the photophysical behavior of the transient enamine generated under the reaction conditions. For this reason, the enamine intermediate was synthesized and carefully characterized. The synthesis of enamine intermediates was achieved by stirring an equimolar mixture of aldehyde **20** or **24** and the chiral amine **IV** over molecular sieves in dry benzene- $d_6$  for 48 hours. Enamines **23** and **25** were quantitatively obtained in high purity (Scheme 4.7).



Scheme 4.7 – Synthesis of enamines **25** and **23**.

The NMR spectra of the enamines are reported in Figure 4.6 – 4.7. A conformational analysis by means of NOESY experiments was conducted.

Careful conformational analysis of the reactive intermediate revealed that enamine **23** was obtained as a single isomer, having an *E* configuration of the double bond, inferred on the basis of a value  $^3J_{\text{H1-H2}} = 14.0$  Hz and a strong nOe between H1 and H3 (Figure 4.6). No traces of the *Z* isomer were detected. Conformational *s-trans* preference was inferred for the exocyclic N-C bond on the basis of a strong nOe between H2 and the two H $\delta$  and H1 and H $\alpha$ . Overall, the conformational behavior of enamine **23** is perfectly consonant with the one of analogous enamine intermediates.<sup>13</sup>

<sup>13</sup> a) Schmid, M. B.; Zeitler, K.; Gschwind, R. M. "Distinct Conformational Preferences of Prolinol Ether Enamines in Solution Revealed by NMR" *Chem. Sci.* **2011**, *2*, 1793. b) Schmid, M. P.; Zeitler, K.; Gschwind, R. M. "Formation and Stability of Prolinol and Prolinol Ether Enamines by NMR: Delicate Selectivity and Reactivity Balances and Parasitic Equilibria" *J. Am. Chem. Soc.* **2011**, *133*, 7065.

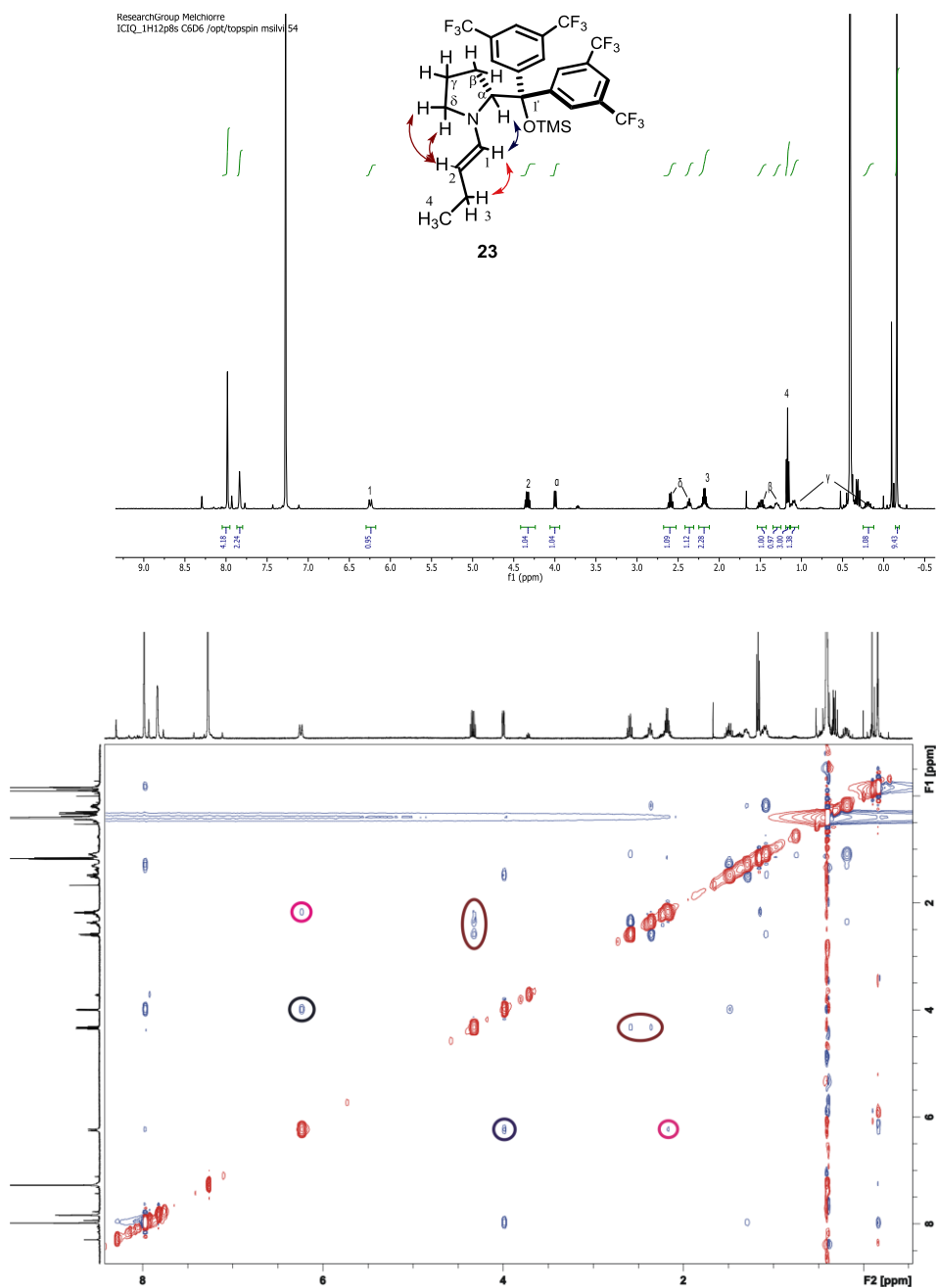
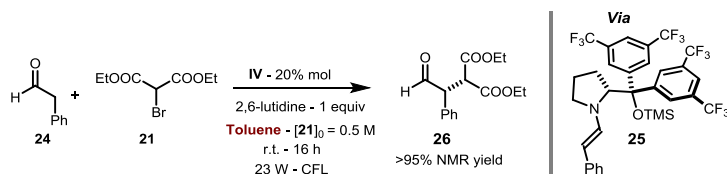


**Figure 4.6** – Selected NMR spectra (<sup>1</sup>H and NOESY) for compound **23**, traces of catalyst **IV** could be detected due to hydrolysis of enamine **23** occurring during NMR experiment.

Unfortunately, the enamine **23** was too unstable for carrying out additional photophysical studies, since it readily hydrolyzed to the corresponding aldehyde and amine in the presence of traces of moisture. For this reason, we considered carrying out the study on the enamine **25**, obtained from phenylacetaldehyde **24**, expecting an improved stability of the compound due to the increased  $\pi$  conjugation.



**Scheme 4.8** – Reaction carried out with phenylacetaldehyde as substrate. Enamine **25** successfully mediates the reaction.

Importantly, phenylacetaldehyde **24** is a competent substrate for the photo-organocatalytic reaction with **21**, providing full conversion into the corresponding product **26** under the reaction conditions (Scheme 4.8). Low enantioselectivity was observed (value between 0 and 50% enantiomeric excess were detected, decreasing during time), as consequence of the tendency of the newly forged benzylic stereocenter to undergo racemization.

The NMR investigation for enamine **25** is reported below, together with a conformational analysis carried out through NOESY technique.

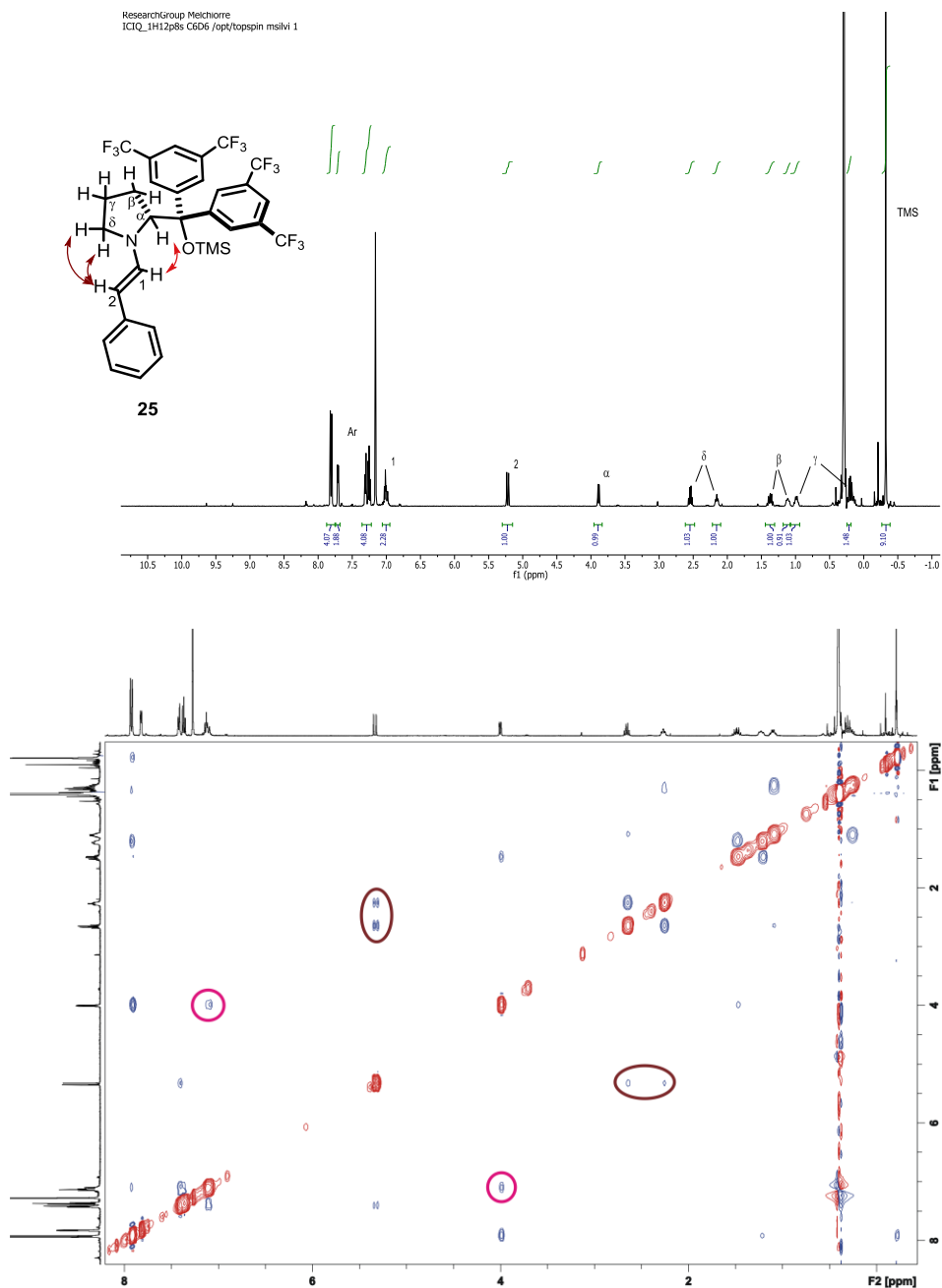


Figure 4-7 – Selected NMR spectra ( $^1\text{H}$  and NOESY) for compound **25**.

In analogy with compound **23**, the enamine **25** was obtained as single isomer which shows a strong conformational rigidity, with identical geometry features.

We were pleased to observe that enamine **25** showed a high stability and no traces of hydrolysis were detected upon dissolution in anhydrous solvents or after storing for one week in the fridge in toluene or benzene solution. The improved stability provided us the possibility to carry out the desired photochemical investigations on the chiral enamine **25**.

### 4.3.2 Photophysical studies of the enamine

UV-vis absorbance analysis of compound **25** revealed a linear Lambert-Beer correlation at different wavelengths (two of which are shown in Figure 4.8, inserts). The linearity of the Lambert-Beer correlation further confirms the stability of **25** under the conditions of the photophysical investigation.

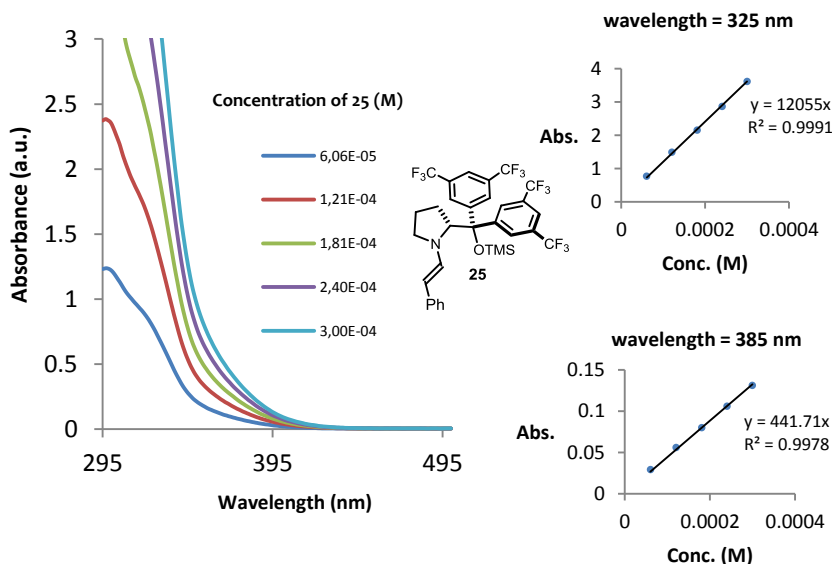
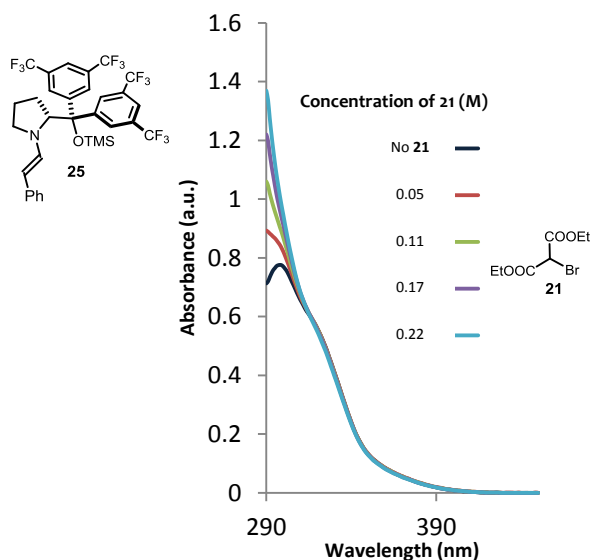


Figure 4.8 – Absorption spectrum of enamine **25** at different wavelengths in toluene. Insert: Lambert-Beer correlation different wavelengths.

The absence of EDA complex charge transfer bands or of any other supramolecular ground state aggregation between enamine **25** and malonate **21** was further confirmed by additional UV-vis absorbance analysis, presented in Figure 4.9. The spectrum of enamine **25** remained completely unaltered upon addition of increasing amounts of malonate **21** (the increase in absorbance in the region  $\lambda < 320$  nm is due to the additive absorption of malonate **21**, which can absorb high energy light, see Figure 4.2), further confirming the absence of ground state interactions between the two compounds.



**Figure 4.9** – Absorption spectra of a  $5 \cdot 10^{-5}$  M solution of enamine **25** in toluene at different concentrations of additive diethyl bromomalonate. The increase of absorption at  $\lambda < 320$  nm is due to the additive absorption of diethyl bromomalonate **21**. The spectrum of enamine **25** remained completely unvaried by the addition of the alkyl halide.

In order to glean some insights into the behavior of enamine **25** in its excited state, we carried out luminescence studies, since this technique furnishes information about transient excited-state species. Irradiation of a solution of enamine **25** with a 365 nm monochromatic light resulted in a luminescence phenomenon. The emission spectrum of the excited enamine is shown in Figure 4.10.

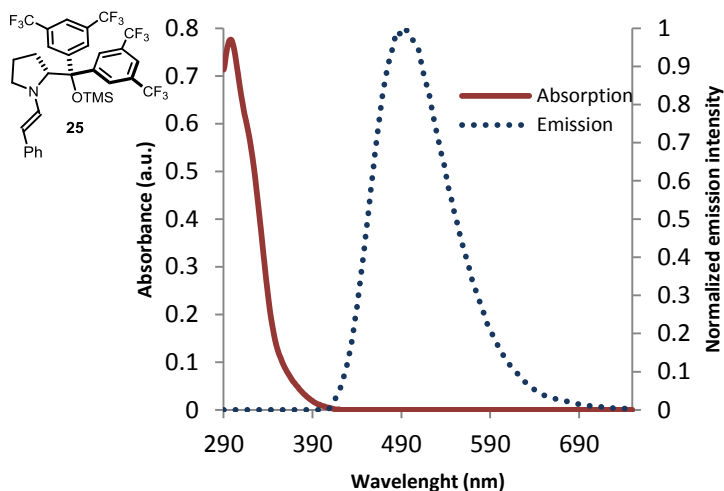


**Figure 4.10** – Absorption spectrum (red line) and normalized emission spectrum (blue dashed line) of a  $5 \cdot 10^{-5}$  M solution of the chiral enamine **25** in toluene solution.

Importantly, blank experiments revealed that irradiation of solutions of amine **IV** or aldehyde **20** did not lead to any luminescence phenomenon, indicating that the emission observed in Figure 4.10 was not due to the presence of traces of starting material arising from hydrolysis.

As a final control experiment, the excitation spectrum associated to the luminescence experiment was compared to the absorption spectrum of enamine **25**. The two spectra show good overlap, indicating that the observed emission was due to the enamine species, and not to the presence of small amounts of fluorescent impurities.<sup>14</sup>

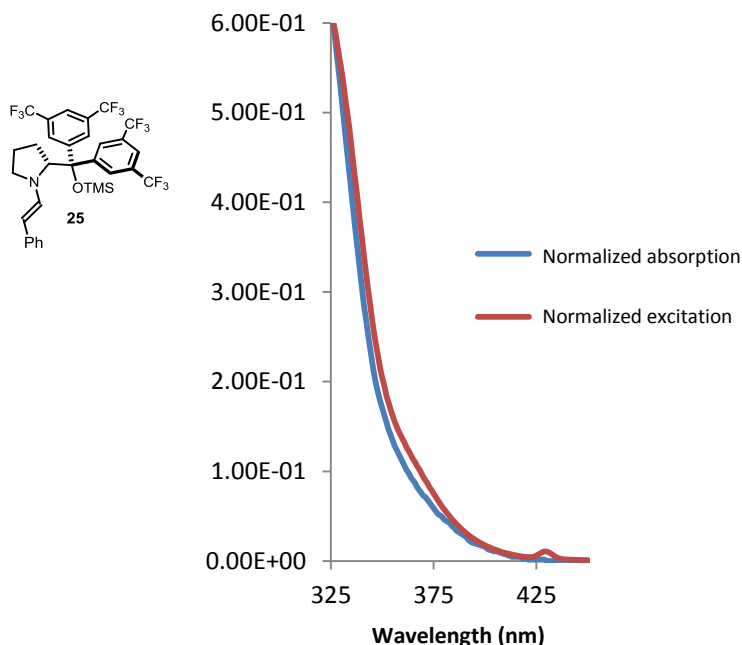


**Figure 4.11** – Overlay between normalized excitation spectrum obtained from the fluorescence experiment and normalized absorption spectrum of enamine, the good overlap indicates that the emission observed is originated by enamine **25**.

We next decided to carry out luminescence quenching studies, in order to reveal possible interactions between the excited enamine **25** and bromomalonate **21**. The addition of increasing amounts of **21** to a solution of enamine **25** effectively quenched the enamine emission. The data analysis revealed a typical linear Stern-Volmer correlation (Figure 4.12, insert).

<sup>14</sup> Anslyn, E. V.; Dougherty, D. A. "Fluorescence" Chapter 16, p. 946 in *Modern Physical Organic Chemistry*, 2006, University Science Books.

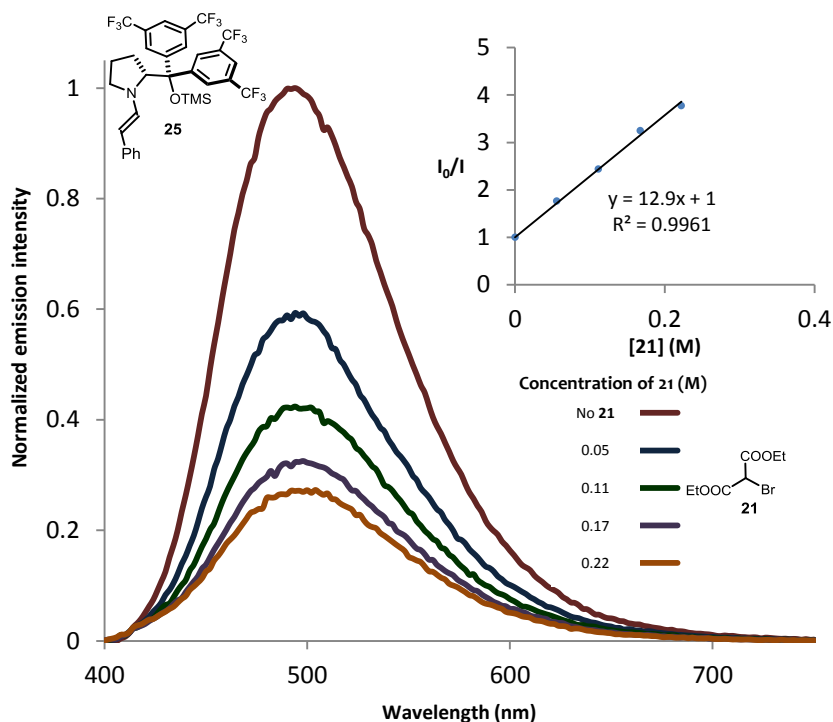


**Figure 4.12** – Fluorescence spectrum of a solution  $5 \cdot 10^{-5}$  M of enamine **25** in toluene solution at different concentrations of diethyl bromomalonate **21**. Insert: Stern-Volmer plot shows a linear correlation between  $I_0/I$  and the concentration of bromomalonate added.

In general three types of fluorescence quenching are known, the trivial fluorescence quenching, also known as *inner-filter* effect, the dynamic fluorescence quenching and the static fluorescence quenching.<sup>15</sup>

*Inner-filter* effect may arise in the case that the quencher compound absorbs light in the same wavelength region used for sample irradiation. As a consequence, the fluorophore will be irradiated less efficiently and fluorescence quenching is observed. This type of quenching is usually a drawback to avoid in Stern-Volmer quenching analysis because it can lead to wrong conclusions. In order to avoid the occurrence of *inner-filter* effect, we carried out the entire analysis irradiating the sample with 365 nm monochromatic light, where our quencher (bromomalonate **21**) does not show any light absorption (see Figure 4.2 and 4.9).

Fluorescence dynamic quenching arises when the lifetime of the excited states is reduced due to interactions with a quencher, usually caused by electron transfer, energy transfer or the formation of an excited complex (also known with the term *exciplex*). Macroscopically, a reduced fluorescence intensity is registered in the presence of the quencher.

<sup>15</sup> Lakowicz, J. R. "Fluorescence Quenching" Chapter 9, p. 258 in *Principles of Fluorescence Spectroscopy* 1983, Premium Press.



Static fluorescence quenching may arise in case that an interaction between the fluorophore and the quencher occurs in the ground state (complex formation, reactions). In case that the new species formed at the ground state does not show luminescence phenomena, a decrease of fluorescence intensity is observed due to the reduction of free fluorophore concentration. Since in the latter case ground-state interactions occur, absorbance spectral variations are usually observed. In our specific studies, we have excluded any possible ground state aggregation between the enamine and the bromomalonate.

In the case that only a single quenching phenomenon occurs, a linear Stern-Volmer correlation is detected ( $I/I_0$  vs  $[Q]$  displays a linear correlation, where  $[Q]$  is the quencher species concentration and  $I$  is the fluorescence emission intensity). In our case, the absence of absorbance spectral variation, together with the linear Stern-Volmer quenching correlation observed, are strong indications of the occurrence of a dynamic quenching.

Overall, our mechanistic studies (absorbance spectra, emission spectra, results of the reaction carried out with monochromatic light source) reveal the previously hidden ability of transiently generated enamines to directly reach an electronically excited state upon light absorption while successively triggering the formation of reactive radical species from the bromomalonate.

We next sought to acquire some information about the electrochemical properties of the enamine **25** in order to evaluate its redox properties.

### 4.3.3 Enamine redox properties

Cyclic voltammetry analysis of the enamine **25** revealed that this species is an extremely electron rich compound. A single irreversible oxidation peak with  $E_{A}^P = 0.6$  V (vs Ag/AgCl) was observed; this result is consonant with reported experiments carried out on similar enamines.<sup>16</sup>

---

<sup>16</sup> Van Humbeck, J. F.; Simonovich, S. P.; Knowles, R. P.; MacMillan, D. W. C. "Concerning the Mechanism of the FeCl<sub>3</sub>-Catalyzed  $\alpha$ -Oxyamination of Aldehydes: Evidence for a Non-SOMO Activation Pathway" *J. Am. Chem. Soc.* **2010**, *132*, 10012.

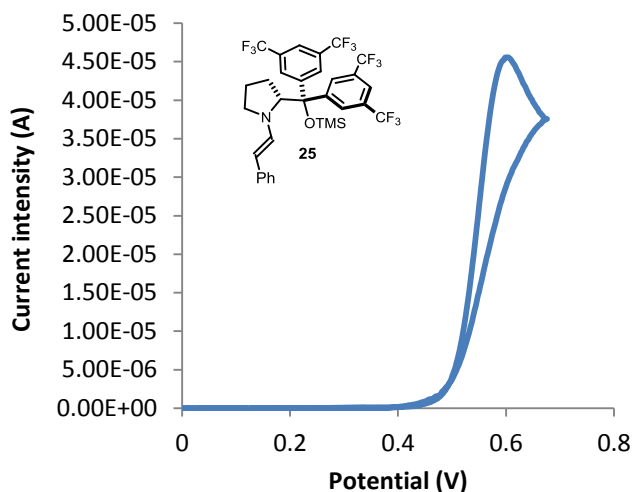


**Figure 4.13** – Cyclic voltammety of enamine **25** (0.01 M acetonitrile solution) in the presence of tetrabutylammonium hexafluorophosphate (0.1 M) as support electrolyte. The oxidation potential was measured using a glassy carbon working electrode, a platinum wire counter electrode, and a NaCl saturated Ag/AgCl reference electrode at 5 mV/s scan rate.

No reversibility was observed increasing the scan rate until 5000 mV/s, which indicates the high instability of the radical cation derived from the enamine oxidation.

The knowledge of the ground-state potential may allow calculating the redox potential of the electronically excited molecule. It is important to remind that *electronically excited molecules are both better electron donors and better electron acceptors than the corresponding ground-state molecules*.<sup>17</sup> This concept is graphically explained in Figure 4.14.

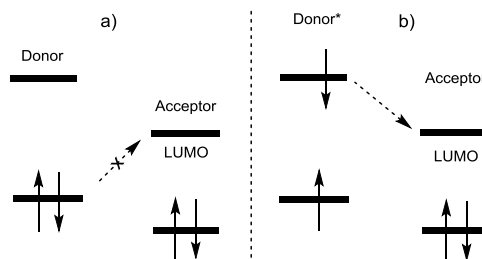


**Figure 4.14** – An endergonic electron transfer reaction between a donor and an acceptor. Electronic excitation of the donor promotes an electron from the HOMO to the LUMO orbital. Electron transfer from excited donor species  $D^*$  is now thermodynamically favorable.

<sup>17</sup> Balzani, V.; Ceroni, P.; Juris, A. “Excited states: Physical and chemical properties, electron transfer” Chapter 4, p. 114 in *Photochemistry and photophysics*, 2014, Wiley-VCH.

Light excitation of an electron-rich compound (donor in Figure 4.14a) leads to the formation of a high energy electronically excited molecule, in which an electron has been promoted to a high energy LUMO orbital (Figure 4.14b). The energy furnished to the system by the photon provides the thermodynamic guidance for electron transfer processes that would otherwise be endergonic.

The knowledge of the energy gap between electronic states gives the possibility to calculate the redox potential of the electronically excited molecule from the corresponding ground-state potential. Unfortunately, a precise calculation of this energy is not always trivial, and this strongly complicates a correct calculation of a redox potential. From spectroscopic measurements, we can roughly estimate the energy gap between the excited state and the ground state in order to calculate an approximate potential. According to Balzani *et al.*, the radiative energy associated to the higher wavelength tail of the electronic spectrum corresponds to a good approximation for the HOMO – LUMO energy gap.<sup>17</sup>

In the case of the enamine **25**, which has a tail of absorption at 400 nm (see Figure 4.10) an approximate energy of 3.10 eV could be calculated. Equation (1) was employed to estimate the excited state potential of enamine **25**:<sup>18</sup>

$$\text{eq. (1)} \quad E_{1/2}[\text{IV}^+/\text{IV}^*] = E_{1/2}[\text{IV}^+/\text{IV}] - E_{0,0}[*\text{IV}/\text{IV}]$$

Due to the irreversibility of the oxidation of the enamine **25**, a precise value for  $E_{1/2}(\text{IV}^+/\text{IV})$  is unavailable, but we can use the  $E_A^P$  measured through cyclic voltammetry analysis and reported in Figure 4.13 as a good approximation of this value.<sup>19</sup> The value of excited state potential could then be calculated as:

$$E_{1/2}(\text{IV}^+/\text{IV}^*) = 0.6 - 3.10 = -2.50 \text{ V (vs Ag/AgCl)}$$

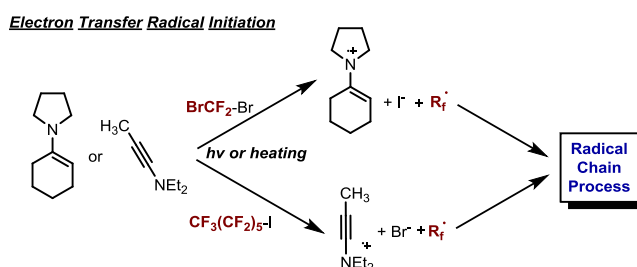
---

<sup>18</sup> a) Kavarnos, G. J. "Excited-State Redox Potentials" Chapter 1, p. 29 in *Fundamentals of Photoinduced Electron Transfer*, **1993**, VCH. b) See also ref. 17. For practical examples of application of equation 1 see: c) Germain, M. E.; Vargo, T. R.; Khalifah, P. G.; Knapp, M. J. "Fluorescent Detection of Nitroaromatics and 2,3-Dimethyl-2,3-dinitrobutane (DMNB) by a Zinc Complex: (salophen)Zn" *Inorg. Chem.* **2007**, 46, 4422. d) Wu, P.; He, C.; Wang, J.; Peng, X.; Li, X.; An, Y.; Duan, C. "Photoactive Chiral Metal-Organic Frameworks for Light-Driven Asymmetric  $\alpha$ -Alkylation of Aldehydes" *J. Am. Chem. Soc.* **2012**, 134, 14991. e) Cummings, S. D.; Eisenberg, R. "Tuning the Excited-State Properties of Platinum(II) Diimine Dithiolate Complexes" *J. Am. Chem. Soc.* **1996**, 118, 1949.

<sup>19</sup>  $E_A^P$  can be used for estimate the redox potential of organic compounds which show irreversible oxidations. Another way is to apply an empiric equation which correlates the ionization potential (measured by means of photoelectron spectroscopy measurements) to the half wave potential. Applying the equation  $E_{1/2} = 0.89(\text{IP}) - 6.04$ , considering the known ionization potential of the parent pyrrolidine derived enamine reported in eV, a value of 0.70 V was calculated, fairly close to the value estimated by electrochemical measurements. Miller, L. L.; Nordblom, G. D.; Mayeda, E. A. "A simple, Comprehensive Correlation of Organic Oxidation and Ionization Potentials" *J. Org. Chem.* **1972**, 37, 916. For the value of IP see ref. 2.

Despite the fact that this value should be considered with caution due to the approximations done, it is an indication of the strong tendency of the excited enamine **25** to transfer an electron to electron poor compounds. Similar negative values of redox potentials are typical of excited electron rich nitrogen compounds such as anilines, well-known strong reducing species which readily participate in photoinduced electron transfer with electron poor alkyl compounds.<sup>20</sup>

Due to the low value of  $E_{1/2}$  associated to the enamine, we consider feasible the possibility of an electron transfer occurring in the photoinitiation step. This possibility is consonant with literature reports.<sup>21</sup> In early studies about the radical reactions of enamines with electron-poor alkyl halides, an electron transfer from a sacrificial amount enamine donor was proposed to initiate radical chain processes (see Scheme 4.9).



Furthermore, fluorescence dynamic quenching of similar electron rich nitrogen compounds, like aromatic amines, operated by electron poor alkyl halides has been widely studied,<sup>22</sup> and electron transfer processes were unambiguously inferred by transient absorption spectroscopy.<sup>23</sup> This literature reports are consonant with our Stern-Volmer quenching studies and supports our hypothesis of an electron transfer mechanism from the excited enamine to the bromomalonate.

### 4.3.4 Proposed mechanism

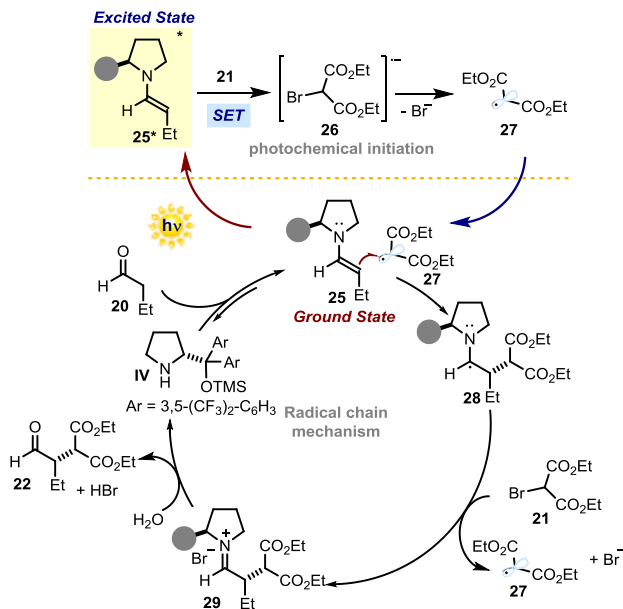
On the basis of the studies performed, we propose the mechanism reported in Scheme 4.10:

<sup>20</sup> Banerjee, A.; Falvey, D. E. "Protecting Groups That Can Be Removed through Photochemical Electron Transfer: Mechanistic and Product Studies on Photosensitized Release of Carboxylates from Phenacyl Esters" *J. Org. Chem.* **1997**, *62*, 6245.

<sup>21</sup> a) Rico, I.; Cantacuzene, D.; Wakelman, C. "Condensation of  $\text{CF}_2\text{Br}_2$ ,  $\text{CF}_2\text{BrCl}$  and  $\text{BrCF}_2\text{CF}_2\text{Br}$  with Enamines and Ynamines" *Tetrahedron Lett.* **1981**, *22*, 3405. b) Wakselman, C. "Single Electron Transfer Processes in Perfluoroalkyl Halides Reactions" *J. Fluorine Chem.* **1992**, *59*, 367.

<sup>22</sup> For a selected example: Iwasaki, T.; Sawada, T.; Okuyama, M.; Kamada, H. "The Photochemical Reaction of Aromatic Amines with Carbon Tetrachloride" *J. Phys. Chem.* **1978**, *82*, 371.

<sup>23</sup> Wyrzykowska, K.; Grodowsky, M.; Weiss, K.; Latowski, T. "Mechanism of the Photochemical Reaction of Diphenylamines with Carbon Tetrachloride" *Photochem. Photobiol.* **1978**, *28*, 311.



**Scheme 4.10** – Proposed catalytic cycle for the photochemical  $\alpha$ -alkylation reaction of butyraldehyde with diethyl bromomalonate.

The enamine **25**, upon light absorption, can reach an electronically excited state (**25\***), generating a highly reducing species (estimated  $E_{1/2} = -2.55$  V vs SCE)<sup>24</sup>. As a consequence, enamine **25** can act as a photoinitiator triggering the formation of the electron deficient radical **27** through the reductive cleavage of the bromomalonate ( $E_{1/2} = -0.49$  V vs SCE)<sup>25</sup> via single electron transfer. The resulting  $\alpha$ -amino radical **28** is a strong reductant ( $E_{1/2} < -0.95$  V vs SCE)<sup>26</sup> and redox process with alkyl halide **21** is expected to induce reductive cleavage through an outer-sphere electron transfer generating the radical and propagating a redox radical chain mechanism.

In the mechanism proposed, enamine **25** plays a central, dichotomous role. Firstly, as electronically excited species it acts as a photoinitiator generating electrophilic radicals from the electron poor alkyl halide **21**. At the same time, the ground state reactivity effectively drives the radical addition with high stereocontrol and efficiency.

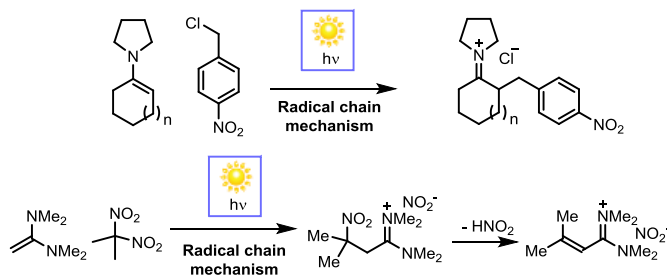
The mechanism proposed in Scheme 4.10 is consonant with the studies reported by Russell *et al.* who performed mechanistic studies on the thermal and photochemical reactions on preformed

<sup>24</sup> The value has been converted from Ag/AgCl reference electrode.

<sup>25</sup> Wu, P.; He, C.; Wang, J.; Peng, X.; Li, X.; An, Y.; Duan, C. "Photoactive Chiral Metal-Organic Frameworks for Light-Driven Asymmetric  $\alpha$ -Alkylation of Aldehydes" *J. Am. Chem. Soc.* **2012**, *134*, 14991.

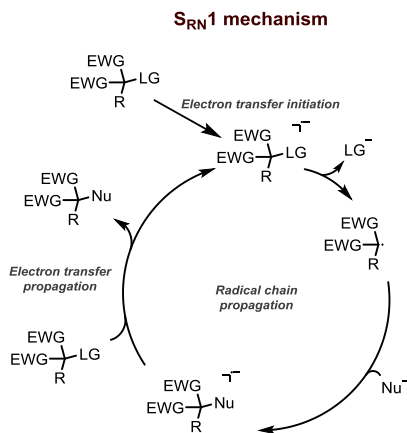
<sup>26</sup> a) Andrieaux, C. P.; Saveant, J. M. "Electrodimerization – II. Reduction Mechanism of Imonium Cations" *J. Electroanal. Chem.* **1970**, *28*, 446. b) Wayner, D. D. M.; Dannenberg, J. J.; Griller, D. "Oxidation Potentials of  $\alpha$ -Aminoalkyl Radicals: Bond Dissociation Energies for Related Radical Cations" *Chem. Phys. Lett.* **1986** *131*, 189.

enamines with electron poor alkyl halides and nitrocompounds, proposing an analogous radical chain mechanism based on electron transfer event propagation.<sup>27</sup>



**Scheme 4.11** – Radical chain reactions of preformed enamines with electron-poor alkyl halides reported by Russell *et al.*

The radical chain mechanism that we propose shows interesting analogies with  $S_{\text{RN}}1$  reactions, which are radical chain reactions of neutral or anionic nucleophiles based on electron transfer propagation events (Scheme 4.12).<sup>28</sup>



**Scheme 4.12** – General  $S_{\text{RN}}1$  mechanism reaction.

Additional control experiments revealed that our photochemical reaction was completely suppressed by the addition of a radical scavenger (TEMPO). Conducting the reaction under air, the reactivity was also completely inhibited, with a concomitant high level of degradation of

<sup>27</sup> Russell, G. A.; Wang, K. "Homolytic Alkylation of Enamines by Electrophilic Radicals" *J. Org. Chem.* **1990**, *56*, 3475.

<sup>28</sup>a) Anslyn, E. V.; Dougherty, D. A. "The  $S_{\text{RN}}1$  Reaction – Electron Pushing" Chapter 11, p. 670 in *Modern Physical Organic Chemistry* **2006**, University Science Books. b) Kornblum, N. "Substitution Reaction Which Proceed *via* Radical Anion Intermediates" *Angew. Chem. Int. Ed.* **1975**, *14*, 734.

aldehyde and catalyst, presumably due to quenching of radical **27** by molecular oxygen.<sup>29</sup> These observations support a radical chain mechanism and are consonant with the studies reported by Kornblum *et al.* about classical  $S_{RN}1$  reactivity.<sup>28b,30</sup>

### 4.3.5 Scope of the reaction

We next evaluated the synthetic potential of the photo-organocatalytic strategy by varying the reaction partner. As detailed in Figure 4.15, variously substituted bromomalonates effectively participated in the enantioselective alkylation of butanal **20** (products **22a–d**). As typically observed in similar radical chain processes, the reaction was insensitive to steric bulkiness, and the tertiary alkyl halide 2-methyl-2-bromo diethylmalonate **21b** readily underwent the chemical transformation with high efficiency and improved stereoselectivity (products **22b**, **22g**). Aldehydes bearing a long alkyl fragment, an internal olefin, or a heteroatom moiety were also alkylated stereoselectively to afford **22e–g**. Additionally, natural solar light effectively promoted the process: simply placing the reaction mixture in ordinary Pyrex glass vessels on a rooftop effected the asymmetric catalytic alkylation with diethyl 2-bromo-2-methylmalonate **21b** (product **22b**, 98% yield, 91% ee).

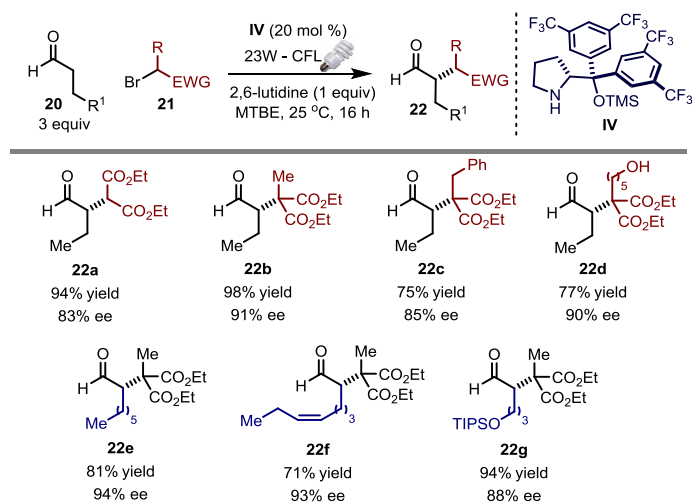
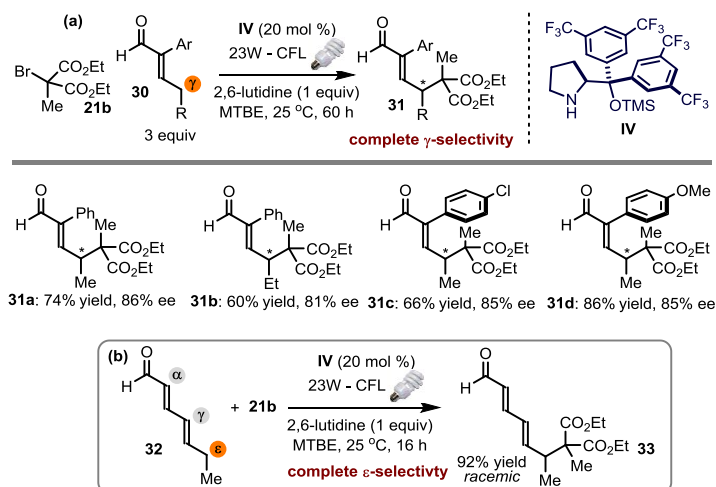


Figure 4.15 – Scope of the  $\alpha$ -alkylation of aldehydes with bromomalonates.

<sup>29</sup> Detectable amounts of 2-hydroxy-diethylmalonate (5% based on NMR experiments) were observed. No traces of this compound were observed carrying out the reaction under strict anaerobic conditions or in the absence of irradiation. Analogous observations were reported by Kornblum *et al.* for classical  $S_{RN}1$  reactivity (see ref. 28b).

<sup>30</sup> During the preparation of this manuscript it was demonstrated that even the ruthenium sensitized version of the reaction studied in this chapter follows a radical chain propagation mechanism, see: Cismesia, M. A.; Yoon, T. P. "Characterizing Chain Processes in Visible Light Photoredox Catalysis" *Chem. Sci.* DOI: 10.1039/C5SC02185E.

This photo-organocatalytic alkylation approach demonstrated potential for targeting stereocenters remote from the carbonyl moiety. We found that extended enamine intermediates, formed from  $\alpha$ -branched enals **30**, could efficiently trap the photogenerated radical while setting a new stereocenter at a distant  $\gamma$ -position (Figure 4.16 a). The capacity for controlling the site selectivity was further corroborated by the experiment detailed in Figure 4.16 b, where hepta-2,4-dienal **32** was exclusively alkylated at the more remote  $\epsilon$ -carbon with full regioselectivity, albeit at the expense of stereocontrol.



**Figure 4.16** – Scope of the reaction of remote functionalizations of unsaturated aldehydes with bromomalونات. The absolute configuration of compounds **31** was not unambiguously assigned.

## 4.4 Towards novel applications: formal asymmetric methylation of aldehydes

The photoinduced radical reaction of enamines with bromomalonate gave the possibility to access  $\alpha$ -alkylated products with high stereoselectivity. Our next step was to find a novel, synthetically useful reaction based on this concept. We investigated the possibility of employing the electron-poor alkyl halide **34**, bearing a sulfone moiety, which is a highly versatile functional group in organic synthesis.<sup>31</sup> The idea arose considering the similar value of  $E_{1/2}$  reported for compounds **34** and **21** (Scheme 4.13),<sup>32</sup> which suggested the possibility of the excited enamine

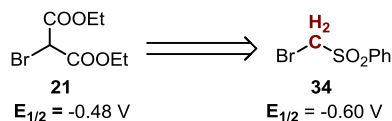
<sup>31</sup> Simpkins, N. S. "Sulfones in Organic Synthesis" **1993**, Pergamon press.

<sup>32</sup> Compounds **34** and **46** potentials: Bordwell, F. G.; Clemens, A. H. "Correlation between the Basicity of Carbanions and Their Ability to Transfer an Electron" *J. Org. Chem.* **1981**, *46*, 1035.



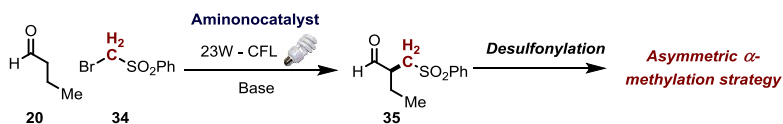
to induce a productive reductive cleavage upon single electron transfer with the sulfone derivative **34**.

#### Rational design



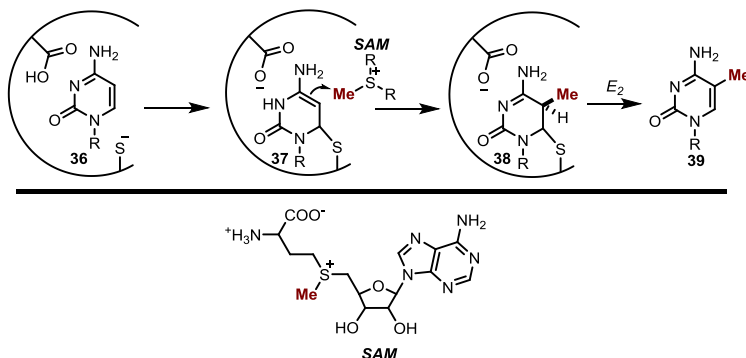
Scheme 4.13 – Starting material rational design.

Furthermore, direct cleavage of the sulfonyl group in **35** could also provide a synthetic strategy for achieving a formal asymmetric methylation of aldehydes.



Scheme 4.14 – Asymmetric photochemical  $\alpha$ -alkylation of aldehydes with  $\alpha$ -bromo methyl sulfones.

Methylation reaction is ubiquitous in biochemistry and is important for a variety of processes, *i.e.* the DNA modifications.<sup>33</sup> Methylation of nucleic bases is operated by DNA methyltransferase enzymes, whose catalytic activity is linked to the cofactor *S*-adenosyl methionine (SAM or AdeMap), an electrophilic methylation agent. The methylation of cytosine, for instance, is operated by the enzyme DNMT-1. Electrophilic SAM-methylation of enamine intermediate **37** affords the 5-methyl cytosine **39** (Scheme 4.15).<sup>34</sup>

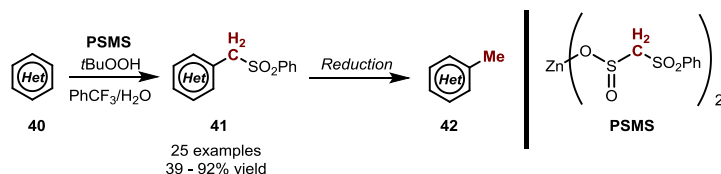


Scheme 4.15 – SAM-mediated DNMT-1 catalyzed methylation of cytosine.

<sup>33</sup> Voet, D.; Voet, J. G. "DNA Methylation and Trinucleotide Repeat Expansion" Chapter 30, p. 1246 in *Biochemistry, fourth edition*, 2011, Wiley.

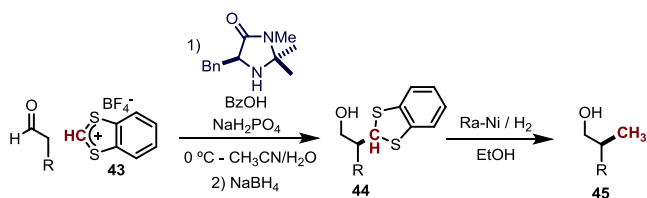
<sup>34</sup>a) Dhe-Paganon, S.; Syeda, F.; Park, L. "DNA Methyl Transferase 1: Regulatory Mechanisms and Implications in Health and Disease" *Int. J. Biochem. Mol. Biol.* **2011**, *2*, 58. b) Santi, D. V.; Normant, A.; Garrett, C. E. "Covalent Bond Formation Between a DNA-Cytosine Methyltransferase and DNA Containing 5-Azacytosine" *Proc. Natl. Acad. Sci. USA* **1984**, *81*, 6993.

Baran *et al.* recently reported a remarkable methylation of heteroaromatic compounds through radical chemistry.<sup>35</sup> Methyl sulfonyl radicals were generated by oxidation of sulfinate salts **PSMS** and trapped by heteroaromatic compounds **40**. Cleavage of the sulfonyl moiety of the products **41** under reductive conditions afforded the desired methylated heterocyclic compound **42** (Scheme 4.16).



**Scheme 4.16** – Baran approach for formal methylation of heteroaromatic compounds.

The direct catalytic asymmetric methylation of aldehydes is a highly challenging reaction and no methodologies have been reported for this transformation in organocatalysis to date. An indirect way to obtain an asymmetric methylation reaction has been reported in 2011 by Cozzi *et al.*<sup>36</sup>



**Scheme 4.17** – Asymmetric alkylation reaction of aldehydes with benzodithiolium salt **43**. Treatment of the product with Ra-Ni/H<sub>2</sub> leads to the desired  $\alpha$ -methylated product.

Analogous products could be obtained with the planned transformation depicted in Scheme 4.14. Indeed, phenyl sulfone moiety could be removed under reductive conditions (magnesium in methanol) to afford the  $\alpha$ -methylated product. Such a strategy could be an alternative approach for achieving a formal methylation procedure while giving the possibility to exploit the synthetic versatility of the sulfonyl moiety to further elaborate the product scaffold (*i.e.* Julia olefination, alkylation reactions etc.).

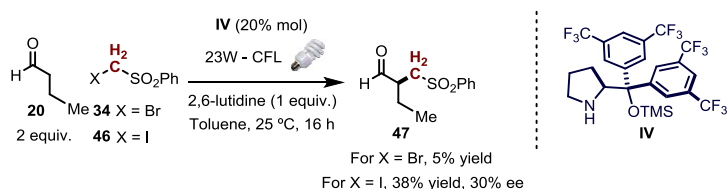
<sup>35</sup> Gui, J.; Zhou, Q.; Pan, C.-M.; Yabe, Y.; Burns, A. C.; Collins, M. R.; Ornelas, M. A.; Ishihara, Y.; Baran, P. "C-H Methylation of Heteroarenes Inspired by Radical SAM Methyl Transferase" *J. Am. Chem. Soc.* **2014**, *136*, 4853.

<sup>36</sup> Gualandi, A.; Emer, E.; Capdevila, M. G.; Cozzi, P. G. "Highly Enantioselective  $\alpha$ -Alkylation of Aldehydes with 1,3-Benzodithiolium Tetrafluoroborate: A Formal Organocatalytic  $\alpha$ -Alkylation of Aldehydes by the Carbenium Ion" *Angew. Chem. Int. Ed.* **2011**, *50*, 7842.

### 4.4.1 Preliminary optimization studies

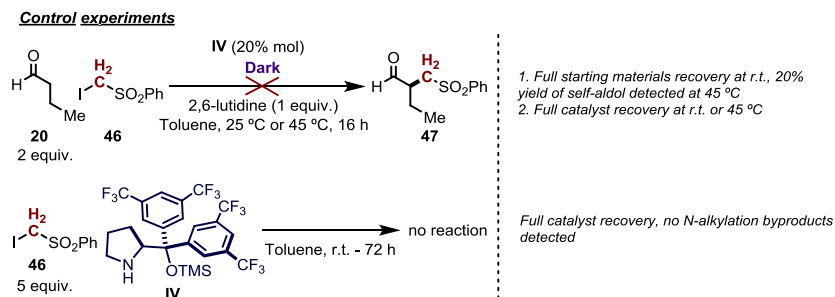
Compact fluorescent lamp (CFL) irradiation of a toluene solution of commercially available bromomethyl sulfone **34**, aldehyde **20**, catalyst **IV** and 2,6-lutidine as acid scavenger, leads to the detection of traces of the desired  $\alpha$ -alkylated compound **47**. Notably, as in the case of diethyl bromomalonate alkylation, no color developed after the addition of the reagents, suggesting the absence of EDA complexes.

Interestingly, the employment of iodomethyl phenylsulfone **46**, easily synthesized in a one-step procedure, resulted in evident yield improvements. The reason of such better yield is probably related to easier mesolysis of the corresponding radical anion and to the slightly increased redox potential of **46**.<sup>32</sup>



**Scheme 4.18** –  $\alpha$ -alkylation reaction of aldehyde **20** with bromomethyl phenylsulfone **34** or iodomethyl phenylsulfone **46**. Replacing the bromide with iodide greatly improved the results. Yields obtained by <sup>1</sup>H NMR analysis of the reaction mixture using trichloroethylene as the internal standard.

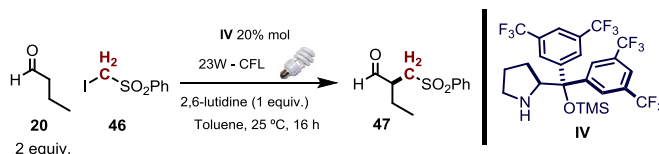
Prior to further optimization studies, a series of control experiments were carried out. Careful exclusion of light resulted in no reaction, ruling out a thermal process. Notably, the catalyst was highly stable under the reaction conditions until 45 °C, since no *N*-alkylation byproducts were observed and full catalyst recover was inferred by NMR analysis (using trichloroethylene as the internal standard). The reluctance for catalyst *N*-alkylation was further demonstrated stirring the catalyst in the presence of the alkylating agent: no reactions were observed.



**Scheme 4.19** – Control experiments on  $\alpha$ -alkylation reaction of aldehyde **20** with iodomethyl phenylsulfone **46**.

We next focused on improving the enantioselectivity and the efficiency of the transformation. During our optimization studies, we realized that a racemization process was occurring under the reaction conditions (Table 4.1).

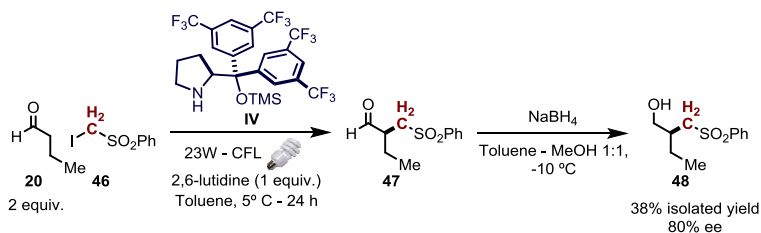
**Table 4.1** – Decrease of the enantiomeric excess of product **47** during the time.



Entry	Reaction time (h)	yield (%)	ee (%)
1	6	35	60
2	25	40	15
3	116	40	0

Yields obtained by NMR analysis using trichloroethylene as internal standard. Enantiomeric excess determined by HPLC analysis on a chiral stationary phase.

We were delighted to observe that the racemization process could be completely suppressed carrying out the reaction at slightly lower temperature (5 °C) and in situ reducing (NaBH<sub>4</sub> in MeOH) the aldehydic product **47** to the corresponding alcohol prior to workup. Changing the catalyst scaffold or modifying the reaction parameters (solvent, concentration, light sources) did not lead to significant improvements and the best result obtained so far is reported in Scheme 4.20.



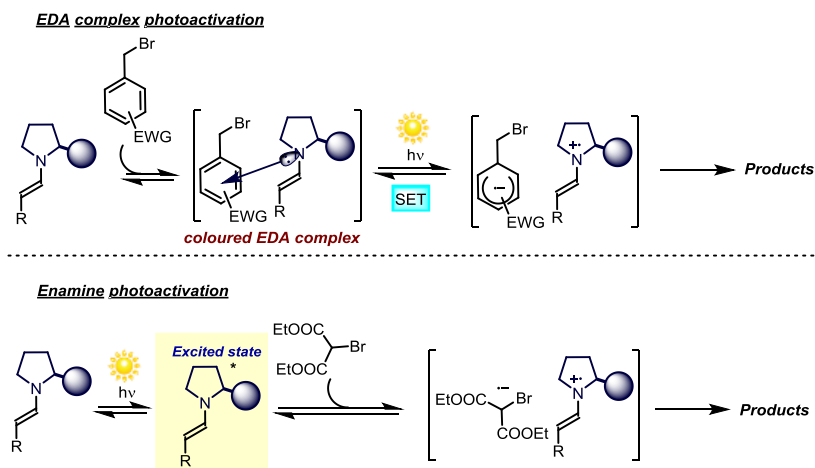
**Scheme 4.20** – Best results obtained for  $\alpha$ -alkylation reaction of butyraldehyde with iodomethyl sulfone **46**.

Unfortunately, the reaction was plagued by degradation of the sulfone substrate **46**, and the yield obtained was associated to a high level of starting material consumption. Further optimization studies are currently ongoing in our research laboratories to improve the yield and the enantioselectivity of this photochemical organocatalytic enantioselective transformation.

## 4.5 Conceptual implications and conclusions

The chemistry detailed in the present chapter establishes the ability of chiral enamines to act as photoinitiators upon excitation by simple light irradiation, and to trigger the formation of reactive open-shell species under mild conditions. At the same time, the chiral organocatalyst ensures effective stereochemical control. We used this approach, where stereoselection and photoactivation conjugate in a sole organocatalytic intermediate, to develop light-driven enantioselective transformations that cannot be realized under thermal activation. This novel photo-organocatalytic strategy, which capitalizes upon the dichotomous reactivity profile of enamines in the ground and the excited states, can offer new opportunities for designing photochemical enantioselective transformations.

At first sight, the difference between the two activations depicted in Scheme 4.21 (the EDA complex activation, better discussed in Paragraph 4.1.2, and on the other the direct photoexcitation of enamines) could appear subtle.

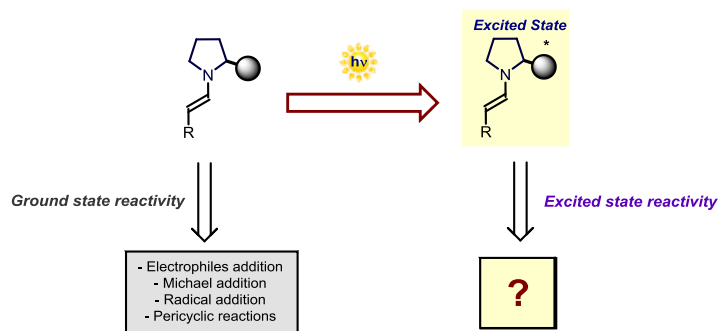


**Scheme 4.21** – Comparison between EDA complex photoexcitation and enamine direct photoexcitation approaches.

Both photochemical strategies aim to access reactive radical species under mild conditions, but they profoundly diverge mechanistically: the first strategy uses the ground state reactivity of the organocatalytic intermediates, since the transient EDA complexes are generated in the ground state and can be photoexcited at a later stage. The second strategy relies on the intrinsic photoactivity of the sole enamine in the excited state.

Our studies suggest the attractive prospect that the enamine, an intermediate with an established ground state reactivity widely employed in asymmetric synthesis (from the

pioneering Stork's enamine chemistry to asymmetric aminocatalysis),<sup>37,38</sup> could be exploited also in its electronically excited state. The to date hidden ability of enamines to reach an electronically excited state upon simple light absorption can open up new opportunities for making chiral molecules through the development of novel, photochemical transformations (Scheme 4.22).



**Scheme 4.22** – Shining light on a reactive intermediate that is well-known for its ground state reactivity can open novel possibilities.

The concept of developing chemistry from excited state organocatalytic intermediates is not limited to the excitation of enamines, as it will be presented in the next chapter. It has more general implications and could provide unexplored routes to asymmetrically functionalize unmodified carbonyl compounds.

## 4.6 Experimental section

**General Information:** The NMR spectra were recorded at 400 MHz and 500 MHz for  $^1\text{H}$  or at 100 MHz and 125 MHz for  $^{13}\text{C}$ . The chemical shifts ( $\delta$ ) for  $^1\text{H}$  and  $^{13}\text{C}$  are given in ppm relative to residual signals of the solvents ( $\text{CHCl}_3$  @ 7.26 ppm  $^1\text{H}$  NMR, 77.16 ppm  $^{13}\text{C}$  NMR). Coupling constants are given in Hz. The following abbreviations are used to indicate the multiplicity: s, singlet; d, doublet; t, triplet; q, quartet; m, multiplet; bs, broad signal.

High-resolution mass spectra (HRMS) were obtained from the ICIQ High Resolution Mass Spectrometry Unit on Waters GCT gas chromatograph coupled time-of-flight mass spectrometer (GC/MS-TOF) with electron ionization (EI) or MicroTOF II (Bruker Daltonics): HPLC-MS-TOF (ESI).

<sup>37</sup> Stork, G.; Brizzolara, A.; Landesman, H.; Szmuszkovicz, J.; Terrell, R. "The Enamine Alkylation and Acylation of Carbonyl Compounds" *J. Am. Chem. Soc.* **1963**, *85*, 207.

<sup>38</sup> Mukherjee, S.; Yang, J. W.; Hoffmann, S.; List, B. "Asymmetric Enamine Catalysis" *Chem. Rev.* **2007**, *107*, 5471.

Optical rotations were measured on a Polarimeter Jasco P-1030 and are reported as follows:  $[\alpha]_D^{rt}$  (c in g per 100 mL, solvent).

UV-vis measurements were carried out on a Shimadzu UV-2401PC spectrophotometer equipped with photomultiplier detector, double beam optics and D<sub>2</sub> and W light sources.

The emission spectra were recorded in a Fluorolog Horiba Jobin Yvon spectrofluorimeter equipped with photomultiplier detector, double monochromator and 350 W xenon light source. Cut-off and band-pass photochemical experiments have been performed using a 300 W xenon lamp (*Asashi Spectra Co., Ltd.*) to irradiate the reaction mixture.

Cyclic voltammetry studies were carried out on a Princeton Applied Research PARSTAT 2273 potentiostat offering compliance voltage up to  $\pm 100$  V (available at the counter electrode),  $\pm 10$  V scan range and  $\pm 2$  A current range.

The <sup>1</sup>H and <sup>13</sup>C NMR spectra of known compounds are available in literature and are not reported in the present dissertation.<sup>1</sup>

**General Procedures:** All reactions were set up under an argon atmosphere in oven-dried glassware using standard Schlenk techniques, unless otherwise stated. Synthesis grade solvents were used as purchased and the reaction mixtures were degassed by three cycles of freeze-pump-thaw. Chromatographic purification of products was accomplished using force-flow chromatography (FC) on silica gel (35-70 mesh). For thin layer chromatography (TLC) analysis throughout this work, Merck precoated TLC plates (silica gel 60 GF<sub>254</sub>, 0.25 mm) were employed, using UV light as the visualizing agent and basic aqueous potassium permanganate (KMnO<sub>4</sub>) stain solutions, and heat as developing agents. Organic solutions were concentrated under reduced pressure on a Büchi rotatory evaporator.

**Determination of Enantiomeric Purity:** HPLC analysis on chiral stationary phase was performed on an Agilent 1200-series instrumentation. Daicel Chiralpak IA or IC columns with hexane:iPrOH or hexane:iPrOH:DCM as the eluents were used. HPLC traces were compared to racemic samples prepared using a catalytic amount of morpholine (30 mol%) for the  $\alpha$ -alkylation of aldehydes (products **22**) or an equimolar mixture of catalysts (*R*)- and (*S*)-**IV** (total 20 mol%) for the  $\gamma$ -site alkylation of enals (products **31**) and  $\alpha$ -alkylation of butyraldehyde with iodomethyl phenylsulfone.

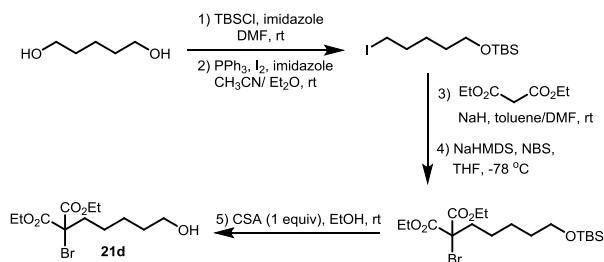
**Materials:** Reagents were purchased at the highest commercial quality from Sigma Aldrich, Fluka, and Alfa Aesar and used as received, without further purification, unless otherwise stated. The chiral secondary amine catalyst **IV** is commercially available; catalyst **IV** was purified by flash column chromatography prior to use and stored at 4 °C under argon to avoid undesired desilylation that would affect the catalytic potential of the amine.

Butyraldehyde **20**, isovaleraldehyde, octanal, 2-phenylpropanal, (*E*)-2-phenylpent-2-enal are commercially available and distilled prior to use. 5-((Triisopropylsilyloxy)pentanal was

synthesized following a two-steps procedure from 1,5-pentanediol, as described in the literature.<sup>39</sup> Dienals **30** were prepared as reported in the literature.<sup>40</sup>

Most of the alkyl halides used within the study are commercially available. Diethyl-2-bromo-2-benzyl malonate **21c** was prepared by alkylating diethyl 2-bromomalonate with benzyl bromide,<sup>41</sup> whereas methyl iodosulfone **46** was prepared by sulfinic acid sodium salt alkylation as reported.<sup>42</sup>

### Preparation of Diethyl 2-bromo-2-(5-hydroxypentyl)malonate **21d**



Scheme 4.23 – Synthesis of compound **21d**.

**STEP 1:**<sup>43</sup> A solution of TBSCl (8 g, 53.1 mmol) in DCM (8 mL) was slowly added at room temperature to a stirred solution of imidazole (7.95 g, 117 mmol, 2.2 equiv) and 1,5-pentanediol (50 mL, 478 mmol, 9.0 equiv) in DMF (50 mL). After stirring for 2 hours at rt, the mixture was partitioned between 200 mL Et<sub>2</sub>O and 100 mL water. The aqueous phase was extracted 3 times with 50 mL of Et<sub>2</sub>O and the combined organic phases were washed twice with 100 mL water, dried (Na<sub>2</sub>SO<sub>4</sub>), filtered, and concentrated under reduced pressure to give the crude 5-((*tert*-butyldimethylsilyloxy)pentan-1-ol as a colorless oil, that is used as such in the next step.

**STEP 2:**<sup>43</sup> The crude product previously obtained is dissolved in Et<sub>2</sub>O (40 mL)/CH<sub>3</sub>CN (15 mL). Then, imidazole (7.57 g, 111 mmol, 3.0 equiv) and triphenylphosphine (14.59 g, 55.6 mmol, 1.5 equiv) were sequentially added to this solution. The mixture was cooled at 0 °C and I<sub>2</sub> (14.6 g, 55.6 mmol, 1.5 equiv) was added portion-wise. After stirring for 30 min at 0 °C (reaction

<sup>39</sup> Crimmins, M. T.; Vanier, G. S. "Enantioselective Total Synthesis of (+)-SCH 351448" *Org. Lett.* **2006**, *8*, 2887.

<sup>40</sup> Cassani, C.; Melchiorre, P. "Direct Catalytic Enantioselective Vinylogous Aldol Reaction of  $\alpha$ -branched Enals with Isatins" *Org. Lett.* **2012**, *14*, 5590.

<sup>41</sup> Makhija, M. T.; Kasliwal, R. T.; Kulkarni, V. M.; Neamati, N. "De novo design and synthesis of HIV-1 integrase inhibitors" *Bioorg. Med. Chem.* **2004**, *12*, 2317.

<sup>42</sup> Pospíšil, J.; Robiette, R.; Satoa, H.; Debrus, K. "Practical synthesis of  $\beta$ -oxo benzo[d]thiazolyl sulfones: Scope and limitations" *Org. Biomol. Chem.* **2012**, *10*, 1225.

<sup>43</sup> Jurberg, I. D.; Odabachian, D.; Gagosz, F. "Hydroalkylation of Alkynyl Ethers via a Gold(I)-Catalyzed 1,5-Hydride Shift/Cyclization Sequence" *J. Am. Chem. Soc.* **2010**, *132*, 3543.



progress monitored by TLC), the reaction was quenched with 50 ml an aqueous saturated solution of  $\text{Na}_2\text{S}_2\text{O}_3$ . The organic phases were separated, dried ( $\text{Na}_2\text{SO}_4$ ), and concentrated under reduced pressure. The crude product was purified by flash column chromatography (9:1 hexane:AcOEt) to furnish *tert*-butyl((5-iodopentyl)oxy)dimethylsilane as a yellow oil (10.2 g, 34.1 mmol, 92% yield).

**STEP 3:** A round bottomed flask was charged with NaH (60% in mineral oil, 1.17 g, 129.2 mmol, 1.2 equiv) and a 1:1 mixture of toluene:DMF (10 mL total). The flask was cooled to 0 °C and a solution of diethyl malonate (7.43 mL, 4.7 mmol, 2 equiv) in toluene/DMF (20 mL total, 1:1 ratio) was slowly added to this suspension. The reaction was allowed to warm up to r.t. and stirring was continued at this temperature for 20 minutes, during which time the cloudy suspension became an homogeneous solution. The flask was cooled again to 0 °C and a solution of *tert*-butyl((5-iodopentyl)oxy)dimethylsilane (8 g, 24.4 mmol, 1 equiv) in toluene:DMF (20 mL total, 1:1 ratio) was slowly added. The reaction was allowed to warm up to rt and stirring at this temperature was continued overnight. Upon reaction completion (as checked by TLC), the reaction was quenched with 100 ml of water followed by extraction with AcOEt (3 times x 50 ml). The combined organic phases were washed 5 times with 50 ml water and one with 50 ml of brine. Then they were dried ( $\text{Na}_2\text{SO}_4$ ), and concentrated under reduced pressure. The residue was purified by flash column chromatography (10:1 hexane:AcOEt) to afford diethyl 2-(5-((*tert*-butyldimethylsilyl)oxy)pentyl)malonate as a colorless oil (5.7 g, 15.9 mmol, 65% yield).

**STEP 4:**<sup>44</sup> NaHMDS (2 M in THF, 8.3 mL, 16.6 mmol, 1.2 equiv) was added to a solution of 2-(5-((*tert*-butyldimethylsilyl)oxy)pentyl)malonate (5 g, 13.9 mmol) in anhydrous THF (110 mL) at -78 °C, and the mixture allowed to stir for 15 min at this temperature. NBS (3.0 g, 16.6 mmol, 1.2 equiv) was then added while slowly warming up the mixture to 0 °C (over 6 h). After completion of the reaction (as checked by TLC), the reaction was quenched with 100 ml of water. The mixture was extracted 3 times with 100 ml of AcOEt, washed with 100 ml brine, dried over  $\text{Na}_2\text{SO}_4$ , and concentrated under reduced pressure. The residue was purified by flash column chromatography (10:1 hexane:AcOEt) to afford diethyl 2-bromo-2-(5-((*tert*-butyldimethylsilyl)oxy)pentyl)malonate as a colorless oil (6.1 g, 13.8 mmol, 99 %).

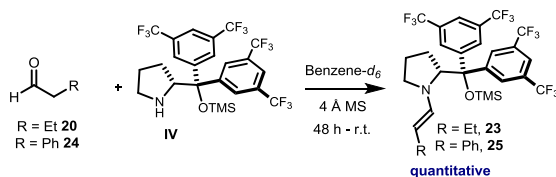
**STEP 5:** A solution of 2-bromo-2-(5-((*tert*-butyldimethylsilyl)oxy)pentyl)malonate (6 g, 13.7 mmol) in absolute EtOH (250 mL) was cooled down to 0 °C and (-)-CSA (3.17g, 13.7 mmol) added portion-wise. After 1 hour, the TLC analysis showed complete consumption of the starting material. A saturated solution of  $\text{Na}_2\text{CO}_3$  (100 mL) was added and the bulk of the solvent removed on a rotary evaporator. The remaining mixture was extracted with 3 times with 50 ml

---

<sup>44</sup> Fürstner, A.; Bonnekessel, M.; Blank, J.T.; Radkowski, K.; Seidel, G.; Lacombe, F.; Gabor, B.; Mynott, A.; "Total Synthesis of Myxovirescin A1" *Chem. Eur. J.* **2007**, *13*, 8762.

AcOEt and the combined organic phases were washed with 50 ml of brine, dried ( $\text{Na}_2\text{SO}_4$ ), and concentrated under reduced pressure. The residue was purified by flash column chromatography (gradient from 4:1 hexane/AcOEt to 1:1 hexane/AcOEt) to afford the final compound, diethyl 2-bromo-2-(5-hydroxypentyl)malonate (**21d**), as a colorless oil (4.5 g, 12.2 mmol, 89%).  $^1\text{H}$  NMR (500 MHz,  $\text{CDCl}_3$ ):  $\delta$  4.26 (q,  $J = 7.1$  Hz, 4H), 3.63 (t,  $J = 6.5$  Hz, 2H), 2.29 – 2.23 (m, 2H), 1.58 (dq,  $J = 9.1\text{Hz}$ ,  $J = 6.5$  Hz, 2H), 1.48 – 1.40 (m, 4H), 1.28 (t,  $J = 7.1$  Hz, 6H).  $^{13}\text{C}$  NMR (125 MHz,  $\text{CDCl}_3$ )  $\delta$  167.1 (x2), 63.6, 63.1 (x2), 62.8, 38.2, 32.5, 25.5, 25.2, 14.0 (x2). HRMS calculated for  $\text{C}_{12}\text{H}_{21}\text{BrO}_5\text{Na}$  ( $\text{M}+\text{Na}^+$ ): 347.0465, found: 347.0470

### Synthesis of the enamines **23** and **25**:



Scheme 4.24 – Synthesis of enamines **23** and **25**.

All manipulations have been conducted under rigorous dry conditions. A Schlenk tube with carefully greased joints was charged with freshly activated 4 Å molecular sieves (in powder). 250  $\mu\text{L}$  of freshly dried benzene- $d_6$ , 0.025 mmol of freshly distilled aldehyde, and 15 mg (0.025 mmol) of **IV** were then added under a positive pressure of argon. The mixture was stirred under an argon atmosphere until full conversion of the starting material was obtained (48 h). The reaction mixture was then filtered over Celite® under an argon atmosphere in order to remove the powder and then diluted to 2 mL with dry toluene (SPS system) over freshly activated pellets 4 Å molecular sieves (stock solution concentration =  $1.25 \cdot 10^{-2}$  M). The solution of the enamine **25**, which was maintained under an argon atmosphere, was employed for spectroscopic studies just after the preparation, whereas enamine **23** could not be employed for further photophysical studies due to its intrinsic instability.

### General Procedures for carrying out absorption and emission spectra:

#### Reagents absorption profile

All the spectra were recorded in MTBE using the same concentrations as in the reaction conditions and better detailed in Figure 4.2. Due to the high concentration of the solutions, short light path cuvettes have been employed in order to avoid fast signal saturation. 1 mm Hellma Quartz SUPRASIL® cuvettes have been used to record all the spectra.

*Lambert-Beer studies of the preformed Enamine 25*

Solutions at different concentration of the enamine **25** (obtained by opportunely diluting the original stock solution with freshly dried toluene spectrophotometric grade as detailed in Figure 4.8) were introduced in a 1 cm path length quartz cuvette equipped with Teflon® septum under an argon atmosphere and analyzed at the spectrophotometer. The absorbance shows a typical Lambert-Beer linear correlation with the concentration at different wavelengths.

*Fluorescence spectrum of the preformed enamine 25*

The emission spectra were recorded in a Fluorolog Horiba Jobin Yvon spectrofluorimeter equipped with photomultiplier detector, double monochromator and 350 W xenon light source. 2 mL of a  $5 \cdot 10^{-5}$  M solution (dry toluene) of the enamine **25** were placed in a 10x10 mm light path quartz fluorescence cuvette equipped with Silicone/PTFE 3.2 mm septum under an argon atmosphere. The excitation wavelength was fixed at 365 nm (incident light slit regulated to 1 mm), while the emission light was acquired from 400 nm to 750 nm (emission light slit regulated to 15 mm). A solvent blank was subtracted from the measurement.

The regulation of the excitation light slit width was crucial for the experiment in order to avoid the occurrence of an undesired photochemical process (double bond isomerization) of the enamine, resulting in detectable spectral variations (both emission and absorption). Under the conditions described above, the undesired isomerization process was completely suppressed.

*Luminescence quenching studies of the preformed enamine 25 by malonate 21*

The samples were prepared mixing the enamine **25** ( $[25] = 5 \cdot 10^{-5}$  M) with the required amount of **21** in a total volume of 2 mL of dry toluene in a 10x10 mm light path quartz fluorescence cuvette equipped with Silicone/PTFE 3.2 mm septum under an argon atmosphere. The samples were vigorously bubbled with dry argon for 5 minutes prior to the measurement. The excitation wavelength was fixed at 365 nm (incident light slit regulated to 1 mm), the emission light was acquired from 400 nm to 750 nm (emission light slit regulated to 15 mm). A solvent blank was subtracted from all the measurements.

The excitation wavelength was chosen in order to avoid *inner-filter effect* due to the absorption of **21**.

The Stern-Volmer plot shows a linear correlation between the amounts of **21** and the ratio  $I_0/I$ , where  $I_0$  is the normalized emission intensity at 495 nm in the absence of the quencher and  $I$  is the normalized emission intensity at 495 nm in the presence of the quencher. On the basis of the following Equation (2), it is possible to calculate the Stern-Volmer constant  $K_{SV}$ .

$$(2) \quad I_0/I = 1 + K_{SV}[Q]$$

The graph is depicted in Figure 4.12. We calculated a Stern-Volmer quenching constant of  $12.9 \text{ M}^{-1}$ .

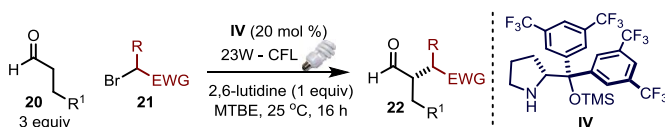
#### General Procedures for electrochemical measurements:

Electrochemical grade tetrabutylammonium hexafluorophosphate (116 mg, 0.300 mmol) was added to a 0.01 M solution of enamine **25** in 3 mL of dry acetonitrile and the solution was vigorously bubbled with  $\text{N}_2$  for 5 minutes prior to the measurement. The oxidation potential was measured using a glassy carbon working electrode, a platinum wire counter electrode, and a NaCl saturated Ag/AgCl reference electrode at 5 mV/s scan rate.

A completely irreversible oxidation wave was observed with  $E_{\text{A}}^{\text{P}} = 0.60 \text{ V}$ .

The cyclic voltammetry of the individual catalyst **IV** and phenylacetaldehyde was also carried out, using the same experimental conditions and concentrations. As expected, no oxidation waves were detected for phenylacetaldehyde in the range 0 – 1.5 V, while the cyclic voltammetry curve of the catalyst didn't show oxidations peak before 1 V, thus confirming that the oxidation wave observed at 0.60 V in the case of enamine **25** was not due to the generation of starting material due to hydrolysis phenomena.

#### General Procedures for the Photochemical Organocatalytic Enantioselective Alkylation of Aldehydes:



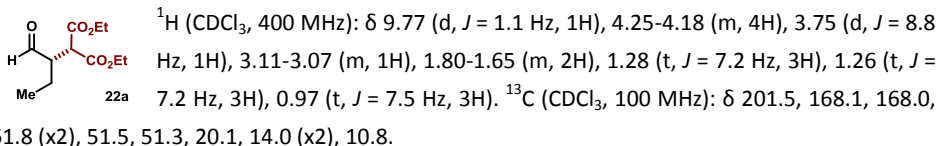
Scheme 4.25 – Photochemical alkylation of aldehydes with malonates.

A 10 mL Schlenk tube was charged with the aminocatalyst **IV** (20 mol%), MTBE (0.5 M referring to the alkyl bromide **21**), the aldehyde **20** (3 equiv), 2,6-lutidine (1 equiv) and the alkylating agent **21** (1 equiv). The reaction mixture was degassed via freeze pump thaw (x3), and the vessel refilled with argon. After the reaction mixture was thoroughly degassed, the vial was sealed and positioned approximately 5 cm away from the two light sources. A set of two household full spectrum 23 W compact fluorescent light (CFL) bulbs was used for irradiating the reaction mixture. After stirring for the indicated time, the crude mixture was purified by flash column chromatography to afford the title compound **22** in the stated yield and optical purity.

#### (S)-diethyl 2-(1-oxobutan-2-yl)malonate (**22a**)

Prepared following the general using the aminocatalyst **IV** (0.02 mmol, 12 mg, 0.2 equiv), MTBE (0.5 M, 200  $\mu\text{L}$ ), 2,6-lutidine (0.1 mmol, 12  $\mu\text{L}$ , 1 equiv), butyraldehyde (0.3 mmol, 27  $\mu\text{L}$ , 3 equiv) and diethyl 2-bromomalonate (0.1 mmol, 17  $\mu\text{L}$ , 1 equiv), after degassing the reaction was

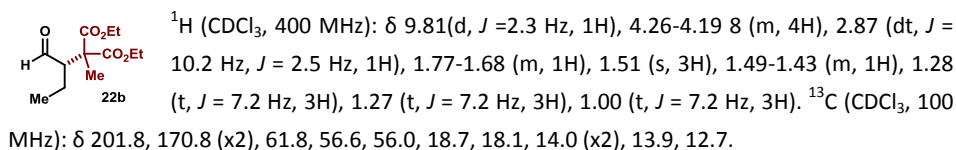
stirred 4 h at r.t. Purification by flash column chromatography (10:1 hexane:AcOEt) afforded the title compound (94% yield, 83% ee) as a colorless oil. The enantiomeric excess was determined by HPLC analysis on a Daicel Chiralpak IA column, eluent 97:3 hexane:<sup>i</sup>PrOH, flow rate 1.00 mL/min,  $\lambda = 215$  nm;  $\tau_{\text{major}} = 8.6$  min,  $\tau_{\text{minor}} = 9.3$  min. HRMS: calculated for C<sub>11</sub>H<sub>17</sub>O<sub>5</sub> (M-H): 229.1076, found 229.1072.  $[\alpha]_{\text{D}}^{25} = +54.9$  (c = 1.0, CHCl<sub>3</sub>, 83% ee).



### (S)-diethyl 2-methyl-2-(1-oxobutan-2-yl)malonate (22b)

Prepared according to the general procedure using the aminocatalyst **IV** (0.02 mmol, 12 mg, 0.2 equiv), MTBE (0.5 M, 200  $\mu$ L), 2,6-lutidine (0.1 mmol, 12  $\mu$ L, 1 equiv), butyraldehyde (0.3 mmol, 27  $\mu$ L, 3 equiv) and diethyl 2-methyl-2-bromomalonate (0.1 mmol, 19.1  $\mu$ L, 1 equiv). Reaction time 16 h. Purification by flash column chromatography (gradient eluent from hexane to 95:5 hexane:AcOEt) afforded the title compound (25 mg, 98% yield, 91% ee) as a colorless oil. The enantiomeric excess was determined by HPLC analysis on a Daicel Chiralpak IC column, 68:32 hexane:<sup>i</sup>PrOH flow rate 1.00 mL/min,  $\lambda = 218$  nm;  $\tau_{\text{major}} = 6.0$  min,  $\tau_{\text{minor}} = 6.8$  min. HRMS: calculated for C<sub>12</sub>H<sub>11</sub>N<sub>2</sub>O<sub>3</sub> (M-H): 231.0775, found: 231.0779.  $[\alpha]_{\text{D}}^{25} = +19.4$  (c = 1.0, CHCl<sub>3</sub>, 92% ee).

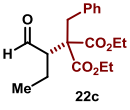
**Chemistry on the Roof: Sunlight driven-reaction** In a second experiment, the reaction was set-up under the usual conditions and the vial was exposed to natural sunlight irradiation on the roof-top of the ICIQ, Tarragona (Spain), on a partially cloudy day (28-Oct-2012). Stirring was continued over 9 hours (from 9 am to 6 pm). Purification by flash column chromatography (20:1 hexane:AcOEt) afforded the title compound (25.2 mg, 98% yield, 92% ee) as a colorless oil.



**Figure 4.14** The simple set-up for the sunlight-driven reaction.

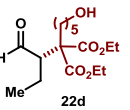
**(S)-diethyl 2-benzyl-2-(1-oxobutan-2-yl)malonate (22c)**

Prepared according to the general procedure using the amino catalyst **IV** (0.02 mmol, 12 mg, 0.2 equiv), MTBE (0.5 M, 200  $\mu$ L), 2,6-lutidine (0.1 mmol, 12  $\mu$ L, 1 equiv), butyraldehyde (0.3 mmol, 27  $\mu$ L, 3 equiv) and diethyl 2-benzyl-2-bromomalonate (0.1 mmol, 33 mg, 1 equiv). Reaction time 16 h. Purification by flash column chromatography (gradient eluent from hexane to 95:5 hexane:AcOEt) afforded the title compound (24 mg, 75% yield, 85% ee) as a colorless oil. The enantiomeric excess was determined by HPLC analysis on a Daicel Chiralpak IC column, 80:10:10 hexane:*i*-PrOH:DCM, flow rate 1.00 mL/min,  $\lambda$  = 254 nm:  $\tau_{\text{major}}$  = 5.8 min,  $\tau_{\text{minor}}$  = 10.3 min. HRMS: calculated for  $\text{C}_{18}\text{H}_{24}\text{O}_5\text{Na}$  (M+Na): 343.1521, found: 343.1519.  $[\alpha]_{\text{D}}^{25}$  = +50.0 (c = 1.0,  $\text{CHCl}_3$ , 85% ee).

  
 $^1\text{H}$  ( $\text{CDCl}_3$ , 300 MHz):  $\delta$  9.71 (d,  $J$  = 2.6 Hz, 1H), 7.30-7.21 (m, 3H), 7.13-7.09 (m, 2H), 4.32-4.08 (m, 4H), 3.40 (d,  $J$  = 14.4 Hz, 1H), 3.28 (d,  $J$  = 14.4 Hz, 1H), 2.60 (dt,  $J$  = 10.5 Hz,  $J$  = 2.6 Hz, 1H), 1.69-1.63 (m, 1H), 1.60-1.50 (m, 1H), 1.22 (t,  $J$  = 7.2 Hz, 3H), 1.21 (t,  $J$  = 7.2 Hz, 3H), 0.95 (t,  $J$  = 7.4 Hz, 3H).  $^{13}\text{C}$  ( $\text{CDCl}_3$ , 75 MHz):  $\delta$  201.5, 169.9, 169.6, 135.3, 130.2, 128.4, 127.3, 61.8 (x2), 60.8, 54.3, 38.6, 18.3, 13.9 (x2), 12.4.

**(S)-diethyl 2-(5-hydroxypentyl)-2-(1-oxobutan-2-yl)malonate (22d)**

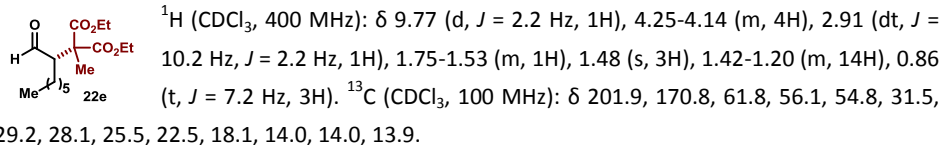
Prepared according to the general procedure using the amino catalyst **IV** (0.02 mmol, 12 mg, 0.2 equiv), MTBE (0.5 M, 200  $\mu$ L), 2,6-lutidine (0.1 mmol, 12  $\mu$ L, 1 equiv), butyraldehyde (0.3 mmol, 27  $\mu$ L, 3 equiv) and diethyl 2-bromo-2-(5-hydroxypentyl)malonate (0.1 mmol, 32.4 mg, 1 equiv). Reaction time 16 h. Purification by flash column chromatography (gradient eluent from hexane to 7:3 hexane:AcOEt) afforded the title compound (24 mg, 77% yield, 90% ee) as a colorless oil. The enantiomeric excess was determined by HPLC analysis on a Daicel Chiralpak IC column, 70:30 hexane:*i*-PrOH, flow rate 1.00 mL/min,  $\lambda$  = 218 nm:  $\tau_{\text{major}}$  = 9.7 min,  $\tau_{\text{minor}}$  = 14.6 min. HRMS: calculated for  $\text{C}_{16}\text{H}_{26}\text{O}_6\text{Na}$  (M+Na): 339.1784, found: 339.1772.  $[\alpha]_{\text{D}}^{25}$  = +27.9 (c = 1.0,  $\text{CHCl}_3$ , 90% ee).

  
 $^1\text{H}$  ( $\text{CDCl}_3$ , 400 MHz): (OH cannot be unambiguously assigned)  $\delta$  9.75 (d,  $J$  = 2.5 Hz, 1H), 4.27-4.16 (m, 4H), 3.63 (t,  $J$  = 6.5 Hz, 2H), 2.72-2.67 (m, 1H), 2.00-1.85 (m, 2H), 1.63-1.48 (m, 5H), 1.42-1.33 (m, 3H), 1.27 (t,  $J$  = 7.0 Hz, 3H), 1.25 (t,  $J$  = 7.0 Hz, 3H), 0.94 (t,  $J$  = 7.4 Hz, 3H).  $^{13}\text{C}$  ( $\text{CDCl}_3$ , 100 MHz):  $\delta$  201.8, 170.5, 170.1, 62.7, 61.7, 61.6, 59.4, 55.3, 33.2, 32.3, 26.0, 24.1, 18.2, 14.0 (x2), 12.7.

**(S)-diethyl 2-methyl-2-(1-oxooctan-2-yl)malonate (22e)**

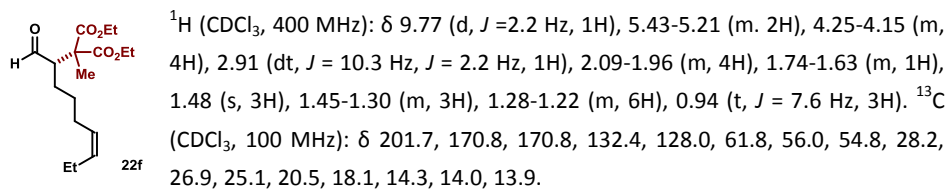
Prepared according to the general procedure using the aminocatalyst **IV** (0.02 mmol, 12 mg, 0.2 equiv), MTBE (0.5 M, 200  $\mu$ L), 2,6-lutidine (0.1 mmol, 12  $\mu$ L, 1 equiv), octanal (0.3 mmol, 47  $\mu$ L, 3 equiv) and diethyl 2-methyl-2-bromomalonate (0.1 mmol, 19.1  $\mu$ L, 1 equiv). Reaction time 16 h. Purification by flash column chromatography (gradient eluent from hexane to 10:1 hexane:Et<sub>2</sub>O) afforded the title compound (81% yield, 94% ee) as a colorless oil. The enantiomeric excess was

determined by HPLC analysis on a Daicel Chiralpak IC column, 80:20 hexane:<sup>i</sup>PrOH flow rate 1.00 mL/min,  $\lambda = 215$  nm;  $\tau_{\text{major}} = 6.6$  min,  $\tau_{\text{minor}} = 7.1$  min. HRMS: calculated for  $\text{C}_{16}\text{H}_{28}\text{NaO}_5$  (M+Na): 323.1829, found: 323.1832.  $[\alpha]_{\text{D}}^{25} = +9.4$  ( $c = 0.3$ ,  $\text{CHCl}_3$ , 94% ee). The value has been compared to the one reported in literature in order to assign the absolute configuration of compounds **22**.<sup>2</sup>



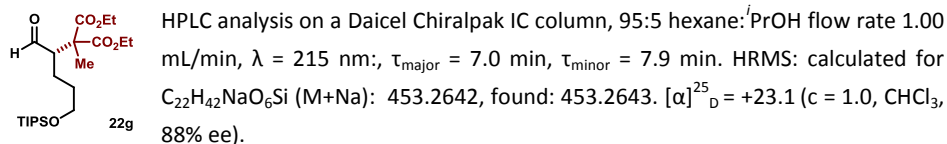
### (S, Z)-diethyl 2-methyl-2-(1-oxonon-6-en-2-yl)malonate (**22f**)

Prepared according to the general procedure using the aminocatalyst **IV** (0.02 mmol, 12 mg, 0.2 equiv), MTBE (0.5 M, 200  $\mu\text{L}$ ), 2,6-lutidine (0.1 mmol, 12  $\mu\text{L}$ , 1 equiv), cis-6-nonenal (0.3 mmol, 50  $\mu\text{L}$ , 3 equiv) and diethyl 2-methyl-2-bromomalonate (0.1 mmol, 19.1  $\mu\text{L}$ , 1 equiv). Reaction time 16 h. Purification by flash column chromatography (gradient eluent from hexane to 20:1 hexane:Et<sub>2</sub>O) afforded the title compound (71% yield, 93% ee) as a colorless oil. The enantiomeric excess was determined by HPLC analysis on a Daicel Chiralpak IC column, 97:3 hexane:<sup>i</sup>PrOH flow rate 1.00 mL/min,  $\lambda = 215$  nm;  $\tau_{\text{major}} = 20.1$  min,  $\tau_{\text{minor}} = 21.9$  min. HRMS: calculated for  $\text{C}_{17}\text{H}_{28}\text{NaO}_5$  (M+Na): 335.1829, found: 335.1831.  $[\alpha]_{\text{D}}^{25} = +6.1$  ( $c = 0.4$ ,  $\text{CHCl}_3$ , 93% ee).



### (S)-diethyl 2-methyl-2-(1-oxo-5-((triisopropylsilyl)oxy)pentan-2-yl)malonate (**22g**)

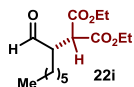
Prepared according to the general procedure using the aminocatalyst **IV** (0.02 mmol, 12 mg, 0.2 equiv), MTBE (0.5 M, 200  $\mu\text{L}$ ), 2,6-lutidine (0.1 mmol, 12  $\mu\text{L}$ , 1 equiv), 5-((triisopropylsilyl)oxy)pentanal (0.3 mmol, 77.4 mg, 3 equiv) and diethyl 2-methyl-2-bromomalonate (0.1 mmol, 19.1  $\mu\text{L}$ , 1 equiv). Reaction time: 16 h. Purification by flash column chromatography (gradient eluent from hexane to 20:1 hexane:AcOEt) afforded the title compound (94% yield, 88% ee) as a colorless oil. The enantiomeric excess was determined by



<sup>1</sup>H (CDCl<sub>3</sub>, 400 MHz):  $\delta$  9.78 (d,  $J = 2.2$  Hz, 1H), 4.23-4.14 (m, 4H), 3.71-3.62 (m, 2H), 2.94 (dt,  $J = 10.1$  Hz,  $J = 2.2$  Hz, 1H), 1.78-1.49 (m, 5H), 1.48 (s, 3H), 1.28-1.21 (m, 8H), 1.06-1.00 (m, 18H). <sup>13</sup>C

(CDCl<sub>3</sub>, 100 MHz):  $\delta$  201.8, 170.9, 170.8, 62.8, 61.8, 56.1, 54.7, 31.4, 22.0, 18.2, 18.0, 14.0, 13.9, 11.9.

**(S)-diethyl 2-(1-oxooctan-2-yl)malonate (22i)** Prepared according to the general procedure



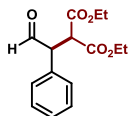
using the amino catalyst **IV** (0.02 mmol, 11.9 mg, 0.2 equiv), MTBE (0.5 M, 200  $\mu$ L), 2,6-lutidine (0.1 mmol, 11.7  $\mu$ L, 1 equiv), octanal (0.3 mmol, 46.8  $\mu$ L, 3 equiv), diethyl bromomalonate (0.1 mmol, 17  $\mu$ L, 1 equiv). Reaction time: 7 h.

Purification by flash column chromatography (gradient eluent from hexane to 9:1 hexane:AcOEt) afforded the title compound (27 mg, 94 % yield, 80% ee) as a colorless oil. In order to calculate the enantiomeric purity, the compound was homologated as a methyl ester, and the enantiomers were separated by HPLC using a Daicel Chiralpak IC-3 column, 90:10 hexane:<sup>i</sup>PrOH, flow rate 0.80 mL/min,  $\lambda$  = 215nm:  $\tau_1$  = 12.6 min,  $\tau_2$  = 13.7 min.  $[\alpha]_D^{25}$  = -48.0 ( $c$  = 1.0, CH<sub>2</sub>Cl<sub>2</sub>, 80% ee).

<sup>1</sup>H NMR (CDCl<sub>3</sub>, 500 MHz)  $\delta$  9.79 (d,  $J$  = 1.1 Hz, 1H), 4.34 – 4.14 (m, 4H), 3.75 (d,  $J$  = 8.6 Hz, 1H), 3.19 – 3.07 (m, 1H), 1.77 – 1.68 (m, 1H), 1.65 – 1.55 (m, 1H), 1.44 – 1.22 (m, 16H), 0.92 – 0.88 (m, 3H). <sup>13</sup>C (CDCl<sub>3</sub>, 125 MHz):  $\delta$  201.6, 168.1, 168.0, 61.8, 61.8, 51.8, 50.3, 31.5, 29.3, 27.1, 26.5, 22.5, 14.0, 14.0.

**(S)-diethyl 2-(2-oxo-1-phenylethyl)malonate**

Prepared according to the general procedure using the aminocatalyst (*S*)-**IV** (0.02 mmol, 12 mg, 0.2 equiv), MTBE (0.5 M, 200  $\mu$ L), 2,6-lutidine (0.1 mmol, 12  $\mu$ L, 1 equiv), phenyl acetaldehyde (0.3 mmol, 35.1  $\mu$ L, 3 equiv) and diethyl bromomalonate (0.1 mmol, 17.0  $\mu$ L, 1 equiv). Reaction time: 48 h. Purification by flash column chromatography (gradient eluent from hexane to 20:1 hexane:AcOEt) afforded the title compound (98% yield, 18% ee) as a colorless oil. We noticed that the enantiomeric excess of the final product erodes during the reaction, because of the racemization of the benzylic stereocenter: other reactions, conducted under the same reaction conditions but at different time, gave different optical purity in the product (ee's in the range of 18-48%). The enantiomeric excess was determined by HPLC analysis on a Daicel Chiralpak IC-3 column, 90:10 hexane:<sup>i</sup>PrOH flow rate 0.80 mL/min,  $\lambda$  = 215 nm:  $\tau_{\text{major}}$  = 16.6 min,  $\tau_{\text{minor}}$  = 21.0 min. HRMS: calculated for C<sub>15</sub>H<sub>18</sub>O<sub>5</sub>Na (M+Na): 301.1046, found: 301.1055.



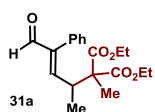
$[\alpha]_D^{25}$  = +31.9 ( $c$  = 1.0, CHCl<sub>3</sub>, 18% ee).

<sup>1</sup>H (CDCl<sub>3</sub>, 400 MHz):  $\delta$  9.68 (s, 1H), 7.43 – 7.28 (m, 3H), 7.31 – 7.15 (m, 3H), 4.48 (d,  $J$  = 11.2 Hz, 1H), 4.24 (q,  $J$  = 7.1 Hz, 1H), 4.13 (d,  $J$  = 11.2 Hz, 1H), 3.93 (q,  $J$  = 7.1 Hz, 2H), 1.29 (t,  $J$  = 7.1 Hz, 3H), 0.95 (t,  $J$  = 7.1 Hz, 3H). <sup>13</sup>C (CDCl<sub>3</sub>, 100 MHz):  $\delta$  196.8, 167.8, 167.6, 131.5, 130.0, 129.3, 128.7, 62.2, 61.7, 58.0, 53.0, 14.1, 13.9.



**(E)-diethyl 2-methyl-2-(5-oxo-4-phenylpent-3-en-2-yl)malonate (31a)**

Prepared according to the general procedure using the amino catalyst **IV** (0.02 mmol, 12 mg, 0.2 equiv), MTBE (0.5 M, 200  $\mu$ L), 2,6-lutidine (0.1 mmol, 12  $\mu$ L, 1 equiv), (*E*)+(*Z*)-2-phenylpent-2-enal (0.3 mmol, 48  $\mu$ L, 3 equiv) and diethyl 2-bromo-2-methylmalonate (0.1 mmol, 19  $\mu$ L, 1 equiv). Reaction time: 60 h. Purification by flash column chromatography (gradient eluent from hexane to 9:1 hexane:AcOEt) afforded the title compound (74 % yield, 86% ee) as a pale yellow oil. The enantiomeric excess was determined by HPLC analysis on a Daicel Chiralpak IC column, 70:30 hexane:PrOH, flow rate 1.00 mL/min,  $\lambda = 254$  nm:  $\tau_{\text{minor}} = 8.5$  min,  $\tau_{\text{major}} = 13.0$  min. HRMS: calculated for  $C_{19}H_{24}O_5Na$  (M+Na): 355.1520, found: 355.1516.  $[\alpha]_D^{25} = -4.8$  ( $c = 1.0$ ,  $CHCl_3$ , 78 % ee).



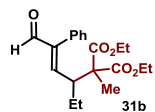
$^1H$  (CDCl<sub>3</sub>, 400 MHz):  $\delta$  9.60 (s, 1H), 7.44-7.32 (m, 3H), 7.16-7.13 (m, 2H), 6.81 (d,  $J = 10.6$  Hz, 1H), 4.27-4.05 (m, 4H), 3.32 (dq,  $J = 10.6$  Hz,  $J = 6.9$  Hz, 1H), 1.43 (s, 3H), 1.23 (t,  $J = 7.2$  Hz, 3H), 1.20 (t,  $J = 7.2$  Hz, 3H), 1.12 (d,  $J = 6.9$  Hz, 3H).

$^{13}C$  (CDCl<sub>3</sub>, 100 MHz):  $\delta$  193.8, 170.9 (x2), 155.3, 144.1, 132.3, 129.1, 128.4,

128.1, 61.4 (x2), 56.5, 38.3, 18.4, 16.0, 14.0, 13.9.

**(E)-diethyl 2-methyl-2-(6-oxo-5-phenylhex-4-en-3-yl)malonate (31b)**

Prepared according to the general procedure using the amino catalyst **IV** (0.02 mmol, 12 mg, 0.2 equiv), MTBE (0.5 M, 200  $\mu$ L), 2,6-lutidine (0.1 mmol, 12  $\mu$ L, 1 equiv), (*E*)-2-phenylhexen-2-enal (0.3 mmol, 52 mg, 3 equiv) and diethyl 2-bromo-2-methylmalonate (0.1 mmol, 19  $\mu$ L, 1 equiv). Reaction time: 60 h. Purification by flash column chromatography (gradient eluent from hexane to 20:1 hexane:AcOEt) afforded the title compound (60 % yield, 81 % ee) as a pale yellow oil. The enantiomeric excess was determined by HPLC analysis on a Daicel Chiralpak IC column, 70:30 hexane:PrOH, flow rate 1.00 mL/min,  $\lambda = 254$  nm:  $\tau_{\text{minor}} = 7.7$  min,  $\tau_{\text{major}} = 11.2$  min. HRMS: calculated for  $C_{20}H_{26}O_5Na$  (M+Na): 369.1672, found: 369.1672.  $[\alpha]_D^{25} = -7.8$  ( $c = 1.1$ ,  $CHCl_3$ , 81 % ee).



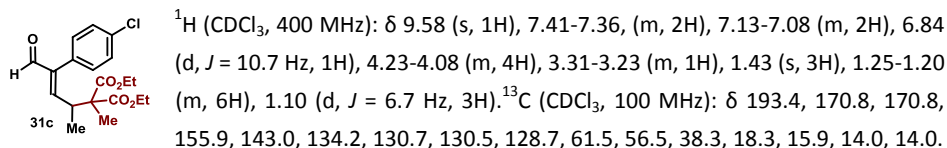
$^1H$  (CDCl<sub>3</sub>, 400 MHz):  $\delta$  9.64 (s, 1H), 7.41-7.36 (m, 2H), 7.36-7.30 (m, 1H), 7.19-7.15 (m, 2H), 6.67 (d,  $J = 11.3$  Hz, 1H), 4.24-4.13 (m, 3H), 4.12-4.04 (m, 1H), 3.15 (dt,  $J = 10.9$  Hz,  $J = 2.6$  Hz, 1H), 1.74-1.65 (m, 1H), 1.51-1.44 (m, 1H), 1.44 (s, 3H), 1.24 (t,  $J = 7.2$  Hz, 1H), 1.19 (t,  $J = 7.2$  Hz, 1H), 0.76 (t,  $J = 7.5$  Hz, 1H).

$^{13}C$  (CDCl<sub>3</sub>, 100 MHz):  $\delta$  193.8, 1701.0, 170.8, 154.0, 146.1, 132.4, 129.5, 128.2, 127.9, 61.4, 61.4, 57.0, 45.1, 23.9, 19.0, 14.0, 13.9, 12.7.

**(E)-diethyl 2-(4-(4-chlorophenyl)-5-oxopent-3-en-2-yl)-2-methylmalonate (31c)**

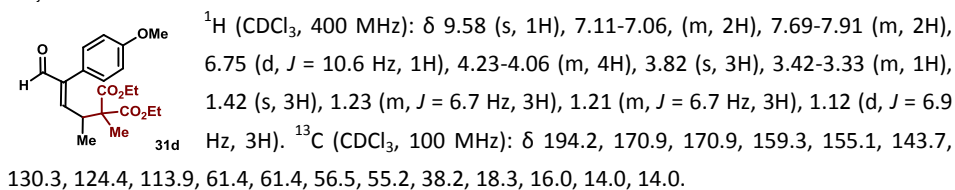
Prepared according to the general procedure using the amino catalyst **IV** (0.02 mmol, 12 mg, 0.2 equiv), MTBE (0.5 M, 200  $\mu$ L), 2,6-lutidine (0.1 mmol, 12  $\mu$ L, 1 equiv), (*E*)-2-(4-chlorophenyl)pent-2-enal (0.3 mmol, 58 mg, 3 equiv) and diethyl 2-bromo-2-methylmalonate (0.1 mmol, 19  $\mu$ L, 1 equiv). Reaction time: 60 h. Purification by flash column chromatography (gradient eluent from

hexane to 5:1 hexane: Et<sub>2</sub>O) afforded the title compound (66 % yield, 85 % ee) as a colorless oil. The enantiomeric excess was determined by HPLC analysis on a Daicel Chiralpak IC column, 70:30 hexane:<sup>i</sup>PrOH, flow rate 1.00 mL/min, λ = 254 nm: τ<sub>minor</sub> = 7.0 min, τ<sub>major</sub> = 9.8 min. HRMS: calculated for C<sub>19</sub>H<sub>23</sub>O<sub>5</sub>Na (M+Na): 389.1126, found: 389.1131. [α]<sub>D</sub><sup>25</sup> = -7.3 (c = 1.0, CHCl<sub>3</sub>, 85 % ee).



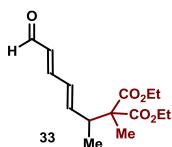
### (*E*)-diethyl 2-(4-(4-methoxyphenyl)-5-oxopent-3-en-2-yl)-2-methylmalonate (31d)

Prepared according to the general procedure using the amino catalyst IV (0.02 mmol, 12 mg, 0.2 equiv), MTBE (0.5 M, 200 μL), 2,6-lutidine (0.1 mmol, 12 μL, 1 equiv), (*E*)-2-(4-methoxyphenyl)pent-2-enal (0.3 mmol, 57 mg, 3 equiv) and diethyl 2-bromo-2-methylmalonate (0.1 mmol, 19 μL, 1 equiv). Reaction time: 60 h. Purification by flash column chromatography (gradient eluent from hexane to 20:1 hexane: AcOEt) afforded the title compound (86 % yield, 85 % ee) as a colorless oil. The enantiomeric excess was determined by HPLC analysis on a Daicel Chiralpak IC column, 70:30 hexane:<sup>i</sup>PrOH, flow rate 1.00 mL/min, λ = 254 nm: τ<sub>minor</sub> = 12.0 min, τ<sub>major</sub> = 18.1 min. [α]<sub>D</sub><sup>25</sup> = 10.5 (c = 1, CHCl<sub>3</sub>, 85% ee).



### (±)-diethyl 2-methyl-2-((3*E*,5*E*)-7-oxohepta-3,5-dien-2-yl)malonate (33)

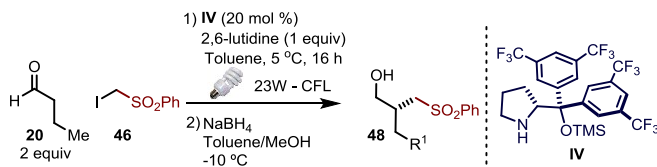
Prepared according to the general procedure using the amino catalyst IV (0.02 mmol, 6.6 mg, 0.2 equiv), MTBE (0.5 M, 200 μL), 2,6-lutidine (0.1 mmol, 12 μL, 1 equiv), (2*E*,4*E*)-hepta-2,4-dienal (0.3 mmol, 38 μL, 3 equiv), 2-bromo-2-methylmalonate (0.1 mmol, 19 μL, 1 equiv). Reaction time: 16 h. Purification by flash column chromatography (gradient eluent from hexane to 9:1 hexane:AcOEt) afforded the title compound (27 mg, 92 % yield, racemic) as a pale yellow oil. The



enantiomers were separated by HPLC using a Daicel Chiralpak IC column, 70:30 hexane:<sup>i</sup>PrOH, flow rate 1.00 mL/min, λ = 254 nm: τ<sub>1</sub> = 13.7 min, τ<sub>2</sub> = 14.8 min. HRMS: calculated for C<sub>15</sub>H<sub>22</sub>O<sub>5</sub>Na (M+Na): 305.1359, found: 305.1364. <sup>1</sup>H (CDCl<sub>3</sub>, 500 MHz): δ 9.52 (d, *J* = 8.0 Hz, 1H), 7.06 (dd, *J* = 15.4 Hz, *J* = 9.9 Hz, 1H), 6.39-6.23 (m, 2H), 6.09 (dd, *J* = 15.4 Hz, *J* = 8.0 Hz, 1H), 4.21-4.12 (m, 4H), 3.12 (pent, *J* = 7.0 Hz, 1H), 1.37 (s, 3H), 1.24 (t, *J* = 7.1 Hz, 3H), 1.23 (t, *J* = 7.1 Hz, 3H), 1.11 (d, *J* = 7.0 Hz, 3H). <sup>13</sup>C

(CDCl<sub>3</sub>, 125 MHz):  $\delta$  193.7, 171.0 (x2), 152.0, 146.4, 131.1, 129.6, 61.4 (x2), 57.2, 41.7, 17.1, 15.2, 14.0 (x2).

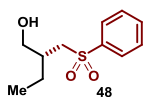
### Procedure for the Photochemical Organocatalytic Enantioselective Alkylation of butyraldehyde with iodomethyl sulfone:



Scheme 4.26 – Photochemical alkylation of aldehydes with malonates.

A 10 mL Schlenk tube was charged with the aminocatalyst **IV** (0.02 mmol, 11.9 mg, 0.2 equiv), Toluene (400  $\mu$ L), butyraldehyde (2 equiv, 0.2 mmol, 18.0  $\mu$ L), 2,6-lutidine (1 equiv, 0.1 mmol, 11.7  $\mu$ L) and iodomethyl sulfone **46** (1 equiv., 28.2 mg). The reaction mixture was degassed via freeze pump thaw (x3), and the vessel refilled with argon. After the reaction mixture was thoroughly degassed, the vial was sealed and positioned in a 5 °C thermostated bath and irradiated with a 23W – CFL (distance 5 cm). After stirring for 24 hours, the reaction was cooled to -10 °C by means of a NaCl/ice bath and methanol (400  $\mu$ L) was added to the reaction. (75.6 mg, 20 equiv) of NaBH<sub>4</sub> was added to the solution and the mixture was stirred for 30 minutes. The reaction was quenched by adding 5 mL of saturated NH<sub>4</sub>Cl solution. The mixture was extracted 4 times with 5 ml of dichloromethane, after which the organic phase were collected, dried over sodium sulfate and the solvents were removed under reduced pressure. The reaction was then purified through gradient silica gel chromatography (Hexane – Hexane:EtOAc 60:40) to afford compound **48** (8.6 mg, 38% yield) as a colorless oil.

### (*R*)-2-((phenylsulfonyl)methyl)butan-1-ol (**48**)



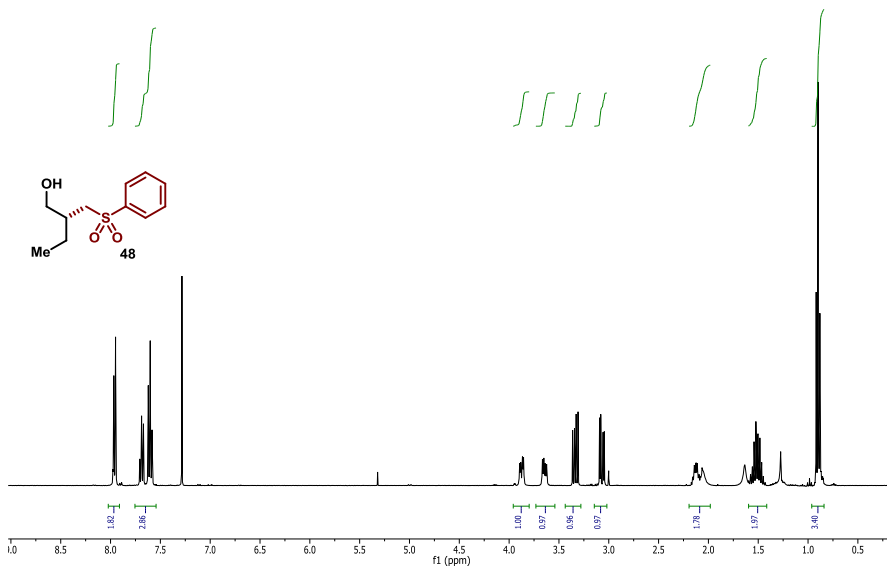
The enantiomers were separated by HPLC using a Daicel Chiralpak IC column, 70:30 heptane:iPrOH, flow rate 0.80 mL/min,  $\lambda$  = 215 nm;  $\tau_1$  = 13.9 min,  $\tau_2$  = 16.8 min.  $[\alpha]_D^{20}$  = -6.8 ( $c$  = 1.0, CH<sub>2</sub>Cl<sub>2</sub>, 80 % ee). HRMS: calculated for C<sub>11</sub>H<sub>16</sub>O<sub>3</sub>SNa (M+Na): 251.0712, found: 251.0720.

<sup>1</sup>H NMR (CDCl<sub>3</sub>, 400 MHz)  $\delta$  8.02 – 7.91 (m, 2H), 7.76 – 7.54 (m, 3H), 3.87 (dd,  $J$  = 11.2, 4.3 Hz, 1H), 3.64 (dd,  $J$  = 11.2, 5.5 Hz, 1H), 3.34 (dd,  $J$  = 14.2, 7.6 Hz, 1H), 3.07 (dd,  $J$  = 14.2, 4.7 Hz, 1H), 2.19 – 1.98 (m, 2H), 1.60 – 1.41 (m, 2H), 0.90 (t,  $J$  = 7.4 Hz, 3H). <sup>13</sup>C (CDCl<sub>3</sub>, 100 MHz):  $\delta$  139.9, 133.7, 129.3, 127.8, 63.5, 57.5, 37.7, 24.3, 11.0.

**(R)-2-((phenylsulfonyl)methyl)butan-1-ol (48)**

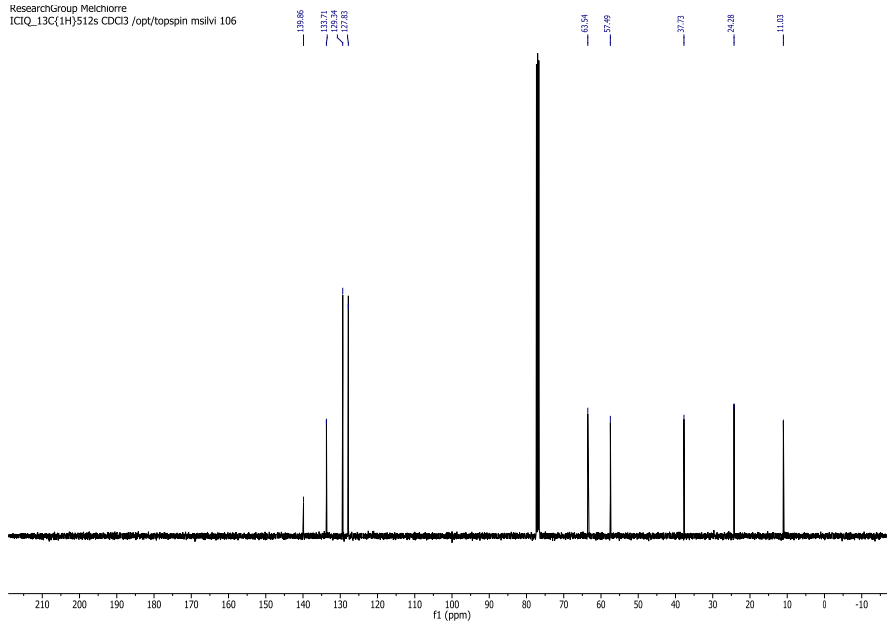
$^1\text{H}$  NMR ( $\text{CDCl}_3$ , 400 MHz)

ResearchGroup Melchiorre  
ICIQ\_1H12p8s CDCl3 /opt/topspin msilvi 106



$^{13}\text{C}$  NMR ( $\text{CDCl}_3$ , 100 MHz)

ResearchGroup Melchiorre  
ICIQ\_13C(1H)512s CDCl3 /opt/topspin msilvi 106



UNIVERSITAT ROVIRA I VIRGILI

NEW DIRECTIONS IN AMINOCATALYSIS: VINYLOGY AND PHOTOCHEMISTRY

Mattia Silvi

## Chapter V

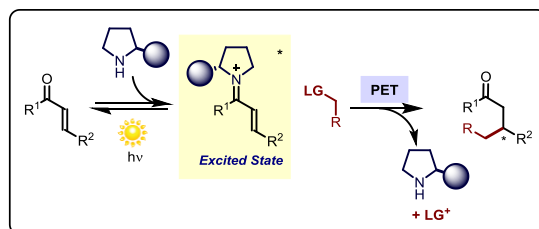
# Iminium ion photochemistry: a novel route for the unconventional asymmetric $\beta$ -functionalization of enals

### Target

Asymmetric, metal free, photochemical  $\beta$ -functionalizations of aldehydes hardly achievable through classical polar chemistry.

### Tool

Tendency of photoexcited iminium ions to undergo photoinduced electron transfer with opportune donor molecules under mild conditions.



## 5.1 Introduction

Observing the physical aspect of a reaction (color, presence of solids in the mixture, temperature increase etc.) is usually a very important aspect in the development of a synthetic methodology and it is often the first recommendation that every supervisor gives to young PhD students. In particular cases, a careful observation of the physical state of a reaction can also lead to the discovery of a novel reactivity, as in the case reported in the present chapter.

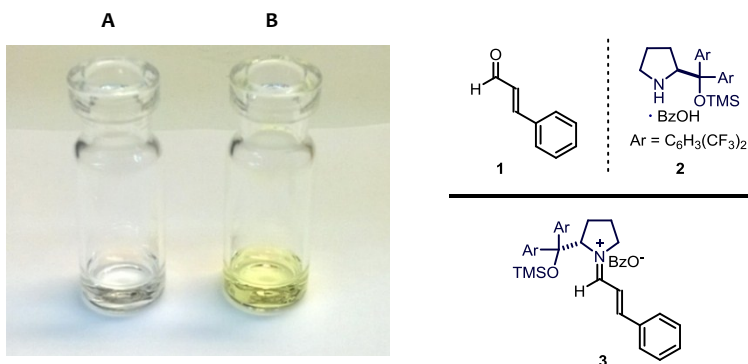


**Figure 5.1** – Pictures of a 0.5 M acetonitrile solution of **1** (vial **A**), and of a 0.5 M acetonitrile solution of **1** upon addition of 20% mol of **2** and after 1 h incubation (vial **B**). The color change is due to the transient formation of the iminium ion **3**.

During our experience in iminium ion-mediated reactions, we noticed that, when mixing conjugated unsaturated aldehyde **1** and the aminocatalyst **2** in organic solvents, a strong yellow color developed, due to the formation of a highly conjugated iminium ion **3** in solution (Figure 5.1). Although this can be considered an “everyday observation” for a chemist involved in asymmetric organocatalysis, the idea of exploiting the photochemistry of this colored transient species has never been exploited to-date.

Motivated by the golden color of the iminium ion solution, attempts to develop new synthetic strategies based on the photochemistry of this reactive intermediate has been a constant goal from the very beginning of my PhD. In initial attempts, I wondered if the chemistry of Rhodopsin, a protein involved in the chemistry of vision, could be emulated. In this enzyme, a photoisomerization process occurs within an iminium ion intermediate formed between a lysine residue and the unsaturated aldehyde retinal, leading to the relay of chemical information in biological systems.<sup>1</sup> The idea, as presented in Figure 5.2, was to translate this photoisomerization process in the context of stereoselective catalytic synthesis. The ability to switch the geometry of a transient chiral iminium ion could indeed provide a mechanism to reverse the chiral induction of a single chiral catalyst using light. A photoinduced *E/Z* isomerization of the iminium ion would result in a new isomeric intermediate where the bulky substituent of the chiral catalyst would shield the opposite prochiral face (Figure 5.2). The following nucleophilic attack (Michael-type addition) would generate the two antipodes of the chiral product using a single chiral catalyst controlled by light.

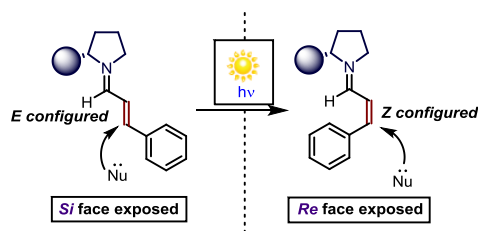


**Figure 5.2** – Light-induced *E/Z* isomerization of chiral iminium ions may lead to the obtaining of both enantiomeric products with the same chiral catalyst.

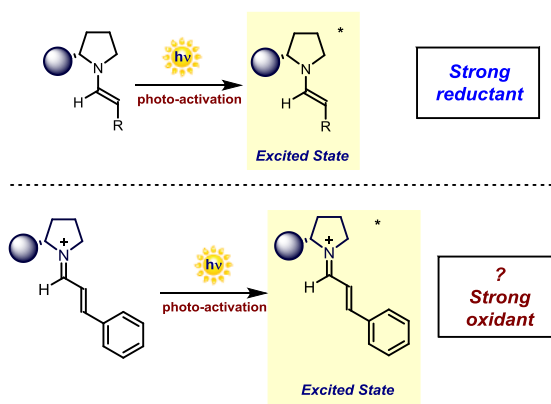
Unfortunately, all the attempts carried out on this ground resulted in failure.<sup>2</sup> Despite the initial disappointment, we later realized that the idea of exploiting the photochemistry of iminium ions was not chemically unfeasible, but that our knowledge of photochemistry was still too preliminary at that time for achieving this goal.

<sup>1</sup> Voet, D.; Voet, J. G. “Bacteriorhodopsin Is a Light-Driven Proton Pump” Chapter 22, p. 851 in *Biochemistry, fourth edition*, 2011, Wiley.

<sup>2</sup> The addition of simple nucleophiles (i.e. dioxindole, see Chapter 3) to cinnamaldehyde was attempted, but light did not affect the outcome of the reaction.

### 5.1.1 From enamine excitation to iminium ion excitation: the idea of exploiting the redox properties of the excited iminium ion

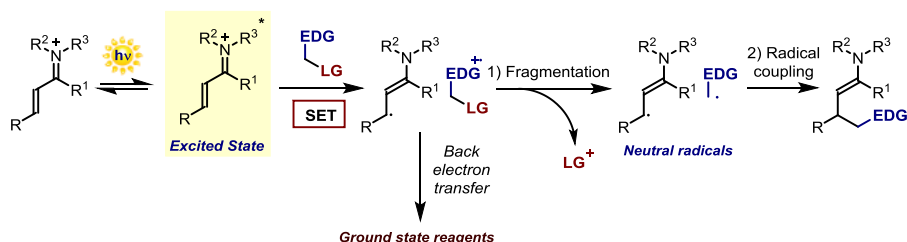
The lesson learnt during our studies on the photochemistry of enamine intermediates (Chapter 4) provided us with a new conceptual framework which was crucial for developing the chemistry reported in this chapter. We questioned whether it could be possible to exploit the photochemistry of transiently generated iminium ions in photoinduced electron transfer (PET): in much the same way as excited electron rich enamines can serve as strong single electron reductant, could excited electron poor iminium ions act as powerful oxidants?



**Scheme 5.1** – A possible analogy between enamine redox photochemistry and iminium ion redox photochemistry.

A common obstacle of PET reactions is the back electron transfer (BET), which returns the ground state reagents. The BET is a non-productive energy wasting process that competes with the desired photochemical reaction, strongly affecting the quantum yield of the process (see Chapter 4). In order to exploit the PET phenomenon for synthetic purposes, BET has to be prevented by a sequential irreversible chemical transformation on the transiently generated, high energy open-shell species.

We envisioned the possibility to use an irreversible fragmentation strategy of the high energy radical cation generated after electron transfer from the donor compound to the strong oxidant excited iminium ion (Scheme 5.2).

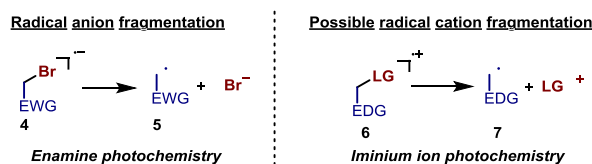


**Scheme 5.2** – Possible PET reaction on transiently formed iminium ions. EDG = electron-donor group; LG = leaving group.



This event would generate stabilized neutral radicals, which could eventually couple in a productive carbon-carbon bond forming process.

The hypothetical fragmentation of the donor partner in Scheme 5.2 recalls the concept of fragmentation used in enamine photochemistry, in which mesolysis of high energy alkyl halide radical anions occurred to afford alkyl radicals.



**Scheme 5.3** – Radical ion fragmentation in order to avoid back electron transfer phenomenon. EWG = electron-withdrawing group; EDG = electron-donor group; LG = leaving group.

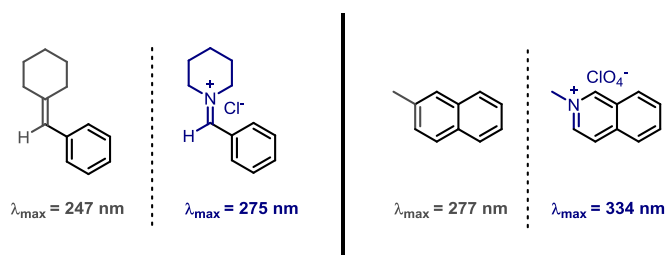
Our studies on the feasibility of this idea started by an extensive literature study about the photophysics and photochemistry of non-vinylogous iminium ions. Despite being structurally and chemically different from the vinylogous intermediate that we planned to exploit, we believed them to show a reminiscent photochemical behavior. Then we focused our attention on the identification of a suitable donor partner, needed to avoid the back electron transfer phenomenon, and the potential application of an iminium ion-mediated photoinduced electron transfer strategy for synthetic purposes.

## 5.1.2 A brief overview of photophysical and electrochemical properties of iminium ions

Most of the photophysical and photochemical properties of iminium ions are directly correlated to the fact that they are isoelectronic with simple olefins, with the nitrogen lone pair completely involved in a conjugative donation to the iminium carbon. A remarkable experimental evidence of this fact is the high rotational barrier around the N-C bond (70-90 kcal/mol), which make the thermal isomerization nearly impossible.

In iminium ions, electronic transitions show analogies with the ones of structurally related olefins:  $\pi-\pi^*$  electronic transitions are only possible and high molar extinction coefficients are usually observed for symmetry reasons.<sup>3</sup> The wavelengths where absorbance maxima occur are comparable to the one of structurally related olefins, although bathochromic shifts are usually observed (Scheme 5.4).

<sup>3</sup> Mariano, P. S. "The Photochemistry of Iminium Salts and Related Heteroaromatic Systems" *Tetrahedron* **1983**, *39*, 3845.



Scheme 5.4 – Absorbance maxima of structurally analogous olefin – iminium ions.<sup>3,4</sup>

The low energy LUMOs in iminium ions enable these species to readily undergo single electron reduction to afford stabilized  $\alpha$ -amino radical (lifetime about 100 ms).  $E_{1/2}$  (half-wave potential values) are in the range of -1.95 and -0.84 volts (vs SCE).<sup>5</sup> The LUMO energy is further lowered in conjugated iminium ions, and this is reflected in both absorbance bathochromic shift and more positive  $E_{1/2}$  values.<sup>3</sup>

Accordingly to the general principle: *electronically excited molecules are both better electron donors and better electron acceptors than the corresponding ground-state species*,<sup>6</sup> after light absorption, iminium ions become extraordinary powerful oxidants. In non-vinyllogous iminium ions the redox potential can reach  $E_{1/2} > 3$  V (vs SCE),<sup>7</sup> rendering them prone to photoinduced electron transfer.

### 5.1.3 The identification of the donor partner

Surmising that the electrochemical and photochemical features of iminium ions could match for the realization of our idea, we next focused on the identification of a suitable donor partner able to fragment as in Scheme 5.2, in order to avoid competing back electron transfer.

An extensive literature study led us to focus on seminal works reported by Mariano in the early 1980s. As presented in Scheme 5.5, the photochemical reaction of preformed cyclic iminium ions **8** with allylsilane **9** or benzylsilane **10** resulted in the formation of  $\alpha$ -substituted allyl or benzyl pyrrolidines **16** or **17**.<sup>8,9</sup>

<sup>4</sup> a) Hodgkins, J.E.; Woodyard, J. D.; Stephenson, D. L. "Stereochemistry of the Reaction of Benzal Chloride with Olefins" *J. Am. Chem. Soc.* **1964**, *86*, 4080. b) Bohme, H.; Anterhoff, G. "In  $\alpha$ -Stellung Durch Aromatische Oder Heterocyclische Reste Substituierte Carbimoniumhalogenide" *Chem. Ber.* **1971**, *104*, 2013.

<sup>5</sup> Andrieaux, C. P.; Saveant, J. M. "Electrodimerization – II. Reduction Mechanism of Imonium Cations" *J. Electroanal. Chem.* **1970**, *28*, 446.

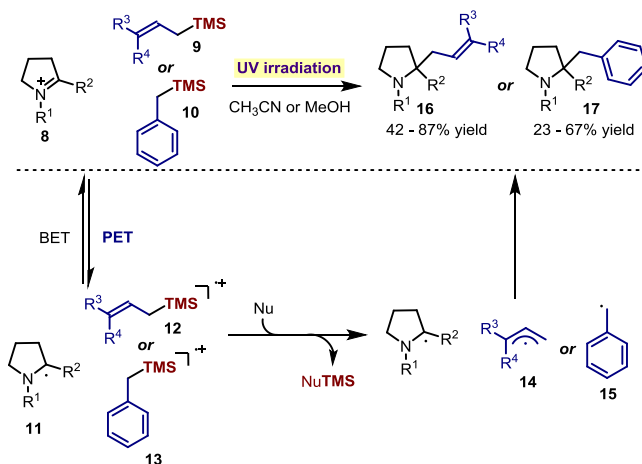
<sup>6</sup> Balzani, V.; Ceroni, P.; Juris, A. "Excited states: Physical and chemical properties, electron transfer" Chapter 4, p. 114 in *Photochemistry and photophysics*, **2014**, Wiley-VCH.

<sup>7</sup> Mariano, P.S. "Electron-transfer Mechanisms in Photochemical Transformations of Iminium Salts" *Acc. Chem. Res.* **1983**, *16*, 130.

<sup>8</sup> Ohga, K.; Mariano, P. S. "Electron Transfer Initiated Photoaddition of Allylsilanes to 1-Methyl-2-phenylpyrrolinium Perchlorate. A Novel Allylation Methodology" *J. Am. Chem. Soc.* **1982**, *104*, 617.

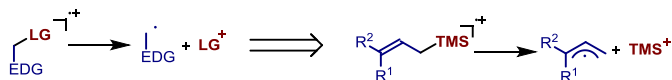
<sup>9</sup> a) Lan A. J. Y.; Quiillen, S. L.; Heuckeroth, R. O.; Mariano, P. S. "Arene-Iminium Salt Photochemistry. Dramatic Effects of Sequential Electron-Transfer-Desilylation Pathways on the Nature and Efficiency of

Careful mechanistic studies highlighted the occurrence of a PET process between the excited iminium ion and the silane to generate an  $\alpha$ -amino radical **11** and a silane radical cation **12** or **13**. Nucleophile mediated desilylation (operated by solvent or water) generated stabilized allyl or benzyl radicals **14** or **15**. Radical coupling finally led to the formation of the desired product **16** or **17**.



**Scheme 5.5** – Photochemical benzylation and allylation of cyclic non-vinyllogous iminium ions.

We realized that the strategy reported by Mariano was consonant with our initial idea of avoiding the back electron transfer by inducing a fragmentation event on the reactive radical cation (Scheme 5.6). In analogy with his report, we considered using silanes as potential reaction partners for the chemistry we wished to develop.



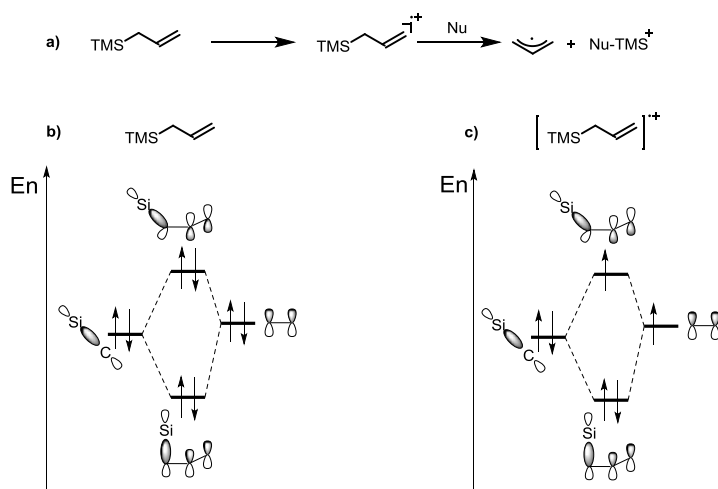
**Scheme 5.6** – Silane moiety can be a good leaving group and provides the desired fragmentation process.

Alkyl silanes have been widely employed in electrochemical reactions because of their low  $E_{1/2}$  and their tendency to undergo nucleophile mediated radical cation fragmentation to generate neutral alkyl radicals (Scheme 5.7-a).<sup>10</sup>

Scheme 5.7 rationalizes the effect that the presence of a  $\beta$ -silicon substituent has on the electrochemical properties of an olefin.

Photoaddition and Photocyclization Processes" *J. Am. Chem. Soc.* **1984**, *106*, 6439. b) Borg, R. M.; Heuckeroth, R. O.; Lan, A. J. Y.; Quillen, S. L.; Mariano, P. S. "Arene-Iminium Salt Electron-Transfer Photochemistry. Mechanistically Interesting Photoaddition Processes" *J. Am. Chem. Soc.* **1987**, *109*, 2728.

<sup>10</sup> Yoshida, J.; Kataoka, K.; Horcajada, R.; Nagaki, A. "Modern Strategies in Electroorganic Synthesis" *Chem. Rev.* **2008**, *108*, 2265.

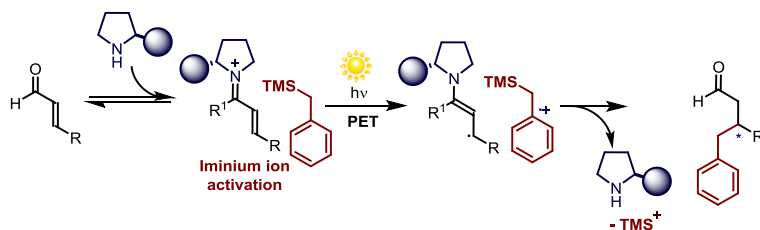


**Scheme 5.7** – FMO explanation for electrochemical behavior of silane compounds.

The low reduction potential of organic silanes is ascribed firstly to a  $\sigma_{\text{C-Si}}-\pi_{\text{C-C}}$  filled orbitals interaction in the neutral molecule that tends to increase the energy of the HOMO orbital (Scheme 5.7b). Secondly, an interaction between the  $\sigma_{\text{C-Si}}$  filled orbital with the single electron occupied  $\pi_{\text{C-C}}$  orbital in the radical cation, resulting from oxidation (Scheme 5.7c), causes a net stabilization of this species. The interaction depicted in Scheme 5.7c also increases the polarization of C-Si bond, rendering it particularly prone to nucleophilic attack, eventually releasing allylic radicals (Scheme 5.7-a).

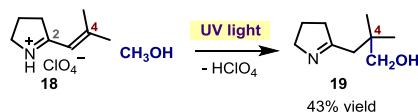
## 5.2 Target of the project

The initial idea of exploiting the photochemistry of transient iminium ions, as well as the literature survey discussed, prompted us to attempt a catalytic enantioselective direct  $\beta$ -allylation and benzylation of  $\alpha,\beta$ -unsaturated systems triggered by light (Scheme 5.8). Successfully developed, this strategy would demonstrate that the excited state reactivity of chiral iminium ions can greatly expand the scope of asymmetric aminocatalysis, providing the possibility to realize transformations inaccessible to classical ground state chemistry of iminium ions.



Scheme 5.8 – The envisioned photochemical strategy for the asymmetric catalytic  $\beta$ -benzylation of enals.

It is pertinent to highlight an observation by Mariano *et al.*, who reported that vinylogous iminium ion **18** reacts at the remote 4 position when exposed to light (Scheme 5.9).<sup>11</sup> This precedent further encouraged us to exploit the iminium ion activation for developing unprecedented  $\beta$ -functionalization of enals triggered by light.



Scheme 5.9 – Vinylogous photochemical reaction of a preformed vinylogous iminium ion.

### 5.3 Catalytic asymmetric conjugate allylation and benzylation of electron-poor olefins: challenging reactions

The catalytic asymmetric conjugate addition to electron-poor olefins is a key transformation for carbon-carbon bond formation. It is usually achieved with the use of organometallic reagents, contextually employing transition metal catalysts, generally Cu, Ni or Rh, in the presence of chiral ligands.<sup>12,13,14</sup> Despite these organometallic strategies are reliable synthetic tools and have

<sup>11</sup> Only the example depicted in Scheme 5.9 was found in literature, which was reported in the review article cited as Reference 3.

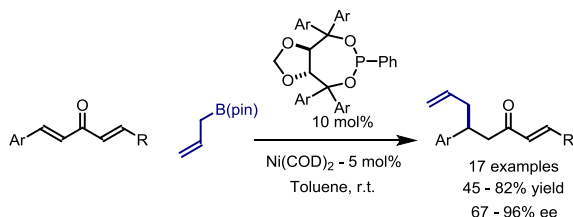
<sup>12</sup> For reviews on copper catalyzed conjugate additions: a) Alexakis, A.; Bäckvall, J. E.; Krause, N.; Pàmies, O.; Diéguez, M. "Enantioselective Copper-Catalyzed Conjugate Addition and Allylic Substitution Reactions" *Chem. Rev.* **2008**, *108*, 2796. b) Feringa, B.; Naasz, R.; Imbos, R.; Arnold, L. A. "Copper-Catalyzed Enantioselective Conjugate Addition Reactions of Organozinc Reagents" Chapter 7, p. 224 in *Modern Organocopper Chemistry*, **2002**, Wiley-VCH.

<sup>13</sup> For early examples of nickel catalyzed conjugate additions: a) "Soai, K.; Yokoyama, S.; Hayasaka, T.; Ebihara, K. "Catalytic Asymmetric Induction in Enantioselective Conjugate Addition of Dialkylzincs to Enones" *J. Org. Chem.* **1988**, *53*, 4148. b) Bolm, C.; Ewald, M. "Optically Active Bipyridines in Nickel Catalyzed Enantioselective Conjugate Addition to Enones" *Tetrahedron Lett.* **1990**, *35*, 5011.

<sup>14</sup> For reviews on rhodium catalyzed conjugate addition: a) Hayashi, T.; Yamasaki, K. "Rhodium-Catalyzed Asymmetric 1,4-Addition and Its Related Asymmetric Reactions" *Chem. Rev.* **2003**, *103*, 2829. b) Tian, P.; Dong, H. Q.; Lin, G. Q. "Rhodium-Catalyzed Asymmetric Arylation" *ACS Catal.* **2012**, *2*, 95.

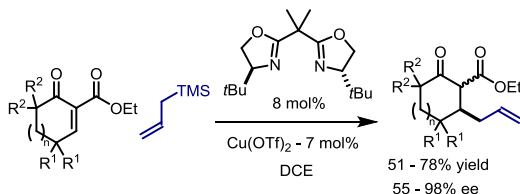
become benchmark reactions in asymmetric catalysis, general catalytic allylation and benzylation procedures remain hardly achievable.<sup>15</sup>

In 2008, a remarkable stereoselective catalytic conjugate allylation of activated enones was reported. However, the reaction required a double conjugated  $\pi$  system to be effective (Scheme 5.10).<sup>15</sup>



**Scheme 5.10** – Enantioselective catalytic conjugate allylation of enones. Using an enone with a double  $\pi$ -system was crucial.

Allylic or benzylic fragments could also be introduced using a conjugate version of the Hosomi-Sakurai reaction; this strategy requires the employment of Lewis acidic metals or activated substrates and is usually plagued by the presence of byproducts generated by competing 1,2-addition pathways.<sup>16</sup> Recently, a remarkable catalytic asymmetric version of this challenging transformation was reported using allyl silane as nucleophile and activated ketones (Scheme 5.11).<sup>17</sup>



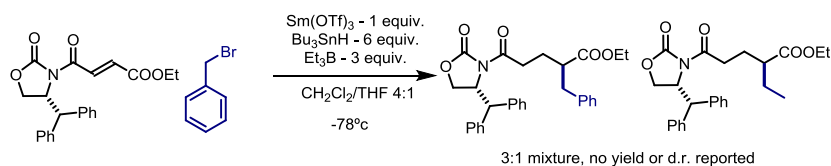
**Scheme 5.11** – Catalytic enantioselective conjugate Hosomi-Sakurai reaction of activated unsaturated  $\beta$ -ketoesters.

<sup>15</sup> We are not aware of catalytic asymmetric conjugate benzylation reactions. For the only two examples of catalytic conjugate allylation of double bonds on special scaffolds using boron or tin precursors, see: a) Sieber, J. D.; Morken, J. P. "Asymmetric Ni-Catalyzed Conjugate Allylation of Activated Enones" *J. Am. Chem. Soc.* **2008**, *130*, 4978. b) Kuang, Y.; Liu, X.; Chang, L.; Wnag, M.; Lin, L.; Feng, X. "Catalytic Asymmetric Conjugate Allylation of Coumarins" *Org. Lett.* **2011**, *13*, 3814.

<sup>16</sup> Allylation reactions: a) Majetich, G.; Casares, A. M.; Chapman, D.; Behnke, M. "Chemoselectivity in the Conjugate Addition of Allylsilanes to Michael Acceptors" *Tetrahedron Lett.* **1983**, *24*, 1909. b) Schultz, A. G.; Lee, J. "Stereoselective Conjugate Additions of Allyl Silanes and Enol Silyl Ethers to a Chiral 2-Substituted-2-Cyclohexen-1-one" *Tetrahedron Lett.* **1992**, *33*, 4397. Benzylation reaction: Ricci, A.; Fiorenza, M.; Grifagni, M. A.; Bartolini, G. "Fluoride Ion Induced Reactions of Organosilanes with Saturated Lactones and  $\alpha,\beta$ -Enones" *Tetrahedron Lett.* **1982**, *23*, 5079.

<sup>17</sup> Shizuka, M.; Snapper, M. L. "Catalytic Enantioselective Hosomi-Sakurai Conjugate Allylation of Cyclic Unsaturated Ketoesters" *Angew. Chem. Int. Ed.* **2008**, *47*, 5049.

Conjugate alkylation-type products could be obtained exploiting radical chemistry as well, trapping chemically-generated nucleophilic radicals with  $\alpha,\beta$ -unsaturated carbonyl compounds.<sup>18</sup> In one of the works reported in this field by Sibi *et al.*, an asymmetric benzylation of electron poor olefins through the employment of chiral auxiliaries (Scheme 5.12) was reported (as a single entry). Nor yield nor stereoselectivity were specified in the original paper, but the compound was identified in a complex mixture.<sup>19</sup>



**Scheme 5.12** – Single example of radical diastereoselective benzylation of electron-poor olefins.

Alkylation and benzylation of electron-poor olefins has also been achieved using photochemical strategies through the employment of organic or metal-based sensitizers, though no enantioselective versions have been reported to date.<sup>20</sup>

## 5.4 Results and discussion

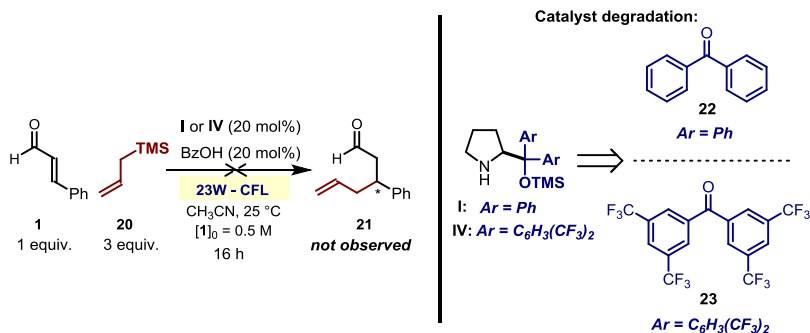
The feasibility of our idea was tested against the asymmetric allylation of cinnamaldehyde in presence of the commercially available chiral amines **I** or **IV**, benzoic acid, and allyl silane **20** (Scheme 5.13). The yellow solution was irradiated with a common household 23 W compact fluorescent light (CFL) bulb for 16 hours. Disappointingly, no traces of the desired product were observed, and starting materials **1** and **20** were recovered at the end of the reaction. Interestingly, it was not possible to recover the catalysts **I** and **IV**. GC-MS analysis of the crude

<sup>18</sup> For an early example, see: a) Brown, H. C.; Kabalka, G. W. "The Oxygen-Induced Reactions of Organoboranes with the Inert  $\alpha,\beta$ -unsaturated Carbonyl Derivatives" *J. Am. Chem. Soc.* **1970**, *92*, 714. For enantioselective versions, see: b) Sibi, M. P.; Ji J. "Chiral Lewis Acid Catalysis in Radical Reactions: Enantioselective Conjugate Radical Additions" *J. Am. Chem. Soc.* **1996**, *118*, 9200. c) Sibi, M. P.; Ji, J. "Practical and Efficient Enantioselective Conjugate Radical Additions" *J. Org. Chem.* **1997**, *62*, 3800. d) Sibi, M. P.; Chen, J. "Enantioselective Tandem Radical Reactions: Vicinal Difunctionalization in Acyclic Systems with Control over Relative and Absolute Stereochemistry" *J. Am. Chem. Soc.* **2001**, *123*, 9472.

<sup>19</sup> Sibi, M. P.; Liu, P.; Ji, J.; Hajra, S.; Chen, J. "Free-Radical Conjugate Additions. Enantioselective synthesis of Butyrolactone Natural Products: (-)-Enterolactone, (-)-Arctigenin, (-)-Isoarctigenin, (-)-Nephrosteranic Acid and (-)-Roccellaric Acid" *J. Org. Chem.* **2002**, *67*, 1738.

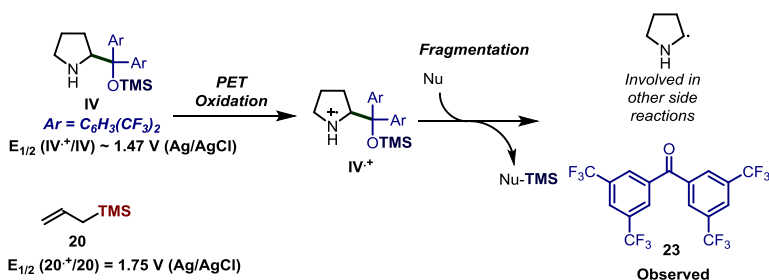
<sup>20</sup> a) Fagnoni, M.; Mella, M.; Albini, A. "Radical Addition to Alkene via Electron Transfer Photosensitization" *J. Am. Chem. Soc.* **1995**, *117*, 7877. b) Cermenati, L.; Richter, C.; Albini, A. "Solar Light Induced Carbon-Carbon Bond Formation via  $\text{TiO}_2$  Photocatalysis" *Chem. Commun.* **1998**, 805. c) Montanaro, S.; Ravelli, D.; Merli, D.; Fagnoni, M.; Albini, A. "Decatungstate as Photoredox Catalyst: Benzylation of Electron-Poor Olefins" *Org. Lett.* **2012**, *14*, 4218.

reaction mixture revealed complete catalyst degradation and generation of consistent amounts of benzophenones **22** or **23**.<sup>21</sup>



**Scheme 5.13** – Catalyst degradation during preliminary attempts of photochemical organocatalytic conjugate allylation of cinnamaldehyde **1**.

The combination of catalyst **I** and benzoic acid is a catalytic system successfully employed for a wide array of iminium ion mediated reactions and usually high catalyst stability is observed under the reaction conditions.<sup>22</sup> We surmised that the degradation phenomenon could be ascribable to a photo-induced oxidation process.



**Scheme 5.14** – Rationale for catalyst degradation.

As presented in Scheme 5.14, on the basis of redox proprieties, the aminocatalyst **IV** is more prone to oxidation than the allyl silane **20**. For this reason, the excited iminium ion is expected to induce facile catalyst oxidation under the reaction conditions.<sup>23</sup> The formation of

<sup>21</sup> The identity of the byproducts was unambiguously inferred by comparison of retention time and mass spectrum achieved by injecting pure samples of the two benzophenones. Benzophenone **22** is commercially available, while compound **23** was synthesized as reported in the experimental part.

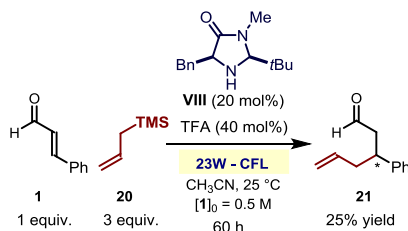
<sup>22</sup> Jensen, K. M.; Dickmeiss, G.; Jiang, H.; Albrecht, L.; Jørgensen, K. A. "The Diarylprolinol Silyl Ether System: A General Organocatalyst" *Acc. Chem. Res.* **2012**, *45*, 248.

<sup>23</sup> a) *Allylsilane potential*: Asami, R.; Fuchigami, T.; Atobe, M. "Development of an Anodic Substitution Reaction System Using Acoustic Emulsification" *Chem. Commun.* **2008**, 244. b) *Aminocatalyst potential*: Silvi, M.; Arceo, E.; Cassani, C.; Melchiorre, P. "Enantioselective Organocatalytic Alkylation of Aldehydes and Enals Driven by the Direct Photoexcitation of Enamines" *J. Am. Chem. Soc.* **2015**, *137*, 6120.



benzophenone **23** could be rationalized by a nucleophile-induced desilylation/fragmentation of the radical cation **IV**<sup>+</sup>.<sup>24</sup>

In order to avoid catalyst degradation, a different catalyst scaffold was tested (Scheme 5.15).



**Scheme 5.15** – First observation of product formation in the photochemical  $\beta$ -allylation of cinnamaldehyde.

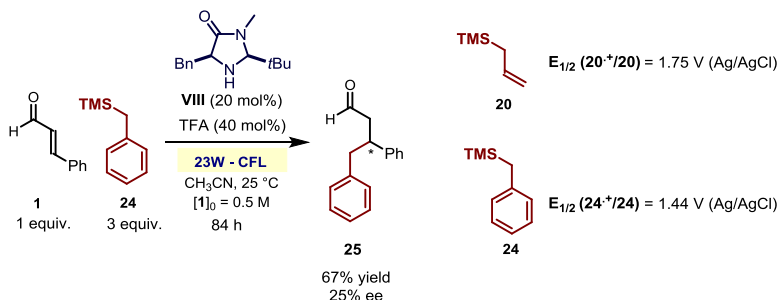
Employing the MacMillan-type imidazolidinone catalyst **VIII**, the desired compound **21** was finally observed in the reaction mixture, albeit in a moderate yield (25% based on NMR analysis).<sup>25</sup> Total catalyst degradation was detected at the end of the reaction, but this catalyst was probably stable enough to allow for the production of a small amount of the target allylated compound **21**. We speculated that the increased catalyst stability could be ascribed to the absence of a readily fragmenting group (the silyl moiety in the case of catalyst **IV**). Furthermore, the absence of acid labile groups in catalyst **VIII** offered the possibility of employing strongly acidic additives like trifluoroacetic acid, which lowered the amount of free amine in solution, thus minimizing the possible oxidation by the excited iminium ion.

Control experiments revealed that careful exclusion of light completely suppressed the process, confirming the photochemical nature of the reaction. Unfortunately, standard reaction parameters screening (solvent, acid, light source) did not lead to significant improvements in reaction efficiency.

In order to develop an efficient methodology, we tuned the redox potential of the silane in order to reduce the catalyst degradation issue. Allylsilane **20** is a moderate electron-rich compound with  $E_{1/2} = 1.75 \text{ V}$  (vs  $\text{Ag}/\text{AgCl}$ ), whereas benzylsilane is more prone to oxidation having  $E_{1/2} = 1.44 \text{ V}$  (vs  $\text{Ag}/\text{AgCl}$ ), comparable to the one of the chiral amines employed as organocatalysts. On the basis of this data, we predicted benzylsilane to be a better reaction partner. Gratifyingly, subjecting benzylsilane **24** to the reaction conditions, the desired compound **25** was obtained in 67% of isolated yield, albeit in an enantiomeric excess as low as 25% (Scheme 5.16).

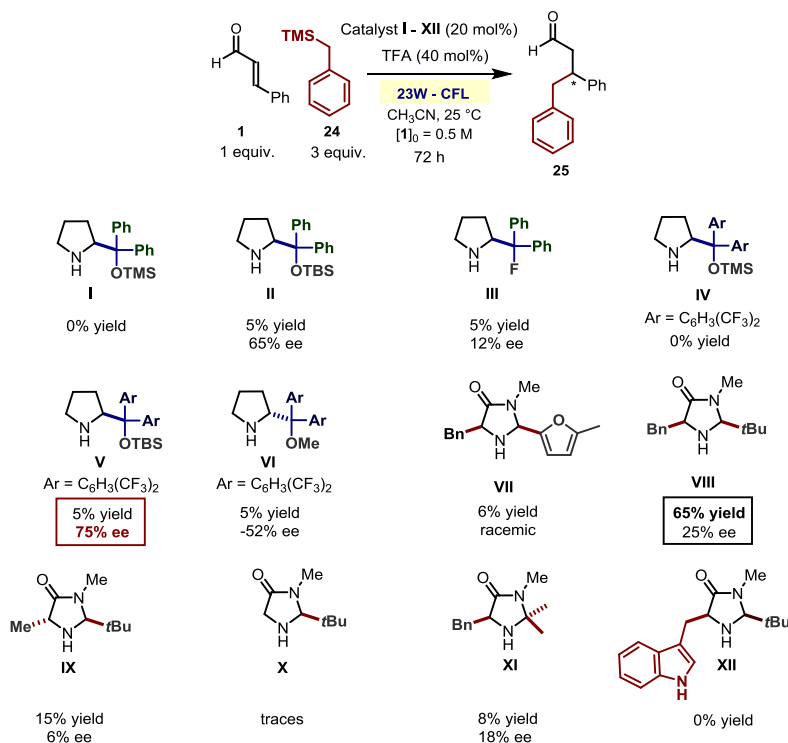
<sup>24</sup> For an analogous fragmentation reaction of structurally related ammonium cations, see: Lucia, L. A.; Burton, R. D.; Schanze, K. S. "Direct Observation of C-C Bond Fragmentation in  $\alpha$ -Amino Alcohol Radical Cations" *J. Phys. Chem.* **1993**, *97*, 9078.

<sup>25</sup> The identity of the desired compound was unambiguously inferred for comparison of spectral properties: Ooi, T.; Kondo, Y.; Maruoka, K. "Conjugate Allylation to  $\alpha,\beta$ -Unsaturated Aldehydes with the New Chemzyme *p*-F-ATPH" *Angew. Chem. Int. Ed. Engl.* **1997**, *36*, 1183.



**Scheme 5.16** – Photochemical conjugate benzylation of cinnamaldehyde: the lower redox potential of benzylsilane is crucial for reaction efficiency.

With these results in hand, we started an optimization phase in order to improve the enantioselectivity of the transformation. Screening of standard reaction parameters using catalyst **VIII** (solvents, acids) gave disappointing results and no stereoselectivity improvements were obtained. Several chiral aminocatalysts were then subjected to the reaction conditions.

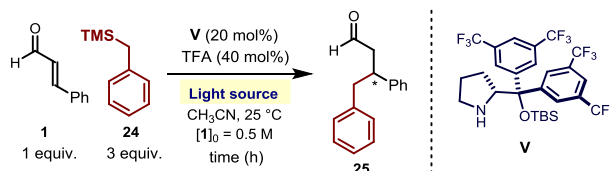


**Scheme 5.17** – Catalyst scaffold optimization for the photochemical conjugate benzylation of cinnamaldehyde. Reaction yields calculated by <sup>1</sup>H NMR analysis of the crude reaction mixtures employing trichloroethylene as the internal standard.

The use of other chiral amines in the presence of trifluoroacetic acid (TFA) as the acid co-catalyst led to poor reactivity (Scheme 5.17). However, the diarylprolinol scaffold was effective in terms of stereoselectivity, albeit low yields were always observed (catalysts **I** – **VI**). Decorating the diarylprolinol catalyst scaffold with a suitable bulky silicon protecting group was crucial for improving the catalyst stability under the reaction conditions, and catalyst **V** was the only one to be recovered quantitatively at the end of the reaction (>90% catalyst load recovery based on NMR analysis). When this catalyst was employed, product **25** was formed in low yield but good level of stereoselectivity (75% enantiomeric excess).

Encouraged by the high enantioselectivity observed employing catalyst **V** and by its stability under the reaction conditions, we decided to modify some reaction parameters in order to improve the efficiency of the chemical transformation. The employment of different solvents or acids did not lead to any improvement of reactivity, but the type of light source had a strong effect on the reaction yield (Table 5.1).

**Table 5.1** – Screening of the light sources for the photochemical  $\beta$ -benzylation of cinnamaldehyde



Entry	Light source	time (h)	yield (%)	s.m.r. (%)	ee (%)
1	23 W CFL Bulb	72	5	>90	75
2	19.2 W White LED Stripe	72	5	>90	75
3	16 W Black Light Bulb	72	6	>90	75
4	100 W medium pressure Hg lamp	11	25	0	40
5	300 W xenon lamp	16	37	15	59
6	300 W xenon lamp – LP filter 380 nm	15	46	15	61
<b>7</b>	<b>7.2 W Black Light LED Strip</b>	40	<b>59 (55)</b>	0	<b>76</b>

Reactions carried out on a 0.1 mmol scale, yield determined by  $^1\text{H}$  NMR analysis using trichloroethylene as the internal standard. Starting material recovery (s.m.r.) determined by  $^1\text{H}$  NMR analysis using trichloroethylene as the internal standard. Enantiomeric excesses determined by HPLC analysis using a chiral stationary phase. The yield of the isolated **25** obtained after chromatographic purification is reported in brackets.

The employment of UV light strongly influenced the reaction outcome. Strong light sources (entries 4 - 6) led to moderate yields with consistent starting material degradation. Phosphorus coated 16 W black light bulb irradiation was ineffective for the reaction (entry 3), probably due

to the low emission intensity of this light source. The employment of commercially available black light LED (light emitting diode) strips provided the best result, and the final product **25** was obtained in 59% NMR yield (55% isolated yield) and 76% ee (entry 7).<sup>26</sup> Details of the reaction set up, including a picture of the employed black LED strip, are reported in the Experimental Section (see Figure 5.5).

### 5.4.1 Spectroscopic investigations and mechanistic considerations

In order to gain some insights into the reaction mechanism, we carried out spectroscopic investigations. When mixing the catalyst **V** with aldehyde **1** and trifluoroacetic acid in acetonitrile, a new band in the UVA region was observed (maximum at 350 nm). The new band could be ascribed to the absorption of the transiently generated iminium ion intermediate.<sup>27</sup>

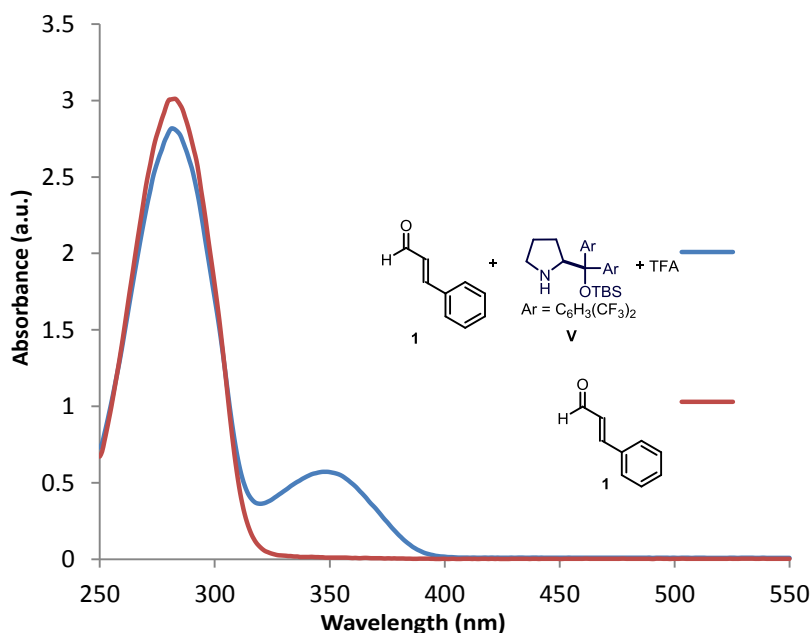


**Figure 5.3** – Absorption profile of a 111  $\mu\text{M}$  acetonitrile solution of cinnamaldehyde (red line) and of a 111  $\mu\text{M}$  acetonitrile solution of cinnamaldehyde upon addition of 20% mol of catalyst **V** and 40% mol of TFA after 2 h of incubation time (blue line). A new band is observed in the near-UV.

The recorded absorption spectrum allows also to rationalize the better results obtained in the photochemical conjugate benzylation of cinnamaldehyde when using black LED strips as the light

<sup>26</sup> The reason of the low mass balance is currently under investigation. It was not possible to isolate appreciable amounts of any byproducts after chromatographic purification.

<sup>27</sup> The absorption profile is consonant with the one reported for structurally related compounds: Lakhdar, S.; Tokuyasu, T.; Mayr, H. "Electrophilic Reactivities of  $\alpha,\beta$ -Unsaturated Iminium Ions" *Angew. Chem. Int. Ed.* **2008**, *47*, 8723.

source (Table 5.1, entry 7). This light source shows a maximum emission at 365 nm, further suggesting that the direct irradiation of the transient iminium ion is crucial for the reaction to occur.

Preliminary UV absorption studies suggested no formation of a photo-absorbing EDA aggregation in the ground state between the transient iminium ion and the silane **24**, since the absorption spectrum of the reaction mixture (green line in Figure 5.4) perfectly overlaid the absorption of the iminium ion, generated upon condensation of the catalyst **V** with **1** (red line in Figure 5.4). This observation is consonant with literature precedents reported by Mariano *et al.*, who did not observe any formation of ground state EDA complexes between pre-formed iminium ions and allyl silanes.<sup>8,28</sup>

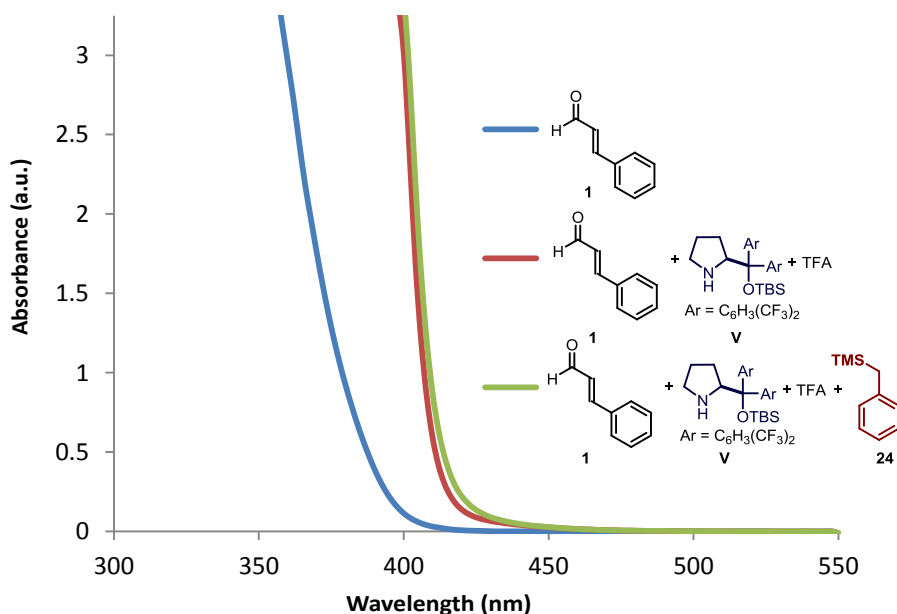
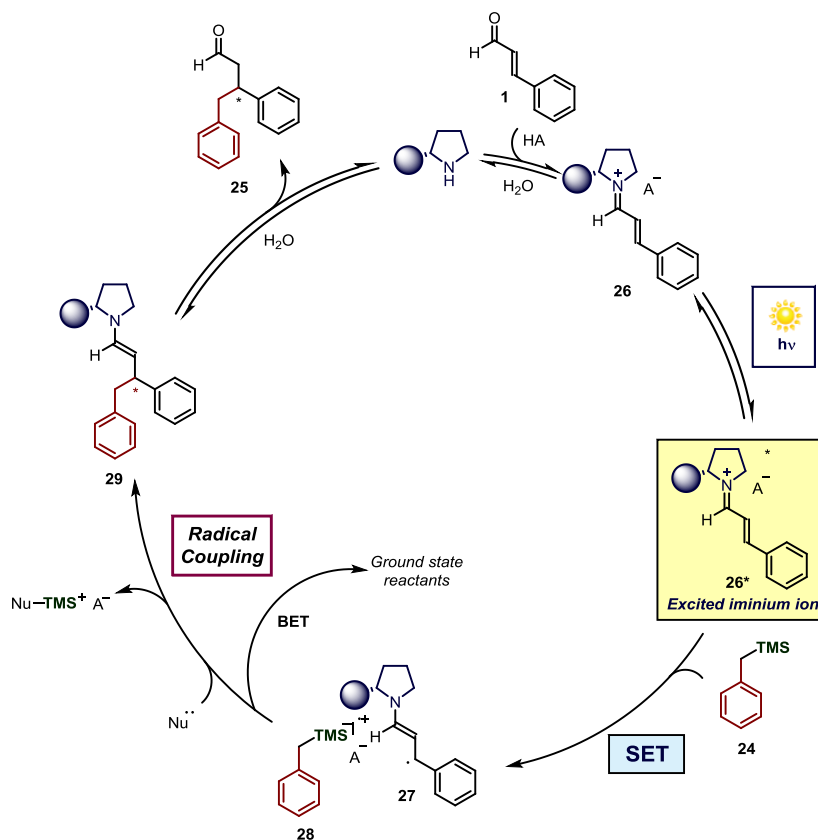


**Figure 5.4** – Optical absorption spectra acquired in acetonitrile in 1 mm path quartz cuvettes. Absorption profile of a 0.5 M solution of cinnamaldehyde (blue line), a 0.5 M solution of cinnamaldehyde upon addition of 20% mol of catalyst **V** and 40% mol of TFA after 2 h of incubation time (red line), and a 0.5 M solution of cinnamaldehyde upon addition of 20% mol of catalyst **V**, 40% mol of TFA, and 3 equivalents of benzylsilane **24**. All measurement carried out in acetonitrile solution. No evident new absorption bands are observed.

On the basis of these preliminary studies and our literature survey about the photochemistry of preformed iminium ions, we propose the following reaction mechanism (Scheme 5.18).

<sup>28</sup> Ohga, K.; Yoon, U. C.; Mariano, P. S. "Exploratory and Mechanistic Studies of the Electron Transfer Initiated Photoaddition Reactions of Allylsilane-Iminium ion Systems" *J. Org. Chem.* **1983**, *49*, 213.



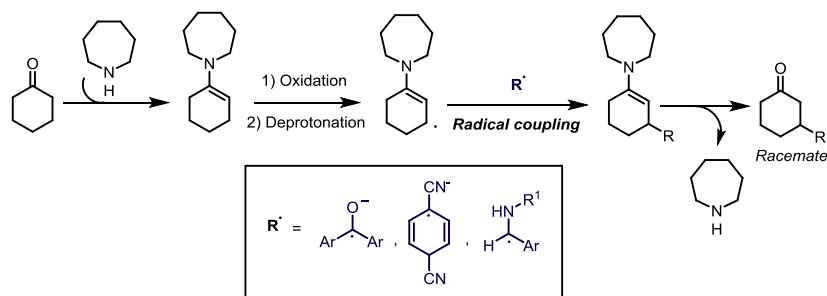
**Scheme 5.18** – Proposed reaction mechanism for the photochemical asymmetric organocatalytic conjugate benzoylation of cinnamaldehyde.

Condensation of the aminocatalyst with enal **1** leads to the transient iminium ion **26**. This chiral intermediate can reach an excited state upon light absorption, generating the excited species **26\***. Electron transfer is then expected to occur between the benzylsilane **24** (acting as a reductant) and the electron poor excited iminium ion **26\*** to generate the  $5\pi\sigma^-$  system  $\beta$ -enaminy radical **27** and the radical cation **28**. Preliminary experiments did not provide any evidence of EDA complex formation, so electron transfer is expected to occur through the formation an encounter complex or an exciplex between **26\*** and **24**. The solvent or traces of water could mediate the crucial radical cation **28** fragmentation, leading to a benzyl radical. This process is in competition with the back electron transfer (BET), which regenerates the ground state reagents. Radical-radical coupling between the long-lived species **27**<sup>29</sup> and the benzyl

<sup>29</sup> An EPR spectrum of analogous enaminy radicals (obtained upon oxidation/deprotonation of an enamine) has been recently reported, showing a surprisingly long lifetime for this kind of radicals: Terrett, J. A.; Clift,

radical provides the product enamine **29**, which after hydrolysis releases the  $\beta$ -functionalized aldehyde **25**. The radical nature of the transformation is corroborated by the complete inhibition observed carrying out the reaction in the presence of a stoichiometric amount of radical scavengers such as TEMPO. Further mechanistic studies, mainly focused at investigating the photo-physical behaviour of the iminium ions (emission and Stern-Volmer quenching studies), will be needed to better detail the reaction mechanism. Notably, the mechanism depicted in Scheme 5.18 is consonant with the photochemistry of preformed non-vinylous iminium ion reported by Mariano *et al.* where a radical coupling between  $\alpha$ -amino radicals and benzyl radicals occurs to afford an alkylated amine (see Scheme 5.5).

The chemistry of  $\beta$ -enaminy radical has been recently explored by MacMillan *et al.* who generated this species through a completely different approach. Specifically, an oxidation-deprotonation of an enamine, mediated by a metal-based photoredox catalyst, led to the formation of the  $\beta$ -enaminy radical (Scheme 5.19). This rather long-lived radical<sup>29</sup> readily underwent radical coupling with electron-rich radicals to furnish  $\beta$ -alkylated products starting from aliphatic ketones.<sup>30</sup> The approach has been used for the  $\beta$ -functionalization of saturated aldehydes but has never been employed in asymmetric catalysis.



Scheme 5.19 – Radical coupling of  $\beta$ -enaminy radicals.

## 5.5 Future directions

### 5.5.1 Introduction of $-\text{CH}_2\text{X}$ fragments in $\beta$ position of enals

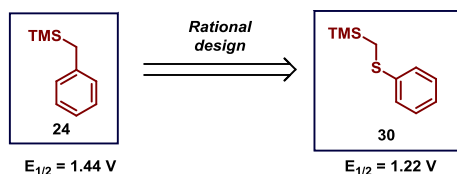
The photochemical strategy discussed in this chapter could be useful for the development of a variety of  $\beta$ -functionalizations of enals which cannot be realized using ground state reactivity. A

---

M. D.; MacMillan, D. W. C. "Direct  $\beta$ -Alkylation of Aldehydes via Photoredox Organocatalysis" *J. Am. Chem. Soc.* **2014**, *136*, 6858.

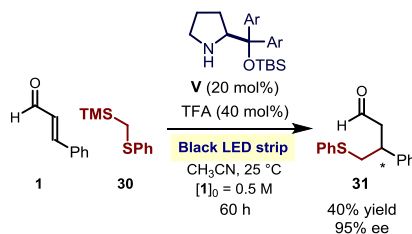
<sup>30</sup> a) Pirnot, M. T.; Rankic, D. A.; Martin, D. B. C.; MacMillan D. W. C. "Photoredox Activation for the Direct  $\beta$ -Arylation of Ketones and Aldehydes" *Science* **2013**, *339*, 1593. b) Petronijević, F. R.; Nappi, M.; MacMillan, D. W. C. "Direct  $\beta$ -Functionalization of Cyclic Ketones with Aryl Ketones via the Merger of Photoredox and Organocatalysis" *J. Am. Chem. Soc.* **2013**, *135*, 18323. c) Jeffrey, J. L.; Petronijević, F. R.; MacMillan, D. W. C.. "Selective Radical-Radical Cross-Couplings: Design of a Formal  $\beta$ -Mannich Reaction" *J. Am. Chem. Soc.* **2015**, *137*, 8404.

rational design of the reaction partner could be drawn on the basis of redox potentials. For instance, methyl heteroatom fragments (where heteroatom is sulfur, oxygen, nitrogen etc.) could be introduced starting from the opportune silane donor.<sup>10</sup> For testing the feasibility of this hypothesis, we synthesized compound **30**, which can be readily oxidized under the reaction conditions.



Scheme 5.20 – Rational starting material design.

Gratifyingly, compound **30** readily reacts with cinnamaldehyde under the best reaction conditions found for the photochemical conjugate benzylation, and the product **31** was obtained with excellent stereocontrol and moderate yield (Scheme 5.21).



Scheme 5.21 – Catalytic asymmetric introduction of methyl-sulfide fragment at the  $\beta$ -position of cinnamaldehyde **1**.

This result provides a poof-of-concept that this novel light-driven methodology can allow synthetic disconnections that are usually unavailable to classical polar ground state reactivity.

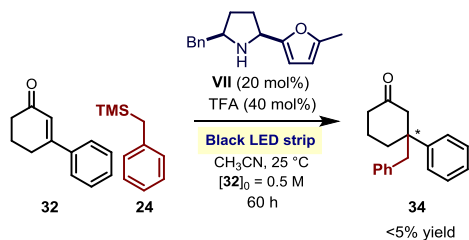
## 5.5.2 The employment of trifluoroborate salts: forging quaternary stereocenters

Quaternary carbon stereocenters are commonly found in natural compounds and are particularly challenging to forge in a catalytic asymmetric fashion.<sup>31</sup> We envisioned the possibility to access compounds bearing quaternary carbon stereogenic centers exploiting our novel photocatalytic strategy. We tested the possibility of extending the benzylation method to

<sup>31</sup> Quasdorf, K. W.; Overman, L. E. "Catalytic Enantioselective Synthesis of Quaternary Carbon Stereocenters" *Nature* **2014**, *516*, 181.

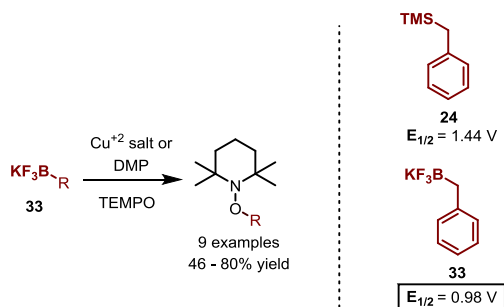


include the  $\beta$ -substituted enone **32**.<sup>32</sup> Unfortunately, only traces of the final product **34** were detected in the reaction mixture.



Scheme 5.22  $\beta$ -benzylation of  $\beta$ -substituted cyclohexenones: forging quaternary stereocenters.

The detection of traces of the desired compound in the reaction mixture motivated us to attempt an optimization of the conditions in order to render the process synthetically useful. It was recently reported that free radicals could be generated starting from trifluoroborates under oxidative conditions.<sup>33</sup> Due to their anionic nature, trifluoroborates are better reducing agents compared to silanes,<sup>34</sup> and this is reflected in their lower  $E_{1/2}$  values (Scheme 5.23).<sup>34</sup>



Scheme 5.23 – Generation of radicals from trifluoroborate salts. DMP = Dess-Martin periodinane.

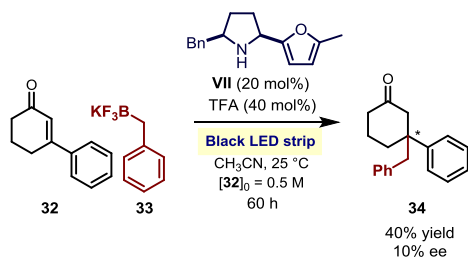
Given the high electron donor ability of compound **33** in comparison to compound **24**, we used trifluoroborate salt **33** in iminium ion PET chemistry in order to improve the results reported in Scheme 5.22.

Gratifyingly, subjecting the trifluoroborate salt **33** to the reaction conditions, the compound **34**, bearing a quaternary stereogenic center, was formed with increased efficiency (Scheme 5.24).

<sup>32</sup> For an example of asymmetric catalyzed copper catalyzed conjugate addition of trimethylalluminium on cyclohexenone **32** see: Palais, L.; Mikhel, I. S.; Bournaud, C.; Micouin, L.; Falciola, C. A.; Vuagnoux-d'Augustin, M.; Rosset, S.; Bernardinelli, G.; Alexakis, A. "SimplePhos Monodentate Ligands: Synthesis and Application in Copper-Catalyzed Reactions" *Angew. Chem. Int. Ed.* **2007**, *46*, 7462.

<sup>33</sup> Sorin, G.; Martinez Mallorquin, R.; Contie, Y.; Baralle, A.; Malacria, M.; Goddard, J.; Fensterbank, L. "Oxidation of Alkyl Trifluoroborates: An Opportunity for Tin-Free Radical Chemistry" *Angew. Chem. Int. Ed.* **2010**, *49*, 872.

<sup>34</sup> Redox potential of trifluoroborate **33**: Nishigaichi, Y.; Orimi, T.; Takuwa, A. "Photo-Allylation and Photo-Benzylation of Carbonyl Compounds Using Organotrifluoroborate Reagents" *J. Organomet. Chem.* **2009**, *694*, 3837.



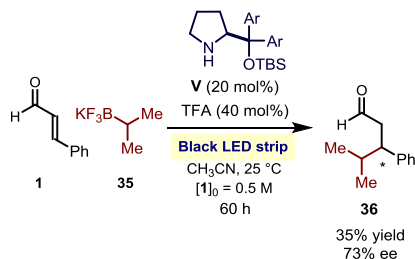
**Scheme 5.24** – Forging quaternary stereocenters through the employment of alkyl trifluoroborates.

Further optimization studies are currently ongoing in our laboratory in order to improve the efficiency and the stereoselectivity of the process reported in Scheme 5.24. We strongly believe that the employment of trifluoroborate salts can increase the generality of the chemistry introduced in this chapter, and extensive studies are currently ongoing along this direction.

### 5.5.3 Iminium photochemistry and trifluoroborate salts, a general alkylation strategy?

The successful employment of trifluoroborate salts for the chemistry presented in this chapter may provide the seductive possibility to use unactivated alkyl trifluoroborate salts for developing a general photochemical organocatalytic strategy for  $\beta$ -alkylation of cinnamaldehyde.

When attempting the reaction depicted in Scheme 5.25, the product **36** was isolated in 35% yield and 73% ee, demonstrating the feasibility of the approach.



**Scheme 5.25** – Asymmetric introduction of an isopropyl fragment into cinnamaldehyde.

This preliminary result is a further evidence of the general applicability of our novel photochemical organocatalytic strategy.

## 5.6 Conclusions

The photochemical, iminium ion-mediated enantioselective  $\beta$ -functionalization of  $\alpha,\beta$ -carbonyl compounds has been developed. The methodology offers a direct access to reactivities which are not available through the classical ground state reactivity. The reactions occur under mild conditions, at ambient temperature and using readily available black light LEDs strips. Initial mechanistic studies support a mechanism where transiently generated chiral iminium ions, classical intermediate of ground state organocatalysis, directly reach an electronically excited state upon light absorption. In their excited states, they can act as powerful oxidants triggering the formation of reactive radical species from electron rich organic compounds bearing silyl or boron fragmenting groups.

Further optimization studies, scope investigation, and mechanism studies are currently underway in our laboratory.

## 5.7 Experimental section

### General information

The  $^1\text{H}$  NMR spectra were recorded at 400 MHz and 500 MHz while  $^{13}\text{C}$  NMR at 100 MHz and 125 MHz. The chemical shifts ( $\delta$ ) for  $^1\text{H}$  and  $^{13}\text{C}$  are given in ppm relative to residual signals of the solvents ( $\text{CHCl}_3$  @ 7.26 ppm  $^1\text{H}$  NMR, 77.16 ppm  $^{13}\text{C}$  NMR). Coupling constants are given in Hz. The following abbreviations are used to indicate the multiplicity: s, singlet; q, quartet; p, pentuplet; m, multiplet.

High-resolution mass spectra (HRMS) were obtained from the ICIQ High Resolution Mass Spectrometry Unit on Waters GCT gas chromatograph coupled time-of-flight mass spectrometer (GC/MS-TOF) with electron ionization (EI) or MicroTOF II (Bruker Daltonics): HPLC-MS-TOF (ESI). UV-vis measurements were carried out on a Shimadzu UV-2401PC spectrophotometer equipped with photomultiplier detector, double beam optics and D2 and W light sources.

Cut-off and photochemical experiments have been performed using a 300 W xenon lamp (Asashi Spectra Co., Ltd.). In Table 5.1 the following light sources were employed: commercially available 23 W bulb compact fluorescent lamp or 16 W black light bulb lamp; 100 W medium pressure mercury lamp UV-Technik Meyer gmbh; White LED: Ledxon modular 9009046 LED, HP double, 19.2W, 1 m length; Black LED: Paulmann Function BlackLight LED Stripe Set, 7.2W, 1 m length.

**General Procedures:** All reactions were set up under an argon atmosphere using standard Schlenk techniques. Synthesis grade solvents were used as purchased and the reaction mixtures were degassed by three cycles of freeze-pump-thaw, no precautions were adopted to avoid moisture in solvents. Chromatographic purification of products was accomplished using force-flow chromatography (FC) on silica gel (35-70 mesh). For thin layer chromatography (TLC) analysis throughout this work, Merck precoated TLC plates (silica gel 60 GF254, 0.25 mm) were

employed, using UV light as the visualizing agent and phosphomolibdic acid stain solution and heat as developing agents. Organic solutions were concentrated under reduced pressure on a Büchi rotatory evaporator.

**Materials:** Reagents were purchased at the highest commercial quality from Sigma Aldrich, Fluka, and Alfa Aesar and used as received, without further purification, unless otherwise stated.

All the catalysts used in this chapter are commercially available apart from catalysts **II**, **V** and **XII** which were prepared following literature procedures.<sup>35,36,37</sup>

Ketone **32** and trifluoroborate salt **33** were prepared following literature procedures.<sup>32,38</sup>

**Determination of Enantiomeric Purity:** HPLC analysis on chiral stationary phase was performed on an Agilent 1200-series instrumentation. Daicel Chiralpak ID-3 or IC-3 columns with hexane:iPrOH as the eluents was used. HPLC traces were compared to racemic samples prepared using a catalytic amount of a racemic mixture of the catalyst employed for the transformation (total loading 20 mol%).

**Determination of Yields in the Optimization Studies:** The starting material recovery (s.m.r.) and the yield of product **25** in the optimization studies were determined by <sup>1</sup>H NMR on the crude reaction mixture employing 1 equivalent (9 μL, 0.1 mmol) of trichloroethylene (1H, singlet, δ = 6.2 ppm) as the internal standard. The yield was obtained integrating the signal of the benzylic proton (δ = 3.52 (p)), identical results were obtained integrating the aldehydic proton (δ = 9.62 (t)). Control experiments revealed that yields of the isolated product were in excellent agreement with NMR yield.

**Reagents absorption profile:** All the spectra were recorded in Shimadzu UV-2401PC spectrophotometer in acetonitrile solutions using the same concentrations as in the reaction conditions as better detailed in Figure 5.3 and 5.4. Due to the high concentration of the solutions, short light path cuvettes have been employed in order to avoid fast signal saturation. 1 mm Hellma Quartz SUPRASIL<sup>®</sup> cuvettes have been used to record all the spectra.

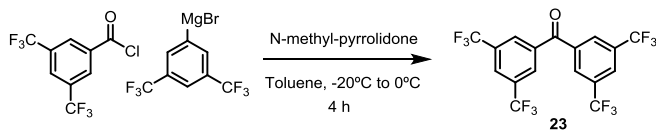
---

<sup>35</sup> Lin, Q.; Meloni, D.; Pan, Y.; Xia, M.; Rodgers, J.; Shepard, S.; Li, M.; Galya, L.; Metcalf, B.; Yue, T.; Liu, P.; Zhou, J. "Enantioselective Synthesis of Janus Kinase Inhibitor INCB018424 via an Organocatalytic Aza-Michael Reaction" *Org. Lett.* **2009**, *11*, 1999.

<sup>36</sup> Hayashi, Y.; Gotoh, H.; Hayashi, T.; Shoji, M. "Diphenylprolinol Silyl Ethers as Efficient Organocatalysts for the Asymmetric Michael Reaction of Aldehydes and Nitroalkenes" *Angew. Chem. Int. Ed.* **2005**, *44*, 4212.

<sup>37</sup> Samulis, L.; Tomkinson, N. C. O. "Preparation of the MacMillan imidazolidinones" *Tetrahedron* **2011**, *67*, 4263.

<sup>38</sup> Molander, G. A.; Ito, T. "Cross-Coupling Reactions of Potassium Alkyltrifluoroborates with Aryl and 1-Alkenyl Trifluoromethanesulfonates" *Org. Lett.* **2001**, *3*, 393.



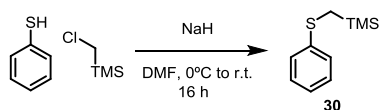
**Scheme 5.26** – Preparation of compound **23**.

**Preparation of compound 23:** (3,5)-bis-trifluoromethyl benzoyl chloride (160  $\mu\text{L}$ , 0.88 mmol) was added dropwise to a solution of *N*-methyl-pyrrolidone (92  $\mu\text{L}$ , 0.96 mmol in 3 ml of toluene) at 0  $^{\circ}\text{C}$  over a period of 15 minutes. This solution was cooled down to -10  $^{\circ}\text{C}$  and 880  $\mu\text{L}$  of a 1 M solution of (3,5)-bis-trifluoromethyl phenyl magnesium bromide was then added over a period of 20 minutes. The reaction was stirred for further 4 hours at room temperature, after which it was quenched with 3 mL of saturated solution of ammonium chloride. The mixture was then transferred in a separatory funnel, 50 mL of water were added and the aqueous phase was extracted 3 times with 30 mL of ethyl acetate. The organic layers were collected, washed with saturated brine solution and dried over sodium sulfate. Evaporation of volatiles and recrystallization from boiling hexanes afforded 295 mg (0.65 mmol, 81% yield) of compound **23** as white crystals.

$^1\text{H}$  NMR (400 MHz,  $\text{CDCl}_3$ ):  $\delta$  8.23 (s, 4H), 8.19 (s, 2H).

$^{13}\text{C}$  NMR (100 MHz,  $\text{CDCl}_3$ ):  $\delta$  190.9, 137.8, 133.1 (q,  $J = 34$  Hz), 129.9 (m), 126.9 (m), 122.7 (q,  $J=273$  Hz).

Spectral data match with the one reported in literature.<sup>39</sup>



**Scheme 5.27** – Preparation of compound **30**.

**Preparation of compound 30:** 165  $\mu\text{L}$  (1.60 mmol) of thiophenol was added dropwise at 0  $^{\circ}\text{C}$  to stirred suspension of NaH (65 mg of 60% suspension in mineral oil, 1.60 mmol) in 5 mL of dry DMF. The reaction was stirred for 20 minutes after which 216  $\mu\text{L}$  (1.45 mmol) of iodomethyl trimethylsilane was added over a period of 5 minutes. The reaction was warmed at room temperature and vigorously stirred for 16 h. The reaction was quenched with 5 mL of water, after which it was transferred in a separatory funnel. 100 mL of ethyl acetate was added and the solution, which was washed 6 times with 50 mL of water and one time with saturated brine. After drying with sodium sulfate and removal of the solvent, the crude reaction mixture was purified through silica gel chromatography (gradient pure hexane – hexane/ethyl acetate 98:2)

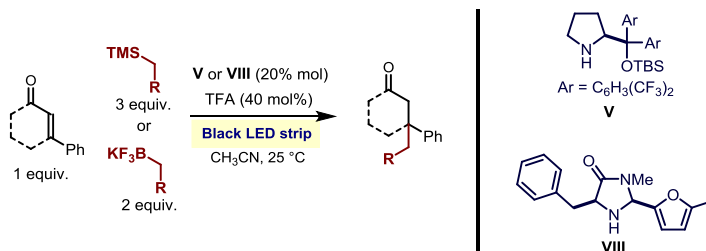
<sup>39</sup> Wang, X.; Liu, F., Tu, H.; Zhang, A. "One-Pot Synthesis of Diarylmethanones through Palladium-Catalyzed Sequential Coupling and Aerobic Oxidation of Aryl Bromides with Acetophenone as a Latent Carbonyl Donor" *J. Org. Chem.* **2014**, *79*, 6554.

to afford 260 mg (1.32 mmol - 91% yield) of phenylthiomethyl trimethylsilane (**30**) as a colorless liquid.

$^1\text{H}$  NMR (400 MHz,  $\text{CDCl}_3$ )  $\delta$  7.31 – 7.20 (m, 4H), 7.14 – 7.03 (m, 1H), 2.17 (s, 2H), 0.15 (s, 9H).

$^{13}\text{C}$  NMR (100 MHz,  $\text{CDCl}_3$ )  $\delta$  140.47, 128.80, 126.15, 124.75, 18.34, -1.46.

Spectral data match with the one reported in literature.<sup>40</sup>



**Scheme 5.28** – General reaction scheme for the  $\beta$ -alkylation of  $\alpha,\beta$ -unsaturated carbonyl compounds.

**General procedure for the  $\beta$ -alkylation of  $\alpha,\beta$ -unsaturated carbonyl compounds:** a 10 mL Schlenk tube was charged with the aminocatalyst **VII** or **VIII** (0.02 mmol), acetonitrile (200  $\mu\text{L}$ ) and trifluoroacetic acid (3.0  $\mu\text{L}$ , 0.04 mmol). The carbonyl compound was added to the mixture (0.1 mmol) followed by the alkylating agent (0.3 mmol or 0.2 mmol). The reaction mixture was degassed via freeze pump thaw (x 3) and the vessel refilled with argon. The vial was sealed and positioned in the center of a beaker equipped with black LED strips, approximately 5 cm away from the light sources (as depicted in Figure 5.5). The reaction was refrigerated with a strong flow of compressed air in order to avoid heating due to the light source. After the stated time, the reaction mixture was directly subjected to flash column chromatography purification to afford final product.

<sup>40</sup> Ishibashi, H.; Nakatani, H.; Umei, Y.; Yamamoto, W.; Ikeda, M. "Reaction of [Arylthio(chloro)methyl]trimethylsilanes with Arenes and Alkyl-1-enes in the Presence of Lewis Acid: Syntheses of [Aryl(arylthio)methyl]- and (1-Arylthioalk-3-enyl)-trimethylsilanes" *J. Chem. Soc. Perkin Trans. I* **1987**, 589.

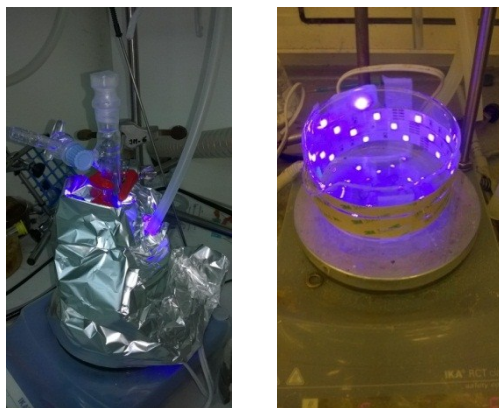
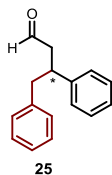


Figure 5.5 – Reaction set up

### 3,4-Diphenyl butanal (**25**)



The reaction was performed following the general procedure, using 12.8 mg of catalyst **V**, 12.6  $\mu\text{L}$  of cinnamaldehyde and 56.8  $\mu\text{L}$  (0.3 mmol, 3 equiv) of benzyl trimethylsilane **24**.

After stirring for 40 hours, the crude mixture was directly subjected to flash column chromatography purification (gradient hexane - hexane/ethyl acetate 95:5) to afford 12.3 mg (55% yield) of the title compound **25** in 75% enantiomeric excess.

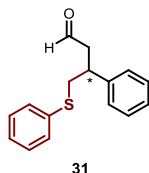
The enantiomeric excess was determined by HPLC analysis on a Daicel Chiralpak ID-3 column: 99:1 hexane/isopropanol flow rate 0.80 ml/min,  $\lambda=215$  nm:  $\tau_{\text{major}} = 15.7$  min,  $\tau_{\text{minor}} = 17.6$  min.  $[\alpha_D]^{25} = -43.94$  ( $c = 0.63$ ). MS (EI) :  $m/z$  206.1 ( $M^+ - \text{H}_2\text{O}$ , 10), 180 (100), 105 (85), 91 (75), 77 (25).

$^1\text{H}$  NMR (400 MHz,  $\text{CDCl}_3$ )  $\delta$  9.62 (t,  $J = 2.0$  Hz, 1H), 7.34 – 7.17 (m, 8H), 7.11 – 7.06 (m, 2H), 3.52 (p,  $J = 7.4$  Hz, 1H), 2.99 (dd,  $J = 13.5, 7.4$  Hz, 1H), 2.91 (dd,  $J = 13.5, 7.4$  Hz, 1H), 2.81 – 2.75 (m, 2H).  $^{13}\text{C}$  NMR (100 MHz,  $\text{CDCl}_3$ )  $\delta$  201.7, 143.4, 139.4, 129.4, 128.7, 128.5, 127.7, 126.9, 126.5, 49.1, 43.5, 42.2.

Spectral data match with the ones reported in literature.<sup>41</sup>

<sup>41</sup> Bull, S. D.; Davies, S. G.; Nicholson, R. L.; Sanganee, H. J.; Smith, A. D. "SuperQuat N-acyl-5,5-Dimethylloxazolidin-2-ones for the Asymmetric Synthesis of  $\alpha$ -Alkyl and  $\beta$ -Alkyl Aldehydes" *Org. Biomol. Chem.* **2003**, *1*, 2886.

### 3-Phenyl-4-(phenylthio)butanal (**31**)



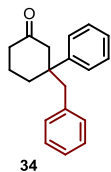
The reaction was performed following the general procedure, using 12.8 mg of catalyst **V**, 12.6  $\mu\text{L}$  of cinnamaldehyde, and 19.6 mg (0.2 mmol, 2 equiv) of phenylthiomethyl trimethylsilane **30**. After stirring for 40 hours, the crude mixture was directly subjected to flash column chromatography purification (gradient hexane - hexane/ethyl acetate 95:5) to afford 9.7 mg (40% yield) of the title compound **31** in 95% ee.

The enantiomeric excess was determined by HPLC analysis on a Daicel Chiralpak IC-3 column: 95:5 hexane/isopropanol flow rate 0.80 ml/min,  $\lambda=215$  nm:  $\tau_{\text{major}} = 16.0$  min,  $\tau_{\text{minor}} = 19.4$  min.

**HRMS** : calculated for  $\text{C}_{16}\text{H}_{16}\text{OSNa}$  (M+Na): 279.0814, found: 279.0807.  $[\alpha_{\text{D}}]^{25} = -40.43$  ( $c = 0.66$ )

$^1\text{H}$  NMR (400 MHz,  $\text{CDCl}_3$ )  $\delta$  9.69 (t,  $J = 1.8$  Hz, 1H), 7.41 – 7.20 (m, 11H), 3.54 – 3.42 (m, 1H), 3.29 (dd,  $J = 12.9, 6.2$  Hz, 1H), 3.16 (dd,  $J = 12.9, 8.0$  Hz, 1H), 3.10 (ddd,  $J = 17.4, 5.8, 1.8$  Hz, 1H), 2.84 (ddd,  $J = 17.4, 8.0, 1.8$  Hz, 1H).  $^{13}\text{C}$  NMR (101 MHz,  $\text{CDCl}_3$ )  $\delta$  200.9, 142.3, 135.8, 129.7, 129.2, 129.0, 127.5, 127.4, 126.5, 48.8, 40.6, 39.6.

### 3-Benzyl-3-phenylcyclohexan-1-one (**34**)



The reaction was performed following the general procedure, using 17.2 mg of ketone **32** and 39.6 mg (0.2 mmol, 2 equiv) of potassium benzyltrifluoroborate **33** and 5.4 mg of catalyst **VII**. After stirring for 60 hours, the crude reaction mixture was directly subjected to flash column chromatography purification (gradient hexane - hexane/ethyl acetate 95:5) to afford 10.6 mg (40% yield) of the title compound **34** in 10% enantiomeric excess.

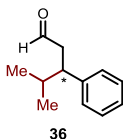
The enantiomeric excess was determined by HPLC analysis on a Daicel Chiralpak IC-3 column: 97:3 hexane/isopropanol flow rate 0.80 ml/min,  $\lambda=215$  nm:  $\tau_{\text{minor}} = 22.9$  min,  $\tau_{\text{major}} = 29.9$  min. MS (EI):  $m/z$  264 ( $\text{M}^+$ , 5), 173 (100), 145 (40), 131 (41), 115 (55), 103 (43), 91 (90), 77 (39).

$^1\text{H}$  NMR (400 MHz,  $\text{CDCl}_3$ )  $\delta$  7.32 – 7.10 (m, 8H), 6.75 – 6.69 (m, 2H), 2.95 (d,  $J = 13.3$  Hz, 1H), 2.89 (d,  $J = 13.3$  Hz, 1H), 2.84 (d,  $J = 14.0$  Hz, 1H), 2.48 (d,  $J = 14.0$  Hz, 1H), 2.41 – 2.32 (m, 1H), 2.24 (dd,  $J = 8.5, 5.5$  Hz, 2H), 2.05 – 1.94 (m, 1H), 1.94 – 1.82 (m, 1H), 1.62 – 1.50 (m, 1H).  $^{13}\text{C}$  NMR (100 MHz,  $\text{CDCl}_3$ )  $\delta$  211.8, 144.7, 137.3, 131.0, 129.0, 128.3, 127.4, 127.0, 126.9, 51.2, 50.8, 47.9, 41.4, 36.4, 22.0.

Spectral data match with the ones reported in literature.<sup>42</sup>

<sup>42</sup> Lin, S.; Lu, X. "Cationic Pd(II)/Bipyridine-Catalyzed Conjugate Addition of Arylboronic Acids to  $\beta,\beta$ -Disubstituted Enones: Construction of Quaternary Carbon Centers" *Org. Lett.* **2010**, *12*, 2536.



**4-methyl-3-phenylpentanal (36)**

The reaction was performed following the general procedure, using 12.8 mg of catalyst **V**, 12.6  $\mu\text{L}$  of cinnamaldehyde, and 30.0 mg (0.2 mmol, 2 equiv) of potassium isopropyltrifluoroborate **35**. After stirring for 16 hours, the crude mixture was directly subjected to flash column chromatography purification (gradient hexane - hexane/ethyl acetate 95:5) to afford 6.2 mg (35% yield) of

the title compound **36** in 73% ee.

The enantiomeric excess was determined by HPLC analysis on a Daicel Chiralpak IC-3 column on the corresponding alcohol obtained through reduction with  $\text{NaBH}_4/\text{MeOH}$ : 97:3 hexane/isopropanol flow rate 0.80 ml/min,  $\lambda=215$  nm:  $\tau_{\text{minor}} = 14.2$  min,  $\tau_{\text{major}} = 16.1$  min.

Spectral data match with the ones reported in literature.<sup>43</sup>

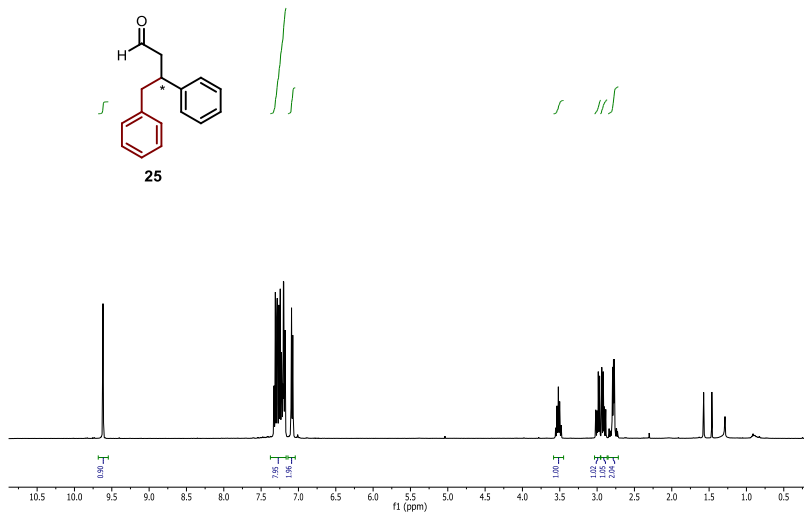
$^1\text{H}$  NMR (500 MHz,  $\text{CDCl}_3$ )  $\delta$  9.60 (dd,  $J = 2.5, 2.0$  Hz, 1H), 7.33 – 7.24 (m, 2H), 7.24 – 7.14 (m, 2H), 7.17 – 7.11 (m, 1H), 3.06 – 2.91 (m, 1H), 2.90 – 2.70 (m, 2H), 1.87 (oct,  $J = 6.7$  Hz, 1H), 0.95 (d,  $J = 6.7$  Hz, 3H), 0.78 (d,  $J = 6.7$  Hz, 3H).  $^{13}\text{C}$  NMR (125 MHz,  $\text{CDCl}_3$ )  $\delta$  202.5, 142.6, 128.4, 128.3, 126.5, 47.2, 47.0, 33.4, 20.6, 20.3.

<sup>43</sup> Arai, N.; Sato, k.; Azuma, K.; Ohkuma, T. "Enantioselective Isomerization of Primary Allylic Alcohols into Chiral Aldehydes with the tol-binap/dbapen/Ruthenium(II) Catalyst" *Angew. Chem. Int. Ed.* **2013**, *52*, 7500.

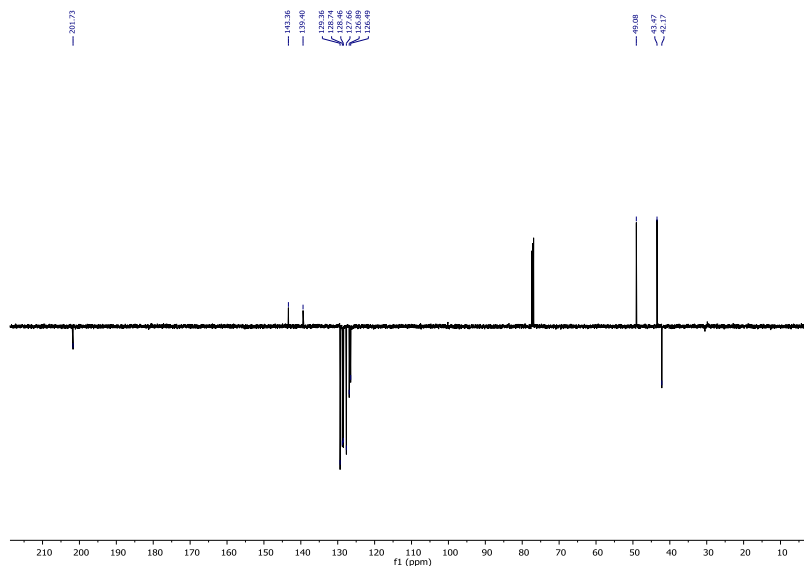
## NMR Spectra

### 3,4-Diphenyl butanal (25)

$^1\text{H}$  NMR ( $\text{CDCl}_3$ , 400 MHz)

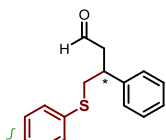


DEPT  $^{13}\text{C}$ -NMR ( $\text{CDCl}_3$ , 100 MHz)

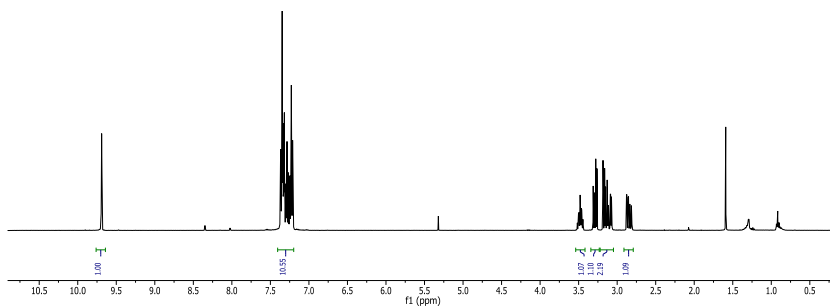


**3-Phenyl-4-(phenylthio)butanal (31)**

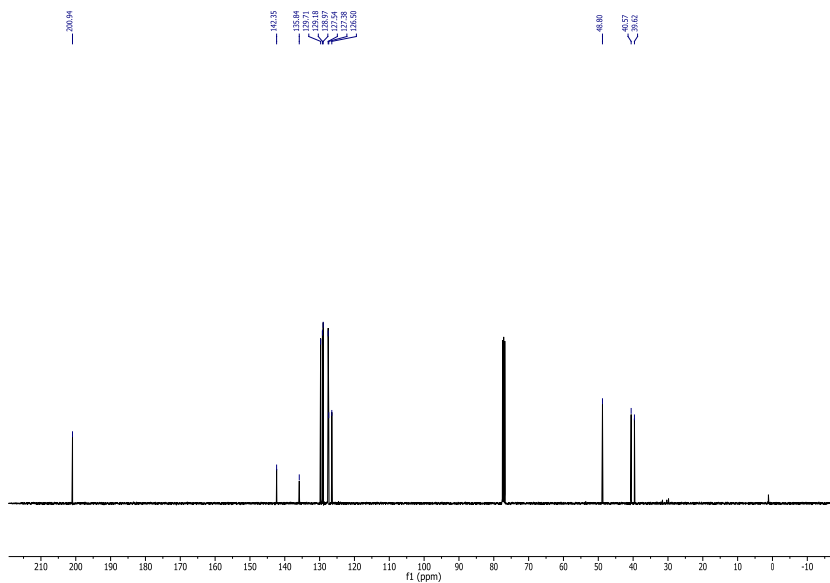
$^1\text{H NMR}$  ( $\text{CDCl}_3$ , 400 MHz)



31

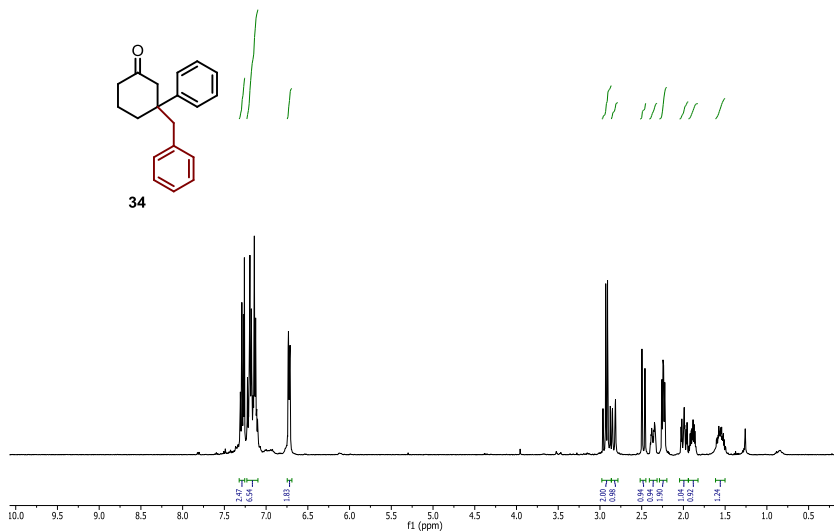


$^{13}\text{C NMR}$  ( $\text{CDCl}_3$ , 100 MHz)

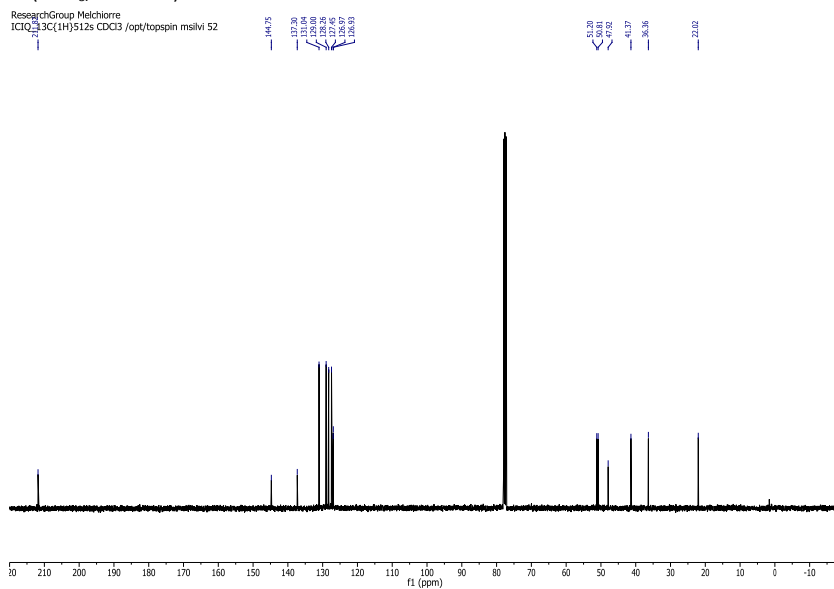


**3-Benzyl-3-phenylcyclohexan-1-one (34)**

$^1\text{H}$  NMR ( $\text{CDCl}_3$ , 400 MHz)



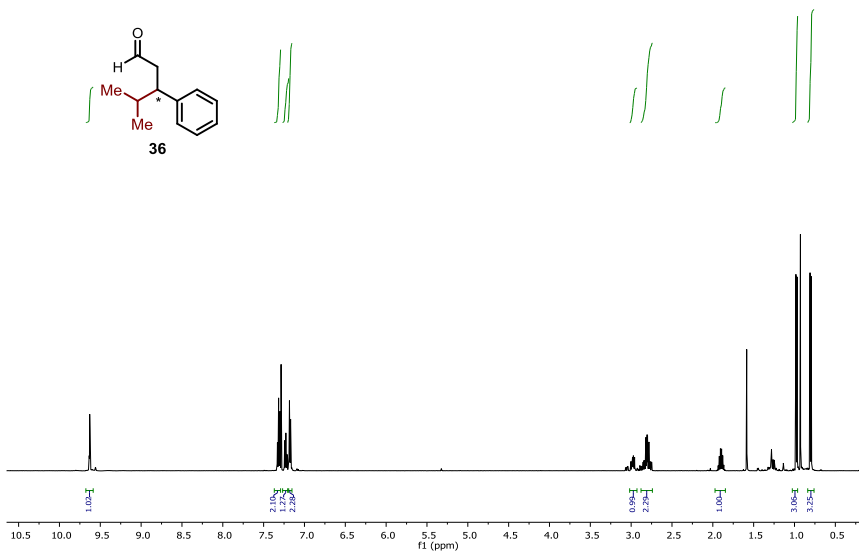
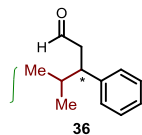
$^{13}\text{C}$  NMR ( $\text{CDCl}_3$ , 100 MHz)



### 4-methyl-3-phenylpentanal (36)

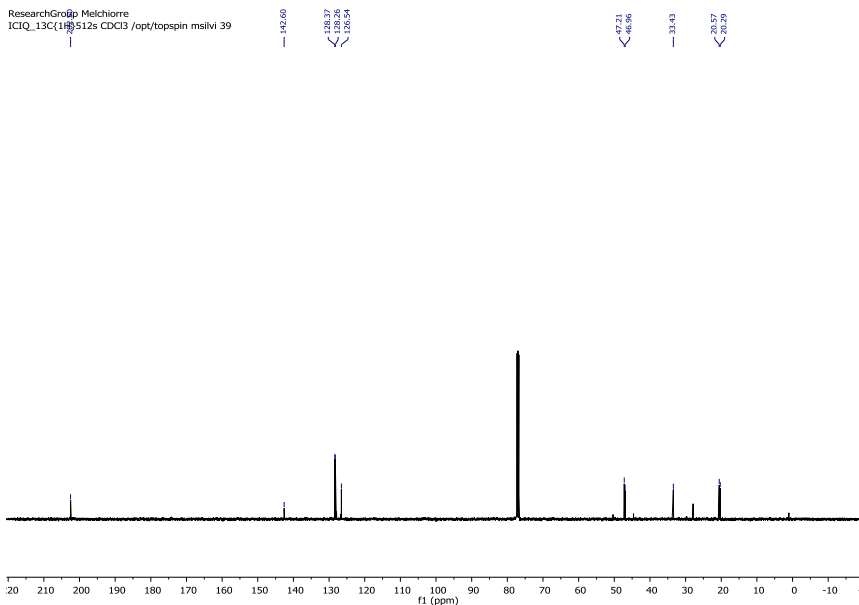
$^1\text{H}$  NMR ( $\text{CDCl}_3$ , 500 MHz)

ResearchGroup Melchiorre  
 ICIQ\_1H12p8s CDCl3 /opt/topspin msilvi 39



$^{13}\text{C}$  NMR ( $\text{CDCl}_3$ , 125 MHz)

ResearchGroup Melchiorre  
 ICIQ\_13C(1H)512s CDCl3 /opt/topspin msilvi 39



UNIVERSITAT ROVIRA I VIRGILI

NEW DIRECTIONS IN AMINOCATALYSIS: VINYLOGY AND PHOTOCHEMISTRY

Mattia Silvi

UNIVERSITAT ROVIRA I VIRGILI

NEW DIRECTIONS IN AMINOCATALYSIS: VINYLOGY AND PHOTOCHEMISTRY

Mattia Silvi